
THE UNIVERSITY
*of* EDINBURGH

# RELAXIN AS A THERAPEUTIC HAEMODYNAMIC MODULATOR IN LIVER DISEASE

Victoria Katherine Snowdon

Submitted for the degree

Doctor of Philosophy

University of Edinburgh

2015

# Declaration

I declare that this thesis is composed by me and that the work presented herein is my own. Some experiments were carried out in collaboration with colleagues. Where this is the case, I have acknowledged it in the appropriate results section. I can confirm that this work has not been submitted for any other degree or professional qualification.

Victoria Katherine Snowdon

# Table of Contents

# Table of Figures and Tables

# Abbreviations

ACh: Acetylcholine

ADH: Antidiuretic hormone

ADMA: Asymmetric dimethylarginine

AGTR1A: Arginine vasopressin receptor 1a

ALT: Alanine Transaminase

ALP: Alkaline phosphatase

AKI: Acute kidney injury

ATN: Acute tubular necrosis

BDL: Bile duct ligation

BOLD MRI: Blood oxygen level dependent magnetic resonance imaging

CPA: Collagen proportionate area

CO: Cardiac output

COX: Cyclo-oxygenase

EDHF: Endothelium-derived hyperpolarisation factor

$CCl_4$: Carbon tetrachloride

CPA: Collagen proportionate area

ET1: Endothelin I

ETA: Endothelin Type A receptor

ETB: Endothelin Type B receptor

GFR: Glomerular filtration rate

HAS: Human albumin solution

H+E: Haematoxylin and Eosin

HRS: Hepatorenal syndrome

HE: Hepatic encephalopathy

HR: Heart rate

IHC: Immunohistochemistry

IF: Immunofluorescence

IP: Intraperitoneal

IV: Intravenous

KPSS: Potassium rich physiological salt solution

LGR: Leucine rich repeats containing G-protein coupled receptor family

L-NAME: L-$N^G$-Nitroarginine methyl ester

LPS: Lipopolysaccharide

MAP: Mean arterial pressure

MMP2: Matrix metalloproteinase 2

MMP9: Matrix metalloproteinase 9

NAFLD: Non-alcoholic fatty liver disease

NO: Nitric Oxide

NOS: Nitric oxide synthase

PAS: Periodic acid-Schiff

PE: Phenylephedrine

PP: Portal pressure

PSS: Physiological Salt Solution

PSR: Picrosirius red

PTN: Portal hypertension

RAAS: Renin angiotensin aldosterone system

RBF: Renal blood flow

RI: Resistive index

RLN: Relaxin (Serelaxin)

RVR: Renal vascular resistance

RXFP: Relaxin family peptide receptors

SD: Sprague –Dawley rats

SC: Subcutaneous

SNP: Sodium nitroprusside

SNS: Sympathetic nervous system

TIPSS: Transjugular intrahepatic portal system shunt

TNFα: Tissue necrosis factor alpha

USS: Ultrasound

VEGF: Vascular endothelial growth factor

VTI: Velocity time integral

# Acknowledgements

I'd like to thank my supervisors Jonathan Fallowfield, John Iredale and Peter Hayes for their excellent support, advice and guidance throughout this work. It has been inspirational to work with them and their input, knowledge and enthusiasm has been invaluable. I'd also like to thank all the members of the Iredale and Forbes research groups with whom I enjoyed working with a lot and learnt a considerable amount from. Many thanks go to Antonella Pellicoro, for her kindness, help at every stage and great friendship.

Particular thanks go to Dr Paddy Hadoke for his invaluable input into this body of work and the excellent scientific guidance he has given me, it has been a privilege to work with him. I'd also like to thank Prof Stuart Forbes for all his support and guidance, both in research and clinically. Finally I would like to thank Will Mungall, without whom, the *in vivo* work would not be what it is.

This research was funded by the Wellcome Trust. I would like to thank my sponsor, Prof David Webb.

Finally, I would like to dedicate this thesis to my Mum and Dad, who are the most supportive parents I could ask for and from whom I have learnt more than anyone and to Chris Hook and Jama, for the time we had in Edinburgh.

# Abstract

**Introduction:** Hepatorenal syndrome (HRS) is a common complication of advanced cirrhosis with a high mortality rate and limited treatment options. Central to its pathogenesis is severe, but potentially reversible, renal vasoconstriction leading to functional renal failure. Current pharmacological treatment using splanchnic vasoconstrictors is suboptimal and prognosis without liver transplantation is dismal. The peptide hormone relaxin (RLN) mediates haemodynamic adaptations to pregnancy including increased renal blood flow (RBF) and glomerular filtration rate (GFR). I hypothesised that exogenous RLN could be used therapeutically to improve RBF and renal function in the context of experimental cirrhosis and HRS.

**Methods:** To address this I generated pathologically distinct rat models of liver cirrhosis with features of human HRS including renal vasoconstriction and renal failure. Compensated cirrhosis was induced in male rats by 16 weeks of i.p. carbon tetrachloride (CCl4) and decompensated cirrhosis by bile duct ligation (BDL). I studied the effects of acute i.v. or sustained (72 hr) s.c. infusion of RLN compared with vehicle on systemic haemodynamics, RBF, GFR and kidney histology. I used blood oxygen dependent-magnetic resonance imaging (BOLD-MRI) to detect changes in kidney parenchymal oxygenation and Doppler ultrasound to monitor changes in RBF (velocity time integral, VTI) and renal arterial resistance (resistive index, RI). Hepatic and renal expression of the relaxin receptor RXFP1 was determined by quantitative polymerase chain reaction (qPCR) and immunohistochemistry (IHC). Vascular functional responses in isolated renal arteries were assessed by wire myography. Relaxin mediated changes in key vaso-regulatory signalling pathways in the kidney and renal vessels were analysed by qPCR, IHC and ELISA.

**Results:** I showed using *in vitro* myography that the pathophysiological mechanism that underlies renal vasoconstriction in experimental cirrhosis models is an impairment of endothelium-dependent vasodilatation. Selective targeting of renal vasoconstriction using relaxin improved renal blood flow, tissue oxygenation, and normalized glomerular filtration rate in both compensated and decompensated rat cirrhosis. Furthermore, relaxin treatment restored endothelium-dependent vasodilation in isolated renal vessels from CCl4 cirrhotic rats. Relaxin-induced effects on renal blood flow and glomerular filtration rate were mediated though activation of the AKT/eNOS/nitric oxide signalling pathway in kidney, though systemic nitric oxide levels were unaffected. Crucially for human translation, relaxin did not reduce mean arterial blood pressure even in advanced cirrhosis.

**Conclusion:** My findings identify relaxin as the first potential targeted treatment reversing the vascular dysfunction which causes HRS and directly improving renal function in HRS. Clinical translation in carefully selected populations is warranted.

# Lay Summary of Thesis

THE UNIVERSITY of EDINBURGH

The lay summary is a brief summary intended to facilitate knowledge transfer and enhance accessibility, therefore the language used should be non-technical and suitable for a general audience. (See the Degree Regulations and Programmes of Study, General Postgraduate Degree Programme Regulations. These regulations are available via: http://www.drps.ed.ac.uk/.)

| | | | |
|---|---|---|---|
| Name of student: | Victoria Katherine Snowdon | UUN | S1066645 |
| University email: | vsnowdon@doctors.org.uk | | |
| Degree sought: | DOCTOR OF PHILOSOPHY | No. of words in the main text of thesis: | 42 000 |
| Title of thesis: | Relaxin as a Therapeutic Haemodynamic Modulator in Liver Disease | | |

Insert the lay summary text here - the space will expand as you type.


In this thesis, work supported by the Wellcome Trust, I investigated a hormone called Relaxin which is known to be responsible for the maternal adaptations to pregnancy including increasing blood supply to the kidney and improving kidney function. The reason this research was undertaken on this hormone is that there is a condition called hepatorenal syndrome, which is a very distinct complication of severe liver dysfunction, which is caused by a critical reduction in blood flow to the kidney leading to decreasing kidney function. Current therapy works in only 40% of patients and death rates from this condition near 80% unless they are able to receive a liver transplant. There is therefore a need for different therapies to try to reverse this condition.

I have used animal models of liver disease, in particular end stage liver disease termed cirrhosis, that mimic human disease to a good extent with reducing blood flow to kidney and decreasing function. When relaxin was given to these models the blood flow to the kidney acutely rose over 30-60 minutes. This has been shown in many ways including using different imaging modalities, ultrasound and MRI. The later measures changes in kidney oxygen levels and we observed that relaxin improved kidney oxygen levels. When relaxin is given over several days not only is the kidney blood supply increased to 60-75% of normal but kidney function was nearly restored. Importantly these effects seemed selective to the kidney and were not associated with any side effects such as a drop in blood pressure.

I have also found, in these models of cirrhosis, that the arteries that supply the kidney do not open up properly (termed vasodilatation) and this appears to be due to a problem with an important mediator of vasodilatation called nitric oxide synthase (NOS). NOS works by producing a substance that allow arteries to dilate and is produced in the inner lining of the artery, which is called the endothelium. Relaxin improves this problem by increasing NOS, allowing the artery to dilate normally.

Bringing all these results together I have shown that relaxin is a very promising therapy for hepatorenal syndrome. It is known to be safe in humans. We hope to study patients with hepatorenal syndrome in the near future.


**Document control**

| | |
|---|---|
| Related policies/regulations: www.docs.sasg.ed.ac.uk/AcademicServices/Regulations/PGR_AssessmentRegulations.pdf | |
| If you require this document in an alternative format please email Academic.Services@ed.ac.uk or telephone 0131 650 2138. | Date last reviewed: 15.05.15 |

# CHAPTER 1- INTRODUCTION

## 1.1 The Clinical Burden of chronic liver disease

Chronic liver disease results from a range of conditions including chronic alcohol excess, non-alcoholic fatty liver disease (NAFLD), chronic viral infection with Hepatitis B or C, parasitic worm infections and numerous immune mediated and metabolic conditions. The prevalence of chronic liver disease is rapidly increasing with 600 000 people having some form of liver disease in England and Wales, of whom 60 000 have cirrhosis. This represents an increase of 62% in liver disease and 40% in cirrhosis in 10 years (Williams, Aspinall et al. 2014). This is predominantly secondary to excess alcohol consumption, NAFLD with obesity and metabolic syndrome and viral hepatitis. Chronic liver injury eventually leads to cirrhosis, portal hypertension (PHT) and its complications. This has resulted in increasing hospital admissions with patients presenting with variceal bleeding, hepatic encephalopathy (HE), ascites, hepatorenal syndrome (HRS), hepatocellular cancer or liver failure requiring treatment. As a result mortality rates have increased 400% since 1970 and in people younger than 65 years has risen by almost five times. Compared to other systems, deaths from liver disease are currently rising (**Fig. 1.1**) and liver disease is now the 3rd commonest cause of premature mortality in the UK.

Although prevention and treatment of the causative agent is an important approach to reducing this burden, much of liver damage is asymptomatic resulting in patients presenting only when they develop cirrhosis and its complications. At which point there are limited therapeutic strategies and the only cure is, for a limited few, liver transplantation. Currently, the demand for organs far outweighs the supply and this will only worsen with the increasing problem. There is therefore a real need for novel therapies that can both reverse the fibrotic process but also treat the complications of cirrhosis and PHT to reduce the mortality and morbidity we are currently seeing and will see more of in the future.

In this thesis, I focus on one of the most important complications of cirrhosis, HRS. This functional kidney failure in the presence of advanced liver disease dramatically reduces life expectancy, presents a significant burden on the NHS with patients requiring prolonged hospital stay, occasional renal replacement therapy and potentially some patients may require a kidney transplant alongside their liver transplant. Importantly, post-transplant outcomes in patients with HRS are not as good as those without HRS (Marik, Wood et al. 2006). Integral to developing novel therapies is the need to fully understand the pathogenic mechanisms that result in this complication.

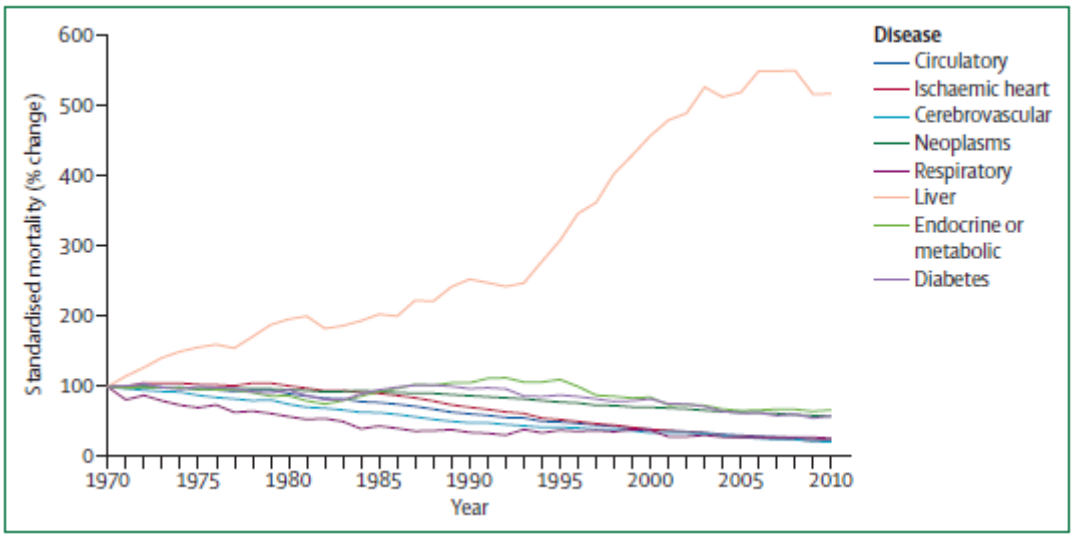


**Figure 1.1 Standardised UK Mortality Rate Data**

Graph showing increasing liver disease associated mortality since 1970 (Williams, Aspinall et al. 2014)

## 1.2 Cirrhosis

Cirrhosis is primarily a histological diagnosis characterised by loss of the normal lobular liver architecture with fibrotic septa separating abnormal nodules of regenerating hepatocytes. The normal liver is relatively free of fibrous tissue, however with chronic liver injury there is progressive accumulation of extracellular matrix proteins including collagen, which distorts the normal liver architecture by producing a scar (Bataller and Brenner 2005). The development of cirrhosis is normally an insidious process that takes 15-30 years, depending on the underlying liver injury. Different chronic liver diseases cause distinct patterns of fibrosis, however the development of cirrhosis represents the final common stage which then leads to similar clinical consequences (Pinzani, Rombouts et al. 2005). It has been shown from rodent models of cirrhosis, autoimmune hepatitis and viral hepatitis in humans that cirrhosis is dynamic and has the capacity to reverse to different degrees (Ramachandran and Iredale 2009; Snowdon and Fallowfield 2011). This evidence has subsequently challenged previous thinking that cirrhosis was a relentlessly progressive and irreversible process.

The idea that cirrhosis represents a single stage of disease is far too simplistic. Our current understanding is that the term cirrhosis represents a spectrum (**Fig 1.2**) of histological parameters (scar thickness and reversibility), clinical parameters (presence or absence of clinically significant PHT) and other complications (Garcia-Tsao, Friedman et al. 2010). Clinically, cirrhosis remains classified according to whether the patient is compensated or decompensated. This is done by the presence of clinically evident complications of cirrhosis, particularly those related to PHT or those secondary to liver failure (i.e. jaundice). However, this terminology should be challenged as the key to defining pathogenesis requires a better understanding of the different histological stages and

biological changes in relation to PHT and clinically evident complications. This would allow better prognostication and therapeutic targeting of 'high risk' cirrhotic populations.

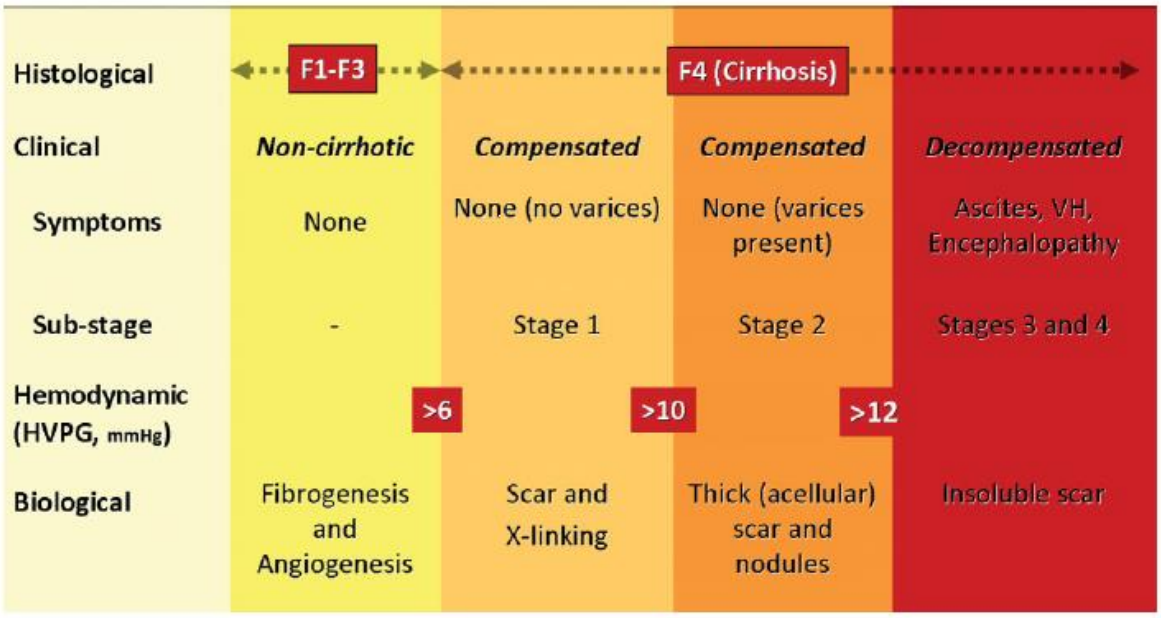


## Figure 1. 2 Classification of chronic liver disease

Classification of chronic liver disease based on histological, clinical, haemodynamic and biological parameters. Adapted from (Garcia-Tsao, Friedman et al. 2010)

## 1.3 Portal Hypertension

Portal hypertension (PHT) is the most important consequence of cirrhosis and is a major contributory factor for most of the morbidity and mortality associated with cirrhosis including variceal bleeding, ascites, HRS and HE (Bosch and Garcia-Pagan 2000). PHT is defined as an increase in the pressure within the portal vein and the current gold standard for measuring PHT and its severity is measurement of the hepatic venous pressure gradient (HVPG). The HVPG is measured invasively by measuring the difference between the wedged hepatic venous pressure (WHVP) and the free hepatic venous pressure (FHVP). A value of 3-5 mmHg is normal with a reading over 10 mmHg being a predictor of clinically significant PHT (de Franchis 2010).

The prognostic value of PHT measurement at different stages in the natural history of chronic liver disease has been well demonstrated, with robust cut-off values for the development of complications (HVPG>10 mmHg) and variceal rupture (HVPG>12 mmHg) (Groszmann, Garcia-Tsao et al. 2005; Ripoll, Groszmann et al. 2007). A reduction in HVPG below 12 mm Hg or by > 20% from baseline is associated with a significant reduction in complications and death. The importance of PHT is summarised in **Fig 1.3,** showing how changes in the HVPG have been shown to affect clinical outcomes.

| HVPG | Prognosis | Reference |
|---|---|---|
| **<10 mmHg** | Predicts patients with cirrhosis that do not decompensate (median 4 year follow up) | (Ripoll, Groszmann et al. 2007) |
| **>10 mm Hg** | Predicts the development of varices | (Groszmann, Garcia-Tsao et al. 2005) |
| **Reducing <12 mm Hg or >20 %** | Prevents re-bleeding (secondary prophylaxis) | (Villanueva, Balanzo et al. 1996) |
| **>20 mm Hg** | Predicts ITU stay, hospital stay, short term and long term mortality in acute variceal bleed | (Moitinho, Eskcorsell et al. 1999) |

## Figure 1.3 Importance of HVPG in Predicting Clinical Outcomes

Table showing the importance of hepatic venous wedge pressure gradient (HVPG) as a surrogate marker of portal hypertension (PHT) and the clinical relevance of its measurement. Adapted from (Snowdon, Guha et al. 2012).

In cirrhosis, PHT is initiated by an increase in intrahepatic vascular resistance (IHVR) and then exacerbated by changes in the systemic and splanchnic circulation that increase the portal inflow. Increased IHVR is caused by mechanical factors (e.g. fibrotic scars and regenerative nodules that distort the hepatic vascular architecture), but also by a reversible dynamic component mediated by an increase in vascular tone due to the active contraction of myofibroblasts around the hepatic sinusoids and in fibrous septa. This dynamic component (which accounts for ~30% of increased IHVR) reflects a functional disturbance of the liver circulation, secondary to increased production of vasoconstrictors (e.g. endothelin-1) and reduced release of endogenous vasodilators (mainly nitric oxide, NO) (Bhathal and Grossman 1985; de Franchis 2000; Rockey 2001; Iwakiri and Groszmann 2007). Decreased expression of endothelial NO synthase (eNOS) protein, decreased phosphorylation

of eNOS by the serine-threonine kinase AKT, the presence of inhibitory substances (e.g. asymmetric dimethylarginine, ADMA) and hypo responsiveness to NO have all been shown to contribute to this endothelial dysfunction (Rockey and Chung 1998; Laleman, Omasta et al. 2005; Iwakiri 2011). In contrast, extra-hepatic endothelial cells have the opposite phenotype producing excessive NO which contributes to splanchnic vasodilation, increased portal blood flow and an increase in PHT.

Angiogenesis has also been shown to influence PHT, with studies demonstrating that the maintenance of increased portal pressure, the hyperkinetic circulation, splanchnic neovascularization and porto-systemic collateralization are regulated by vascular endothelial growth factor (VEGF) and platelet derived growth factor (PDGF) (Fernandez, Mejias et al. 2007). By blocking VEGF and PDGF after development of PHT in rodents, portal pressure and mesenteric blood flow were significantly reduced with no effect on collaterals. In contrast, no anti-portal hypertensive effect was seen in models where PHT was developing, though there was reduced collateral formation.

Most of the research, to date, has focussed on PHT and variceal bleeding, as the latter is a clearly defined end-point whereas there has been less attention on its definitive role in the pathogenesis of the topic of my thesis, HRS. There is no doubt that this is likely to be due to the heterogeneity of this condition and subsequent difficulty in clear diagnosis limiting clinical studies. Although PHT is an important contributory factor, as evidenced by work showing that acutely blocking trans-jugular intrahepatic porto-systemic shunts (TIPSS) causes a robust reduction in renal blood flow (RBF) (Jalan, Forrest et al. 1997) and data showing that responders to treatment of PHT have a lower risk of development of HRS (Abraldes, Tarantino et al. 2003), what is not entirely clear is whether this condition can exist without PHT and more importantly, what the relative contribution of other abnormalities in the cirrhotic circulation is. Below I aim to summarise the current understanding of HRS pathogenesis.

### 1.4 Acute kidney injury (AKI) in cirrhosis

Acute kidney injury (AKI) is commonly seen in decompensated cirrhotic patients, occurring in approximately 20% of hospitalized individuals (Garcia-Tsao, Parikh et al. 2008). Not only does this confer a significantly increased mortality with a 7-fold increase in death and a 1 month mortality nearing 50% (Fede, D'Amico et al. 2012), but it is also a challenge to differentiate the underlying cause for AKI. This can be secondary to volume depletion from diuretics or paracentesis, or intrinsic kidney injury due to sepsis, shock or nephrotoxic drug therapy, or related to HRS (Hartleb and Gutkowski 2012). Conventional criteria for AKI in cirrhosis defined it as an increase in serum creatinine (sCr) over 50% to a final value of over 1.5mg/dL (133 µmmol/L). Recently this definition has been challenged owing to evidence from non-cirrhotics where smaller rises in creatinine were shown to have a detrimental effect on morbidity and mortality (Mehta, Kellum et al. 2007). Substantial work has been undertaken by the International Club of Ascites (ICA-AKI) to establish clear guidance in the cirrhotic population and the resultant definition of AKI is an increase in serum Creatinine (sCr) over 0.3 mg/dL (>26.5µmol/L) within 48 hours, or a percentage increase in sCr >50% from baseline which is known, or presumed, to have occurred within the prior 7 days (Angeli, Gines et al. 2015). Further classification of staging and baseline sCr is summarised in **Fig 1.4**.

| Subject | Definition | | |
|---|---|---|---|
| Baseline sCr | A value of sCr obtained in the previous 3 months, when available, can be used as baseline sCr. In patients with more than one value within the previous 3 months, the value closest to the admission time to the hospital should be used<br>In patients without a previous sCr value, the sCr on admission should be used as baseline | | |
| Definition of AKI | Increase in sCr ≥0.3 mg/dL (≥26.5 μmol/L) within 48 h; ora percentage increase sCr ≥50% from baseline which is known, or presumed, to have occurred within the prior 7 days | | |
| Staging of AKI | Stage 1: increase in sCr ≥0.3 mg/dL (26.5 μmol/L) or an increase in sCr ≥1.5-fold to twofold from baseline<br>Stage 2: increase in sCr >two to threefold from baseline<br>Stage 3: increase of sCr >threefold from baseline or sCr ≥4.0 mg/dL (353.6 μmol/L) with an acute increase ≥0.3 mg/dL (26.5 μmol/L) or initiation of renal replacement therapy | | |
| Progression of AKI | Progression<br>Progression of AKI to a higher stage and/or need for RRT | | Regression<br>Regression of AKI to a lower stage |
| Response to treatment | No response<br>No regression of AKI | Partial response<br>Regression of AKI stage with a reduction of sCr to ≥0.3 mg/dL (26.5 μmol/L) above the baseline value | Full response<br>Return of sCr to a value within 0.3 mg/dL (26.5 μmol/L) of the baseline value |

AKI, acute kidney injury; RRT, renal replacement therapy; sCr, serum creatinine.

**Figure 1.4 International Club of Ascites (ICA-AKI) new definitions for the diagnosis and management of AKI in patients with cirrhosis**

Table showing the new classification of acute kidney injury (AKI). Adapted from (Angeli, Gines et al. 2015)

### 1.5 Hepatorenal syndrome (HRS)

In the presence of cirrhosis and PHT or severe liver dysfunction there is a distinct form of renal failure that can develop, which has been termed HRS. It has been estimated that HRS develops in around 11 % of patients with cirrhosis and ascites (Planas, Montoliu et al. 2006) and the annual incidence of HRS is estimated at 18% by 1 year and 39% by 5 years (Gines, Escorsell et al. 1993). The frequency of HRS in severe acute alcoholic hepatitis and in fulminant liver failure is about 30% and 55%, respectively (Moore 1999; Verma, Ajudia et al. 2006) . HRS is a reversible form of acute or sub-acute renal failure traditionally described as 'functional' largely due to the absence of significant morphological changes in renal histology and largely preserved tubular function, with conservation of sodium and reduced urinary sodium levels. The evidence for functional renal failure stems from the observation that HRS resolves following liver transplantation (Iwatsuki, Popovtzer et

al. 1973) and from the fact that kidneys from patients with HRS function normally when they are transplanted into patients with end-stage renal failure (Koppel, Coburn et al. 1969).

### 1.6 Classification of HRS (past and present)

Historically, two types of HRS have been recognized and classified according to the intensity and form of presentation of renal dysfunction/AKI. Type 1 HRS is characterized by severe and rapidly progressive renal failure and is commonly precipitated by bacterial infections (such as spontaneous bacterial peritonitis). It has a median survival time of only 2 weeks (Arroyo, Guevara et al. 2002; Gines, Guevara et al. 2003). Type 2 HRS is characterized by a moderate and steady decrease in renal function, is usually associated with diuretic-resistant ascites, and carries a slightly better prognosis with a median survival time of about 6 months (Arroyo, Guevara et al. 2002; Gines, Guevara et al. 2003). **Fig 1.5** shows the impact of HRS on survival.

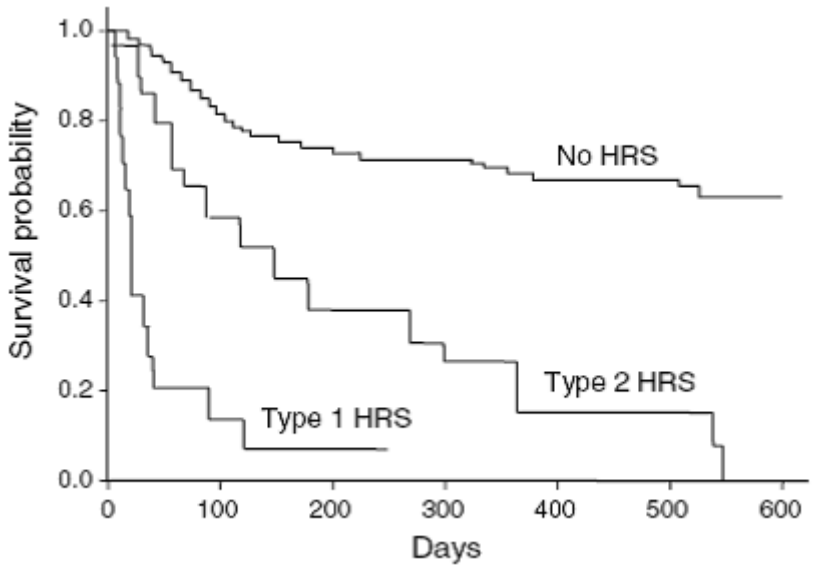

## Figure 1.5 Kaplan-Meier plot showing reduced survival in presence of Hepatorenal Syndrome

Graph highlighting the increased mortality in presence of HRS, with Type 1 HRS having a median survival of 2 weeks and Type 2 HRS having a median survival of 4-6 months. Adapted from (Arroyo, Terra et al. 2007).

The recent change in definition of AKI has led to a change in the definition of HRS-AKI updating the above, with the following criteria needing to be fulfilled to allow diagnosis. Adapted from (Angeli, Gines et al. 2015):

1. Diagnosis of cirrhosis and ascites
2. Diagnosis of AKI according to ICA-AKI criteria (**Fig 1.4**)
3. No response after 2 consecutive day of diuretic withdrawal and plasma volume expansion with albumins 1g/kg bodyweight
4. Absence of shock
5. No contrast or recent use of nephrotoxic drugs (NSAIDs, aminsoglycosides etc)
6. No macroscopic signs of structural kidney injury, as defined:
    a. Absence of proteinuria (>500 mg/day)
    b. Absence of micro haematuria (>550 RBC's per high power field)
    c. Normal findings on renal ultrasonography

### 1.7 Presumed Pathogenesis of HRS

At the centre of HRS pathogenesis is functional renal vasoconstriction as demonstrated by Epstein et al. (1970) using renal angiography in cirrhotic patients with renal failure showing profound

vasoconstriction of the renal vasculature associated with re-distribution of blood flow away from the cortex (**Fig 1.6**) (Epstein, Berk et al. 1970).

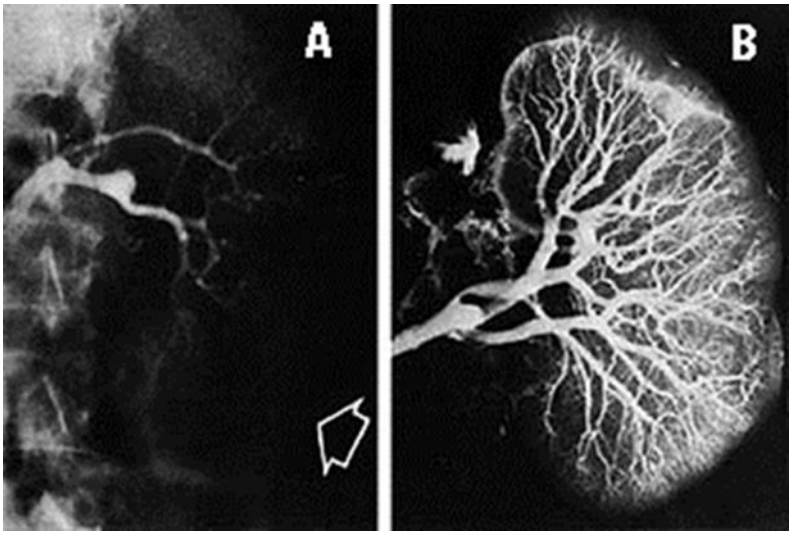


## Figure 1.6 Angiogram of the renal vasculature in a patient with cirrhosis and renal failure

Profound vasoconstriction is seen (A) and after death normal vasculature is seen (B) showing that this is not a structural phenomenon. Adapted from (Epstein, Berk et al. 1970)

This profound vasoconstriction is believed to be the hallmark of HRS (Platt, Ellis et al. 1994; Dagher and Moore 2001) . Renal blood flow in cirrhotic patients has been shown to diminish with increasing severity of liver disease and when this reaches a critical level of hypo-perfusion to the kidney, renal dysfunction and HRS develop (Ring-Larsen 1977).

The current paradigm for HRS pathogenesis is based upon the 'vasodilatation' hypothesis. Vasoconstriction occurs in response to splanchnic and peripheral arterial vasodilatation and impairment of cardiac function (cirrhotic cardiomyopathy) that lead to a reduction in effective

circulating volume and compensatory activation of the renin-angiotensin-aldosterone system (RAAS), sympathetic nervous system (SNS) and increased activity of antidiuretic hormone (Schrier, Arroyo et al. 1988; Krag, Bendtsen et al. 2010). As previously described in **section 1.3**, in PHT the splanchnic vascular bed is vasodilated thought mainly due to endothelial overproduction of NO and VEGF driven angiogenesis (Iwakiri and Groszmann 2007; Huang, Haq et al. 2011). Other vasodilators have also been implicated in this process such as prostacyclins, prostaglandins E2, atrial naturetic peptide (ANP) and kinins. As a result of splanchnic vasodilatation, there is activation of the SNS, RAAS and other vasoconstrictors as effective blood volume is perceived as low (Ring-Larsen, Hesse et al. 1982; Schrier, Arroyo et al. 1988). Renal vascular resistance correlates closely with the activity of the RAAS and SNS and so activation of these systems leads to renal vasoconstriction. HRS is thought to be associated with extreme stimulation of these pathways. Progression of these haemodynamic alterations in cirrhosis and an intra-renal imbalance between vasoconstrictor and vasodilator systems, results in renal blood flow becoming critically dependent on arterial blood pressure, with small changes in perfusion pressure translating into intense renal vasoconstriction and the precipitation of HRS (Stadlbauer, Wright et al. 2008). The plasma concentration of endothelin-1 (ET-1), a vasoconstrictor peptide of endothelial origin, is also increased in cirrhosis and has been proposed as an additional factor in the pathogenesis of HRS (Anand, Harry et al. 2002). Importantly, any process that increases splanchnic vasodilatation (infection, systemic vasodilators or paracentesis) or reduces vascular filling (diarrhoea, diuretics or bleeding) will precipitate this cycle (Belcher, Parikh et al. 2013).

Evidence for the above hypothesis is strong, as standard treatment for HRS aimed at improving mean arterial blood pressure (MAP) using intravascular volume expansion with human albumin solution (HAS) and splanchnic vasoconstrictors (octreotide or terlipressin) results in improved renal function in 40-50% of patients (Angeli, Volpin et al. 1999; Nazar, Pereira et al. 2010). Indeed, in patients that

demonstrated an improvement in serum creatinine there was a strong association with an increase in MAP (Velez and Nietert 2011). However, although HRS reversal significantly improved survival at day 180 and treatment with terlipressin and HAS significantly improved renal function and HRS versus HAS alone, treatment with terlipressin was not associated with improved overall survival (Sanyal, Boyer et al. 2008; Boyer, Sanyal et al. 2011). This was likely related to the significant presence of non-responders in the terlipressin arm. The proportion of patients who do not respond to vasoconstrictor treatment have a dreadful prognosis, with one study showing 100% mortality by 3 months (Moreau, Durand et al. 2002).

As a result of this, it has been more recently hypothesised that other pathogenic mechanisms are likely to be involved as well and that renal dysfunction in cirrhosis may be even more heterogeneous than previously thought. Pooling of blood in the splanchnic circulation (so-called 'splanchnic steal syndrome') likely alters gut permeability and induces bacterial translocation, with the release of endotoxin and various cytokines, which amplify the dysregulated circulation in cirrhosis priming the kidneys for further insults (Newby and Hayes 2002). Evidence for this comes from studies showing gut decontamination with prophylactic antibiotics (norfloxacin) reduced the incidence of renal dysfunction and improved survival (Fernandez, Navasa et al. 2007). This has also been shown in a rodent bile duct ligation (BDL) model of cirrhosis, with norfloxacin treatment reducing pro-inflammatory cytokines (TNFα) and Toll like receptor 4 (TLR) expression in the kidney (Shah, Dhar et al. 2012) . Further evidence for an inflammatory component comes from human studies showing an increased rate of renal dysfunction in cirrhotic patients with systemic inflammatory response syndrome (SIRS) (Thabut, Massard et al. 2007). More recent histological and biomarker studies report that tubular injuries are actually increased in the cirrhotic population, including patients with associated HRS, perhaps explaining why some individuals do not respond to circulatory support even when instigated early (Trawale, Paradis et al. 2010; Fagundes, Pepin et al. 2012). Additionally, a

recent study in cirrhotic patients highlighted the potential contribution of endothelial dysfunction in the development of renal vasoconstriction and renal failure (Garcia-Martinez, Noiret et al. 2014).

Overall, the pathogenesis of HRS remains to be fully elucidated. There is a school of thought that the sepsis/pro-inflammatory renal phenotype may not represent 'true' HRS but an alternative form of renal failure in cirrhosis (Adebayo, Morabito et al. 2015), but this remains unproven and the concept of non-responders may relate to the true possibility that indirectly targeting the renal circulation with albumins and splanchnic vasoconstrictors is insufficient to reverse HRS . All of this is summarised in **Fig 1.7**.

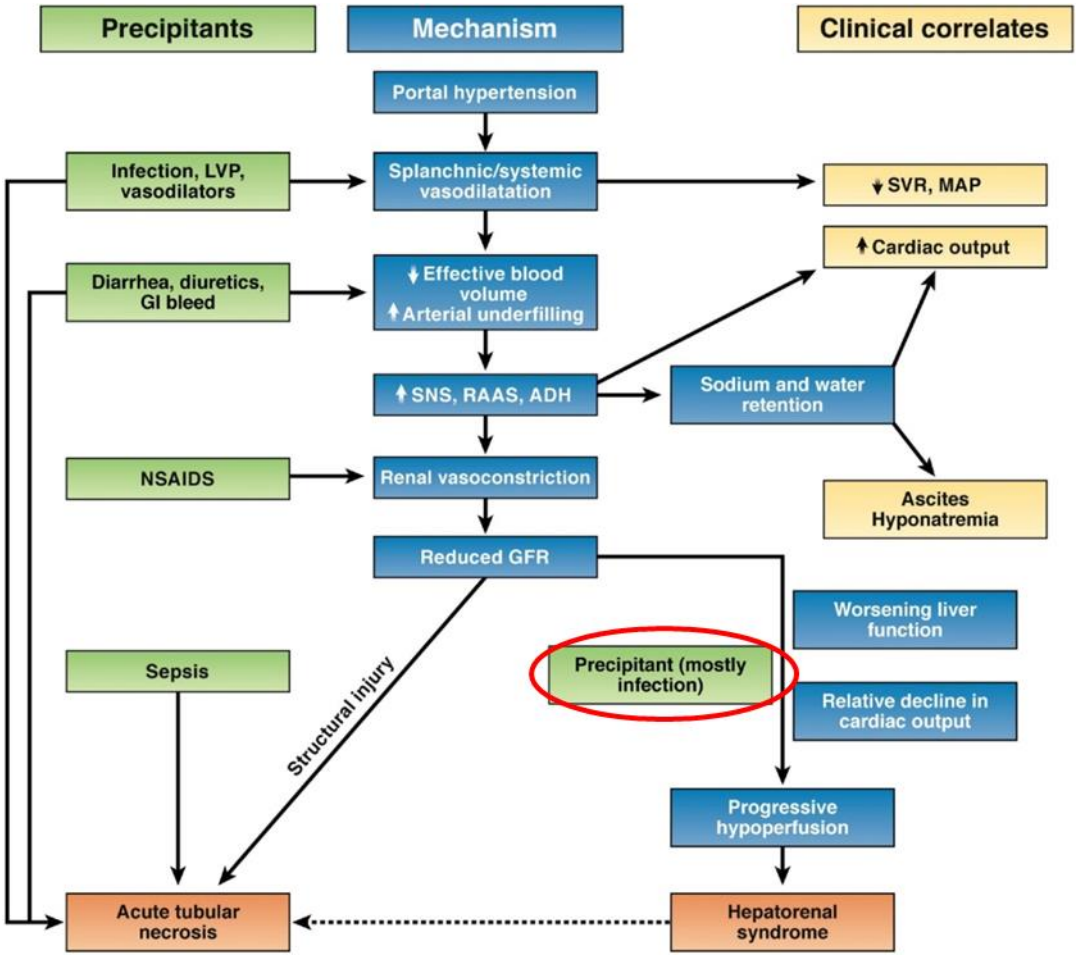

## Figure 1.7 Precipitants, Mechanisms and Clinical correlates of HRS and ATN in cirrhosis

Schematic showing proposed vasodilation hypothesis, adapted from (Belcher, Parikh et al. 2013) Portal hypertension leads to splanchnic and systemic vasodilatation with a decreased perceived effective arterial blood volume. This decrease stimulates activation of the SNS, RAAS, and ADH systems. The increased activity of these vasoconstrictor systems causes renal vasoconstriction and decreased renal perfusion. Any factor that worsens vasodilatation (infection, large volume paracentesis (LVP), vasodilators) or decreases blood volume (diarrhoea, diuretics, bleeding) can decrease renal perfusion further and lead to AKI. In advanced cirrhosis renal blood flow becomes dependent on the MAP and a decline in cardiac output leads to severe renal hypoperfusion and development of HRS. Alternatively, precipitants may be severe enough to produce structural tubular injury (e.g. septic or hypovolemic shock) and AKI. The extent to which prolonged severe HRS can progress to ATN remains unclear and is shown with a dotted line. GI, gastrointestinal; MAP, mean arterial pressure; NSAIDs, nonsteroidal anti-inflammatory drugs; SVR, systemic vascular resistance.

### 1.8 Current treatment of HRS

Current drug therapy for HRS is limited to splanchnic vasoconstrictors. Off label use of intravenous terlipressin (in combination with HAS (Sort, Navasa et al. 1999)) constitutes the treatment of choice for type-1 HRS in the UK, but this is only effective in around 40-50% of patients (Fabrizi, Dixit et al. 2006; Martin-Llahi, Pepin et al. 2008; Sanyal, Boyer et al. 2008; Nazar, Pereira et al. 2010), confers no long term survival advantage, and is associated with a significant increase in cardiovascular side effects (Krag, Moller et al. 2007; Krag, Moller et al. 2011; Gluud, Christensen et al. 2012). Liver transplantation is the optimal treatment for HRS, with the majority of patients recovering renal function. There is, however, a shortfall of donor organs and post-transplant outcomes are inferior compared to non-HRS cirrhotic patients (Gonwa, Morris et al. 1991; Marik, Wood et al. 2006). Additionally, insertion of a TIPSS may be effective in highly selected patients with preserved hepatic

function, where improvement in renal function and ascites and increased survival have been demonstrated in both Type 1 (Guevara, Gines et al. 1998) and 2 HRS (Brensing, Textor et al. 2000; Testino, Ferro et al. 2003). The issues that limit the widespread use of TIPSS are that it is only a viable option in patients with relatively well preserved hepatic function, without hepatic encephalopathy or cardiac impairment, and can only be performed in specialist centers (Salerno, Gerbes et al. 2007).

There is, therefore, an unmet clinical need for new and effective therapies to both treat and prevent AKI/HRS thus reducing mortality in patients with decompensated cirrhosis, and also to improving outcomes after liver transplantation for patients with AKI/HRS.

### 1.9 Relaxin

Relaxin (RLN), a 6kD endogenous peptide hormone (**Fig 1.8**), has been shown to have anti-fibrotic, anti-inflammatory and vasoactive effects in a range of tissues in normal and pathological situations (Samuel, Hewitson et al. 2007; Teichman, Unemori et al. 2009). RLN is secreted by the corpus luteum in females and has well described physiological effects in pregnancy, including remodeling and relaxation of the pelvic ligaments, cervical softening, and mediating the maternal haemodynamic and renovascular adaptations to pregnancy (Sherwood 2004; Conrad 2010). Three RLN genes are present in humans but only one gene product, human-2 (H2-) RLN, is detected in the circulation. H2-RLN circulates in women at low concentrations during the luteal phase of the menstrual cycle (~50 pg/mL) and at increased levels (~1 ng/mL) throughout pregnancy, beginning in the first trimester. Women with ovarian failure who have egg donation and subsequent pregnancy, or pregnant rats treated with RLN neutralizing antibodies, do not exhibit the renovascular adjustments

to the same degree (Novak, Danielson et al. 2001; Smith, Murdoch et al. 2006) suggesting its importance in modulating renovascular haemodynamics.

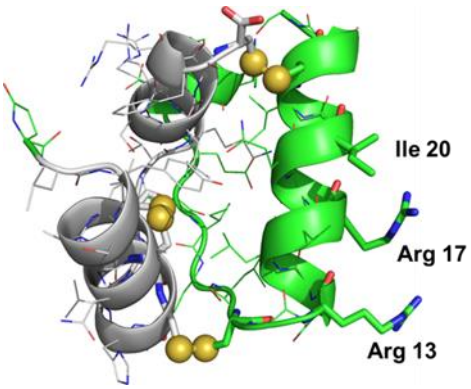


## Figure 1.8 Relaxin peptide

Schematic of RLN 6KDa peptide hormone-showing alpha (grey) and beta (green) chains with binding site/

### 1.10 LGR7/RXFP1

Relaxin's activity is initiated by binding to its cognate G-protein coupled receptor (GPCR), LGR7/RXFP1 (**Fig 1.9**). LGR7/RXFP1 is a member of the leucine-rich repeat containing family of GPCRs which include the relaxin family peptide receptors (RXFP). RXFP1 has been shown to be expressed in a wide range of organs including the renal and systemic vasculature in rodents and humans at the transcript and protein level (Hsu, Nakabayashi et al. 2002; Novak, Parry et al. 2006; Vodstrcil, Tare et al. 2012). The importance of RXFP1 in mediating the effects of RLN were shown in *Rxfp1* knockout mice, which exhibited a complete absence of vasodilation in response to RLN (Debrah 2008).

There is a paucity of data on the exact location of RXFP1 in the vasculature and in particular the renal vasculature. In rodents, RXFP1 has been localized to the small renal and mesenteric arteries and the thoracic aorta in both sexes (Novak, Parry et al. 2006). RXFP1 expression has been shown by RT-PCR and immunohistochemistry, to be greatest in vascular smooth muscle rather than in endothelium, although the relative contribution of receptors in each location in mediating the vasoactive effects of RLN is unknown (Conrad 2010). It has also been shown from myographic studies of isolated vessels that removal of the endothelium obliterates the vascular response to RLN, suggesting that the endothelium is critical, either through the presence of the receptor or through post-receptor signalling pathways (Novak, Ramirez et al. 2002).

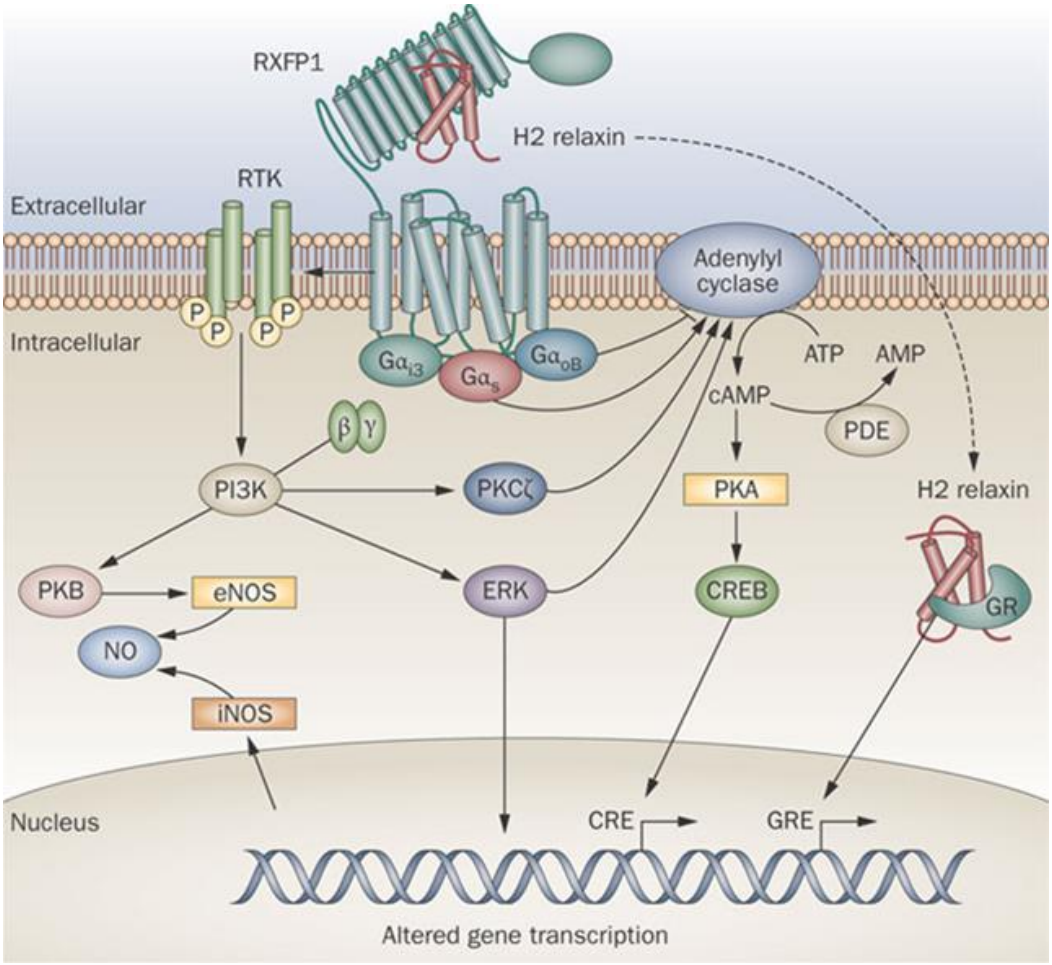


**Figure 1.9 Relaxin - RXFP1 axis**

Schematic of RXFP1 showing multiple possible pathways activated after H2-relaxin binds to its G protein coupled receptor. After binding to RXFP1 there is activation of adenylate cyclase, increasing cAMP and protein kinase A (PKA) with subsequent altered gene transcription or activation of PI3K with activation of endothelial nitric oxide synthase (eNOS) and ERK. Additionally RLN can bind directly to a glucocorticoid receptor (GR). Adapted from (Du, Bathgate et al. 2010).

### 1.11 Relaxin and renal haemodynamics

The haemodynamic changes modulated by RLN in the pregnant rodent include the following - in the systemic circulation: **↑ cardiac output (CO), ↓ systemic vascular resistance (SVR), ↑ global arterial compliance, with maintenance of the mean arterial pressure (MAP) ;** and in the renal circulation**:↓ renal vascular resistance (RVR), ↑ RBF, ↑ GFR, ↓ myogenic reactivity of small renal arteries and↓ vasoconstrictor response to angiotensin II**. Exogenous H2-RLN treatment in male and non-pregnant female rats recapitulated the haemodynamic profile associated with pregnancy (Danielson and Conrad 2003; Danielson, Welford et al. 2006). **Fig 1.10** summarises the experiments contributing to these conclusions. Systemic infusion of recombinant H2-RLN elicited a rapid increase in renal plasma flow, measured by para-aminohippurate, in healthy male and female human volunteers (Smith, Danielson et al. 2006). Additionally, a study in patients with mild scleroderma showed that long-term administration of RLN (for 6 months) resulted in a 15-20% increase in predicted creatinine clearance (Seibold, Korn et al. 2000). Finally, data from clinical studies in acute (Teerlink, Cotter et al. 2013) and chronic (Dschietzig, Teichman et al. 2009) heart failure showed that RLN treatment increased creatinine clearance and reduced serum creatinine, respectively. Importantly, in both preclinical and human studies augmentation of renal blood flow (RBF) by RLN was not accompanied by a significant reduction in systemic arterial blood pressure (Danielson and Conrad 2003; Danielson, Welford et al. 2006; Smith, Danielson et al. 2006).

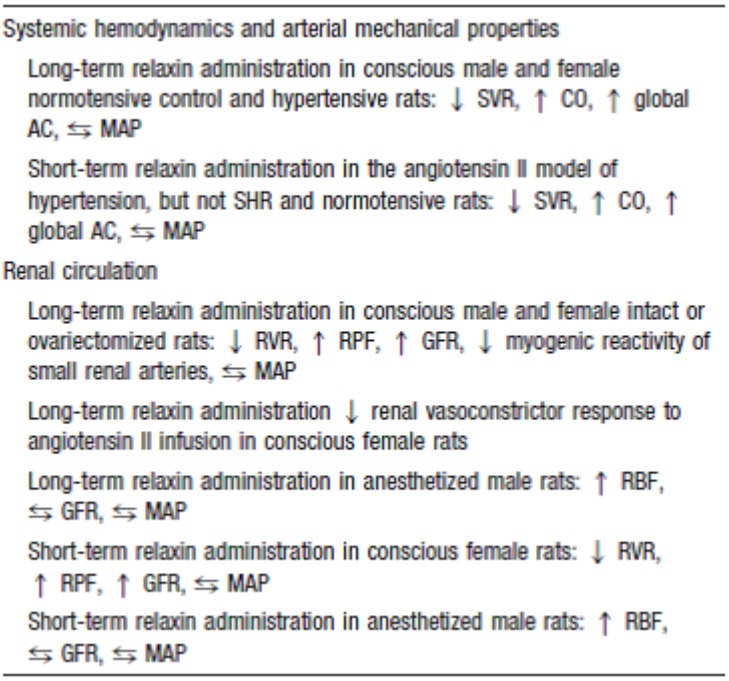


**Figure 1.10 Summary of *in vivo* experiments using exogenous RLN**

Summary of *in vivo* experiments using exogenous relaxin in short term (hours) and long term (days) and its effects on cardiac output (CO), systemic vascular resistance (SVR), global arterial compliance, mean arterial pressure (MAP), renal vascular resistance (RVR), renal blood flow (RBF), glomerular filtration rate (GFR), myogenic reactivity of small renal arteries and vasoconstrictor response to angiotensin II. Adapted from (Conrad 2010).

### 1.12 Proposed mechanisms for the haemodynamic role of relaxin

The molecular mechanisms that underpin the haemodynamic effects of RLN have not been fully defined. The duration of hormone exposure seems to be paramount, and both rapid and sustained vasodilatory responses to RLN have been shown (Fisher, MacLean et al. 2002; Jeyabalan, Novak et al. 2003; McGuane, Debrah et al. 2011). Mechanistic studies using specific inhibitor compounds suggest that RLN induces its sustained vasoactive effects indirectly through the endothelin type-B ($ET_B$) receptor and NO signalling pathway. Administration of a NO synthase (NOS) inhibitor or $ET_B$ antagonist inhibited the RLN mediated decrease in renal vascular resistance, with an associated

reduction in glomerular filtration rate (GFR) and RBF (Danielson, Sherwood et al. 1999). Furthermore, the inhibition of myogenic reactivity seen in renal arteries isolated from rats chronically treated with RLN was restored to control levels after treatment with a NOS inhibitor, $ET_B$ antagonist or removal of the endothelium (Novak, Ramirez et al. 2002). No evidence was found for RLN causing a direct increase in expression of $ET_B$. Further studies have suggested that sustained vasodilatory responses to relaxin are likely to be mediated by up-regulation of arterial gelatinases matrix metalloproteinase-2 (MMP2, MMP9), whereby gelatinase activity leads to processing of big ET to form $ET_{1-32}$ which subsequently activates the endothelial $ET_B$/NO vasodilatory pathway (Jeyabalan, Novak et al. 2003; Jeyabalan, Novak et al. 2007). Elegant studies performed by Jayabalan et al, using inhibitors to MMP2 and 9 *in vivo* and using isolated vessels from RLN treated rats, showed obliteration of the normal vasodilatory and myogenic response to RLN. Recent evidence has also suggested that angiogenic growth factors (e.g. VEGF) may also play a role (McGuane, Danielson et al. 2011). **Fig 1.11** highlights the proposed sustained RLN vasodilation pathway.

Further research is emerging that the effects of chronic administration of RLN (days to weeks) may also be exerted through collagen breakdown and increase in passive compliance of the vasculature. RLN is known to increase vascular collagen degradation through activation of MMPs and down-regulation of expression of tissue inhibitors of metalloproteinases (TIMPs). Administration of exogenous RLN to mice reduced the ratio of collagen to total protein in small renal arteries (Debrah, Debrah et al. 2011).

Very rapid vasodilatory responses to RLN (within minutes) have also been observed in isolated gluteal and subcutaneous human arteries and small rodent renal arteries. In culture, human endothelial cells briefly treated with RLN demonstrated G-protein coupling to PI3 kinase,

phosphorylation of Akt and endothelial NOS activation (Gαi/o-PI3K-AKT-eNOS mechanism) (Fisher, MacLean et al. 2002; McGuane, Debrah et al. 2011). The pathophysiological importance of RLN and RXFP1 signalling pathways in the kidney are completely unknown in the context of cirrhosis and AKI/HRS.

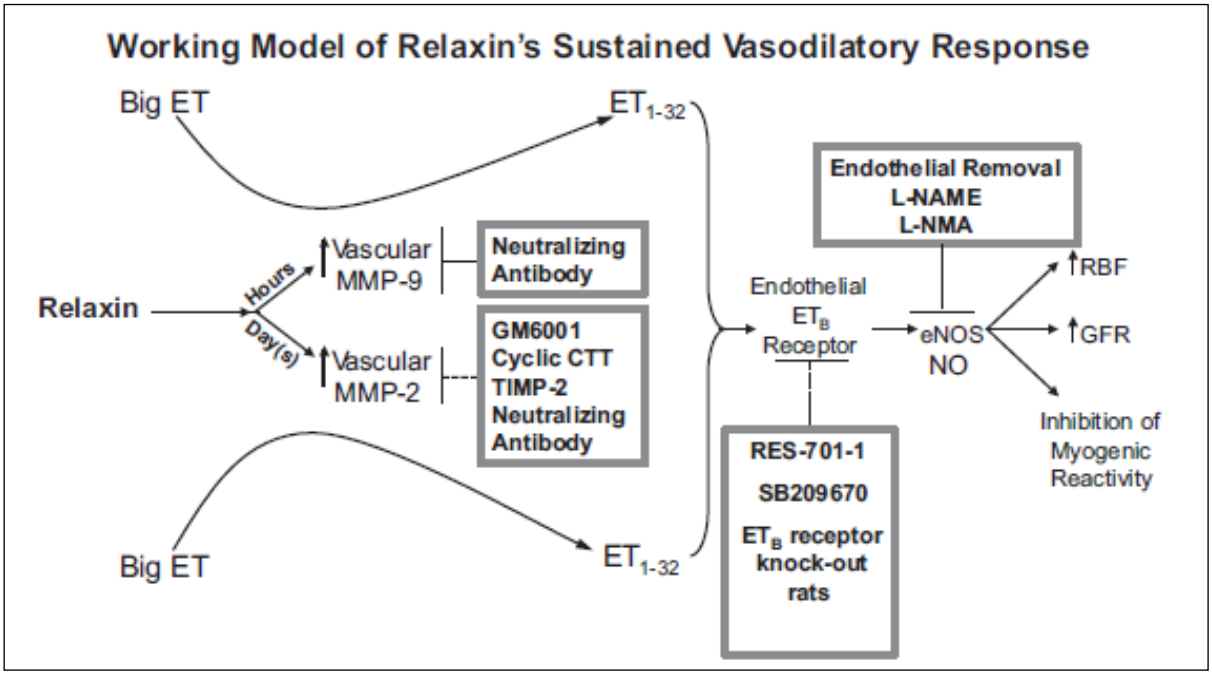


**Figure 1.11 Proposed mechanism for relaxin's sustained vasodilatory effects**

Schematic of the proposed mechanism of RLN's haemodynamic effects. RLN upregulates vascular Matrix metalloproteinase: MMP9 (hours) and MMP2 (days), which cleave Big Endothelin (ET) to $ET_{1-32}$ which bind to the Endothelial $ET_B$ receptor which activates eNOS, with subsequent release of NO to the smooth muscle relaxing vascular tone. Inhibition at any of these stages reduces/abrogates RLN's effects. (Conrad 2010).

### 1.13 Rationale for the use of relaxin in cirrhosis and HRS

RLN has been shown to have promising anti-fibrotic effects in rodent models of cirrhosis (Williams, Benyon et al. 2001) as well as with fibrosis in the lung (Huang, Gai et al. 2011), heart (Samuel 2005) and kidney (Chow, Kocan et al. 2014) . However, the haemodynamic (particularly renal) effects of RLN in cirrhosis have not been fully explored.

As discussed previously, central to HRS pathogenesis is profound renal vasoconstriction (Epstein, Berk et al. 1970). The fact that RLN has been shown to increase RBF and GFR *in vivo*, to reduce myogenic reactivity in isolated vessels *in vitro*, and to preferentially dilate pre-constricted vessels (so called 'anti-vasoconstrictor' effect) makes it a potentially useful therapeutic agent in HRS (Debrah, Conrad et al. 2005; Teichman, Unemori et al. 2009). Furthermore, RXFP1 has been shown to be expressed in the renal circulation, with rapid vasodilatory effects seen in isolated arteries suggesting that a targeted effect on the renal circulation is possible (Fisher, MacLean et al. 2002; McGuane, Debrah et al. 2011). This contrasts with current therapy for HRS which works indirectly through splanchnic vasoconstriction. Furthermore RLN has been shown to have anti-inflammatory effects suggesting that it may also have therapeutic benefit via other relevant mechanisms in the development of renal dysfunction in cirrhosis (Dschietzig, Brecht et al. 2012). Finally, in both pre-clinical studies and human trials with RLN, no significant drop in systemic blood pressure was observed, which is critical for the translation of RLN as a therapy in the cirrhosis/HRS population who may have a lower than normal MAP at baseline.

## 1.14 Hypothesis

Relaxin can modulate renal haemodynamic responses in experimental cirrhosis and be used to increase renal blood flow and improve renal function in HRS.

## 1.15 Aims and Objectives

The overall aim of this thesis is to answer the central research question 'Can the peptide hormone RLN, by virtue of its vasoactive effects, ameliorate renal vasoconstriction and improve renal function in the context of HRS?'

I will address this aim through achieving the following objectives:

- Establishing and characterising robust and reproducible models of cirrhosis with portal hypertension, renal vasoconstriction and renal dysfunction in rats
- Defining the renal haemodynamic effects of RLN in these models
- Evaluating non-invasive measures of RBF in these models
- Determining the expression profile of RXFP1 in the liver, kidney and vascular tissue in rats with cirrhosis and renal dysfunction
- Investigating the downstream signalling pathways activated by RLN in the renal vasculature in experimental models of cirrhosis and renal dysfunction
- Elucidating the pathogenic mechanisms that underpin renal dysfunction in experimental cirrhosis and renal dysfunction

# CHAPTER 2-MATERIALS AND METHODS

## 2.1 Animals

Male Sprague-Dawley rats were used for all the experiments presented in this thesis and were purchased by the University of Edinburgh and bred under specific pathogen free conditions. All procedures involving animals were conducted with approval from the University of Edinburgh Animal Welfare and Ethical Review Body and UK Home Office and in accordance with the Use of Animals in Scientific Procedures Act 1986.

## 2.2 Human tissue

Human tissue was used in accordance with the Human Tissue (Scotland) Act 2006. Non lesional human kidney from nephrectomies was acquired through the Scottish Academic Health Sciences Collaboration (SAHSC) Annotated Human BioResource, ethical research committee reference 10/S1402/33.

## 2.3 Relaxin (Serelaxin)

The investigational product serelaxin has been manufactured using both recombinant and synthetic processes and is identical in structure to the naturally occurring H2-RLN. Serelaxin was kindly provided by Dennis Stewart of Corthera, Inc. (a Novartis company).

## 2.4 Experimental design

All *in vivo* experiments were designed and implemented according to the NC3R ARRIVE guidelines. A sample size of ≥5 rats per group was determined prospectively using the statistical power analysis

tool G*Power Version 3.1.2 (Faul, Erdfelder et al. 2007) to perform a power calculation given $\alpha$=0.05, power (1-$\beta$)=0.9, effect size (d)=2.64 based on preliminary experiments. Cage mates were randomized to treatment (serelaxin) and vehicle groups. Clinically relevant hemodynamic endpoints (portal pressure, RBF, GFR) were analyzed by reference standard invasive methods, in addition to non-invasive measures. All surviving rats at the designated endpoints were included in the data analyses. No animals or potential outliers were excluded from the data sets presented. All biochemical and histological assessments were performed in a blinded manner.

### 2.5 Rat carbon tetrachloride ($CCl_4$) model

Cirrhosis and portal hypertension was induced in 6-8 week old Sprague-Dawley rats by up to 16 weeks administration of $CCl_4$ through twice-weekly intraperitoneal (i.p.) injection (Sigma-Aldrich, UK). A dose of 0.1mL/100g for the first 2 weeks and then 0.05mL/100g, thereafter, diluted 1:1 in olive oil (Sigma-Aldrich, UK) making a total of volume of 0.2mL/100g for the first 2 weeks and thereafter 0.1mL/100g. A subset of rats was given twice-weekly i.p. injections of olive oil vehicle for 16 weeks to serve as a control group. To characterize this model after 8, 12 and 16 weeks of $CCl_4$ or olive oil (24 hrs following the final injection) subgroups of anesthetized rats (*n*=6-8) underwent hemodynamic monitoring without recovery.

### 2.6 Rat bile duct ligation (BDL) model

Biliary cirrhosis and portal hypertension was induced in 6-8 week Sprague-Dawley rats by BDL under isoflurane anaesthesia. A 1cm upper midline incision was made, the common bile duct was

exposed and tied three times with 7-0 silk then ligated, leaving two proximal sutures to the ligation and one distal suture. The abdominal muscle was closed with 5-0 silk and the skin was closed using subcuticular 3-0 silk sutures. Rats were given 0.01mL/100g of Buprenorphine analgesia intra-operatively along with 5mL of subcutaneous (s.c.) 0.9% normal saline (NaCl), both of which were repeated at 12 hr intervals for the first 2 days of the post-operative period if needed based on pain and dehydration scoring systems. Cage mates were randomly allocated to either BDL or sham procedure (controls), where the common bile duct was exposed but not ligated. To characterize this model subgroups of rats underwent haemodynamic monitoring at 14, 21 and 28 days post BDL and 28 days post sham procedure.

**2.7 Haemodynamic measurements**

Haemodynamic monitoring was performed using aseptic technique in rats anesthetized with Inactin (Sigma-Aldrich) 0.1mL/100g (125mg/mL) unless specified. A tracheostomy was performed to allow secretions to be aspirated and a right internal jugular vein was cannulated with PE50 tubing (Smiths Medical, UK). 0.9% NaCl, pre-warmed to 37$^{o}$C was instilled at a rate of 0.05mL/100g/mins throughout surgery and then 0.03mL/100g/mins during stabilization and monitoring (Menzies, Unwin et al. 2013). To determine the GFR rats received 5% inulin-FITC (Sigma-Aldrich) instead of 0.9% NaCl at the same rate as above. Core body temperature was measured by rectal probe and maintained at 37$^{o}$C using a heat mat. Mean arterial pressure (MAP) and heart rate (HR) were measured via a pre-heparinized (heparin 100U/mL in 0.9% NaCl) right femoral artery PE50 catheter (Smiths Medical). Portal pressure was measured using a 24G cannula inserted into the portal vein, and RBF was measured using a perivascular flow probe (MA2PSB, Transonic systems, ADInstruments, UK) sited around the left renal artery proximal to the bifurcation, all connected to a

Powerlab 4/35 system and analyzed using LabChart 7 Pro software (ADInstruments). The urinary bladder was catheterized with PE90 tubing (Smiths Medical) and secured with a purse-string suture. All rats were stabilized for 20 mins prior to starting data recording, based on observations of fluctuations in haemodynamic parameters immediately following surgery. Urine and blood collections were performed for calculation of GFR as described in **section 2.25**. At the end of the experiment blood was collected, tissues were weighed and then either fixed in 10% buffered formalin or methyl Carnoy's solution or snap frozen.

### 2.8 Acute serelaxin *in vivo* hemodynamic study

Groups of control rats (*n*=10) or 16 week $CCl_4$ rats (*n*=14) were randomly allocated to treatment with serelaxin (4µg in 200µL i.v.) or equivalent volume of vehicle (24 hrs following the final injection of $CCl_4$ or vehicle), then anesthetized for continuous hemodynamic monitoring over 60 mins, as described above.

### 2.9 Acute serelaxin *in vivo* ultrasound study

After determining the feasibility of this non-invasive imaging modality in a small pilot study in normal rats with regards to signal obtained and optimal monitoring conditions, groups of 16 week $CCl_4$ rats (*n*=16) were randomized to treatment with serelaxin (4µg in 1.5mL i.v.) or equivalent volume of vehicle (24 hrs following the final injection of $CCl_4$) prior to ultrasound assessment. A group of olive oil control rats (*n*=6) were scanned first to acquire baseline non-cirrhotic data. All rats were anaesthetized using 1.5-2% isoflurane in oxygen-enriched air (0.5L/mins air and 0.5L/mins

oxygen) for ultrasound assessment (Vevo 770, Visualsonics). Animals were placed in a supine position on a heated table (Visualsonics, Fujifilm), then cannulated via tail vein using a 24G cannula attached to pre-heparinized catheter tubing (Vygon, UK). Heart rate was monitored continuously using an electrocardiogram (ECG), core body temperature maintained at 37$^{o}$C using a heated table and a heat lamp as required. The chest and abdominal regions were shaved and remaining hair removed with depilatory cream. Parasternal, long-axis B-mode and M-mode images were taken of the heart at the level of the papillary muscle for quantitative assessment of cardiac function at baseline and at 60 mins post injection of serelaxin or vehicle. Parameters calculated included stroke volume (SV), cardiac output (CO) and ejection fraction (EF). A short-axis image of the right kidney was then obtained and, using pulse-wave Doppler, measurements of RBF were taken from the superior branch of the renal artery distal to the point of renal artery bifurcation at the hilum. Measurement of Doppler blood flow was taken at baseline and every 10 mins for 60 mins after serelaxin or vehicle injection. The renal parameters calculated from the Doppler trace included velocity time integral (**Fig 2.1**) and peak Pourcelot resistance index (**Fig 2.2**).

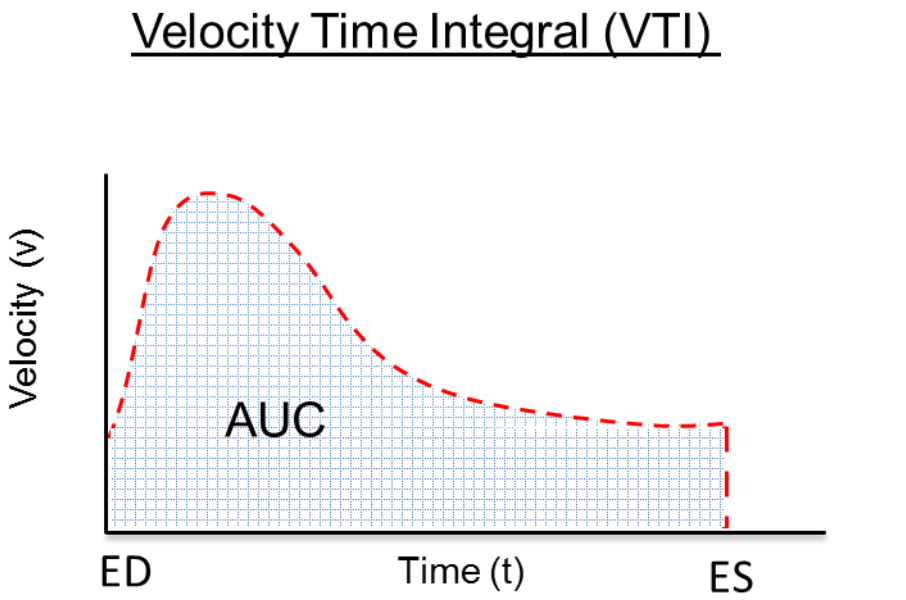


**Figure 2. 1 Velocity Time Integral Measurement**

The area under the curve/Doppler wave form is the velocity time integral (VTI) and represents, in our models, the amount of blood passing through the superior branch of the renal artery distal to the bifurcation. Three measurements, each of 3 cycles, were taken at each time point and averaged.

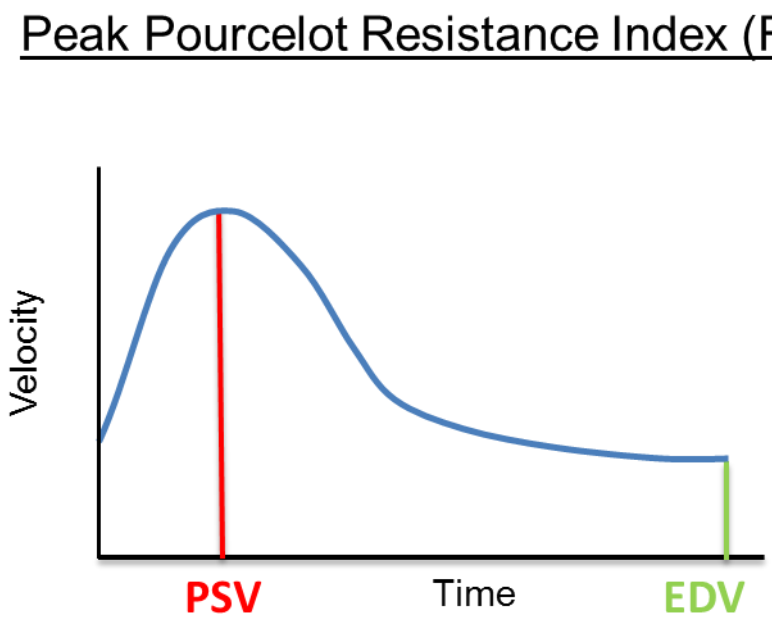


$$\text{Peak Pourcelot Resistance Index (RI)} = \frac{Peak\ systolic\ velocity - End\ Diastolic\ Velocity}{Peak\ systolic\ velocity}$$

**Figure 2. 2 Peak Pourcelot Resistance Index Measurement**

Schematic of how the Peak Pourcelot Resistance Index is calculated. The RI is calculated as shown in the equation above. 3 measurements were taken at each time point and averaged.

### 2.10 Acute serelaxin BOLD MRI study

Measurements were performed using a 7 Tesla preclinical MRI scanner (Agilent Technologies). Control (*n*=10), 8 week $CCl_4$ (*n*=16) and 16 week $CCl_4$ rats (*n*=12) were randomized to treatment with serelaxin (4µg in 1.5mL i.v.) or equivalent volume of vehicle (24 hrs after the final injection of $CCl_4$) then anesthetized with 1.5-2% isoflurane in oxygen-enriched air (0.5L/mins air and 0.5L/mins oxygen). The tail vein was cannulated using a 24G cannula attached to pre-heparinized catheter (Vygon, UK). Rectal temperature was maintained at 37°C, and respiration rate was monitored throughout the scanning protocol. A birdcage volume coil (72-mm diameter) and a 4-channel phased

array surface coil (Rapid Biomedical) were used for radio frequency transmission and signal reception, respectively. BOLD image acquisition used a multiple echo gradient-recalled MRI pulse sequence of ten images weighted in T2*; TE = 4, 8, 12, 16, 20, 24, 28, 32, 36, and 40 ms; TR = 100 ms and flip angle of 30°. An axial slice through the center of the right kidney was selected with 50×40 mm field of view containing a 192×128 acquisition matrix (in-plane resolution = 0.26×0.31 mm). A single axial slice, aligned parallel with the renal artery identified by rapid scout scanning (fast gradient echo, 3 slices in coronal orientation), ensured slice position encompassed the most representative section of the kidney regions. Slice thickness was 2 mm with 14 signal averages. The scan time was 3 mins for each BOLD scan. Three baseline scan were performed and then scans were performed every 3 mins for 60 mins after serelaxin or vehicle injection, with 30 and 60 mins being chosen as analysis points. T2* maps were generated using the scanner software.

Regions of interest (ROI) (**Fig 2.3**) were selected on the T2* maps using ImageJ (NIH, USA) in the kidney cortex and medulla, avoiding regions containing large vessels. The same regions were selected in all animals and all conditions. ROIs were drawn on baseline and subsequent images acquired after treatment to determine the signal intensity of each ROI. T2* values were converted to R2* (1/T2*), where R2* equates to the level of deoxygenated haemoglobin.

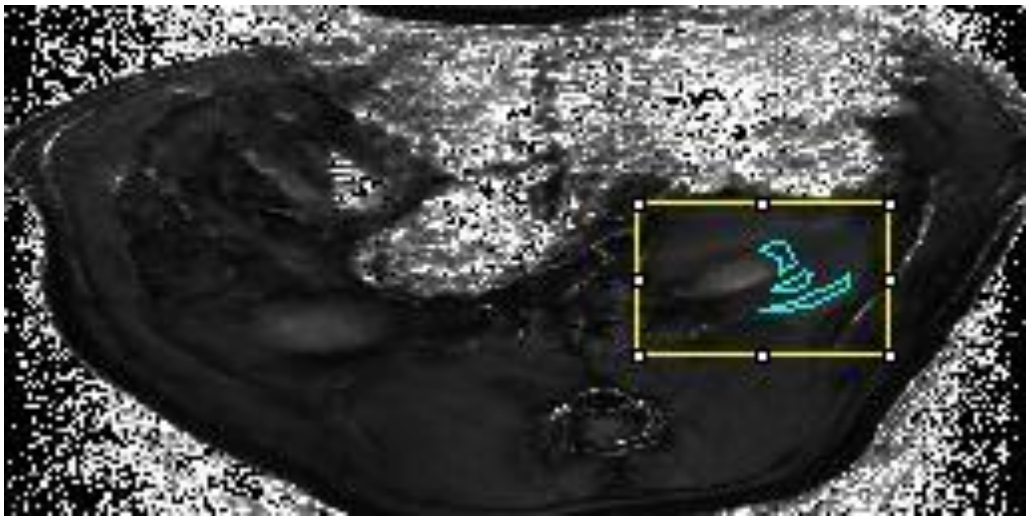

## Figure 2.3 BOLD image of kidney

Example of images obtained through kidney with regions of interest (ROI) shown (cortex, outer and inner medulla).

### 2.11 Acute nitrovasodilator *in vivo* hemodynamic study

To establish the effect of a non-selective vasodilator on MAP and RBF in cirrhosis I chose to use sodium nitroprusside (SNP). SNP is an endothelium independent vasodilator and works through release of NO and has been shown when instilled directly into the hind limb to increase hind limb blood flow at 0.09 and 0.9µg doses (Robertson, Gray et al. 2012). To establish the effect of this drug systemically a groups of 16 week $CCl_4$ rats (*n*=6), 24hrs following the final injection of $CCl_4$ were anesthetized and treated with a range of doses of sodium nitroprusside (SNP; 0.09, 0.9 and 9µg in 200µL i.v.; Sigma Aldrich) or an equivalent volume of vehicle. Between each dose MAP and RBF was allowed to return to baseline. Continuous hemodynamic monitoring was undertaken for 10 mins after each dose, as described above.

### 2.12 Sustained (72hr) serelaxin in vivo hemodynamic study

Both 16 week $CCl_4$ (*n*=16) and 21 day post BDL (*n*=14) rats were randomized to receive continuous treatment for 72 hrs with either serelaxin (4µg/hr) or vehicle via s.c. osmotic minipumps (2ML1 Alzet; Durect, USA). I chose 72 hrs as this is around the time-point in humans when response to current pharmacological therapy is assessed making it a suitable time-point to assess response to RLN (Salerno, Gerbes et al. 2007). Secondly I wanted a time-point that allowed the rats time to recover from insertion of the minipump. Finally, in non-cirrhotic rats sustained infusion of RLN for

24 hours to as long as 5 days have been shown to have effects on RBF and GFR so I chose a mid-point (Danielson and Conrad 2003) .

Groups of $CCl_4$ rats (*n*=12) were also randomly allocated to treatment with serelaxin or vehicle plus co-administration of L-NAME (Sigma-Aldrich) 250 mg/mL in drinking water, starting 24 hrs before osmotic minipump insertion and continuing for the 72 hrs study period. After 72 hrs rats had hemodynamic and renal functional measurements performed under terminal anesthesia using isoflurane anaesthetic and monitored as described above.

**2.13 Wire myography studies**

Wire myography was performed on isolated blood vessels. Groups of rats (normal uninjured *n= 6,* Sham BDL *n=8* , 28 day BDL *n=8*, 16 weeks *n=12,* olive oil *n*=8 and 16 weeks $CCl_4$ + 72 h serelaxin or vehicle n=14) were killed by cervical dislocation and vessels (mesenteric, extra-renal and intra-renal renal arteries-segmental, interlobar and arcuate) were harvested and placed in 4$^oC$ physiological salt solution (PSS) freshly prepared as follows: NaCl 119mM, KCl 4.7mM, $CaCl_2$ 2.5mM, $MgSO_4$ 1.17mM,$NaHCO_3$ 25mM, $KH_2PO_4$ 1.18mM, ethylenediaminetetra-acetic acid di-potassium salt ($K_2$EDTA) 0.026mM and D-glucose 5.5mM and used the same day. Second order mesenteric arteries and the extra-renal, segmental and inter-lobar and arcuate renal arteries were dissected and cleaned of connective tissue. 2mm rings were mounted from each vessel segment onto 40 µm stainless steel wires, one end of which was attached to a force transducer and the other to a micrometer (**Fig 2.4A-B**). The vessel ring was bathed in PSS at 37$^oC$, bubbled with 95% $O_2$ and 5% $CO_2$ and stepwise radial stretching was performed to determine the lumen diameter necessary for optimal force generation. Vessel rings were then stretched to achieve 90% of the diameter expected

if it had been fully relaxed and exposed to a transmural pressure of 13.3 kPa (100 mmHg). The vessel ring was allowed to equilibrate for 30 mins before viability was assessed using three stimulations with a high potassium physiological salt solution( KPSS, 125 mM, made by equimolar substitution of KCl for NaCl in PSS), activated for 2 mins with each solution followed by a 5 mins washout period in PSS to allow full relaxation. Measurement of viability was performed in these vessels to confirm that isolation and mounting of the vessel did not damage the arterial wall. Isolated rings had their endothelium denuded by insertion of a wire into the lumen and the endothelium rubbed circumferentially. The ability of the vessel to respond to contractile and relaxant agents was investigated by producing concentration-response curves (CRCs). CRCs were obtained for phenylephedrine (PE; $1x10^{-9}$-$3x10^{-5}$ M, Sigma-Aldrich), and a concentration that produced 70-80% maximum contraction ($EC_{80}$) was chosen for each individual rat vessel ring. Following contraction, CRCs were obtained to the endothelium-dependent vasodilator acetylcholine (ACh; $1x10^{-9}$-$3x10^{-5}$ M, Sigma-Aldrich, UK) and the endothelium-independent vasodilator SNP ($1x10^{-9}$-$3x10^{-5}$ M, Sigma-Aldrich). To establish the endothelial mechanisms responsible for vasodilation in the renal circulation a group of normal and $CCl_4$ (n=6/group) vessel rings were co-treated for 45 mins with the NOS inhibitor L-NAME ($1x10^{-4}$ M), cyclo-oxygenase inhibitor indomethacin ($1x10^{-5}$M) or the endothelium derived hyperpolarising factor (EDHF) inhibitors apamin ($1x10^{-4}$ M) and charybdotoxin ($1x10^{-5}$M) and further CRC produced to ACh and SNP.

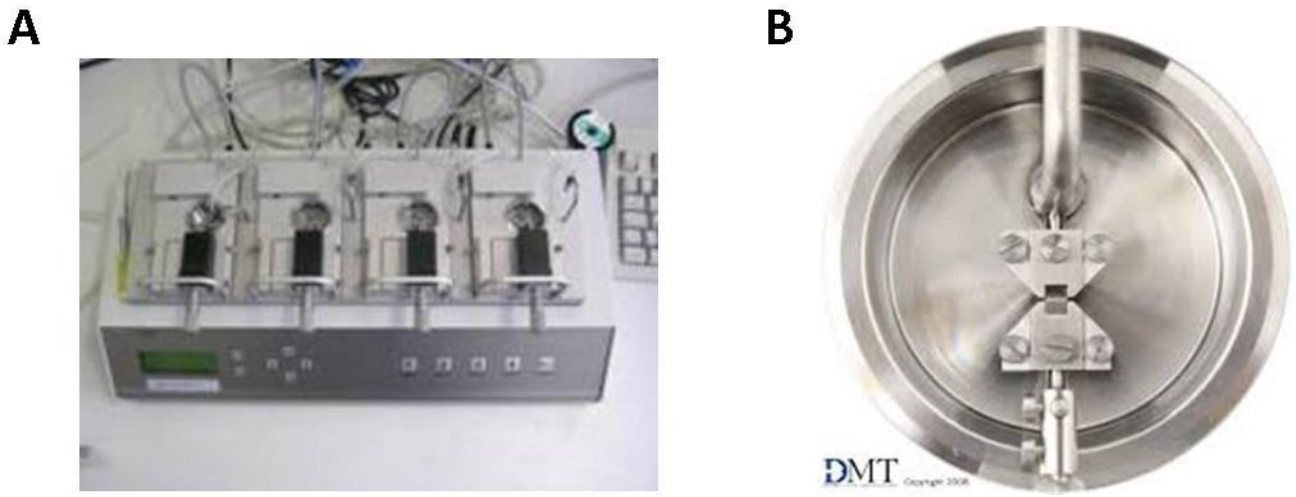


## Figure 2.4 Wire Myography

Photograph of wire myography. (A) showing the water baths and connections, (B) the individual water bath with a vessel on the wire.

### 2.14 Immunohistochemistry

Following harvest, liver tissue was fixed overnight in 10% neutral buffered formalin (Sigma) or methyl Carnoy's (60% Methanol: 30% Chloroform: 10% Glacial Acetic acid) solution, followed by paraffin embedding. Detection of selected proteins was undertaken in 3µm formalin fixed tissue sections, unless otherwise stated, using either standard avidin-biotin staining or single and dual immunofluorescence staining methods. Sections were dewaxed and rehydrated in decreasing concentrations of ethanol (100%, 75%, 65%) . Unless stated, antigen retrieval was performed by boiling for 15 mins in 10mM Sodium Citrate buffer, pH6.

Following the above, endogenous peroxidise activity was inhibited with 3% hydrogen peroxide followed by avidin/biotin block (Vector Labs) and then non-specific binding minimised using appropriate serum block. All primary antibodies were incubated overnight at 4$^{o}$C in species

appropriate serum. For control sections no primary antibody was added. Species appropriate anti-IgG biotinylated secondary antibodies (Vector) were used at 1/400 dilution, at room temperature for 1 hr. Immunostaining was developed using 3,3'-diaminobenzidine (DAB; Dako, UK). Picrosirius red and haematoxylin and eosin staining were performed according to standard performed by the histology department staff. Antibodies used in immunohistochemistry are shown in **Table 2.1.**

| Antibody | Dilution | Antigen retrieval |
|---|---|---|
| **Arginase II H64 (Santa Cruz, USA, 20151)** | 1:200 | 15 mins |
| **Relaxin receptor 1 H160 (Santa Cruz, USA, 50328)** | 1:50 | 20 mins |
| **LGR7 (735-757) (Human) Antibody Phoenix Pharmaceuticals** | 1:200 | 15 mins |

## Table 2.1 Antibiotics used in Immunohistochemistry

Antibodies with their dilution and necessary antigen retrieval condition used in immunohistochemistry.

### 2.15 Single Immunofluorescence

For single immunofluorescence initial preparation of sections was as above including blocking endogenous hydrogen peroxide however non-specific binding was minimised using protein block (DAKO) and the primary antibody was incubated overnight at 4$^{o}$C in antibody diluent (DAKO). Control sections had no primary antibody added. Goat anti-rabbit HRP (**Vector**, 1:500) was then

added to sections for 30 mins at room temperature and TSAT Plus Cyanine 3 System (PerkinElmer NEL744B001KT) applied to amplify the signal for 10 mins at room temperature. All sections were then blocked with 0.1% Sudan Black B (Sigma) and mounted with Dapi (4', 6'-diamidino-2-phenylindole) hard set mounting medium (Vector Labs H1500). All antibodies used in immunofluorescence are shown in **Table 2.2.**

| Antibody | Dilution | Antigen retrieval |
|---|---|---|
| **Arginase II H64 (Santa Cruz, USA, 20151)** | 1:200 | 15 mins |
| **PDGFβ (Abcam; ab32570)** | 1:100 | 15 mins |
| **Caveolin I (Cell Signaling, #3238)** | 1:125 | 10 mins |
| **anti-endothelial cell (RECA-1) (Abcam, UK; ab9774)** | 1:25 | 10 mins |
| **anti-CD31 (Abcam; ab28364)** | 1:100 | 10 mins |
| **Relaxin receptor 1 H160 (Santa Cruz, USA; 50328)** | 1:50 | 15 mins |
| **Anti-GPCR LGR7 antibody - C-terminal(Abcam; ab140903)** | 12µg/mL | 10 mins |
| **Anti-Actin, alpha smooth muscle (Sigma-Aldrich)** | 1:500 | 5 mins |
| **Wilms Tumor 1 antibody (GTX15249, GeneTex, USA)** | 1:100 | 15 mins (TRIS EDTA) |

## Table 2.2 Antibodies used in Immunofluorescence

Antibodies with their dilutions and necessary antigen retrieval condition used in immunofluorescence.

## 2.16 Dual Immunofluorescence

To co-localise the cellular origin of the RXFP1 receptor dual immunofluorescence was undertaken. Sections were dewaxed and rehydrated with decreasing concentrations of ethanol. Antigen retrieval was undertaken as stated above, endogenous peroxidise activity was inhibited with 3% hydrogen peroxide peroxidase and primary antibodies PDGFβ or RECA or CD31 (rat or human sections, respectively) or WT1 applied to formalin fixed sections at concentrations shown above, overnight at 4$^{o}$C. Goat and rabbit HRP (Vector, 1:500) was added to sections and TSAT Plus Cyanine 3 System (PerkinElmer NEL744B001KT) applied for 10 mins to amplify the signal. After washing, further antigen retrieval was undertaken for 5 mins and protein block applied followed by incubation with either relaxin receptor 1 in rat or Anti-GPCR LGR7 antibody - C-terminal in human sections at 4$^{o}$C overnight. Goat anti rabbit HRP was added followed by TSAT Plus Cyanine 3 System (PerkinElmer NEL744B001KT). All sections were then blocked with 0.1% Sudan Black B (Sigma) and mounted with DAPI hard set mounting medium (Vector Labs H1500). For dual immunostaining with the Anti-Actin, alpha smooth muscle antibody, this was applied for 1 hr at room temperature and secondary donkey anti mouse Alexa 555 (Invitrogen A31570), followed by protein block, appropriate RXFP1 antibody overnight at 4$^{o}$C, followed by the Goat anti rabbit HRP and TSAT Plus Cyanine 3 System. Relevant controls were undertaken with either no first primary, no second primary or without both. For all, sections were then blocked with 0.1% Sudan Black B (Sigma) and mounted with Dapi hard set mounting medium (Vector Labs H1500). All photographs were taken using a Nikon Eclipse e600 microscope and camera (DXM1200F) and acquired using NIS–Elements D software (Nikon).

## 2.17 Quantitative digital image analysis of picrosirius red (collagen proportionate area)

For each animal, liver tissue was harvested from 4 separate lobes, sections cut at 3 µm and stained with picrosirius red. Thirty non overlapping brightfield RGB digital images were captured per liver at a single magnification (x50) using a Zeiss Axiovert 200 microscope and AxioCam MRc camera by a blinded observer. Morphometric pixel analysis was undertaken using Adobe Photoshop CS2. Pixel counts of positive staining were shown as a percentage of total pixel count and hence % area. For picrosirius red staining, this was referred to as collagen proportionate area (CPA). Where stated 'relative % area' was calculated by normalising to the mean % area of one group (Control) which was assigned a value of 1.

### 2.18 Quantification of renal acute tubular necrosis (ATN)

Renal ATN was measured on H&E stained kidney sections by a blinded pathologist as previously described (Melnikov, Faubel et al. 2002). Histological changes of ATN were evaluated by calculation of the percentage of tubules that displayed cell necrosis, loss of brush border, cast formation, and tubule dilatation as follows: 0, none; 1, ≤10%; 2,11–25%; 3, 26–45%; 4, 46–75%; and 5, >76%. At least ten fields (×40 magnification) were assessed.

### 2.19 RNA extraction and quantitative RT-PCR

RNA was extracted from rat kidneys, liver, heart, mesentery and renal artery, snap frozen and stored at -80$^{o}$C, using Trizol reagent (Invitrogen) and RNeasy mini columns (Qiagen) according to the manufacturer's protocol, followed by quantification using Nanodrop Spectrophotometer (Thermo Scientific). 2µg of RNA was reversed transcribed using Superscript III (Invitrogen) according to the manufacturer's protocol. Validated primer/probe sets for rat RXFP1 (Rn01495351_m1) and eukaryotic 18S were purchased from Applied Biosystems (UK). qPCR was performed using an ABI

7500 Fast Realtime system with TaqMan Express qPCR master mix (Applied Biosystems, UK). Gene expression was calculated by $2^{-\Delta\Delta}$Ct method relative to the housekeeping gene 18S. Where stated 'relative gene expression' was calculated by normalizing to the mean expression of one group which was assigned a value of 1.

RT2 Profiler Rat Hypertension PCR array (SA Biosciences, Qiagen; PARN-037Z) was performed using RT2 First Strand Kit and RT2 SYBR Green/ROX PCR Master Mix according to manufacturer's instructions. Relative gene expression was analyzed against a panel of 5 housekeeping genes using the RT2 Profiler PCR Array data analysis tool.

**2.20 Nitric oxide synthase activity assay**

Whole kidney tissue was homogenized in phosphate buffered saline (pH 7.4), centrifuged at 10,000g for 10 mins and the supernatant collected. Protein determination was performed using the Bradford assay and 150µg of protein was used to measure NOS activity using an EnzyChrom TM kit (Bioassay Systems, USA).

**2.21 Serum analysis**

At the time of harvest, whole blood was collected from the femoral artery allowed to clot and serum isolated by centrifugation at 8000g for 5 mins. Serum samples were stored at -80$^{o}$C and analysed for Alanine aminotransferase (ALT), Aspartate aminotransferase (AST), Alkaline phosphatase (ALP), Bilirubin and Albumins levels using a standard bioanalyser.

### 2.22 Nitric oxide measurement

Rat urine and serum were filtered using a 10,000Da molecular weight cut-off filter (Millipore, UK). As NO has a short half-life *in vivo* of a few second or less, the levels of its more stable metabolites nitrite (NO2) and nitrate (NO3) can be used as indirect measurements of NO. Determination of these was performed using a Total Nitric Oxide and Nitrate/Nitrate Assay parameter Kit (R&D Systems, UK). Serum samples required a 2 fold dilution. This assay determined the total nitrite concentration by measuring endogenous nitrite using the modified Griess Reaction and then the concentration following enzymatic conversion of nitrate to nitrite by nitrate reductase followed by the modified Griess Reaction. Samples were assayed in duplicate. The reaction was follow by colorimetric detection (with the optical density measured at 540nm with wavelength correction at 690 nm) of nitrite as an azo dye product of the Griess Reaction. Nitrite positive standards were assayed alongside samples in duplicate and a concentration curve constructed of decreasing dilutions of nitrite to allow a standard curve of nitrite concentration versus optical density to be constructed. Sample nitrite concentrations were then interpolated from the curve

### 2.23 Relaxin measurement

Rat serum was prepared as described in **2.21** and diluted 4 fold and relaxin levels measured by Human Relaxin-2 Immunoassay kit (R&D Systems, UK).

### 2.24 TNFα measurement

Rat serum was prepared as described in **2.21** and diluted 3 fold and TNFα measured by Quantikine ELISA kit (R&D Systems, UK).

### 2.25 GFR measurement

Two 20 minute urine samples with midpoint plasma collections were collected for each rat. Samples were thawed overnight and spun down. Urine samples were diluted 1:100 in HEPES buffer (HEPES 1.19g, 450 mL distilled water, pH to 7.4 with 5M NaOH and autoclaved). A 9 point 2 fold dilution series was constructed starting with 1 mg/mL in HEPES buffer (20 µL in 980 µL buffer). All samples were further diluted 1:100 in HEPES buffer and were performed in duplicate. 190µL was loaded per well and fluorescence read at 485nm (excitation) and 538nm (emission). Concentrations of inulin were calculated from the standard curve. The GFR was calculated as follows: [(urine inulin x urine volume/min)/plasma inulin].

### 2.26 Western blotting

Western blot was performed on whole kidney lysates prepared by homogenization in T-PER protein extraction reagent (Thermo Scientific, Hemel Hempstead, UK) containing Halt protease and phosphatase inhibitor cocktail (Thermo Scientific). Protein concentration in kidney homogenates was determined by Bradford Assay (Bio-Rad, UK). 30 µg of protein was loaded per well of pre-cast gels (Biorad, UK) and separated by electrophoresis initially at 60V, increased to 80V when the proteins were into the gel. They were then transferred, using wet transfer, onto nitrocellulose membranes (Whatman, GE, USA) using 240mA for 90 mins in standard buffer with 10% methanol. Successful transfer was assessed by immersing the membrane in 1:10 diluted Ponceau Red which allowed visualizing of proteins. Membranes were then cut so multiple proteins could be assessed. The membranes were blocked in either 5% non-fat dry milk powder/ Tris buffered saline (TBS)-Tween20 (non-phosphorylated proteins) or 5% Bovine Serum Albumin/TBS-Tween20 (phosphorylated proteins) for 1 hr at room temperature and then the primary antibodies were diluted in 5% non-fat

dry milk powder/ TBS-Tween20 (non-phosphorylated proteins) or 5% Bovine Serum Albumin/TBS-Tween20 (phosphorylated proteins) and incubated over night at 4$^{o}$C. The membranes were washed x3 (15 mins) in TBS-T and the secondary antibody: Anti-rabbit IgG, HRP-linked Antibody (Cell Signaling, #7074) was added and incubated with the membrane for 1 h at room temperature. After further washing x3, detection was performed using enhanced chemiluminescence (Millipore, Livingstone, UK) and bands were visualized by X-ray films (Fuji, Bedfordshire, UK). Selected membranes were stripped using western blot stripping buffer (Thermo scientific, UK) to allow the membranes to be re-probed to allow assessment of relative expression of phosphorylated to non-phosphorylated proteins. GAPDH loading control blot was performed for all experiments to ensure even loading. Densitometry analysis was performed using ImageJ (NIH, USA). See **Table 2.3** for list of primary antibodies used.

| Antibody | Dilution |
|---|---|
| **panAKT (#4685) Cell signalling** | 1:1000 |
| **PhosphoAKT Thr308(#C31E5E) Cell signalling** | 1:1000 |
| **eNOS (9572) Cell signalling** | 1:1000 |
| **Phospho-eNOS Ser117 (#9671) Cell signalling** | 1:1000 |
| **Relaxin receptor 1 H160(Santa Cruz, 50328)** | 1: 1000 |
| **Arginase II H64 (Santa Cruz 20151)** | 1:200 |
| **Caveolin I (#3238) Cell Signalling** | 1:1000 |

## Table 2.3 Antibodies used for Western Blot

Table showing antibodies with their dilutions used for Western blot.

### 2.27 Statistical analysis

Primary data are expressed as mean ± standard error of the mean (SEM). GraphPad Prism Version 5.03 (GraphPad Software Inc., USA) was used to perform statistical calculations. Differences among multiple groups were assessed with one-way ANOVA, or repeated measures ANOVA with post-hoc Bonferroni test. Statistical evaluation of two groups was with unpaired two-tailed Student's *t*-test. Concentration response curves (CRC) were constructed as a percentage (%) dilation relative to the

pre-constricted PE dilation. Comparison of both cirrhosis/treatment and concentration between groups was assessed using two-way ANOVA with post-hoc Bonferroni test. Non-linear regression analysis was used to assess differences in sensitivity of vessels ($IC_{50}$ or $EC_{50}$) to vasodilators and vasoconstrictors respectively. $p<0.05$ was considered statistically significant.

# CHAPTER 3 – RESULTS - CHARACTERISATION OF MODELS

### 3.1 Overview of Chapter:

To provide proof of concept of RLN's effect in cirrhosis, I needed to define suitable robust models of cirrhosis with sinusoidal portal hypertension, renal vasoconstriction and renal dysfunction. In this chapter I fully characterised two distinct rat models of cirrhosis in terms of histological, biochemical, systemic and renal haemodynamic parameters. I used $CCl_4$ and BDL models and monitored the rats using invasive monitoring at time points throughout their evolution, with suitable controls, focussing particularly on the effect on renal blood flow and renal function (GFR).

### 3.2 Author contribution:

I performed BDL and all the microsurgical invasive monitoring. Will Mungall did the twice weekly $CCl_4$ injections and also latterly assisted with the BDL surgery. Picrosirius red (PSR), periodic acid-Schiff (PAS) and haematoxylin and eosin (H+E) staining was undertaken by the histology department. Dr Tim Kendall (Consultant Histopathologist, University of Edinburgh) reported all the histology in a blinded manner and serum blood tests were analysed by Dr Forbes Howie (University of Edinburgh).

### 3.3 Background:

HRS in humans, as previously described in the **Introduction**, is diagnosed according to strict criteria, which have recently been updated (Angeli, Gines et al. 2015). However, faithfully recapitulating these diagnostic criteria in preclinical models, as a platform for testing potential novel interventions, is a challenge. The key features are 'functional' (and therefore potentially reversible)

AKI rather than structural kidney disease, and the absence of septic shock, hypovolaemia, or nephrotoxic drugs (Angeli, Gines et al. 2015). Although bile duct ligation (BDL) (Pereira, dos Santos et al. 2008) or galactosamine (Anand, Harry et al. 2002) in rodents have been shown to induce renal failure without obvious intrinsic renal damage, in the presence of cirrhosis and acute liver failure respectively, there are currently no well validated models of HRS. This is largely due to the complexity of this condition, with activation of many signalling pathways meaning that a model of genetic manipulation is unlikely to be successful. Furthermore as our current understanding of HRS pathogenesis is incomplete it is difficult to know how best to approach an animal model system.

Functional renal arterial vasoconstriction is the central mechanism underlying HRS pathogenesis and therefore it is crucial for any model of HRS that this is a reproducible feature (Epstein, Berk et al. 1970; Platt, Ellis et al. 1994; Dagher and Moore 2001). Historically, HRS in humans has been classified into Type 1 and Type 2. Type 1 HRS is defined by doubling of the creatinine over 2 weeks, often precipitated by an event such as sepsis/bleeding/untreated dehydration, whilst Type 2 occurs in a more indolent way with a gradual increase in creatinine often seen in patients with refractory ascites (Arroyo, Guevara et al. 2002). The recent change in definition of AKI has led to a change in the definition of HRS-AKI surpassing the above with the criteria needing to be fulfilled to allow diagnosis in humans shown in Introduction 1.6. (Angeli, Gines et al. 2015). It has been shown that renal vasoconstriction worsens throughout advancing cirrhosis until it reaches a critical perfusion threshold and then AKI occurs and HRS, according to the above criteria, can be diagnosed (Ring-Larsen 1977). I was keen to establish models that were representative of this progression, i.e. pre-ascitic (compensated) cirrhosis and ascitic (decompensated) cirrhosis.

The first model I studied for haemodynamic characterisation was chronic carbon tetrachloride ($CCl_4$) intoxication. $CCl_4$ is the most widely used hepatotoxin in experimental models of fibrogenesis and its resolution. When administered in vivo it is metabolised by the Cyp2E1 enzyme system forming trichloromethyl peroxy free radicals which result in lipid peroxidation, subsequently affecting the integrity of the cell membrane and allowing activation of intracellular calcium-dependent proteases, ultimately resulting in hepatocyte death through both apoptosis and necrosis (Shi, Aisaki et al. 1998; Manibusan, Odin et al. 2007). As Cyp2E1 is predominantly expressed in the centrilobular (Zone 3) hepatocytes, the majority of cell death occurs in these areas. This model shares a similar pathogenesis with human alcohol related liver damage and non-alcoholic steatohepatitis which also affect Cyp2E1, inducing lipid peroxidation causing Zone 3 liver damage (Lieber 2004). Chronic iterative administration results in recurrent hepatic necrosis with wound healing and ultimately fibrosis and cirrhosis, in many respects mimicking human disease in pathological evolution (Perez Tamayo 1983). Through this pattern of progressive fibrosis, sinusoidal portal hypertension develops and as a result this model has been used to study potential therapies for this complication of cirrhosis (Abraldes, Rodriguez-Vilarrupla et al. 2007). However, there has been very little published literature on the renal manifestations of $CCl_4$ cirrhosis.

The second model I characterised was the bile duct ligation (BDL) model of cirrhosis, which is induced by preventing bile outflow leading to progressive cholestasis, biliary inflammation and intense fibrosis. This model has been suggested to have analogous features to human HRS. BDL in rats has been shown to produce a rapid deterioration in renal function, within days (Rivera-Huizar, Rincon-Sanchez et al. 2006) with no signs of acute tubular damage. Pereira et al (2008) showed progressive renal dysfunction over weeks, with rats developing renal impairment evidenced by reduced creatinine clearance and ascites by 4-6 weeks, with no signs on electron microscopy of tubular damage (Pereira, dos Santos et al. 2008). However, unlike humans with HRS they witnessed

increasing urinary sodium excretion and the rats did not become oliguric. Noticeably they did not look at changes to renal blood flow itself. Other groups have observed renal dysfunction by 4 weeks after BDL and used lipopolysaccharide (LPS) as a 'second hit' (Harry, Anand et al. 1999; Shah, Dhar et al. 2012). A possible criticism of this approach is that this second hit, although theoretically akin to a superadded infection in humans, renders the animals moribund and cardiovascularly unstable such that subsequent physiological observations are unpredictable and rather heterogeneous. In BDL and BDL-LPS rats with this more severe phenotype, histological changes are apparent in the tubules that indicate a degree of ATN (Shah, Dhar et al. 2012). However, this may not be a major concern given recent evidence from kidney biopsy series in 'HRS' patients which suggests that tubular damage may occur more frequently than previously thought (Trawale, Paradis et al. 2010; Fagundes, Pepin et al. 2012). Taken together, there is considerable evidence to support BDL in rats as a suitable model in which to study HRS.

I chose to use rats as my rodent species in both models for several reasons. Firstly, our laboratory has extensive experience with $CCl_4$ models of fibrosis in rats (Issa, Zhou et al. 2004). Chronic dosing with $CCl_4$ or BDL in outbred rats leads to a reproducible fibrotic lesion and the development of cirrhosis (Constandinou, Henderson et al. 2005) . Secondly, rats are much more amenable to microsurgical procedures such as BDL and vascular cannulation, which is technically challenging in mice with the risk of increased morbidity and mortality.

### 3.4 Aims of this Chapter:

- To define the phenotype of $CCl_4$ treated rats in terms of:
    - Liver fibrosis and liver function
    - Portal hypertension
    - Systemic and renal haemodynamics
    - Kidney function
    - Kidney histology

- To define the phenotype of BDL treated rats in terms of:
    - Liver fibrosis and liver function
    - Portal hypertension
    - Systemic and renal haemodynamics
    - Kidney function
    - Kidney histology

## RESULTS:

### 3.5 Chronic $CCl_4$ intoxication generates hepatic necro-inflammation with progressive collagen deposition and synthetic dysfunction

I wanted to determine the histological, biochemical and haemodynamic changes that occur in the $CCl_4$ model of fibrosis in rats to enable me to choose appropriate time-points to investigate therapeutic modulation of renal vasoconstriction and renal function with RLN. To do this, 6-8 week

male Sprague-Dawley (SD) rats had intraperitoneal (i.p.) injections of $CCl_4$ or olive oil (vehicle controls) administered twice weekly for up to 16 weeks. The rats underwent haemodynamic monitoring under terminal general anaesthetic after 8, 12 and 16 weeks of $CCl_4$, 24 hrs following the final dose of $CCl_4$ (n= 6-11/ time-point). After haemodynamic monitoring, blood and tissues were harvested. The results expressed below are from two separate $CCl_4$ models run two weeks apart with 3-4 rats analysed at each time-point to ensure reliability and robustness of findings.

In figure **3.1A-C**, liver tissue at each time-point was stained with haematoxylin and eosin (H+E) to visualise lobular architecture and picrosirius red (PSR) to visualise collagen deposition. Hepatic fibrosis was quantified by morphometric pixel analysis (n=5-8/time-point) and expressed as % of total pixels relative to controls, termed relative collagen proportionate area (relative CPA; %). With chronic administration of $CCl_4$ there was progressive hepatic necro-inflammation with loss of the normal lobular liver architecture (**Fig 3.1A**). There were no differences in fibrosis seen in either olive oil or normal controls. Hepatic fibrosis (CPA) increased progressively with duration of $CCl_4$ administration leading to cirrhosis (**Fig 3.1B and C**). Biochemically, I measured serum alanine aminotransferase (ALT) levels, a marker of hepatic injury routinely used in clinical practice, and this was progressively elevated with increased duration of $CCl_4$ (**Fig 3.2A**). I measured hepatic functional impairment using serum albumin, routinely used in clinical practice as a marker of hepatic synthetic function and this was significantly reduced after 16 weeks (**Fig 3.2B**) at a time when liver histology showed advanced cirrhosis.

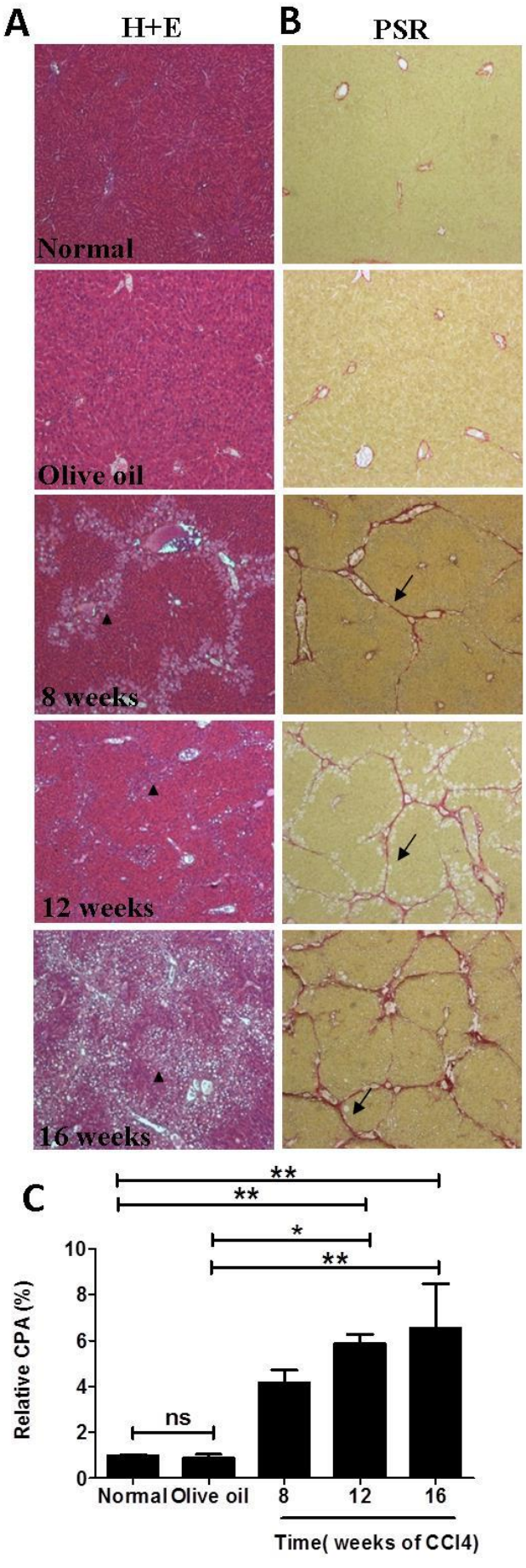
A
H+E
B
PSR
Normal
Olive oil
8 weeks
12 weeks
16 weeks
C
**
**
*
**
ns
Relative CPA (%)
0
2
4
6
8
10
Normal
Olive oil
8
12
16
Time( weeks of CCl4)

# Figure 3.1 $CCl_4$ Model of Cirrhosis

$CCl_4$ model of cirrhosis with representative liver sections stained with H+E (**A**), PSR (**B**). (**A)**. hepatic necro-inflammatory changes (triangle) (**B)**. PSR staining for total collagen (arrow). (**C)**. Hepatic fibrosis was assessed by PSR staining and morphometric pixel analysis (Expressed relative to mean % area of controls; n=4-8 per time point). Data expressed as mean±SEM and analysed by one-way ANOVA with post-hoc Bonferroni test. *p<0.05 **p<0.01 ***p<0.001.

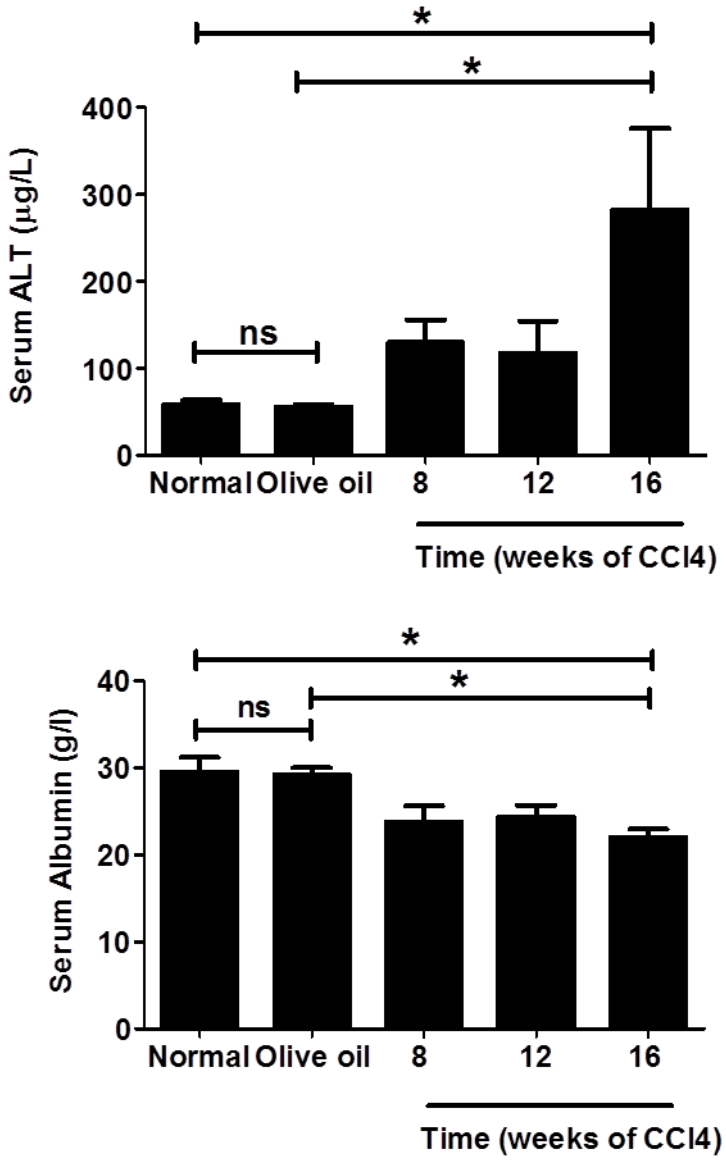


## Figure 3.2 Serum Biochemistry changes in $CCl_4$ model of cirrhosis

**(A)**. Serum Alanine Transaminase (ALT), a marker of hepatic injury, (**B)**. Serum Albumin, a marker of hepatocyte synthetic function were measured in normal, olive oil and 8,12 and 16 week $CCl_4$ rats. Data expressed as mean±SEM and analysed by one-way ANOVA with post hoc Bonferroni test. *p<0.05 **p<0.01 ***p<0.001.

### 3.6 Chronic $CCl_4$ treated rats do not develop ascites despite significant portal hypertension

No $CCl_4$ treated rats developed jaundice or detectable ascites. I measured portal pressure at each time-point, by cannulation of the hepatic portal vein, (**Fig. 3.3**) and this showed elevation at 8 weeks (12.8±0.9 mmHg, $p<0.001$), 12 weeks (12.64±0.9mmHg; $p<0.001$) and 16 weeks $CCl_4$ (11.1±0.7 mmHg, $p<0.05$) compared to normal (7.4±0.4mmHg) and olive oil control rats (7.4±0.7 mmHg).

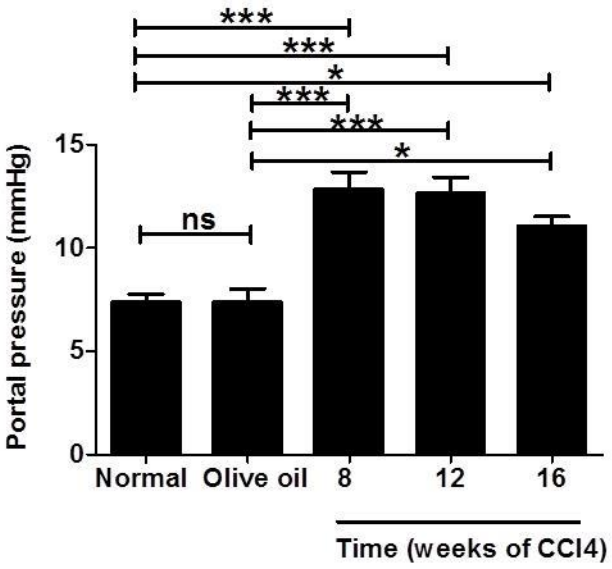


## Figure 3.3 Portal Pressure changes in $CCl_4$ Cirrhosis

Portal pressure, measured by cannulation of the portal vein. Data expressed as mean±SEM and analysed by one-way ANOVA with post hoc Bonferroni test. *p<0.05 **p<0.01 ***p<0.001.

### 3.7 Chronic $CCl_4$ treated rats exhibit renal vasoconstriction and renal dysfunction with no reduction in mean arterial pressure

RBF was measured invasively using a perivascular flow probe attached around the left renal artery immediately proximal to the bifurcation. After 16 weeks of $CCl_4$, RBF (**Fig.3.4A**) was markedly reduced (2.4±0.2 mL/min) compared to normal (6.5±0.5 mL/min; $p<0.05$), olive oil (7.3±1.0 mL/min; $p<0.01$) and 8 week $CCl_4$ treated rats (6.3±0.9 mL/min; $p<0.01$). This was accompanied by a substantial decline in GFR, measured by inulin clearance, (**Fig. 3.4B**) after 16 weeks $CCl_4$ (0.8±0.2 mL/min, $p<0.01$) compared to olive oil controls (2.4±0.4 mL/min). To establish whether this reduction in RBF and GFR was secondary to a reduction in systemic blood pressure, MAP was measured by cannulation of the femoral artery and showed no significant reduction (**Fig 3.4C**).

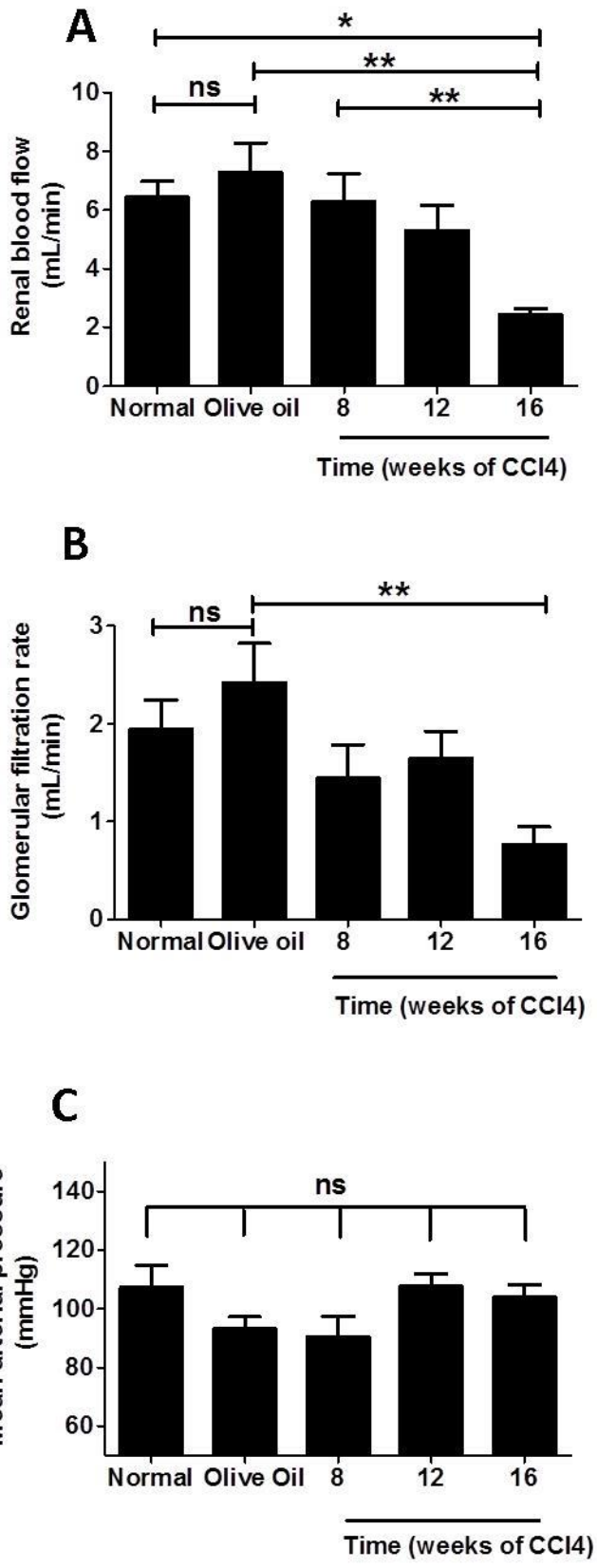
A
*
**
ns
**
Renal blood flow (mL/min)
0
2
4
6
8
10
Normal
Olive oil
8
12
16
Time (weeks of CCl4)
B
**
ns
Glomerular filtration rate (mL/min)
0
1
2
3
Normal
Olive oil
8
12
16
Time (weeks of CCl4)
C
ns
Mean arterial pressure (mmHg)
60
80
100
120
140
Normal
Olive Oil
8
12
16
Time (weeks of CCl4)

## Figure 3.4 Renal Blood Flow, Glomerular Filtration Rate and Mean Arterial Pressure Changes in the CCl4 Model of Cirrhosis

**(A)**. RBF, measured by a flow probe. (**B)**. GFR, measured by inulin clearance. (**C**). MAP, measured by a femoral line were measured in normal, olive oil, 8,12 and 16 week $CCl_4$ rats. Data expressed as mean±SEM and analysed by one-way ANOVA with post hoc Bonferroni test. *p<0.05 **p<0.01 ***p<0.001.

### 3.8 Chronic $CCl_4$ intoxication does not induce histological changes in the kidneys

Despite renal functional impairment, kidney tissues from 16 week $CCl_4$ treated rats stained with H+E and reviewed by a pathologist blinded to the slides, showed no structural damage compared with olive oil controls, and in particular no evidence of acute tubular necrosis (ATN). **Fig 3.5** shows representative images (arrow-glomerulus, triangle-tubular cells).

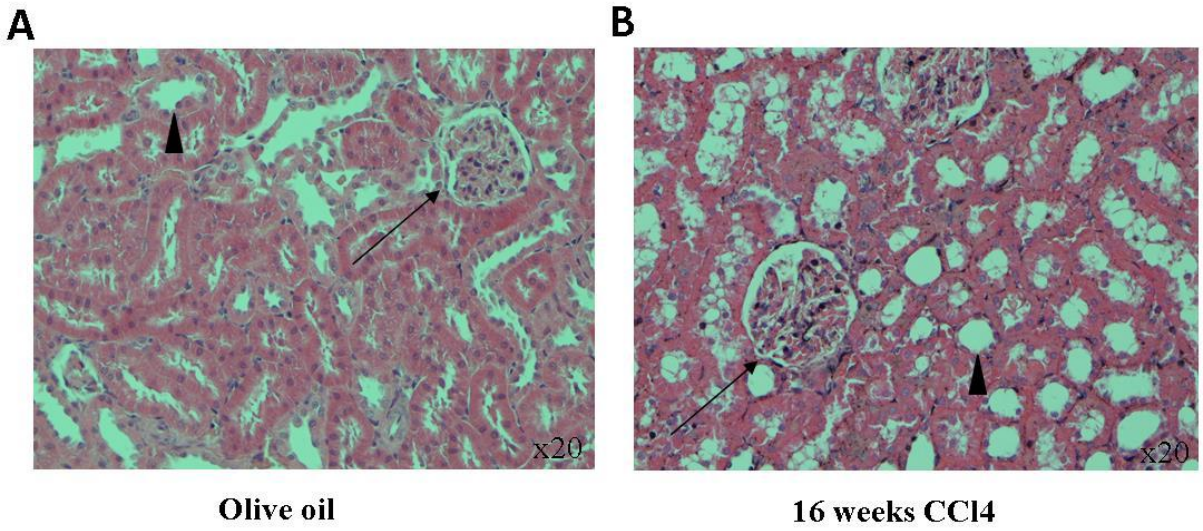


## Figure 3.5 $CCl_4$ Kidney Histology

Representative images of olive oil (**A**) and 16 week CCl4 (**B**) kidneys sections. Original magnification x20. Arrow-Glomerulus, triangle-tubular cells.

### 3.9 Bile duct ligated rats exhibit rapidly progressive biliary fibrosis and development of decompensated cirrhosis

I went on to determine whether I could model HRS using BDL injury. To do this I performed surgical ligation of the common bile duct under general anaesthetic in 6-8 week old S-D rats and subsequently performed haemodynamic monitoring under terminal general anaesthesia with tissue, urine and serum collection every 7 days until 28 days to evaluate changes in these parameters. As a control group I performed a 'sham' operation, exposing the common bile duct but not ligating it and then monitored the rats until 28 days when I undertook identical assessment as for the BDL animals. The sham procedure controls for the potential confounding effects of surgery and anaesthesia in the

BDL model. The results below are pooled from 3 separate cohorts of BDL treated rats that I generated over time, to ensure that the findings were reproducible (n=5-6/ time-point).

Following BDL, rats were jaundiced after 14 days and all had ascites by 28 days. From 14 days post BDL, liver tissue stained with H+E showed florid inflammation (**Fig 3.6A**) and staining with PSR showed progressive deposition of collagen with loss of normal lobular liver architecture (cirrhosis) (**Fig. 3.6B, C**). Serum alkaline phosphatase (ALP, a marker of biliary obstruction) rapidly increased after BDL (**Fig 3.7A**; $p<0.05$). Serum albumin was reduced at 28 days after BDL compared with sham controls (19.6±2.5 g/dL vs. 26.5±1.1 g/dL; $p<0.05$) (**Fig 3.7B**).

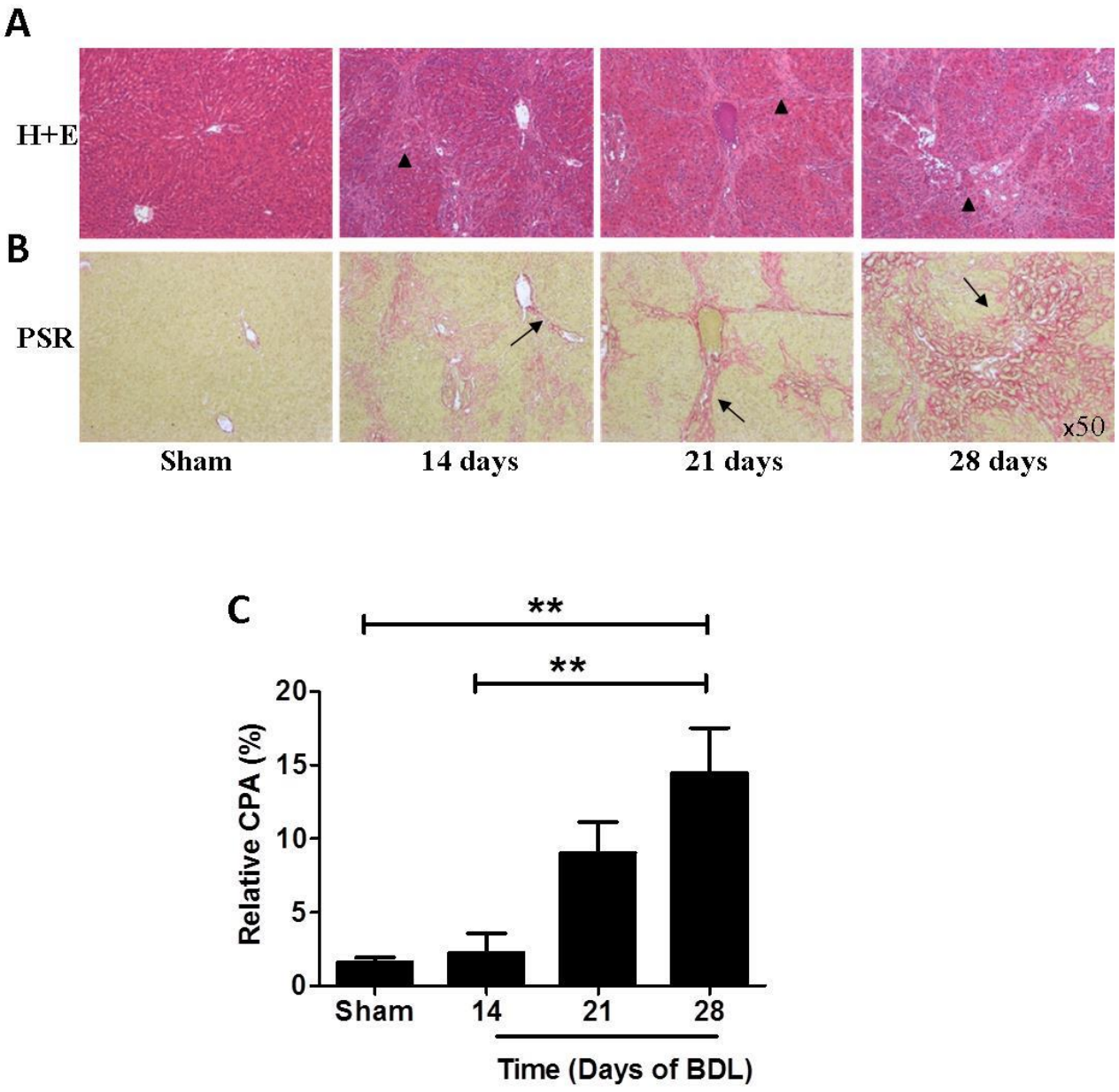


## Figure 3.6 BDL Model of Biliary Cirrhosis

BDL Model of Cirrhosis with representative liver sections stained with H+E (A), PSR (B) in sham, 14, 21 and 28 days post BDL. (**A)**. Hepatic necro-inflammatory changes (triangle) (**B)**. PSR staining for total collagen (arrow). (**C)**. Quantification of PSR by morphometric pixel analysis (Expressed relative to mean % area of sham controls; n=4 per time point). Data expressed as mean±SEM and analysed by one-way ANOVA with post-hoc Bonferroni test. *p<0.05 **p<0.01 ***p<0.001.

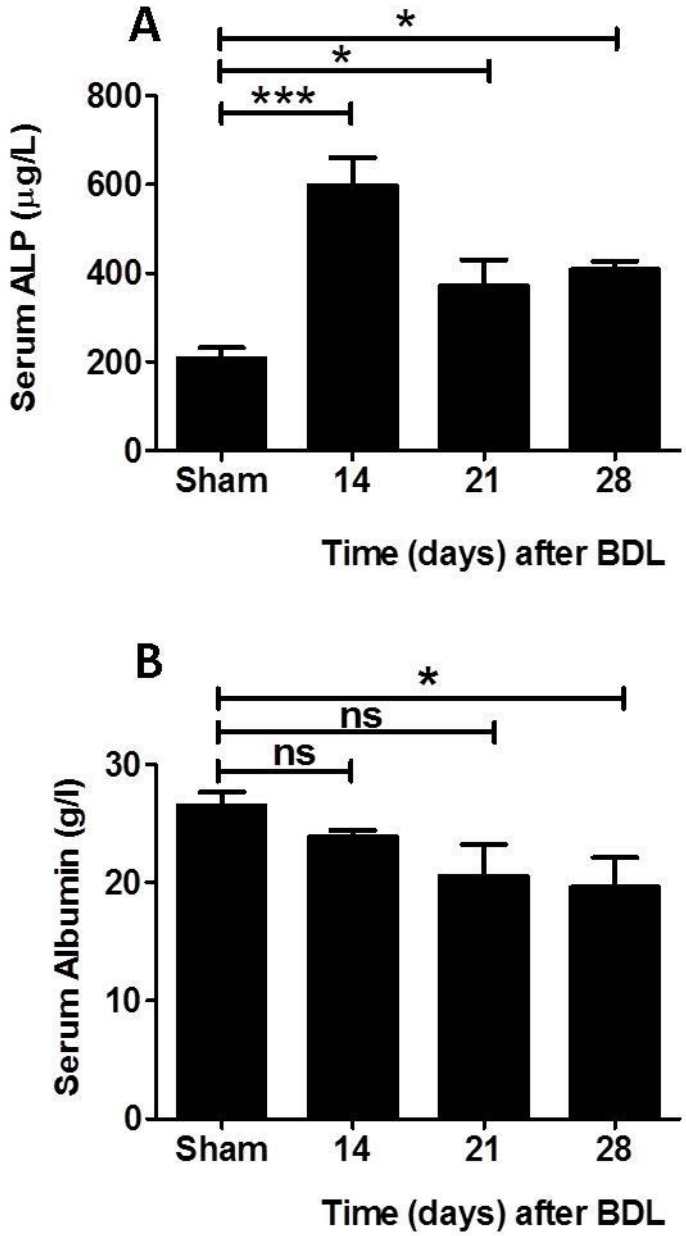


**Figure 3. 7 Serum Biochemistry Changes in BDL model of Cirrhosis**

**(A)**. Serum alkaline phosphatase (ALP), a marker of biliary injury and (**B)**. Serum Albumin, a hepatic synthetic marker were measured in shams, 14,21 and 28 day BDL rats. Data expressed as mean±SEM and analysed by one-way ANOVA with post hoc Bonferroni test. *p<0.05 **p<0.01 ***p<0.001.

### 3.10 Bile duct ligated rats rapidly develop portal hypertension, renal arterial vasoconstriction and renal functional impairment

Following BDL, portal pressure (**Fig. 3.8**) was increased after 14 days (12.0±2.0 mmHg; $p<0.01$), 21 days (16.4±0.4 mmHg; $p<0.001$) and 28 days (14.8±1.5 mmHg; $p<0.001$) compared to sham operated controls (5.2±0.8 mmHg). In addition, RBF (**Fig. 3.9A**) was decreased following BDL (1.9±0.4 mL/min after 14 days, $p<0.01$; 1.6±0.3 mL/min after 21 days, $p<0.01$; 1.5±0.4 mL/min after 28 days, $p<0.01$) compared to sham controls (6.5±1.5 mL/min). Furthermore, there was a parallel reduction in GFR (**Fig. 3.9B**) (1.1±0.3 mL/min after 14 days, $p<0.05$; 0.9±0.2 mL/min after 21 days, $p<0.01$; 0.7±0.3 mL/min after 28 days post BDL, $p<0.01$) compared to sham controls (2.4±0.2 mL/min). Although there was a reduction in MAP (**Fig. 3.9C**) after 21 days (69.4±7.1mmHg;$p<0.05$) compared with sham controls (96.4±7.9mmHg), there was no significant difference at 14 days (84.3±3.1mmHg) or 28 days ( 79.5±5.5mmHg) following BDL.

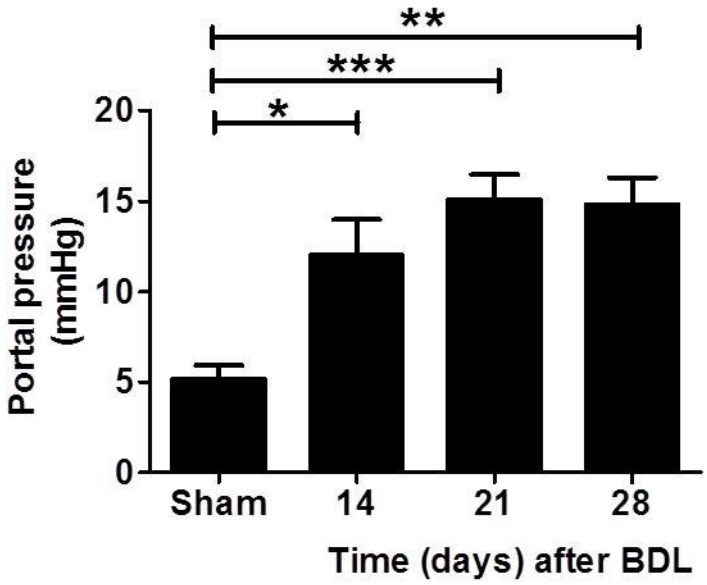


## Figure 3.8 Portal Pressure Changes in BDL Model of Cirrhosis

Portal pressure was measured by cannulation of portal vein in sham, 14, 21 and 28 day BDL rats. Data expressed as mean±SEM and analysed by one-way ANOVA with post hoc Bonferroni test. *p<0.05 **p<0.01 ***p<0.001.

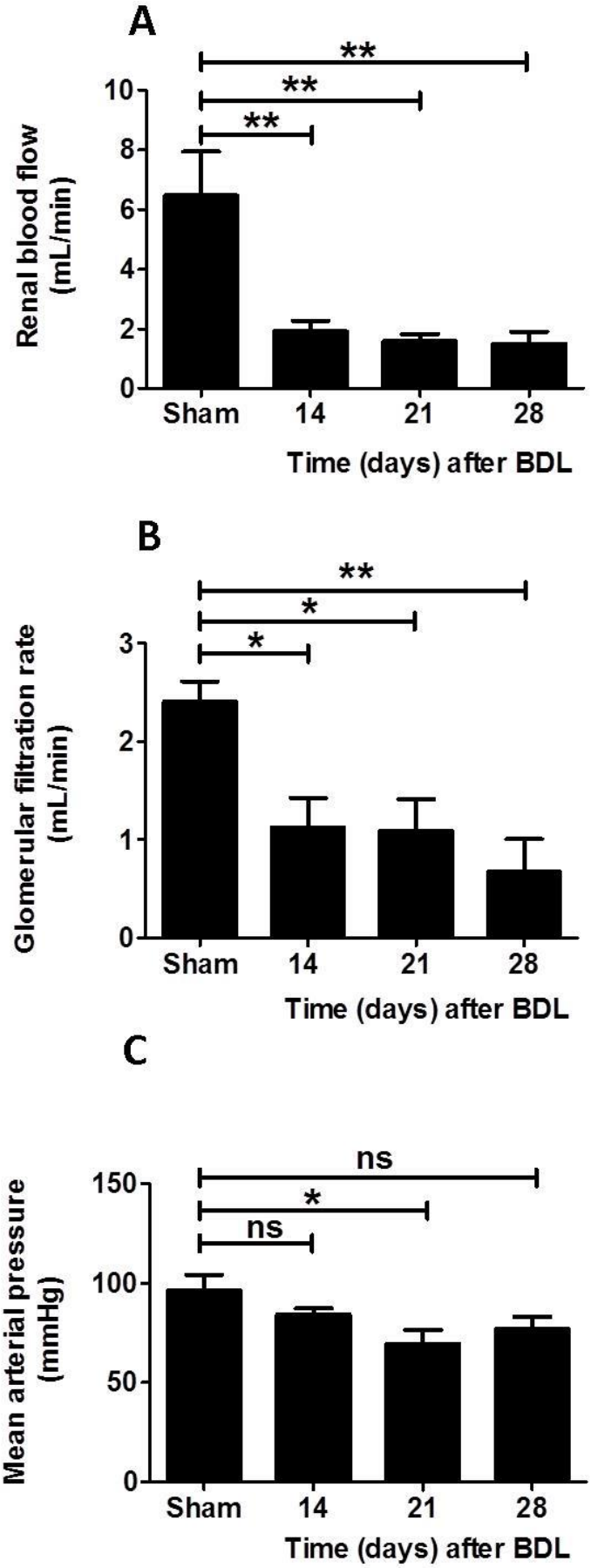
A
**
**
**
Renal blood flow (mL/min)
10
8
6
4
2
0
Sham
14
21
28
Time (days) after BDL
B
**
*
*
Glomerular filtration rate (mL/min)
3
2
1
0
Sham
14
21
28
Time (days) after BDL
C
ns
*
ns
Mean arterial pressure (mmHg)
150
100
50
0
Sham
14
21
28
Time (days) after BDL

## Figure 3.9 Renal Blood Flow, Glomerular Filtration Rate and Mean Arterial Pressure Changes in BDL Cirrhosis

**(A)**. RBF, measured by a flow probe, (**B)**. GFR measured by inulin clearance and (**C)**. MAP measured by a femoral line were measured in sham, 14, 21 and 28 day rats. Data expressed as mean±SEM and analysed by one-way ANOVA with post hoc Bonferroni test. *p<0.05 **p<0.01 ***p<0.001.

### 3.11 BDL kidneys show signs of ischaemic glomerular and tubular damage

To establish whether there was any histological damage to the kidneys, tissue sections from 21 and 28 day BDL rats and sham controls were stained with H+E and periodic acid shiff (PAS), and examined by a blinded pathologist. In contrast to the $CCl_4$ model, extensive acute tubular injury and necrosis (short arrows) were seen on H+E staining (**Fig.3.10A**). PAS staining showed variable glomerular abnormalities with mesangial hypercellularity and podocyte proliferation, in keeping with glomerular ischaemic injury (long arrow: podocyte proliferation, triangle: mesangial hypercellularity). Using a validated histological ATN score (Melnikov, Faubel et al. 2002), an increasing degree of ATN was seen at each consecutive time-point compared to sham controls (**Fig 3.10B**).

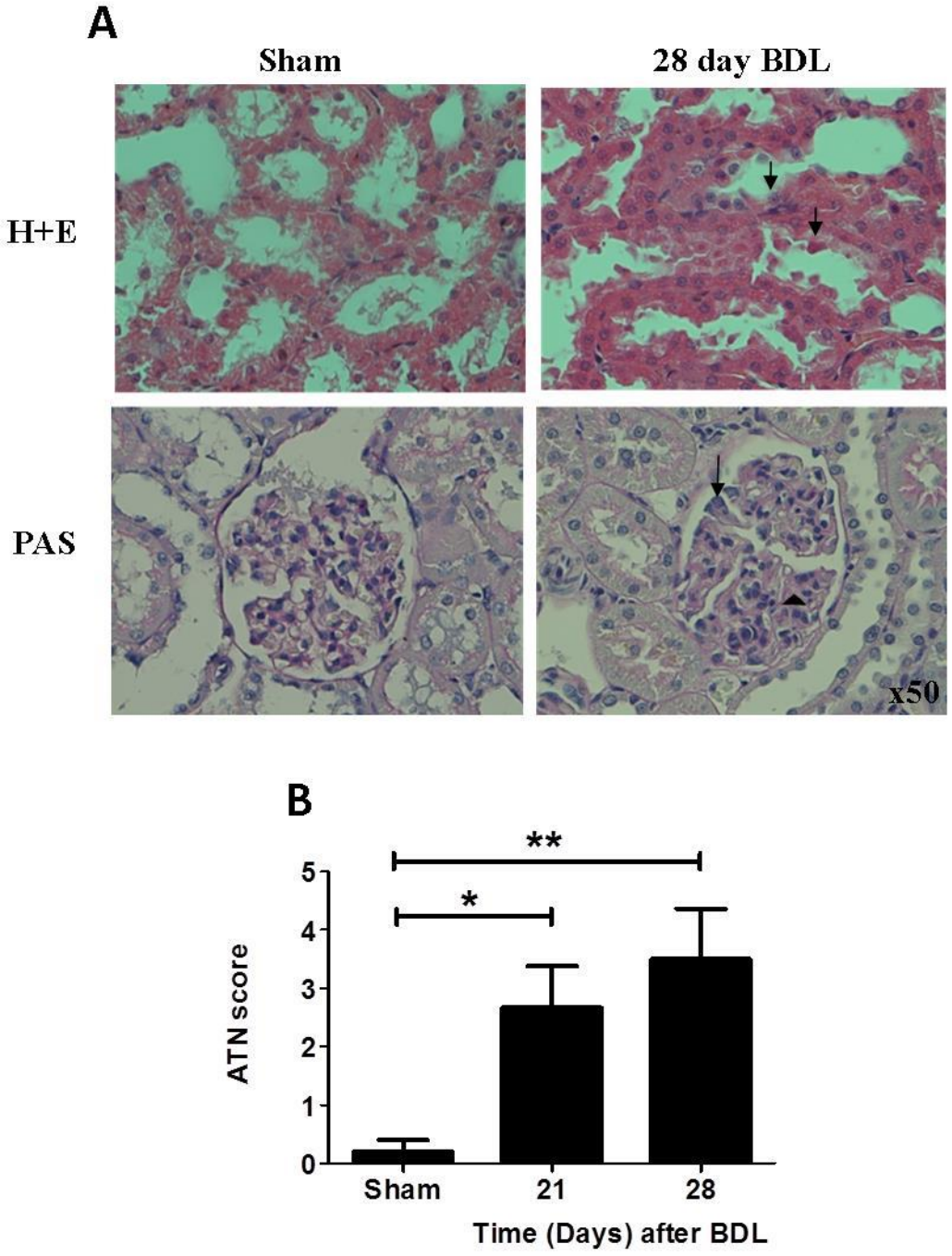


## Figure 3.10 Kidney Histology in BDL Cirrhosis

**(A)**. Representative images of sham and 28 day BDL kidneys sections, stained with PAS and H+E. Original magnification x50. Reviewed by a blinded histopathologist. (long arrow: podocyte proliferation, triangle: mesangial hypercellularity). Acute tubular injury and necrosis (short arrows) (**B).** Validated histological ATN score (Melnikov, Faubel et al. 2002) used to analyse degree of ATN

(n=4/group). Data expressed as mean±SEM, analysed by one way ANOVA with post hoc Bonferroni test. *p<0.05 **p<0.01.

## DISCUSSION

I have characterised two distinct rat cirrhosis models, one a model of repetitive hepatic necro-inflammation that evolves to compensated (pre-ascitic) cirrhosis, the other a model of rapid onset biliary fibrosis that evolves to decompensated cirrhosis and ascites. My aim was to establish two independent models that were suitable for use to investigate the pathophysiology and treatment of renal dysfunction/HRS in cirrhosis. Critically, a central feature of both models is progressive and significant portal hypertension, renal arterial vasoconstriction (demonstrated by a reduction in RBF) and a parallel decline in GFR (**Fig.3.4A and B, Fig 3.9A and B**). The relevance of these models to human liver disease is highlighted further, firstly, by common biochemical markers of hepatic injury (**ALT; Fig 3.2A**) and biliary injury (**ALP; Fig 3.7A**) showing marked abnormalities with increasing hepatic/biliary injury, respectively. Secondly, with portal hypertension developing in both, consistent with what is seen in advancing human cirrhosis (**Fig 3.3 and Fig 3.8**). Taken together, the haemodynamic phenotype shared in these models in many respects resembles human HRS in cirrhosis, although all animal studies are subject to the legitimate criticism that they cannot be considered to truly reflect events in the human condition.

In characterising two pathologically distinct cirrhosis models, it is clear that the key observations are not model dependent, rather they reflect the inevitable consequence of severe portal hypertension regardless of the initial insult. Furthermore, the magnitude of RBF and GFR reduction in these models indicates that an additional insult, such as LPS, is probably unnecessary.

There are some variances in these models that mean under the strict diagnostic criteria (Angeli, Gines et al. 2015) these rats would not necessarily be classified as having 'true' HRS. Specifically, the BDL kidneys showed changes consistent with ATN (**Fig 3.9B**). But does this matter? Although it was previously held that HRS kidneys were structurally 'normal', current evidence derived from human biopsies and urinary markers of structural kidney injury suggests that in many cases some degree of tubular damage in HRS is present (Trawale, Paradis et al. 2010; Fagundes, Pepin et al. 2012). In addition, HRS that does not respond to treatment with vasoconstrictors and albumin will inevitably progress to ATN in time. This suggests that the BDL model might reflect a severe intractable form of human HRS. There has also been debate as to whether the renal dysfunction seen in BDL is actually due to hyperbilirubinaemia distorting the tubules rather than being a reflection of true HRS (Assimakopoulos and Vagianos 2009). This criticism is valid, but it is worth remembering that, in humans, HRS is often precipitated by decompensation (including jaundice) and that this in itself can induce oxidative stress and HRS (Bomzon, Holt et al. 1997). It seems unlikely that the significant reduction in RBF that was observed with BDL (and $CCl_4$) can be accounted for purely by tubular damage from hyperbilirubinaemia.

A criticism of the $CCl_4$ model is that the rats are well compensated and do not have ascites. In humans HRS is predominantly seen in patients with decompensated cirrhosis and ascites or in patients with fulminant liver failure or severe acute alcoholic hepatitis (Moore 1999; Gines, Guevara et al. 2003; Verma, Ajudia et al. 2006). Renal dysfunction (demonstrated by a low GFR) (**Fig 3.4A and B)** was only evident at the extreme end of the $CCl_4$ model (16 weeks). There is some evidence that $CCl_4$ is nephrotoxic (Jaramillo-Juarez, Rodriguez-Vazquez et al. 2008) and that this could

underlie any associated renal phenotype, although this was described in a different strain of rat (Wistar). In my $CCl_4$ model, using SD rats, there was no evidence of nephrotoxicity.

To assess the effect of RLN on RBF and GFR in cirrhosis, I decided that the optimal time-point (associated with portal hypertension, renal vasoconstriction and renal dysfunction) was 16 weeks of $CCl_4$. For the BDL model, identifying the optimal time-point was more complicated. After 14 days the rats exhibit a reduction in RBF and GFR, but they are not yet cirrhotic and do not have ascites. After 28 days the rats have ascites and are deeply jaundiced, but are too unstable to undergo prolonged general anaesthetic and microsurgery. Therefore for future *in vivo* experiments requiring prolonged general anaesthetic I decided to use 21 day BDL rats that showed a significant and reproducible reduction in RBF and GFR, but had better health status/body condition score than 28 day rats. In contrast, for some experiments where general anaesthetic was not required I analysed 28 day BDL rats.

**Summary of important findings:**

- Chronic $CCl_4$ intoxication generates progressive hepatic fibrosis, culminating in cirrhosis with hepatic functional decline and an increase in portal hypertension
- 16 week $CCl_4$ treated rats exhibit renal functional impairment with a reduction in renal blood flow, but no evidence of structural renal injury
- BDL induces an intense biliary cirrhosis with rapid hepatic decompensation
- BDL induces a more rapid (by 14 days) decline in renal blood flow and renal function
- BDL kidneys show histological evidence of glomerular and tubular ischaemic injury

**Next steps:**

Having characterised two pathologically distinct models of rat cirrhosis with a significant and reproducible reduction in renal blood flow and renal function, that were suitable for future use as a platform for evaluating the effects of RLN, the next step was to determine the extent and the distribution of the receptor for H2-RLN (RXFP1) in these models.

# CHAPTER 4 - RESULTS -

# EXPRESSION AND DISTRIBUTION OF RXFP1 IN RAT MODELS OF CIRRHOSIS AND RENAL DYSFUNCTION

## 4.1 Overview of Chapter:

In the previous chapter I fully characterised two distinct models of cirrhosis with sinusoidal hypertension and renal dysfunction. I subsequently needed to confirm that the chief target for RLN, its G-protein coupled receptor, RXFP1, was present in these models and to determine its' cellular location. I used qPCR to monitor transcript expression and immunohistochemistry and western blot to measure protein expression of the RXFP1 receptor. Additionally, I utilised dual immunofluorescence to try to establish cellular location and I validated these findings in both rat and human tissue.

## 4.2 Author contribution:

I performed all the experiments in this chapter.

## 4.3 Background:

The vasoactive actions of RLN are transduced by binding to its cognate receptor LGR7 or RXFP1. LGR7 is a member of the leucine-rich-repeats containing G-protein coupled receptor family (LGR) which are also known as the RLN family peptide (RXFP) receptors. RXFP1 has been shown to be widely expressed in both rodent and human tissues outside the reproductive organs, importantly including the kidney (Hsu, Nakabayashi et al. 2002). As previously described, H2-RLN binds to both RXFP1 and RXFP2, with the former suggested from knockout murine models to be the predominant receptor through which RLN mediates its vascular effects (Novak, Parry et al. 2006; Conrad 2010).

In HRS renal arterial vasoconstriction is central to its pathogenesis (Epstein, Berk et al. 1970). I therefore wanted to focus my investigation on vascular expression of RXFP1. The current literature has evolved during my time undertaking this PhD and is significantly further on than when I started this body of work. The majority of work has been done in rodents. The *Rxfp1* transcript and its' protein determined by Western blot, was initially localized in male and female rats to the small renal, mesenteric arteries and the thoracic aorta (Novak, Parry et al. 2006). At a cellular level, Conrad and colleagues (2010) found that *Rxfp1* transcripts were in greatest abundance in the vascular smooth muscle of arteries rather than the endothelium, although the relative contribution of receptors in each location in mediating the vasoactive effects of RLN remained unknown. It had also been shown, from myogenic studies of isolated rat renal arteries, that removal of the endothelium obliterated the vascular response to RLN, suggesting that the endothelium is critical either through expression of the receptor or for the post binding signalling pathway (Novak, Ramirez et al. 2002). Further evidence for the presence and importance of endothelial RXFP1 comes from a recent abstract showing that vascular reactivity is altered in mice with a conditional knockout of *Rxfp1* in endothelial cells (Woodward W, Rusnak M et al. 2014).

Much of the debate over RXFP1 expression comes from literature that has studied levels of transcription, with much less data on protein expression. Based on the following chapter of work and through personal discussion with different laboratories, also searching for this receptor in other disease states, the reason for this is likely to be secondary to the quality of the antibodies available for this receptor. Recent work from detailed immunohistochemistry in rodents has suggested that RXFP1 is expressed on both endothelial and smooth muscle cells in small renal arteries, mesenteric arteries and veins, aorta, femoral arteries and veins with differing abundance of endothelial versus

smooth muscle expression seen depending on the vessel type (Jelinic, Leo et al. 2014). This appears to affect the myogenic response to RLN in individual vessels. There is still limited expression data reported in human tissues.

RXFP1 is widely expressed outside the vasculature. In the liver we have shown that RXFP1 is expressed on activated myofibroblasts in fibrosis in both rats and humans (Fallowfield, Hayden et al. 2014) and this has also been shown to be the case in the lung (Huang, Gai et al. 2011). It has additionally been found to be expressed on cardiomyocytes in the heart (Moore, Su et al. 2014). None of the work summarised above, apart from our recent paper (Fallowfield, Hayden et al. 2014) based on some of the following work, has been undertaken in cirrhosis. Given what is known about the expression of this receptor and the differing cellular origin in different vascular beds and tissues, it is likely that disease states may also affect RXFP1 expression profile.

**4.4 Aims of this chapter:**

- To determine *Rxfp1* mRNA transcript expression in in the liver, kidney and renal artery of $CCl_4$ and BDL treated cirrhotic rats
- To determine RXFP1 protein expression in the liver, kidney and renal artery of $CCl_4$ and BDL treated cirrhotic rats
- To identify the cellular source(s) of RXFP1 in the kidney and renal artery in rat and human cirrhosis

# RESULTS

## 4.5 Kidney and liver *Rfxp1* mRNA transcript expression increases in cirrhosis

To determine *Rxfp1* mRNA expression I used a pre-made and validated primer/probe set for rat *Rxfp1* (Rn01495351_m1). In normal/uninjured control rat liver the *Rxfp1* transcript is expressed at very low levels. I used tissue from 16 week $CCl_4$ and 28 day BDL rats (n=3-5/group) and compared individual organ expression to their respective control liver (given a value of 1) to view overall *Rxfp1* expression in these models. In **Fig 4.1A** *Rxfp1* mRNA transcript is most highly expressed in the heart in $CCl_4$ cirrhosis compared to other organs (*$p<0.05$). This was also seen in the BDL model (**Fig 4.1B**).

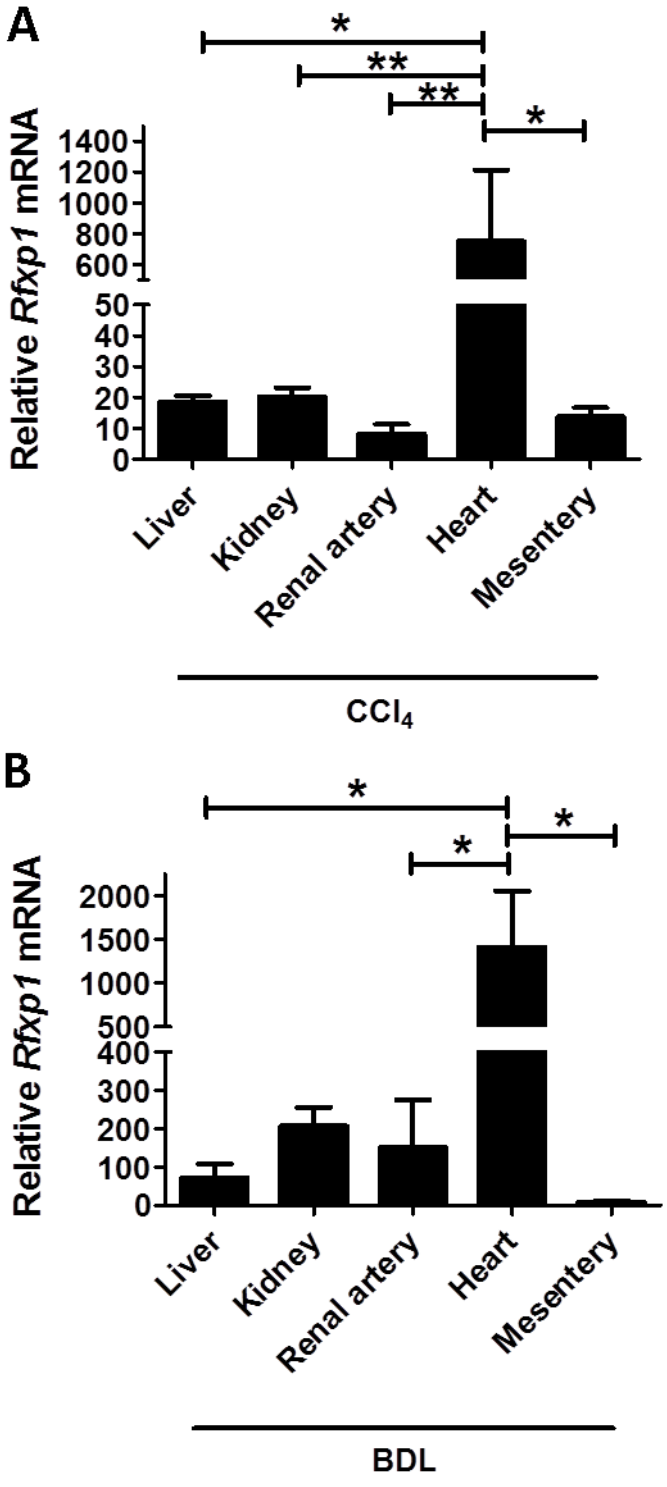


## Figure 4. 1 *Rxfp1* mRNA expression in cirrhosis models

**(A)** Relative *Rxfp1* mRNA transcript expression in 16 week CCl4 cirrhosis (**B)** Relative *Rxfp1* mRNA transcript expression in 28 day BDL cirrhosis. n=3-5/group. Data expressed as mean ±SEM, analysed relative to uninjured liver expression, given value of 1. Analysed by 1 way ANOVA with post hoc Bonferroni correction, *p<0.05 **p<0.01.

To observe the effect of cirrhosis on individual organ *Rxfp1* expression, I compared expression in that organ to expression in their respective control tissue (n=4-5/group). In **Fig 4.2A** and **B** the hepatic expression of *Rxfp1* was increased 40-fold in $CCl_4$ and 70-fold in BDL cirrhosis. This was also seen in the kidney (**Fig 4.2C** and **D**) with a 5- and 19-fold increase in $CCl_4$ and BDL cirrhosis, respectively. Focussing on the renal artery (**Fig 4.2E** and **F**) there was a 2-fold increase in $CCl_4$ cirrhosis with a trend to increase in BDL cirrhosis, that did not reach statistical significance ($p=0.0675$).

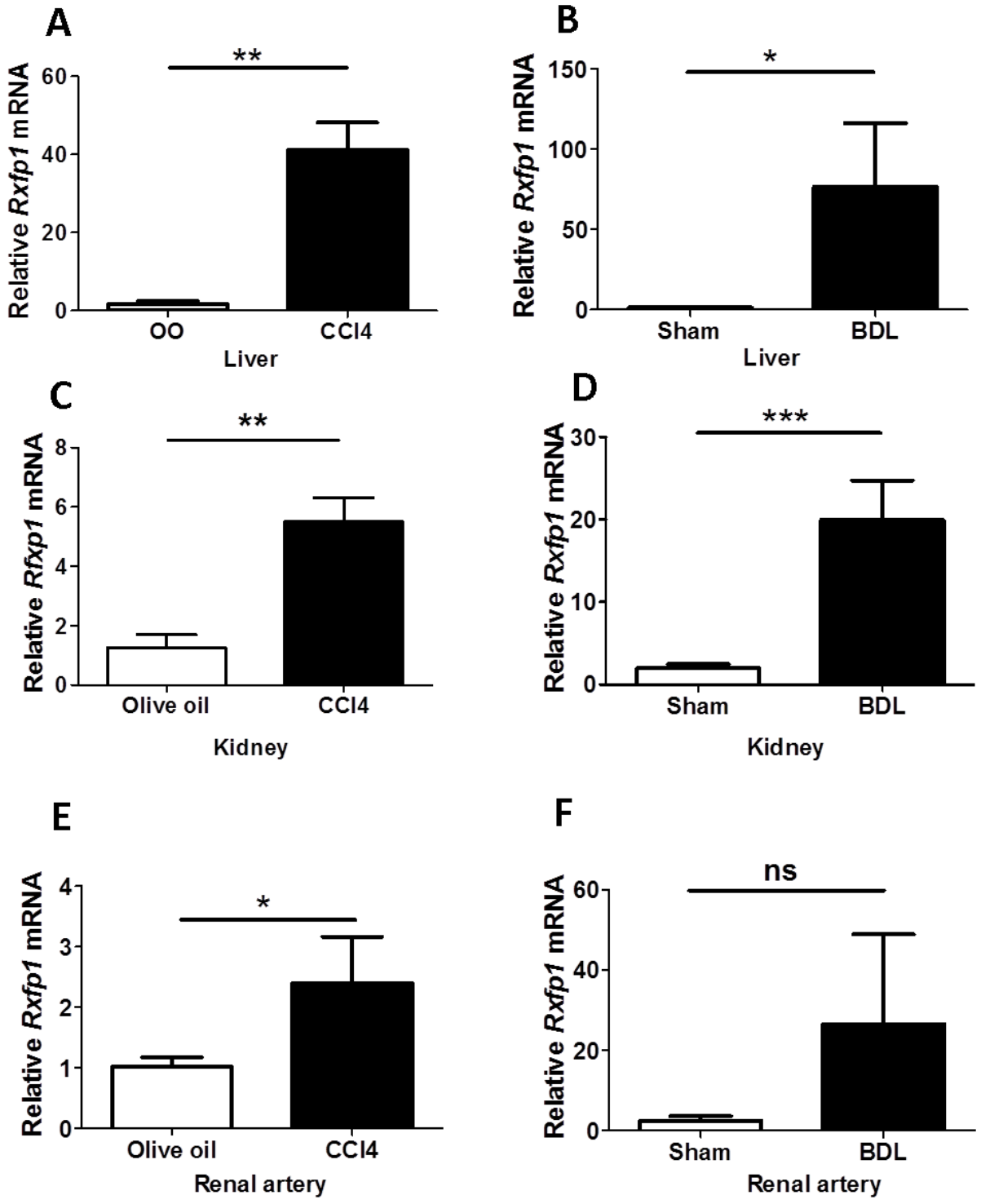


## Figure 4. 2 *Rxfp1* mRNA expression in cirrhosis in the Liver, Kidney and Renal artery

*Rxfp1* transcript expression in in the liver (**A-B**), kidney (**C-D**) renal artery (**E-F**) in 16 week CCl4 and 28 day BDL relative to control tissue. n=4-5/group. Expressed as mean±SEM and analysed relative to expression in uninjured tissue by Students t test, *p<0.05 **p<0.01 ***p<0.001.

### 4.6 RXFP1 receptor protein expression increases in cirrhosis

To establish if mRNA transcript levels translated into increased protein expression I performed DAB immunohistochemistry (IHC). I stained sections of liver tissue from the $CCl_4$ model (n=4 per group) and using ImageJ (NIH, USA) counted the number of stained cells per field (x50 magnification) averaged over 30 non-overlapping fields. Hepatic expression of RXFP1 increased in $CCl_4$ cirrhosis (**Fig 4.3A** and **B**). It appeared to localise along the fibrotic scars.

A

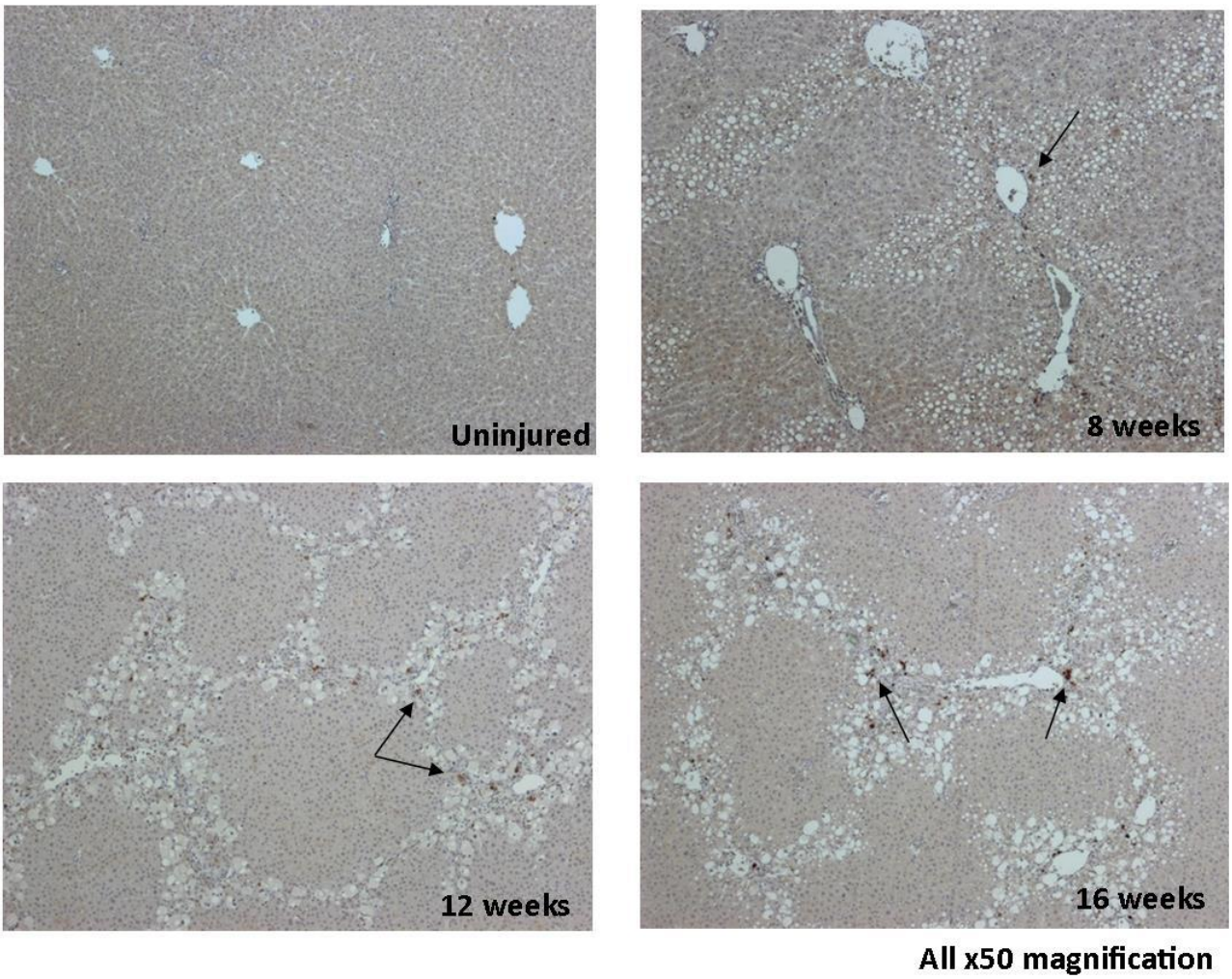


All x50 magnification

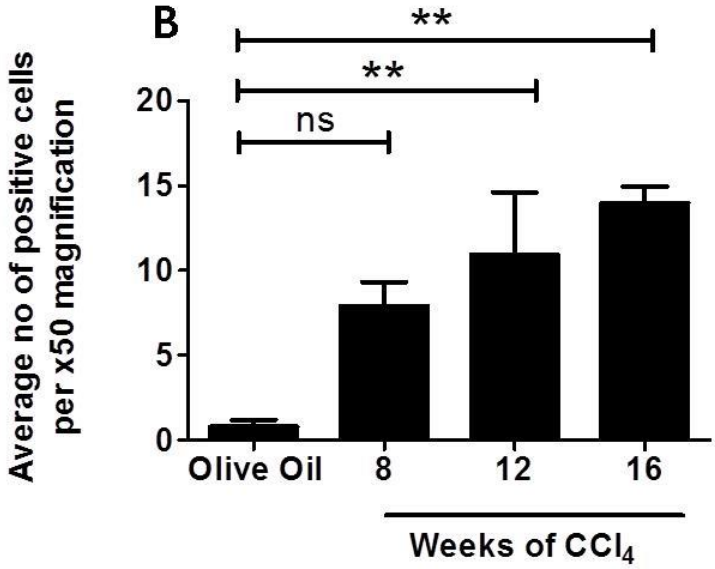

## Figure 4.3 Hepatic RXFP1 protein expression in CCl4 cirrhosis

(**A**) Representative images of RXFP1 staining in the liver by immunohistochemistry in olive oil, 8, 12 and 16 week time-points. Original magnification x50. Arrow shows staining. Quantified in **B** (n=4) per time point by image J analysis, expressed as number of positive cells stained per x50 magnification. Analysed by one way ANOVA with post hoc Bonferroni correction, *p<0.05 **p<0.01.

I also stained kidney sections at the same time-points but the pattern of staining, despite optimisation was not such that I could establish a way to reliably count receptor expression, or use morphometric pixel analysis. I therefore proceeded to analyse RXFP1 protein expression levels quantitatively using Western blot analysis. Western blotting of whole kidney (n=4/group) with densitometry analysis from the $CCl_4$ kidney showed increased expression of RXFP1 (**Fig 4.4A** and **B;*p<0.05**). Whereas with BDL kidneys, although suggesting a similar expression trend (**Fig 4.4C** and **D; p=0.0755**), it did not reach statistical significance with the sample size (n=4) used. Finally, I stained renal arteries from $CCl_4$ rats, with their respective controls (n=4 per group) and there was consistently more staining seen in the cirrhotic renal arteries (**Fig 4.5** shows representative images).

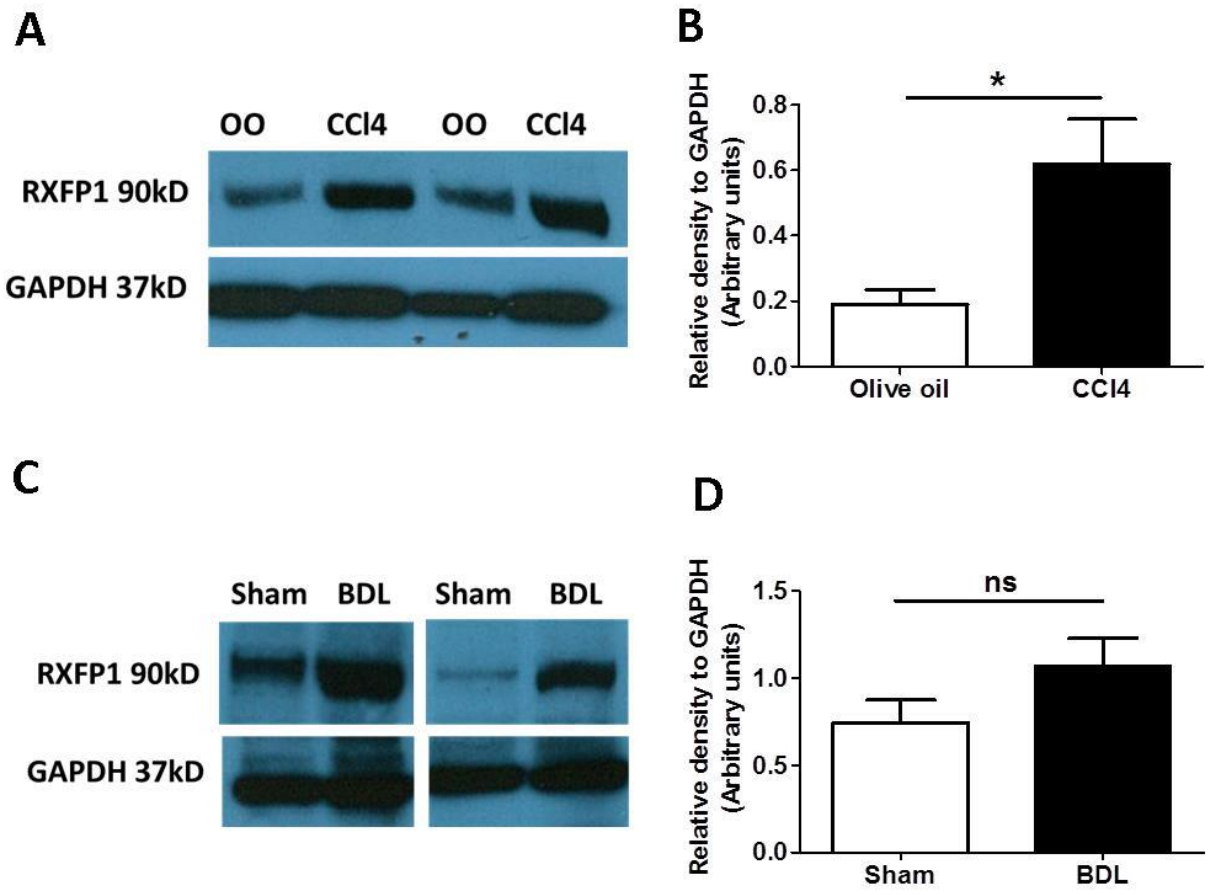


## Figure 4.4 Kidney RXFP1 protein expression in cirrhosis

(**A**) Representative Western Blots of RXFP1 in Olive oil and $CCl_4$ kidney with densitometry analysis, (**B**). **(C)** Representative Western blots of RXFP1 in sham and 28 day BDL kidneys, with densitometry analysis (**D)**. Expressed as mean±SEM relative to GAPDH and analysed by Students t test, *$p<0.05$.

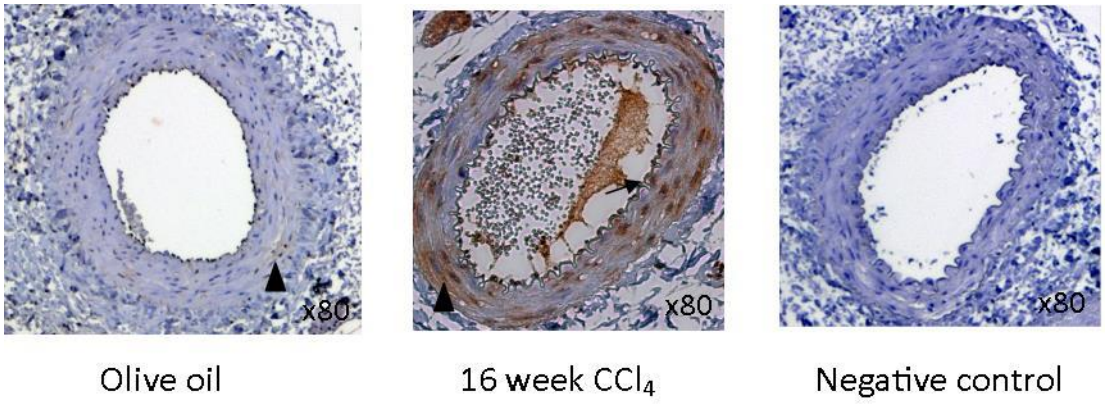


## Figure 4.5 Renal artery RXFP1 expression in cirrhosis

Representative images of renal arteries isolated from olive oil and 16 week $CCl_4$ rats with negative control (no primary RXFP1 antibody). Staining in smooth muscle (triangle) and endothelium (arrow). Magnification as shown.

### 4.7 RXFP1 is expressed abundantly in kidneys from cirrhotic rats

To delineate where RXFP1 is expressed in the kidney and its vasculature I used immunofluorescence (IF) with tyramide enhancement. Optimising this technique over DAB IHC meant that once I had established adequate staining with the single RXFP1 antibody I could then move on to dual IF . I firstly stained mouse uterus as a positive control to show validity of the antibody in IF compared to DAB staining (**Fig 4.6A DAB staining original magnification x80, 4.6B** IF**,** original magnification x100). In 16 week $CCl_4$ kidneys RXFP1 expression was seen throughout the kidney, with expression seen in extra and intra renal arteries, glomerular and peri-tubular capillaries, medullary rays and the renal papilla (**Fig 4.6B)**. This pattern of staining appeared consistent with sections from BDL kidney (**Fig 4.6C**). The distribution of staining suggested that RXFP1 could be expressed in podocytes, endothelial cells, smooth muscle cells and/or PDGFβ-expressing pericytes.

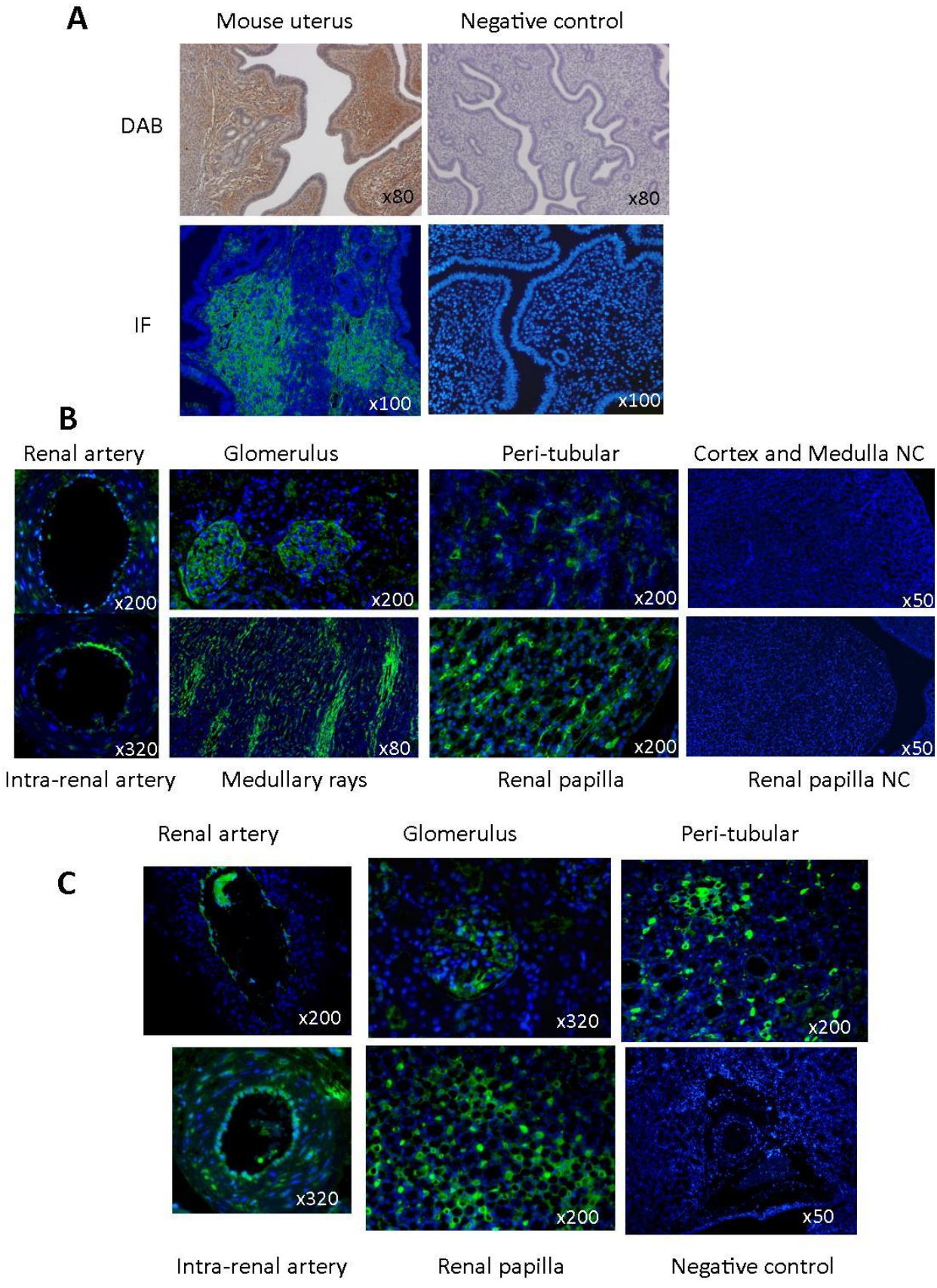
A
Mouse uterus
Negative control
DAB
IF
x80
x80
x100
x100
B
Renal artery
Glomerulus
Peri-tubular
Cortex and Medulla NC
x200
x200
x200
x50
x320
x80
x200
x50
Intra-renal artery
Medullary rays
Renal papilla
Renal papilla NC
C
Renal artery
Glomerulus
Peri-tubular
x200
x320
x200
x320
x200
x50
Intra-renal artery
Renal papilla
Negative control

## Figure 4.6 Distribution of RXFP1 expression in cirrhosis

(**A**). Representative images of RXFP1 DAB and IF staining in mouse uterus which was used as a positive control. (**B**). 16 week $CCl_4$ kidney sections showing RXFP1(green) expression throughout the kidney, in extra and intra renal arteries, glomerulus and peri-tubular region, medullary rays and the renal papilla. (**C**) 28 day BDL kidney sections stained for RXFP1. Magnification as shown.

### 4.8 RXFP1 is expressed in the kidney on endothelial cells, smooth muscle cells and renal pericytes

To establish the key cells expressing RXFP1 in these models I utilised both dual IF and serial section staining. For these co-localisation stains I focussed on the $CCl_4$ tissue as I had shown a consistent expression profile (**Fig 4.6**) between models. **Fig 4.7A and B** shows that there did not appear to be any co-localisation with WT1 expressing podocytes. There was convincing co-localisation with rat endothelial cell antibody (RECA) stained endothelial cells in renal arteries (**Fig 4.8**). Again there was consistent overlap with αSMA positive cells in renal arteries (**Fig 4.9**). Finally, there was possible co-localisation with PDGFβ positive pericytes (**Fig 4.10A-B**).

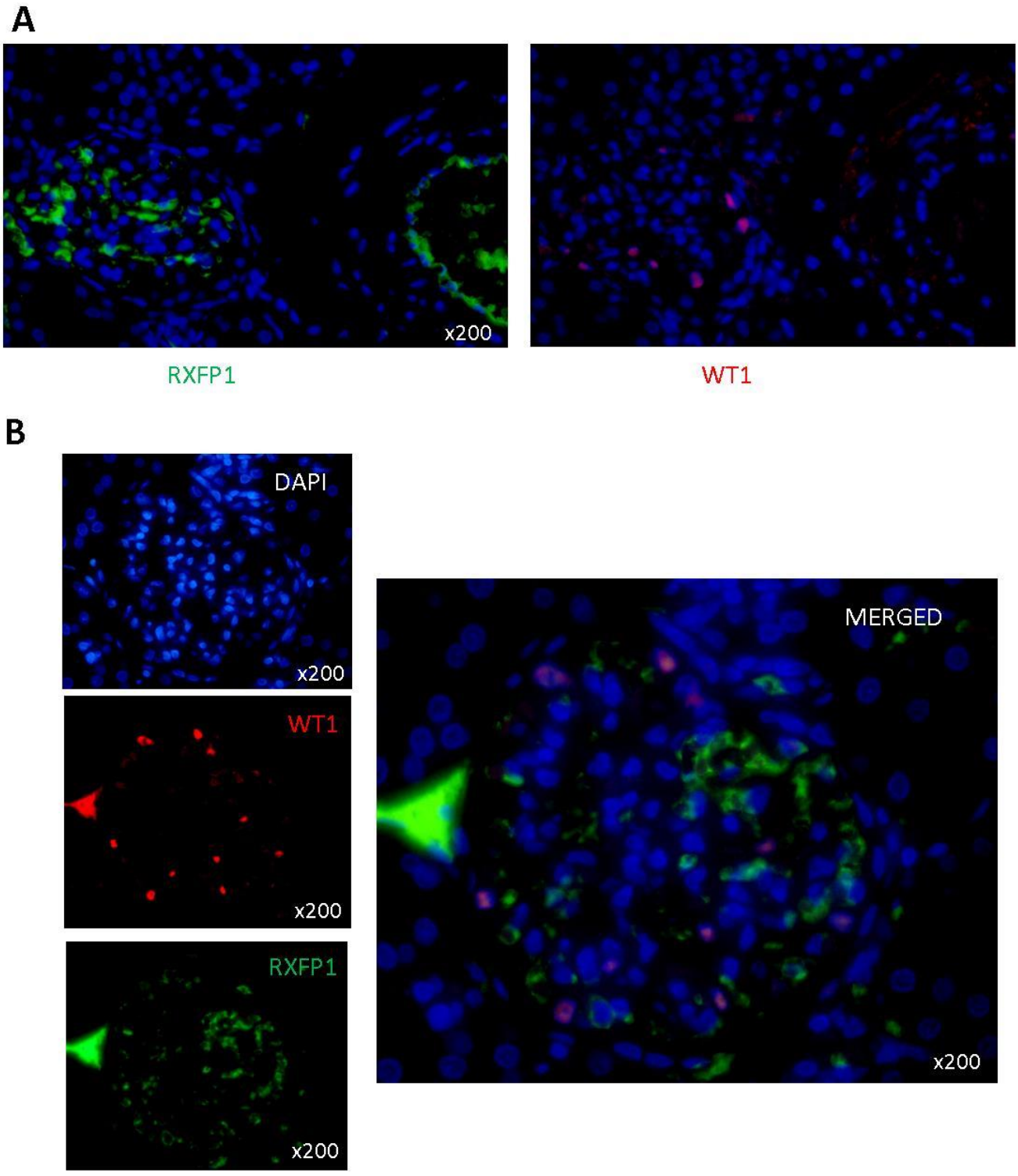


**Figure 4.7 Serial sections and Dual Immunofluorescence of RXFP1 and WT1 expressing podocytes**

(**A**) Serial sections of 16 week $CCl_4$ kidney were stained for RXFP1(green) and WT1(red) and DAPI (blue). (**B**) Dual immunofluorescence. Original magnification x200.

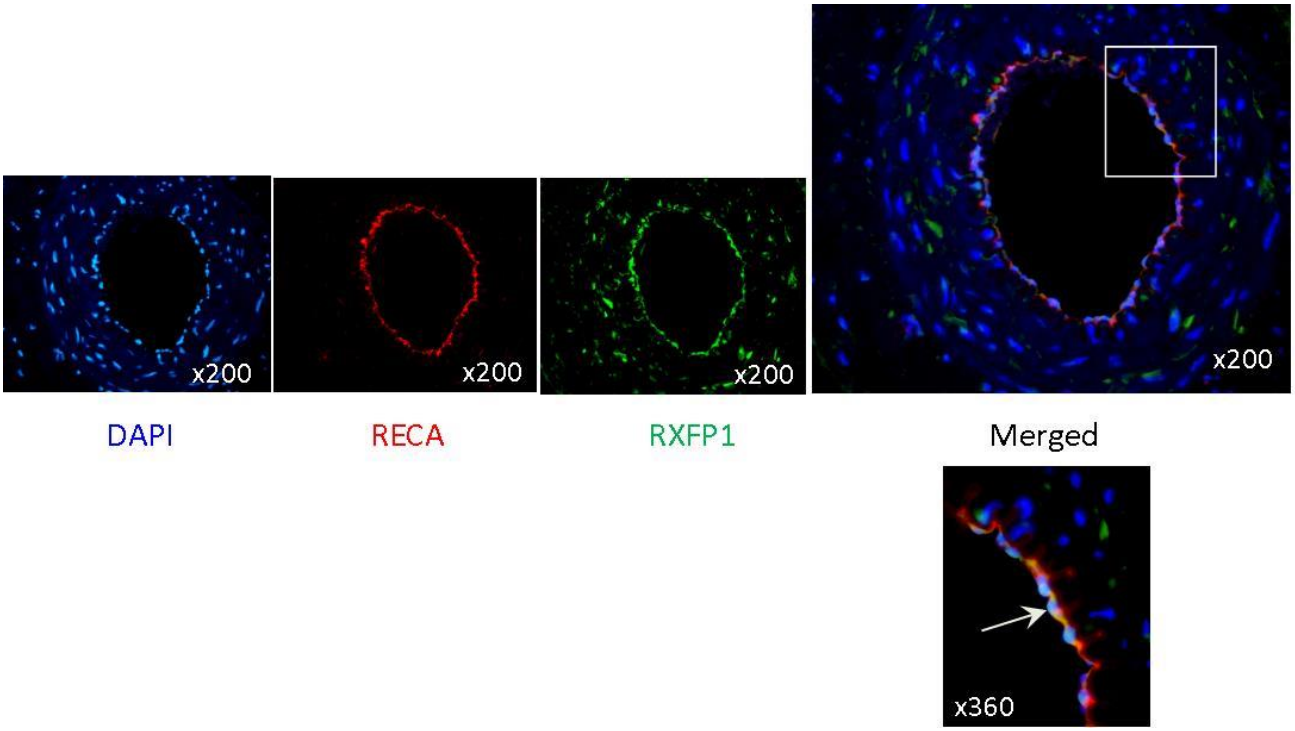


## Figure 4.8 Dual Immunofluorescence of RXFP1 and RECA

16 week $CCl_4$ renal artery sections were stained using dual immunofluorescence for rat endothelial cell marker (RECA;red) and RXFP1(green) with DAPI(blue) for nuclear stain. Co-localisation was seen on the endothelial cells (arrow). Original magnification x 200. Area of co-localisation highlighted with arrow, x360 magnification.

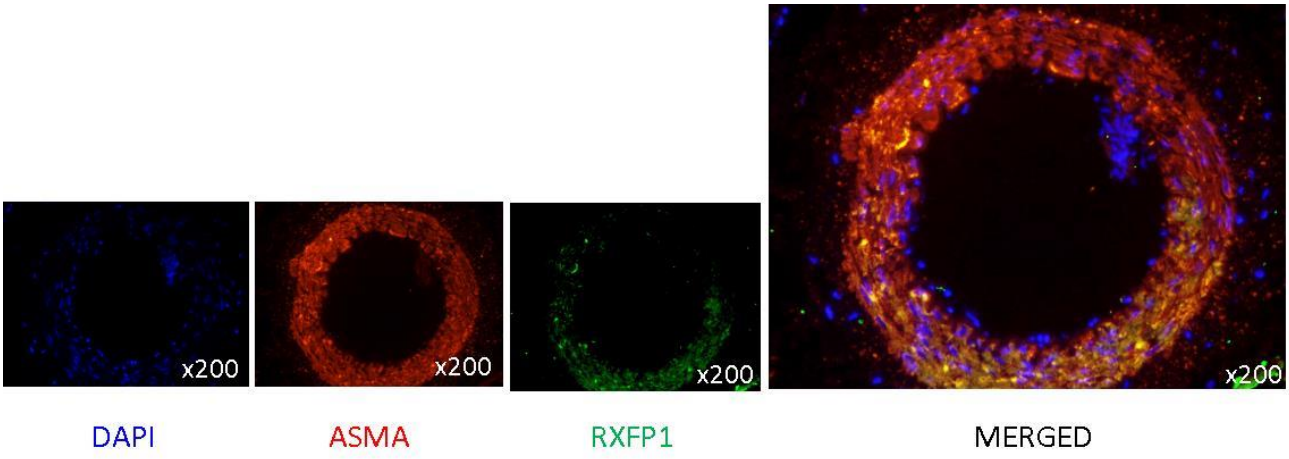


## Figure 4.9 Dual Immunofluorescence of RXFP1 and ASMA

16 week CCl4 renal artery sections were stained using dual immunofluorescence for ASMA and RXFP1. Co-localisation was seen on the smooth muscle cells. Original magnification x 200.

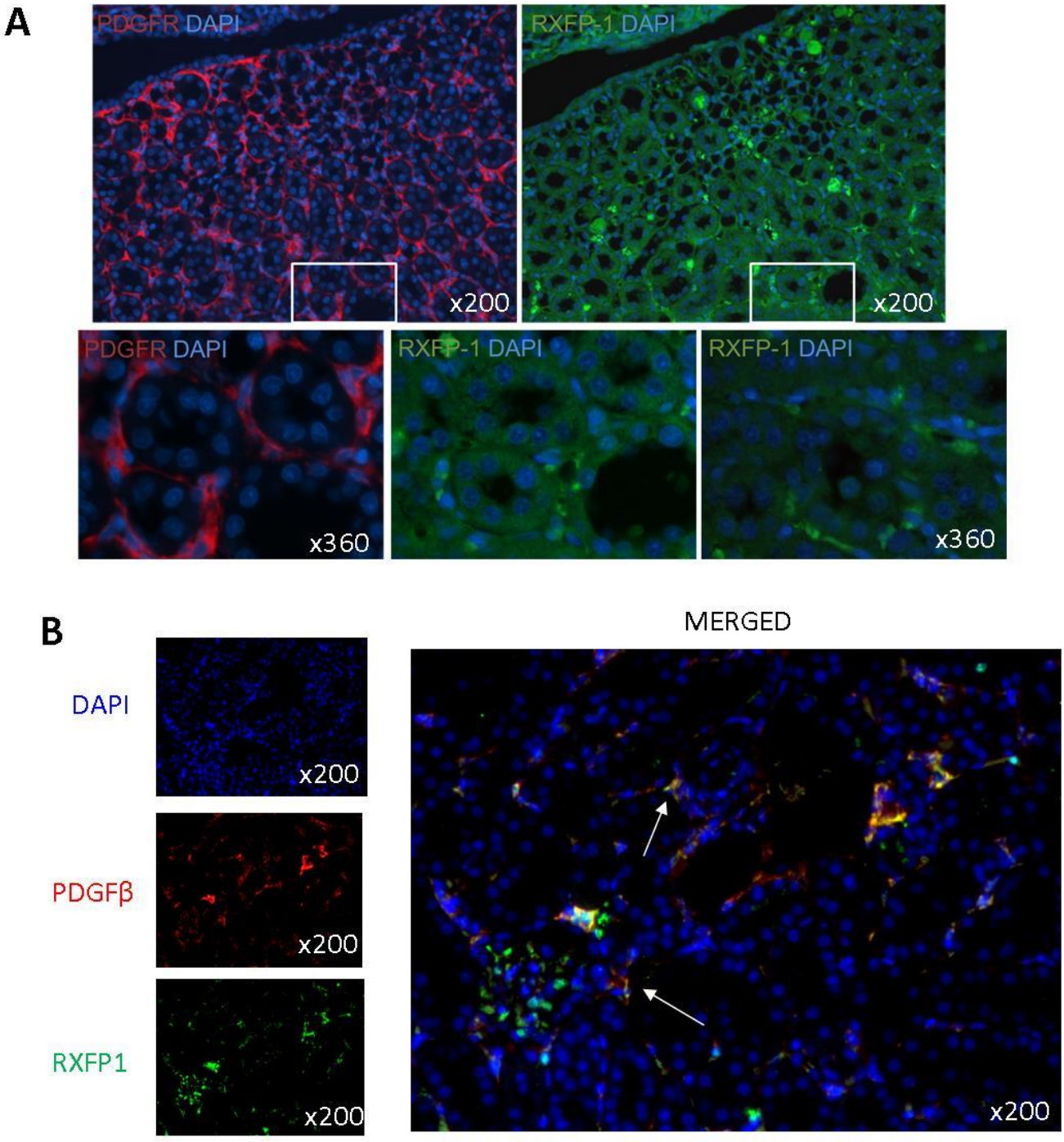


**Figure 4.10 Serial Section and Dual Immunofluorescence of RXFP1 and PBGFβ**

16 week $CCl_4$ kidney serial sections were stained for PDGFβ (red) and RXFP1(green) (**A**). Dual immunofluorescence with PDGFβ and RXFP1 in 16 week kidney tissue (**B**). Possible co-localisation is seen, arrow. Original magnification x 200 and x 360.

### 4.9 RXFP1 is expressed in human kidney on endothelial cells, smooth muscle cells and pericytes

Kidneys are rarely biopsied from cirrhotic patients, even with AKI. Therefore to establish cellular expression of RXFP1 in human HRS remains difficult. I obtained normal human kidney tissue, harvested from organs that had been surgically removed due to cancer. I analysed these tissues firstly, using single stain RXFP1 IF (**Fig 4.11A**), which confirmed a similar staining pattern to both cirrhosis models. Secondly I undertook dual IF with an endothelial marker (CD31), a smooth muscle cell marker (αSMA) and a pericyte marker (PDGFβ). **Fig 4.11 B**,**C and D** show respective co-localisation images, which were in broad agreement with my findings in rat kidney.

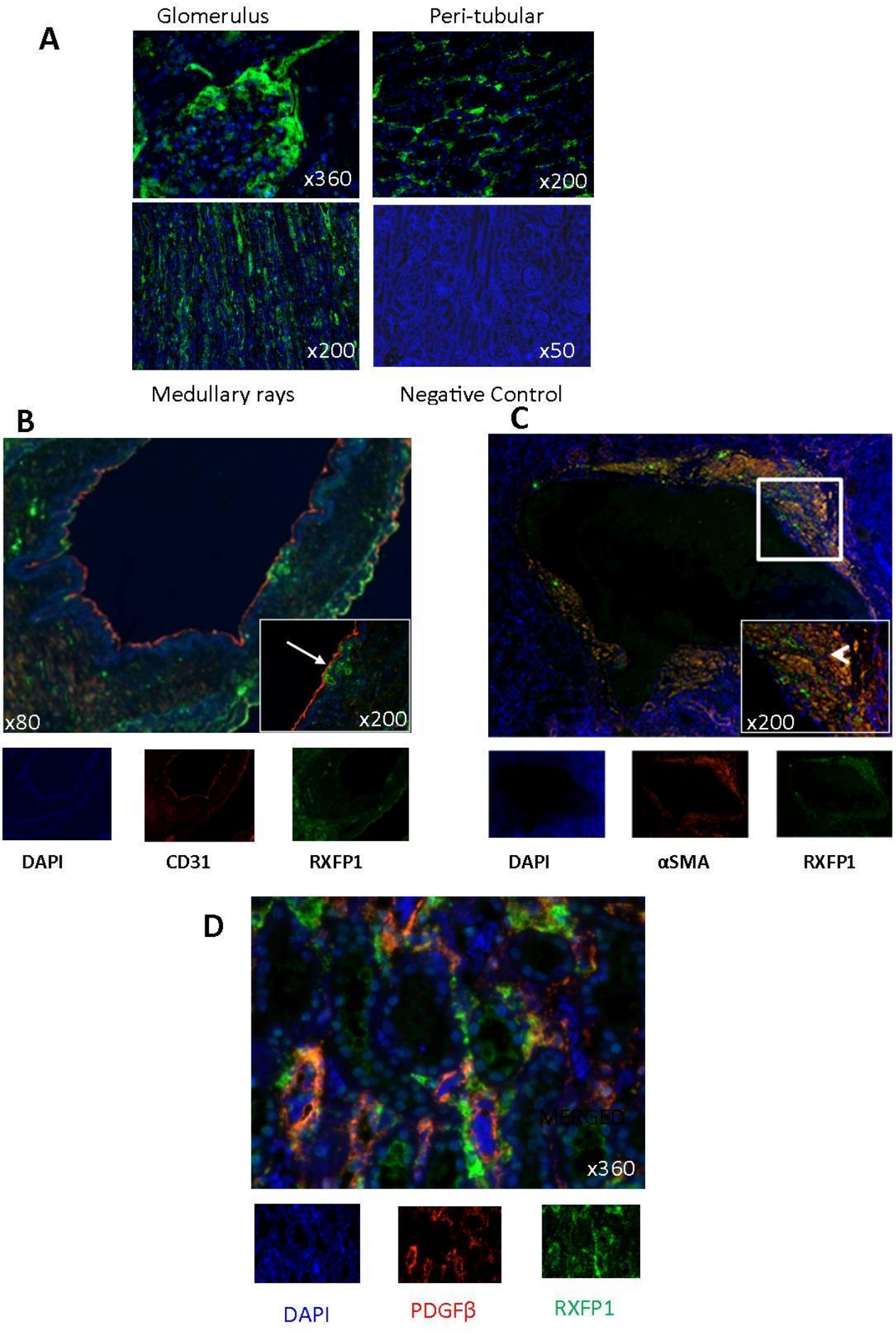
A
Glomerulus
Peri-tubular
x360
x200
x200
x50
Medullary rays
Negative Control
B
C
x80
x200
x200
DAPI
CD31
RXFP1
DAPI
αSMA
RXFP1
D
MERGED
x360
DAPI
PDGFβ
RXFP1

## Figure 4.11 RXFP1 staining in the Human Kidney

Human kidney, stained with single IF for RXFP1 (green) (**A**). Dual IF with CD31 (endothelial marker;red; arrow showing co-localistation;**B**), ASMA (smooth muscle marker;red; triangle showing co-localisation; **C**) and PDGFβ (pericyte marker;red; **D**). Magnification as shown.

## DISCUSSION

I have shown that *Rxfp1* mRNA transcript levels are increased in the $CCl_4$ and BDL models in the liver and kidney with an increase in the renal artery expression in the $CCl_4$ model of cirrhosis and a trend in the BDL model. With regards the renal artery results in BDL, the non-significant results are likely due to the small sample size as I analysed n=4 and the expression was variable. This could be in part due to differences in the relative area of the renal artery that was used in RNA extraction. My aim was to cut across the artery to achieve a cross sectional piece incorporating smooth muscle and endothelium. However, given the small nature of this sample, this may have not been consistent, resulting in greater variation in the renal artery results. Additionally, I have shown that these expression changes are not limited to transcript changes with increasing RXFP1 protein expression in the liver and kidney in $CCl_4$ cirrhosis and a trend to increase in the BDL model. This latter finding may reflect an issue with technique. Using Western blot for measuring expression relies on incorporating an equal amount of cortex/medulla/renal vasculature into the sample, therefore for a set protein amount you may get differing levels of expression depending on what makes up that particular sample, as it is not clear whether there is more expression in the medulla or cortex.

Although detailed investigation of the mechanism of RXFP1 gene regulation in rat cirrhosis models was beyond the scope of this thesis, recent data in myocardium suggested that RXFP1 expression is regulated by α1 and β1 adrenoceptors (Moore, Su et al. 2014). In the liver it is tempting to speculate, given that RXFP1 is known to be expressed on myofibroblasts (Fallowfield, Hayden et al. 2014) that increasing expression of this cell type in fibrogenesis leads to increasing expression of RXFP1. However, this hypothesis cannot explain why it is increased in the renal vasculature and kidney as there is no evidence that either $CCl_4$ or BDL induce fibrosis in the kidney or vasculature. It may well be unique to different organs and vascular beds. To attempt to answer this question I needed to know which cells expressed RXFP1 in the kidney.

From co-localisation staining I have shown expression of RXFP1 on endothelial cells, smooth muscle cells and pericytes (**Fig 4.9** and **4.10**). This is in agreement with previous literature in healthy rodents (Jelinic, Leo et al. 2014). These are all cells integral to renal blood flow regulation and vascular reactivity, making them promising targets for therapeutic modulation. Despite thorough optimisation and the use of tyramide, I had many problems with the secondary antibodies cross reacting with the primary antibodies as my antibodies were all raised in Rabbit. Most of my issues with the methodology in this current chapter of work were due to the quality of RXFP1 antibodies available. I consistently used the Santa Cruz one for all rat IF work to prevent additional variables, such as antibody affinity, compromising my findings. Additionally, despite promising results with the Phoenix antibody in the liver I was unable to get this antibody to work using IF thereby limiting its use in establishing co-localisation. Commercially available RXFP1 antibodies appear to lack specificity, and despite extensive troubleshooting, I did not manage to obtain a completely clear answer to my questions. In situ hybridisation is an alternative technique that could be used in the future to help clarify/confirm the cellular source of RXFP1.

Finally, I have shown that RXFP1 cellular expression in human kidney tissue appears analogous to that in the rodent. This represents an important finding. By sharing a similar expression profile one can postulate that RLN may work in a mechanistically similar way between species.

**Summary of important findings:**

- *Rxfp1* mRNA transcripts are increased in the liver and kidney in both rat cirrhosis models
- RXFP1 protein is detectable in both models of cirrhosis in the kidney and its expression appears to increase in cirrhosis
- RXFP1 co-localised to endothelial cells, smooth muscle cells and pericytes in rat and human kidney tissue - cell types that are implicated in regulation of RBF and GFR

**Next steps:**

Having established the presence of RXFP1 in the renal vasculature and kidneys in both $CCl_4$ and BDL cirrhosis models the next step was to determine the *in vivo* effect of RLN in these models.

# CHAPTER 5 - RESULTS -

# THE EFFECTS OF EXOGENOUS RLN *IN VIVO*

# IN PRE-CLINICAL CIRRHOSIS MODELS

## 5.1 Overview of Chapter:

In this chapter I used both models of cirrhosis with renal vasoconstriction and renal dysfunction to determine the effect of exogenous RLN on renal and systemic haemodynamics. I firstly investigated the pharmacodynamic effects of a single acute bolus of RLN on renal and systemic haemodynamics and then proceeded to study the effect of an extended subcutaneous (s.c.) RLN infusion on renal function, which is the pivotal end point of interest in human HRS. I utilised not only invasive monitoring to study changes in renal and systemic haemodynamics in response to exogenous RLN, but also evaluated the use of non-invasive imaging tools - USS and BOLD MRI - to measure changes in velocity time integral and resistive index and renal oxygenation, respectively.

## 5.2 Author Contribution:

I designed, performed all the invasive experiments in this chapter and did all the analysis. Adrian Thomson operated and optimised the USS technique and Ross Lennen operated and optimised the BOLD MRI imaging.

## 5.3 Background:

Summarising briefly what I discussed in the Introduction, endogenous RLN has been shown to have pleiotropic effects in matrix and collagen turnover, vascular remodelling and haemodynamic adaptations to pregnancy (Conrad 2010). It has been shown to be an important mediator of the maternal haemodynamic adaptations to pregnancy in both humans and rodents (Debrah, Novak et al.

2006; Smith, Murdoch et al. 2006). RLN's effects in the systemic circulation are increased cardiac output, increased global arterial compliance, reduced systemic vascular resistance and in the renal circulation, increased RBF, increased GFR and reduced renal vascular resistance. All these vascular effects have been recapitulated using exogenous H2-RLN in both male and non-pregnant female rodents and importantly no decrease was seen MAP due to the increased cardiac output through increased stroke volume (Conrad, Debrah et al. 2004; Debrah, Conrad et al. 2005; Debrah, Conrad et al. 2005). Arteries from RLN deficient mice show increased myogenic reactivity and reduced compliance (Novak, Parry et al. 2006). Furthermore, a study in healthy human volunteers showed an increase in renal plasma flow as early as 30 minutes in response to exogenous RLN infusion with no drop in MAP (Smith, Danielson et al. 2006). More recent studies in patients with acute and chronic heart failure and a study in patients with scleroderma have also shown that exogenous RLN improved renal function.

Therefore, there is fairly compelling evidence that exogenous RLN may improve RBF and renal function in certain disease states. Given the hypothesis that functional renal arterial vasoconstriction (Epstein, Berk et al. 1970; Gines, Guevara et al. 2003) is central to HRS development, a drug that can modulate this directly could be very beneficial. Previous work has suggested that RLN preferentially vasodilates pre-constricted vessels, adding promise to my hypothesis of its potential beneficial effects in HRS (Debrah, Conrad et al. 2005; Teichman, Unemori et al. 2009). Furthermore, I have shown the presence of RXFP1, RLN's major receptor in the kidneys and particularly the renal arteries of cirrhotic rats and that this expression profile is the same as human kidney.

There has been significant work undertaken in normal rodents on dosing and duration of exogenous H2-RLN to recapitulate the endogenous effects seen in pregnancy, to summarise:

- The first conclusion is that H2-RLN is the functional orthologue of rat and mouse RLN, though their amino acid sequence is not homologous (Halls, van der Westhuizen et al. 2007).
- Second, all studies in these normal rats used H2-RLN and have shown robust effects suggesting that its effects are not limited to its species, summarised in (Conrad 2010).
- Third, given it is also the drug given to humans, it stands to reason that for translational potential I should use the human recombinant form, given that it is also known to have effects in rodents.

Exogenous RLN administration has been shown to produce a U-shaped, biphasic dose response curve (Danielson and Conrad 2003; Debrah, Conrad et al. 2005) with 4µg/hr producing peak renal and systemic effects with serum RLN levels of 10-20ng/mL, whereas 40µg/hr produced serum RLN levels of 80ng/mL with minimal renal effects. I therefore chose 4µg/hr as the dose to work with in my rodent models. It is also known that duration of exposure to RLN also affects the downstream pathway activation (**Section 1.12**). Isolated vessels can rapidly dilate in minutes (Fisher, MacLean et al. 2002), with *in vivo* experiments suggesting that more sustained exposure resulted in an increase in RBF and GFR peaking at 24 hours and persisting with duration of exposure (Danielson, Kercher et al. 2000; Danielson and Conrad 2003).

To date, no other groups have looked at the effect of H2-RLN on renal and systemic haemodynamics in rat models of cirrhosis with renal vasoconstriction and dysfunction.

### 5.4 Aims of this Chapter:

- To define the acute effect of a single i.v. bolus of H2-RLN on renal and systemic haemodynamics in control and cirrhotic rats
- To establish non-invasive imaging techniques to monitor changes in renal and systemic haemodynamics in response to H2-RLN in these models
- To assess the effect of sustained H2-RLN infusion on systemic and renal haemodynamics and renal function

## RESULTS

### 5.5 Renal blood flow is augmented by a single bolus of recombinant human H2-RLN (serelaxin)

In preliminary experiments of n=4 rats, I firstly established that a 200µL volume challenge did not cause a rapid change in RBF (**Fig 5.1A)** though a non-clinically relevant reduction was seen in MAP by 5 mins relative to baseline (0 mins: 105.6±7.5mmHg versus 5 mins: 102.4±7.9mmHg; $p<0.05$) (**Fig 5.1B**) when monitored invasively under general anaesthetic. The question I was trying to answer with this experiment was whether a bolus of 200µL caused relevant changes in these parameters, which would limit observation of RLN's effects. This did not appear to be the case.

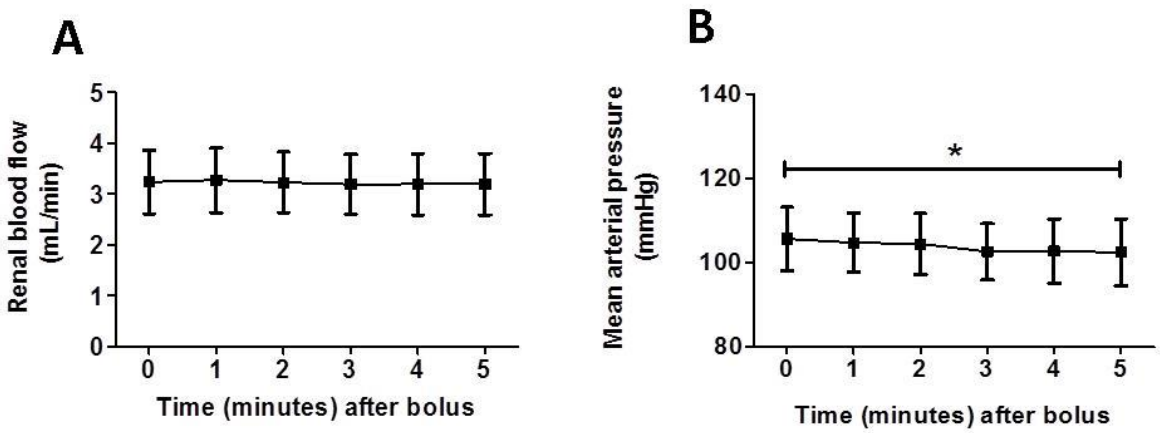


## Figure 5.1 Effect of bolus of Vehicle on Renal Blood Flow and Mean Arterial Pressure

Anaesthetised 16 week $CCl_4$ rats were given an i.v bolus of 200 µL of normal saline and their RBF, measured by flow probe for 5 mins (**A**), MAP , measured by femoral arterial line, for 5 mins. (**B**). Data expressed as mean±SEM and analysed by one-way ANOVA with post hoc Bonferroni test. *p<0.05.

Subsequently, I undertook a small feasibility study to establish that the dosing suggested by the literature was valid in my model. I treated 16 week $CCl_4$ rats, anaesthetised with Inactin, with an i.v. bolus of RLN of 1,4,10 or 20 µg in 200 µL via their jugular vein and monitored them for up to 80 minutes. This was not a formal dose-response study, with only n=1 rat studied per dose. My aim was firstly to establish that with my invasive monitoring, under general anaesthetic, I was able to detect changes in RBF and MAP and, secondly, to ensure that the 4µg dose was sufficient for this acute study. My justification for this approach was that there are good publications on dosing of H2-RLN and, to try to abide by the 3R's philosophy, I felt that the rats were better utilised in establishing novel results rather than repeating experiments. If there had not been sufficient literature to base my dosing decision on, I would have planned a larger scale dose-response study. In **Fig 5.2A** and **B**, there was an observed increase in RBF seen with 1, 4 and 10µg, with 4µg giving the most apparent change from baseline at 60 minutes. With 20µg a reduction in RBF was seen. Furthermore, with 1

and 4µg there was no drop in MAP. However this appeared more labile at higher doses (**Fig 5.2C**). The conclusion I drew from this limited experiment was that I would continue using 4µg of RLN for my acute experiments.

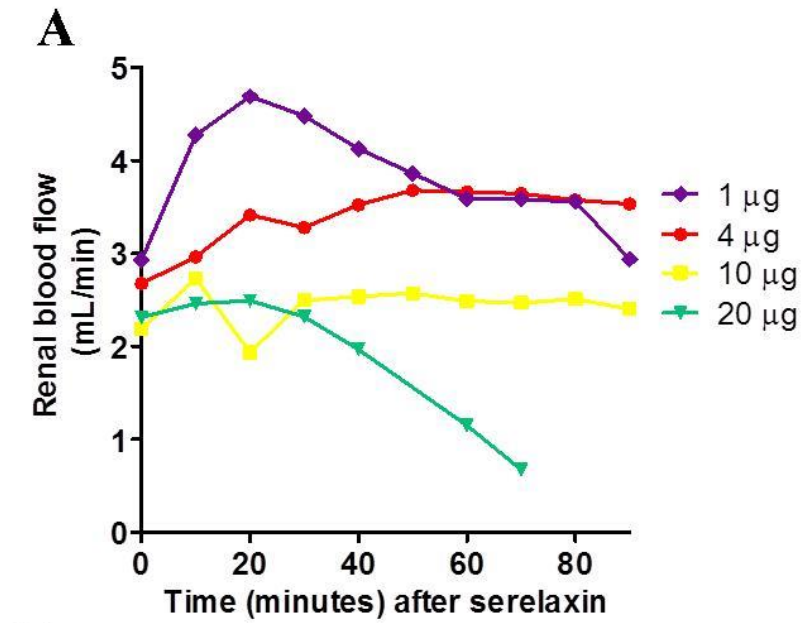
A
Renal blood flow (mL/min)
Time (minutes) after serelaxin
1 µg
4 µg
10 µg
20 µg

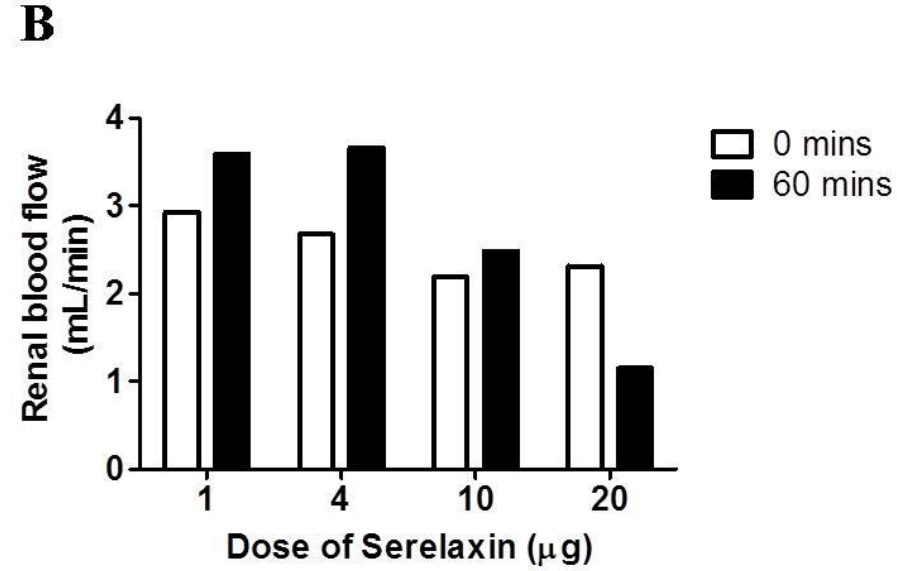
B
Renal blood flow (mL/min)
Dose of Serelaxin (µg)
0 mins
60 mins

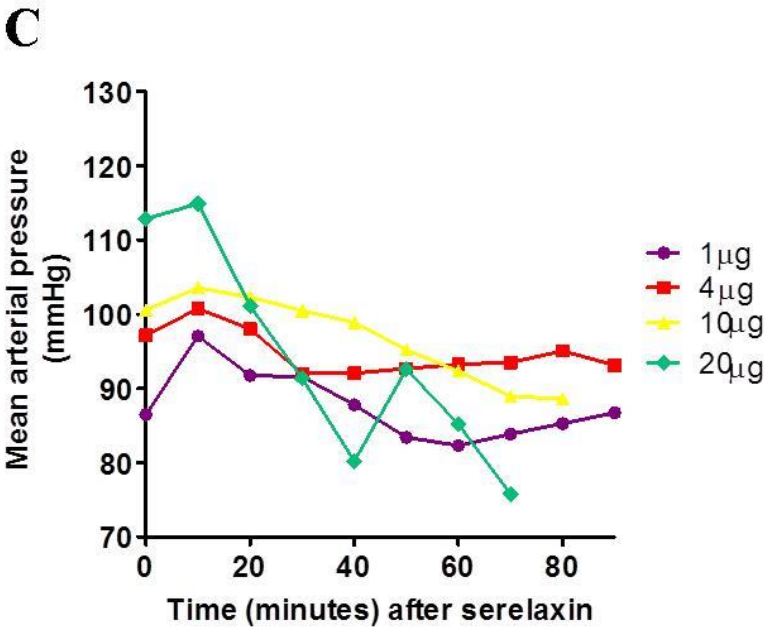
C
Mean arterial pressure (mmHg)
Time (minutes) after serelaxin
1µg
4µg
10µg
20µg

## Figure 5.2 Effect of Different Doses of Relaxin on Renal Blood Flow and Mean Arterial Pressure in 16 week $CCl_4$ cirrhotic rats

16 week CCl4 rats, 24-48 hours after their last $CCl_4$ injected, were anaesthetised and their RBF (**A**) and MAP (**C**) monitored invasively for 80 minutes in response to i.v. bolus of 1, 4, 10 or 20µg of RLN. (**B**) RBF at 0 compared to 60 mins. Data expressed as individual rat, n=1 per dose.

I treated anaesthetized control (uninjured n=5/group) and 16 week $CCl_4$ rats (n=6/group) with either a single i.v. bolus of RLN (4µg in 200 µL via jugular vein) or equivalent volume of vehicle and monitored their RBF, MAP and HR invasively for 60 mins. The mean serum RLN level after 60 mins was 6.0±0.3 ng/mL. **Fig.5.3** shows the relative change in RBF. There was a progressive increase in RBF seen in both the 16 week $CCl_4$ cirrhotic (**Fig. 5.3A**) and control rats (**Fig. 5.3B**) given RLN compared to vehicle. Cirrhotic rats showed an increased relative rise in RBF compared with their uninjured counterparts, in response to RLN (**Fig 5.3C**). Looking at absolute changes, after a single bolus of RLN RBF increased in the $CCl_4$ model from 2.0±0.3mL/min at baseline to 2.79±0.5mL/min at 30 minutes ($p<0.01$) to 3.1±0.5mL/min at 60 minutes ($p<0.001$) **Fig 5.3D**: a 50% increase in RBF.

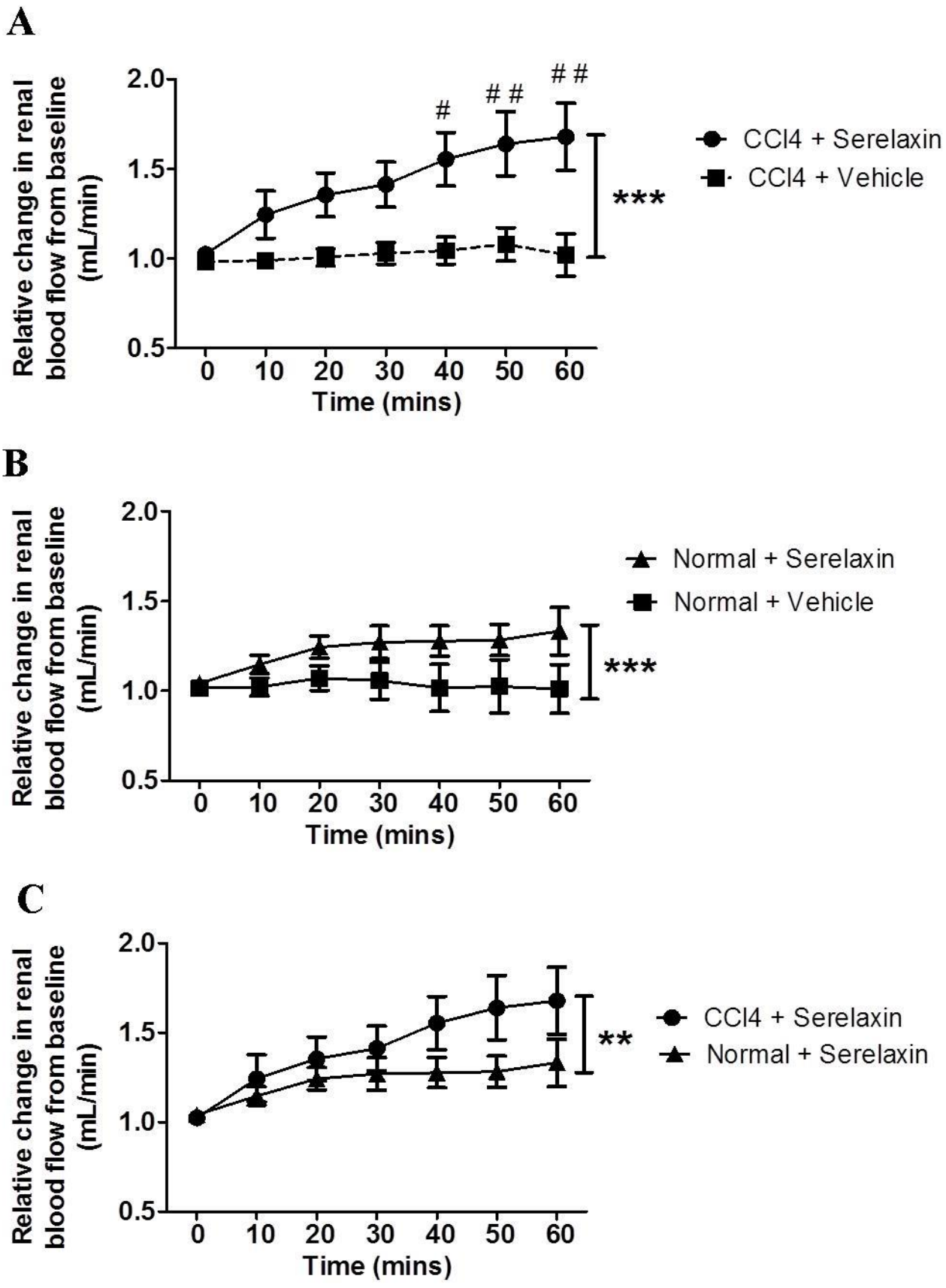
A
Relative change in renal blood flow from baseline (mL/min)
2.0
1.5
1.0
0.5
0
10
20
30
40
50
60
Time (mins)
#
# #
# #
***
CCl4 + Serelaxin
CCl4 + Vehicle
B
Relative change in renal blood flow from baseline (mL/min)
2.0
1.5
1.0
0.5
0
10
20
30
40
50
60
Time (mins)
***
Normal + Serelaxin
Normal + Vehicle
C
Relative change in renal blood flow from baseline (mL/min)
2.0
1.5
1.0
0.5
0
10
20
30
40
50
60
Time (mins)
**
CCl4 + Serelaxin
Normal + Serelaxin

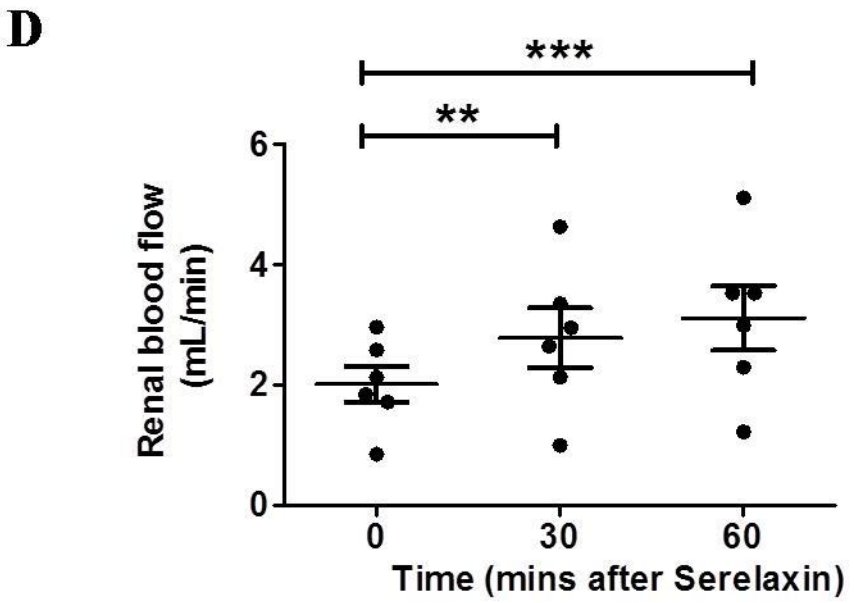


## Figure 5.3 Effect of Single Dose Relaxin on Renal Blood Flow in 16 week $CCl_4$ cirrhotic and normal uninjured rats

Anaesthetized control (uninjured n=5/group) and 16 week $CCl_4$ rats (n=6/group) were treated with a single i.v. bolus of RLN (4µg in 200 µL via jugular vein) or equivalent volume of vehicle and their RBF monitored invasively for 60 minutes. (**A**) RBF change in 16 week $CCl_4$ rats RLN versus vehicle (**B**) RBF in normal uninjured rats, RLN versus vehicle. (**C**) RBF change in 16 week CCl4 versus normal given RLN. Data was expressed relative to mean RBF pre-RLN, which was given the value of 1, and analysed by repeated measures ANOVA with post-hoc Bonferroni test. (**D**) Absolute RBF in CCl4 group given RLN (**D**). Data expressed as individual values and analysed by one way ANOVA with post-hoc Bonferroni test. *p<0.05 **p<0.01 ***p<0.001.

### 5.6 There was no drop in mean arterial pressure after a single bolus of RLN

I monitored the MAP via a femoral arterial line for 60 mins after the i.v. bolus of RLN or vehicle. A potential concern for using any vasodilator is the risk of inducing hypotension, which in cirrhotic patients, as they often have low MAPs, might induce a detrimental reduction. My results show that

even at the extreme of the $CCl_4$ model there was no drop in MAP in response to RLN (**Fig 5.4A**). Furthermore there was no difference in MAP in the rats given RLN versus vehicle (**Fig 5.4B**). The significant increase in RBF after RLN, with no change in MAP, indicates that RLN is acting as a selective renal vasodilator.

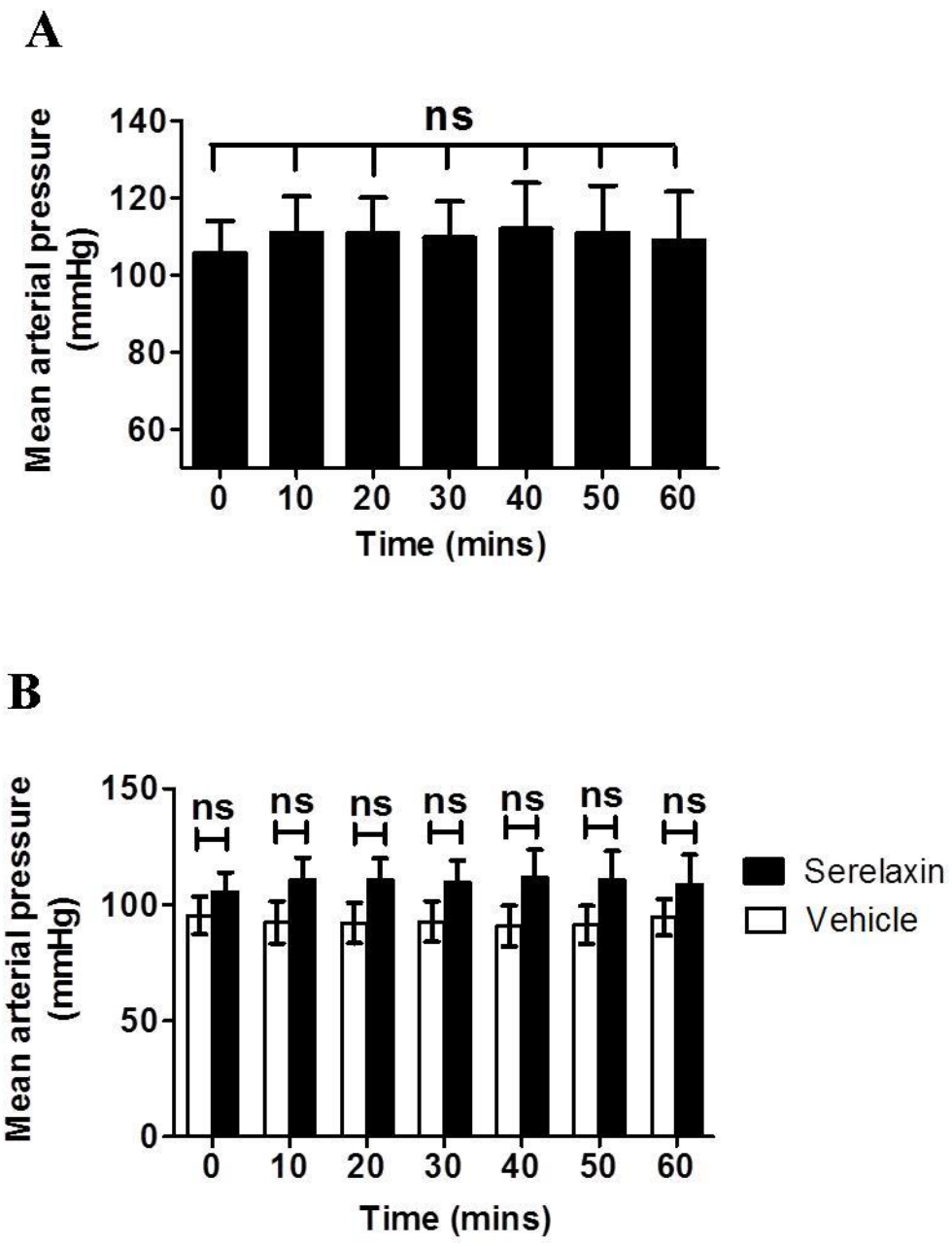

## Figure 5.4 Effect of Single Dose Serelaxin on Mean Arterial Pressure in 16 week $CCl_4$ cirrhotic rats

16 week $CCl_4$ rats. MAP was monitored invasively via the femoral arterial line for 60 mins after RLN or same volume vehicle. **(A)** MAP in rats given RLN. Analysed by repeated measures ANOVA with post-hoc Bonferroni test. **(B)** MAP in RLN versus vehicle, analysed by two way ANOVA with post hoc Bonferroni test.

### 5.7 Non-invasive Doppler ultrasound confirms augmentation of renal blood flow after a single i.v. bolus of RLN

Although invasively monitoring RBF using a renal flow probe wrapped around the renal artery is a well-established technique for monitoring real time changes in renal haemodynamics in rodents, it is not a technique that we would use in humans due to its invasive nature. Additionally, the process of cannulating arteries and veins and performing a laparotomy to visualise the renal artery leads to fluid shifts, which is an additional potentially confounding variable. Although I ensured the surgery was optimised with regards to fluid losses, criticisms still remained as to the validity of using this method to monitor real time changes in response to vasoactive drugs. With this in mind I went on to use Doppler ultrasound. Doppler USS is used routinely in clinical practice and as such remains a potential technique with which to translate findings from murine models to humans more easily. Using this non-invasive technique allowed me to firstly corroborate my invasive findings and secondly to monitor parameters I had not been able to before, such as cardiac output.

16 week $CCl_4$ cirrhotic rats (n=14) were anaesthetised using isoflurane. This inhalational agent was used as it allows the operator more control over the onset and depth of anaesthesia compared to

injectable inactin. A baseline scan was performed and then the Doppler trace was measured continuously for 60 minutes. During this time I collected data every 10 minutes. **Fig. 5.5**, I have shown results of the effect of RLN (4µg i.v.) or vehicle on Velocity Time Integral (VTI). VTI is calculated by measuring the volume under the curve in time (schematic shown in **METHODS Fig 2.1**). An increase in renal arterial VTI (Baseline 2.6±0.3cm vs. 60 min 3.4±0.3cm, $p<0.05$) was seen with RLN (n=8), whereas no effect was seen with vehicle (n=6) (**Fig. 5.5A, B and C).** Examples of images obtained are shown in **Fig 5.5D.**

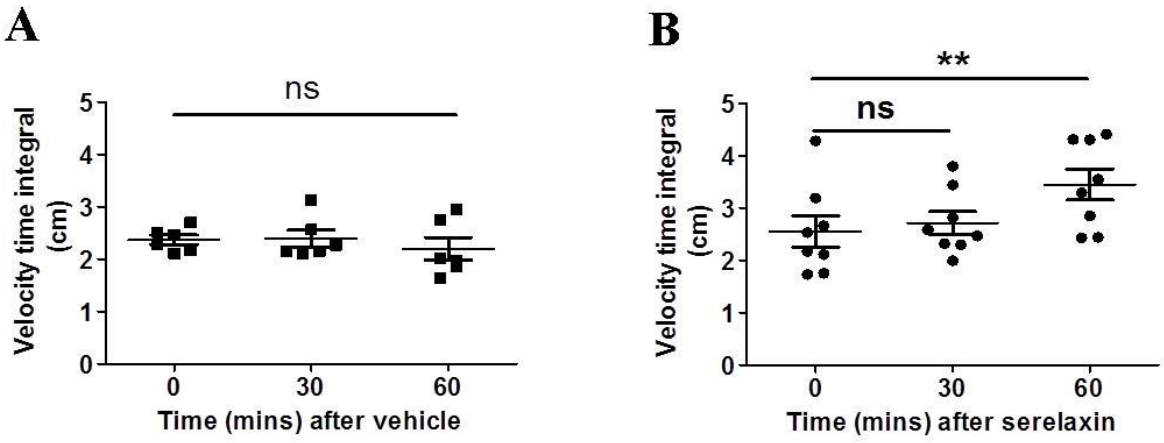
A
ns
Velocity time integral (cm)
Time (mins) after vehicle
B
**
ns
Velocity time integral (cm)
Time (mins) after serelaxin

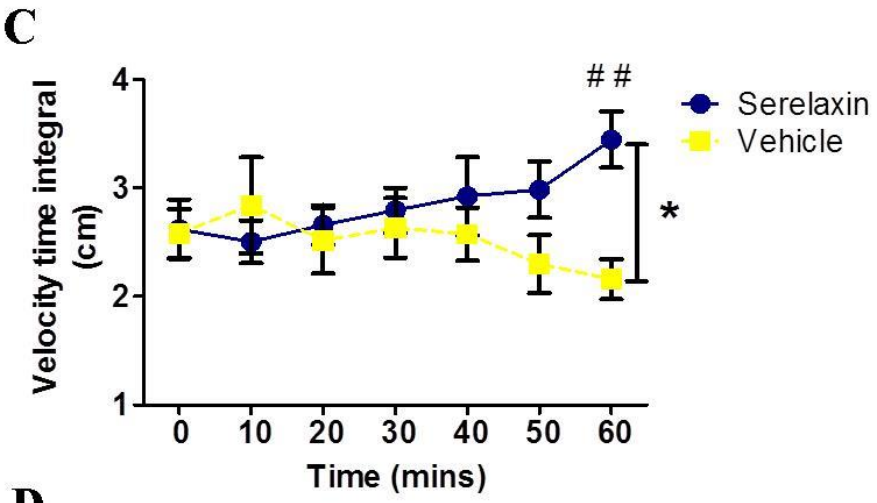
C
##
*
Serelaxin
Vehicle
Velocity time integral (cm)
Time (mins)

D

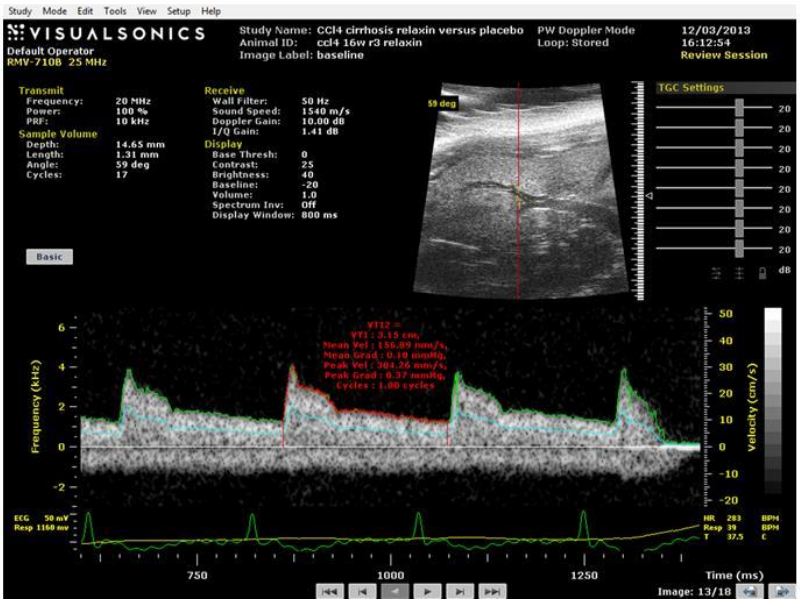
VISUALSONICS
Study Name: CCl4 cirrhosis relaxin versus placebo
Animal ID: ccl4 16w r3 relaxin
Image Label: baseline
PW Doppler Mode
Loop: Stored
12/03/2013
16:12:54
Review Session
Default Operator
RMV-710B 25 MHz
Transmit
Receive
Sample Volume
Display
TGC Settings
Basic
Frequency (kHz)
Velocity (cm/s)
Time (ms)
Image: 13/18

## Figure 5. 5 Effect of Single Dose Relaxin on Velocity Time Integral measured by Ultrasound Doppler

16 week CCl4 rats were anaesthetised and randomised to either vehicle (n=6) or RLN (n=8) and monitored for 60mins. VTI change in rats given vehicle (**A**), VTI change in rats given RLN (4µg i.v; **B**). Data expressed as individual data with mean±SEM and analysed by one way ANOVA with post-hoc Bonferroni test. RLN versus vehicle (**C)**. Data analysed by 2-way ANOVA with post-hoc Bonferroni test. Example of images obtained (**D**). *p<0.05 **p<0.01 ***p<0.001.

### 5.8 Renal Resistive Index is reduced by a single i.v. bolus of RLN

The renal resistive index or peak Pourcelot resistive index (RI) is a measure of renal arterial vasoconstriction. Platt et al were the first to show that RI was increased in HRS (Platt, Ellis et al. 1994). More recently RI has been shown in cirrhosis to correlate with MELD and Child-Pugh score, with higher scores seen in more decompensated patients (Culafic, Stulic et al. 2014) and a recent small study has shown increasing RI with reducing renal function in cirrhosis (Mindikoglu, Dowling et al. 2014). Currently it is not used routinely in clinical practice. A score of 0.6 is considered normal in a human intra-renal artery, with 0.7 the very upper limit of normal in native non-transplanted kidneys. There is limited data in murine models although the suggestion is that it is a similar range to humans (Kong, Chen et al. 2013). The RI is measured as shown in **Fig 2.2**. In our model peak RI decreased following RLN (baseline 0.68±0.02 vs. 60 min 0.63±0.01, p<0.01), with no effect seen with vehicle (**Fig.5.6 A, B)**. **Fig 5.6C** shows the effect on RI, measured every 10 minutes, with RLN reducing RI compared to vehicle. An example of the images obtained is shown **Fig 5.6D**.

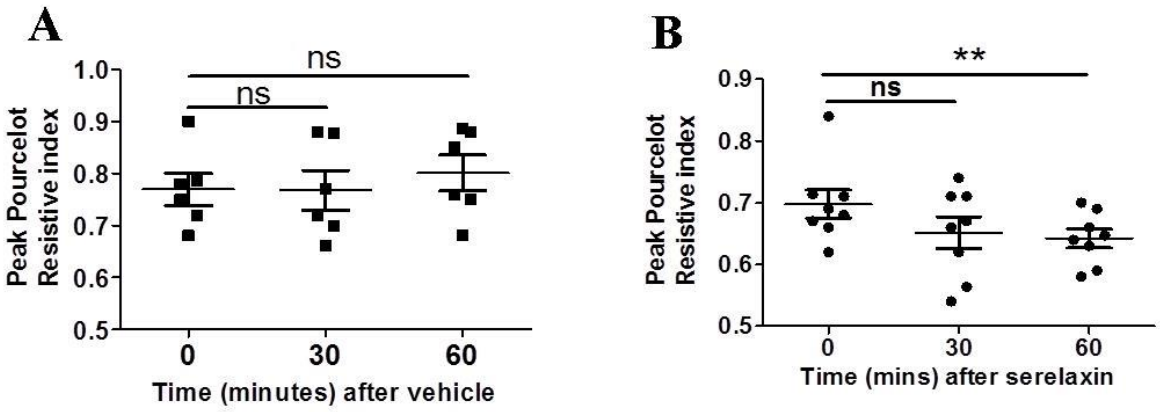
A
ns
ns
Peak Pourcelot Resistive index
1.0
0.9
0.8
0.7
0.6
0.5
0
30
60
Time (minutes) after vehicle
B
**
ns
Peak Pourcelot Resistive index
0.9
0.8
0.7
0.6
0.5
0
30
60
Time (mins) after serelaxin

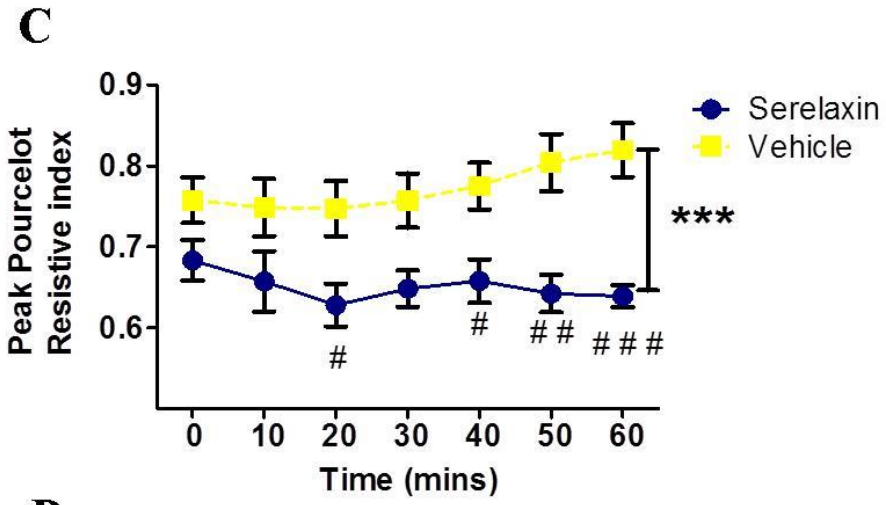
C
Peak Pourcelot Resistive index
0.9
0.8
0.7
0.6
Serelaxin
Vehicle
***
#
#
##
###
0
10
20
30
40
50
60
Time (mins)

D

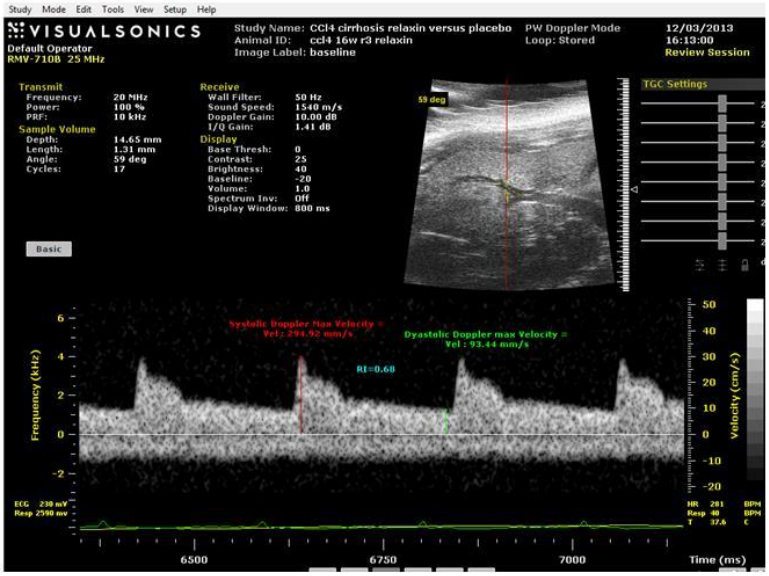
VISUALSONICS
Study Name: CCl4 cirrhosis relaxin versus placebo
Animal ID: ccl4 16w r3 relaxin
Image Label: baseline
PW Doppler Mode
Loop: Stored
12/03/2013
16:13:00
Review Session
Default Operator
RMV-710B 25 MHz
Transmit
Frequency: 20 MHz
Power: 100 %
PRF: 10 kHz
Sample Volume
Depth: 14.65 mm
Length: 1.31 mm
Angle: 59 deg
Cycles: 17
Receive
Wall Filter: 50 Hz
Sound Speed: 1540 m/s
Doppler Gain: 10.00 dB
I/Q Gain: 1.41 dB
Display
Base Thresh: 0
Contrast: 25
Brightness: 40
Baseline: -20
Volume: 1.0
Spectrum Inv: Off
Display Window: 800 ms
TGC Settings
Basic
Systolic Doppler Max Velocity =
Vel: 294.92 mm/s
Dyastolic Doppler max Velocity =
Vel : 93.44 mm/s
RI=0.68
Frequency (kHz)
Velocity (cm/s)
6500
6750
7000
Time (ms)

## Figure 5.6 Effect of Single Dose Relaxin on Resistive Index measured by Ultrasound Doppler

16 week $CCl_4$ rats were anaesthetised and randomised to either vehicle (n=6) or RLN (n=8) and monitored for 60mins. RI change in rats given vehicle (**A**), RI change in rats given RLN (4µg i.v; **B**). Data expressed as individual data with mean±SEM and analysed by one way ANOVA with post-hoc Bonferroni test. RLN versus vehicle (**C)**. Data analysed by 2-way ANOVA with post-hoc Bonferroni test. Example of images obtained (**D**). *p<0.05 **p<0.01 ***p<0.001.

### 5.9 Blood oxygen level dependent MRI showed reduced renal deoxygenated Haemoglobin in response to RLN

To complement my ultrasound blood flow analyses, I also assessed kidney parenchymal oxygenation using blood oxygen level-dependent magnetic resonance imaging (BOLD MRI) in anesthetized $CCl_4$ cirrhotic rats. BOLD MRI uses the paramagnetic properties of deoxyhaemoglobin to acquire images sensitive to local tissue oxygen concentration. As the deoxyhaemoglobin in blood increases the T2* relaxation time decreases and this produces measurable signal loss in these areas. The validity of this technique as a surrogate marker of oxygenation has been shown by studies that found comparable results between invasive measurements of oxygenation and BOLD MRI signal (Li, Halter et al. 2008). The loss of phase coherence (T2*) maps were generated in the kidney and regions of interest (cortex, outer medulla and inner medulla) were selected and R2* values were calculated by 1/T2*. R2* (relaxation rate) correlates inversely with the oxygenation of the kidney and is proportional to the level of deoxyhaemoglobin. As long as the temperature of the rat, sedation (respiration rate) and hydration remain constant so as to not increase R2*, any changes in this parameter should reflect changes to the blood supply of oxygenated blood, thereby making it a suitable non-invasive imaging tool to assess dynamic changes to blood supply.

Three baseline 3 minute scans were performed and RLN or equivalent volume of vehicle given i.v. through a tail vein cannula and 3 minute scans were repeated for 60 minutes post injection. In 8 week $CCl_4$ rats the R2*was reduced after 60 minutes in the renal cortex and outer medulla in response to acute i.v. RLN, which was not seen with same volume of vehicle (**Fig 5.7A-D**; n=7/group;*p<0.05). In the inner medulla these results were not reproduced (**Fig 5.7E-F**). In 16 week $CCl_4$ rats the R2* was reduced after 60 minutes in both the outer and inner medulla in response to RLN whereas no response was seen in the vehicle treated group (**Fig 5.8A-D**, n=4-5/group,*<0.05). However, no significant effect was seen in response to RLN in the cortex (**Fig 5.8E-F**).

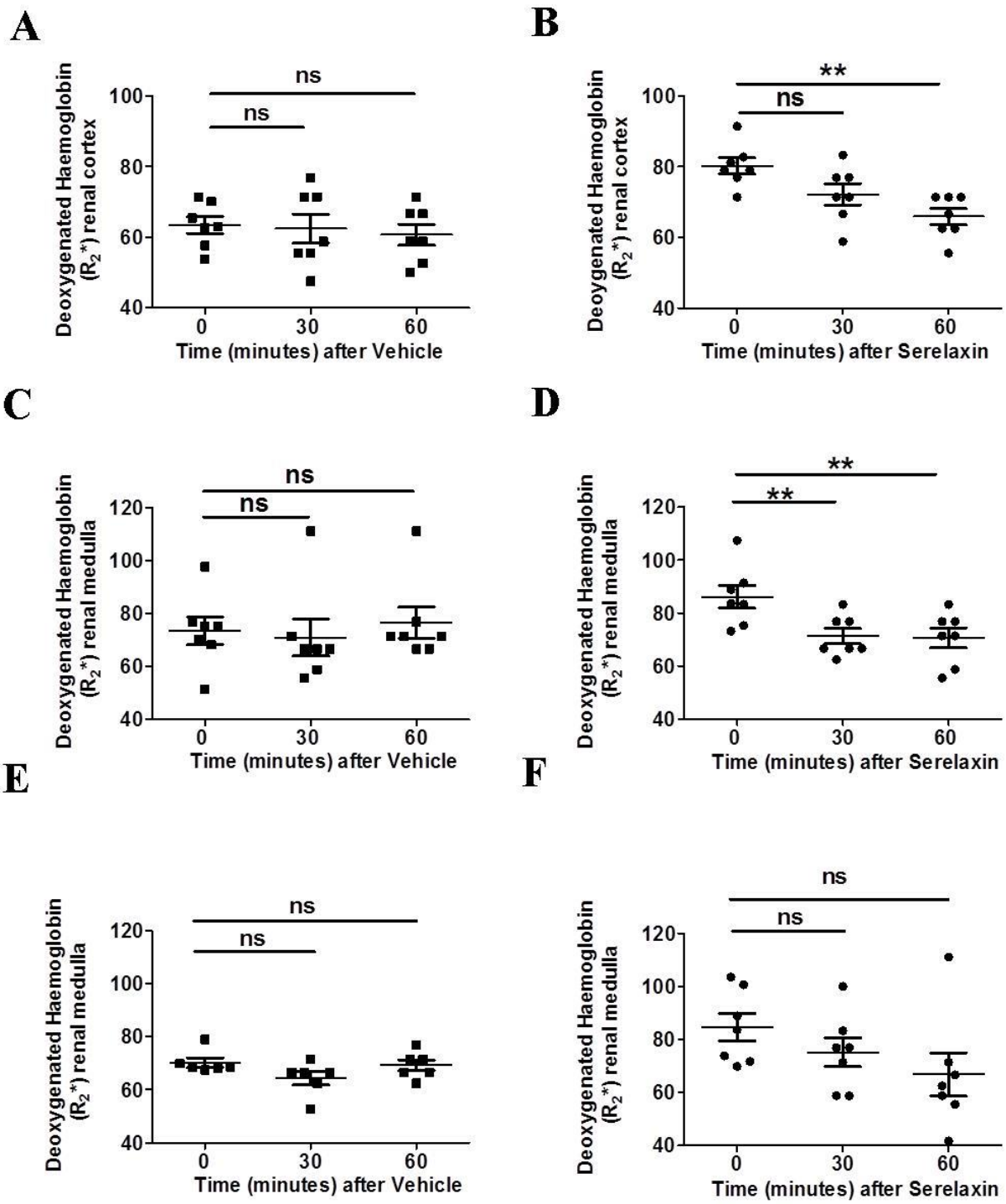
A
B
C
D
E
F
Deoxygenated Haemoglobin ($R_2$*) renal cortex
Deoxygenated Haemoglobin ($R_2$*) renal medulla
ns
**
100
80
60
40
120
0
30
60
Time (minutes) after Vehicle
Time (minutes) after Serelaxin

## Figure 5.7 Effect of Single Dose Relaxin on R2* (Deoxygenated Haemoglobin) in 8 week $CCl_4$ Fibrotic Rats

8 week $CCl_4$ rats were anaesthetized and three baseline 3 minute scans were performed and RLN (n=7) or equivalent volume of vehicle (n=7) given i.v. through a tail vein cannula and 3 minute scans were repeated for 60 minutes post injection. (**A-B**) Cortex in response to vehicle or RLN, (**C-D**) Outer medulla in response to vehicle or RLN, (**E-F**) Inner medulla in response to vehicle or RLN. Data expressed as individual with mean ±SEM and analysed by one way ANOVA with post-hoc Bonferroni test. *p<0.05 **p<0.01 ***p<0.001.

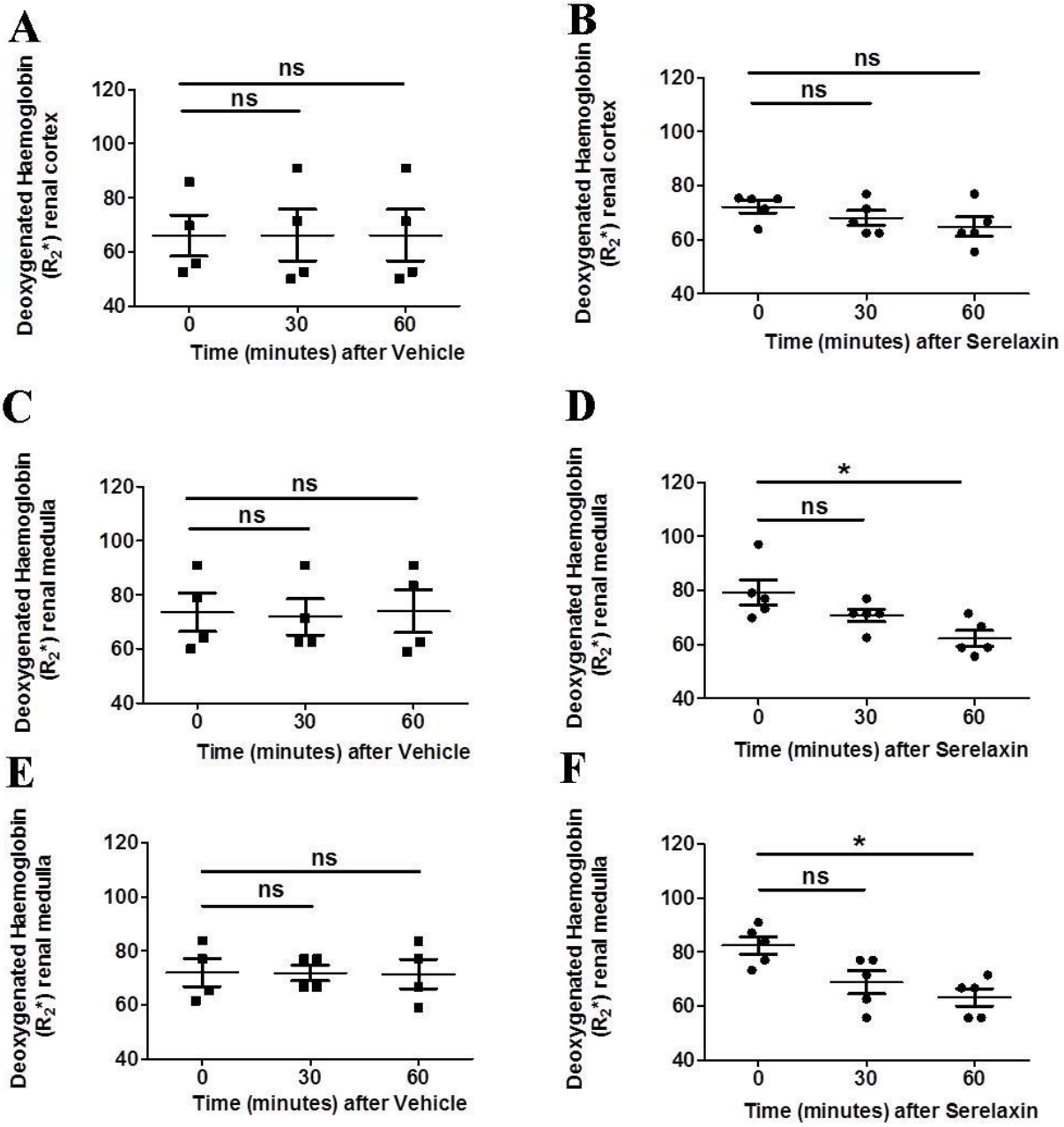
A
Deoxygenated Haemoglobin ($R_2^*$) renal cortex
ns
ns
120
100
80
60
40
0
30
60
Time (minutes) after Vehicle
B
Deoxygenated Haemoglobin ($R_2^*$) renal cortex
ns
ns
120
100
80
60
40
0
30
60
Time (minutes) after Serelaxin
C
Deoxygenated Haemoglobin ($R_2^*$) renal medulla
ns
ns
120
100
80
60
40
0
30
60
Time (minutes) after Vehicle
D
Deoxygenated Haemoglobin ($R_2^*$) renal medulla
*
ns
120
100
80
60
40
0
30
60
Time (minutes) after Serelaxin
E
Deoxygenated Haemoglobin ($R_2^*$) renal medulla
ns
ns
120
100
80
60
40
0
30
60
Time (minutes) after Vehicle
F
Deoxygenated Haemoglobin ($R_2^*$) renal medulla
*
ns
120
100
80
60
40
0
30
60
Time (minutes) after Serelaxin

## Figure 5.8 Effect of Single Dose Relaxin on R2* (Deoxygenated Haemoglobin) in 16 week $CCl_4$ Cirrhotic Rats

16 week CCl4 rats were anesthetized and three baseline 3 minute scans were performed and RLN (n=5) or equivalent volume of vehicle (n=4) given i.v. through a tail vein cannula and 3 minute scans were repeated for 60 minutes post injection. (**A-B**) Cortex in response to vehicle or RLN, (**C-D**) Outer medulla in response to vehicle or RLN, (**E-F**) Inner medulla in response to vehicle or RLN. Data was expressed as individual with mean ±SEM and analysed by one way ANOVA with post-hoc Bonferroni test. *p<0.05 **p<0.01 ***p<0.001.

Having shown results, using 3 modalities, of the dynamic renal vasodilator effects of acute bolus RLN in $CCl_4$ cirrhosis I went on to define its effect on a more translatable and clinically relevant parameter (renal function). This is the parameter we currently monitor in the clinical setting and it is also used in clinical trials to determine the efficacy of drugs on HRS. Previous work has shown it takes several hours to start seeing changes in the GFR in normal conscious rodents (Danielson and Conrad 2003). I chose to give the infusion for 72 hours as this is around the time point that we use to establish whether a patient is responding to current pharmacological therapy for HRS (Salerno, Gerbes et al. 2007).

### 5.10 Sustained RLN infusion elicits renal vasodilation and restores renal function in chronic carbon tetrachloride treated rats

Sustained treatment with RLN (4µg/hr s.c.) for 72h in 16 week $CCl_4$ rats resulted in mean serum RLN levels of 10.2±1.3 ng/mL. Rats treated with RLN had improved RBF compared with vehicle (RLN 3.8±0.3 mL/min vs. vehicle 2.5±0.2 mL/min, p<0.01; **Fig. 5.9A**). This was mirrored by a parallel improvement in GFR (RLN 2.6±0.3 mL/min vs. vehicle 0.7±0.3 mL/min, p=0.001; **Fig.**

**5.9B**). RLN therefore restored the RBF from 37% to 59 % of normal uninjured controls and the GFR was fully normalised.

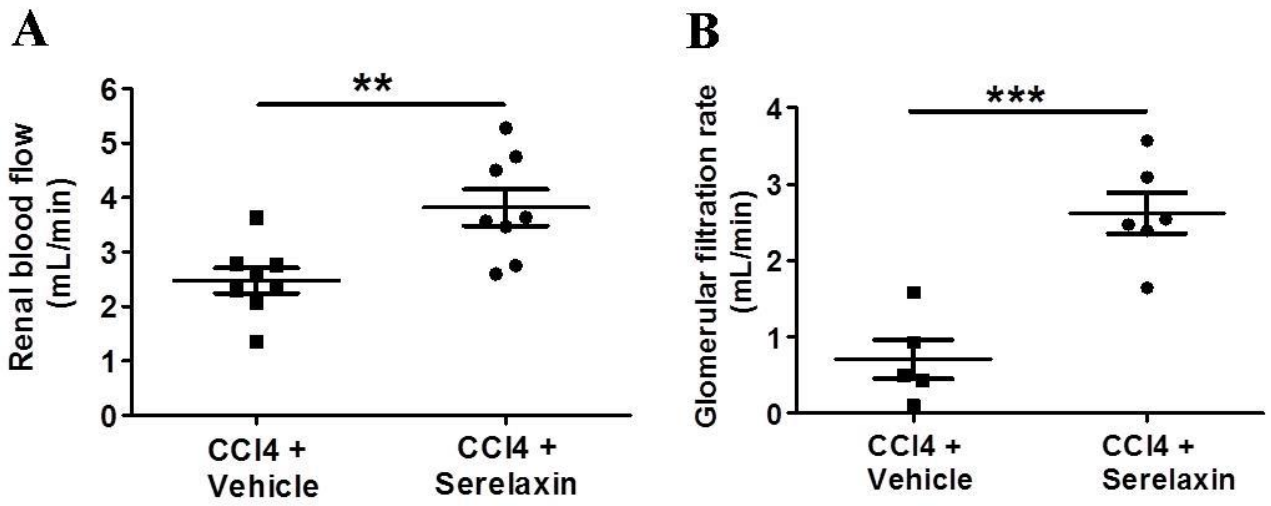


## Figure 5.9 Effect of Sustained 72 Hour Infusion of Relaxin on Renal Blood Flow and Glomerular Filtration Rate in 16 week CCl4 Cirrhotic Rats

Sustained treatment with RLN (4µg/hr s.c.) or vehicle for 72h in 16 week $CCl_4$ rats. Rats were anaesthetised and RBF, measured by flow probe compared with vehicle **(A**). GFR by inulin clearance (**B**). Data expressed as individual data ±SEM and analysed by Students t test. *p<0.05 **p<0.01 ***p<0.001.

### 5.11 Sustained RLN treatment reduces portal pressure but does not affect mean arterial blood pressure or systemic nitric oxide levels in $CCl_4$ cirrhotic rats

There was no difference in MAP between RLN and vehicle treated 16 week $CCl_4$ cirrhotic rats (RLN 105±4 mmHg vs. vehicle 106±4 mmHg, p=0.85; **Fig. 5.10A**). In contrast, there was a significant

reduction in PP in the RLN treated rats which was not seen with vehicle treated rats (RLN 6.1±1.1mmHg vs. vehicle 9.5±0.8mmHg, p<0.01; **Fig 5.10B**). I tested for changes in serum total nitrite as a surrogate for nitric oxide (NO). Central to the 'vasodilatation' theory of HRS development is the concept that excessive circulating NO leads to worsening splanchnic vasodilatation. Given that the results indicated that RLN was causing renal vasodilatation I investigated whether this was associated with increased circulating NO levels. This was not the case as total serum nitrite levels were not different between RLN and vehicle treated rats (RLN 18.6±1.7 µmol/L vs. vehicle 16.5±2.8 µmol/L, p=0.52; **Fig 5.10C**).

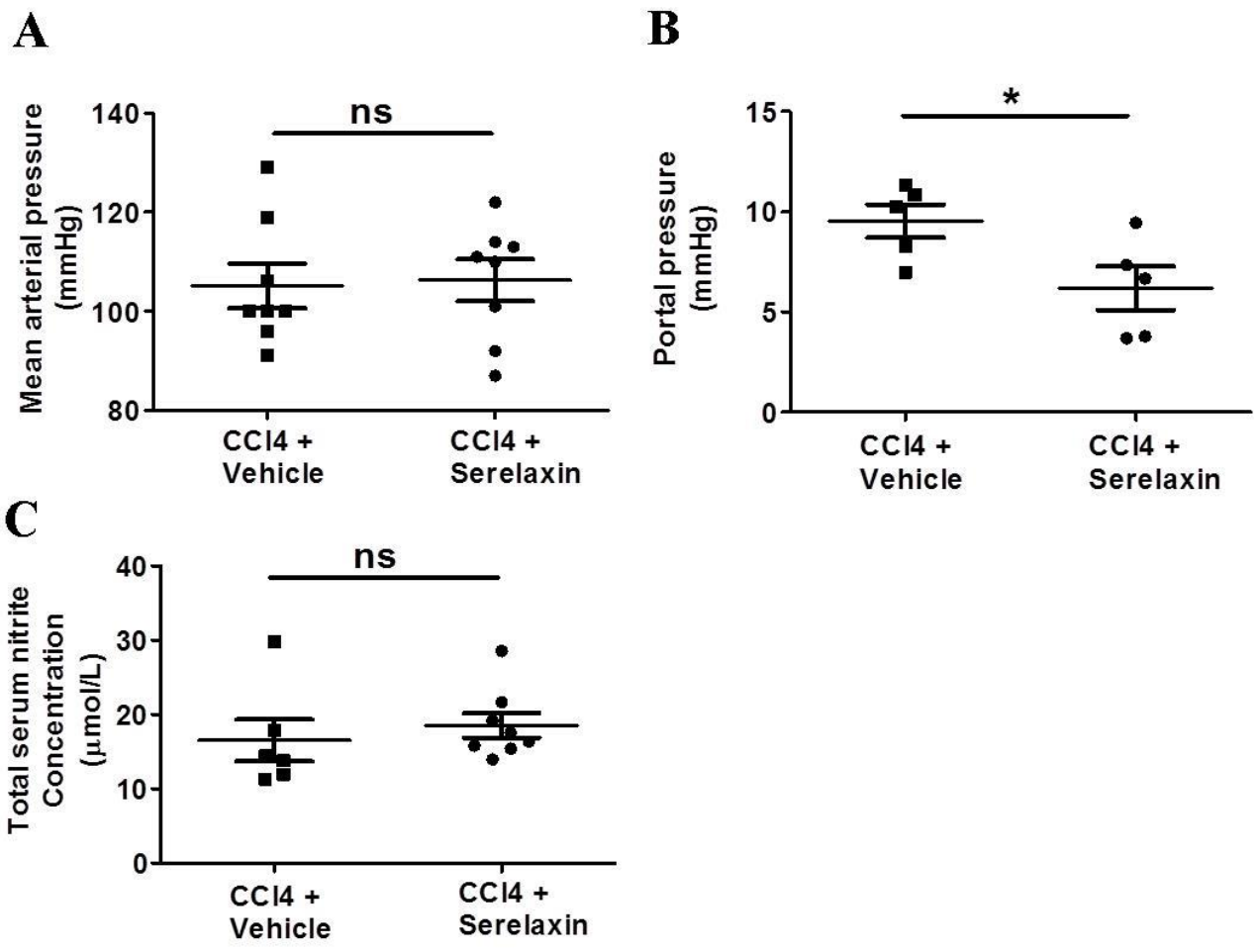

# Figure 5.10 Effect of sustained 72 hour Infusion of Relaxin on Mean Arterial Pressure, Portal Pressure and Serum Nitric Oxide in 16 week $CCl_4$ Rats

MAP was measured by a femoral arterial line in 16 week $CCl_4$ cirrhotic rats post 72 hrs of RLN or vehicle (**A**). PP was measured by portal vein cannulation (**B**). Serum nitrite levels (**C**). Data expressed as individual data ±SEM and analysed by Students t test. *$p<0.05$.

### 5.12 72 hours sustained RLN does not affect hepatic injury or fibrosis but an increased serum albumin is observed

Given that we know the underlying insult leading to HRS is cirrhosis and that RLN has anti-fibrotic effects and an anti-portal hypertensive effect (**Fig 5.10B**; (Fallowfield, Hayden et al. 2014)) , I wanted to investigate whether the effect on RBF could be attributed to improvements in hepatic fibrosis or injury. I measured serum ALT in each group to determine whether there was a difference in the degree of liver injury, but ALT levels were similar (RLN 89±28µmol/L vs. vehicle 80±21µmol/L, p=0.76; **Fig. 5.11A**). Serum albumin, a hepatocyte synthetic marker, was modestly increased with RLN treatment (RLN 27.4±0.7g/L vs vehicle 24.75±0.7g/L, $p<0.05$; **Fig 5.11B**). I quantified PSR staining of liver sections (n=4/group) and found no difference between RLN and vehicle treated rats (collagen proportionate area (CPA); RLN 2.9±0.1% vs. vehicle 2.5±0.1%, p=0.43; **Fig. 5.11C**, representative images shown in **Fig. 5.11D**). In addition there were no histological differences in the kidneys of RLN and vehicle treated groups (images not shown).

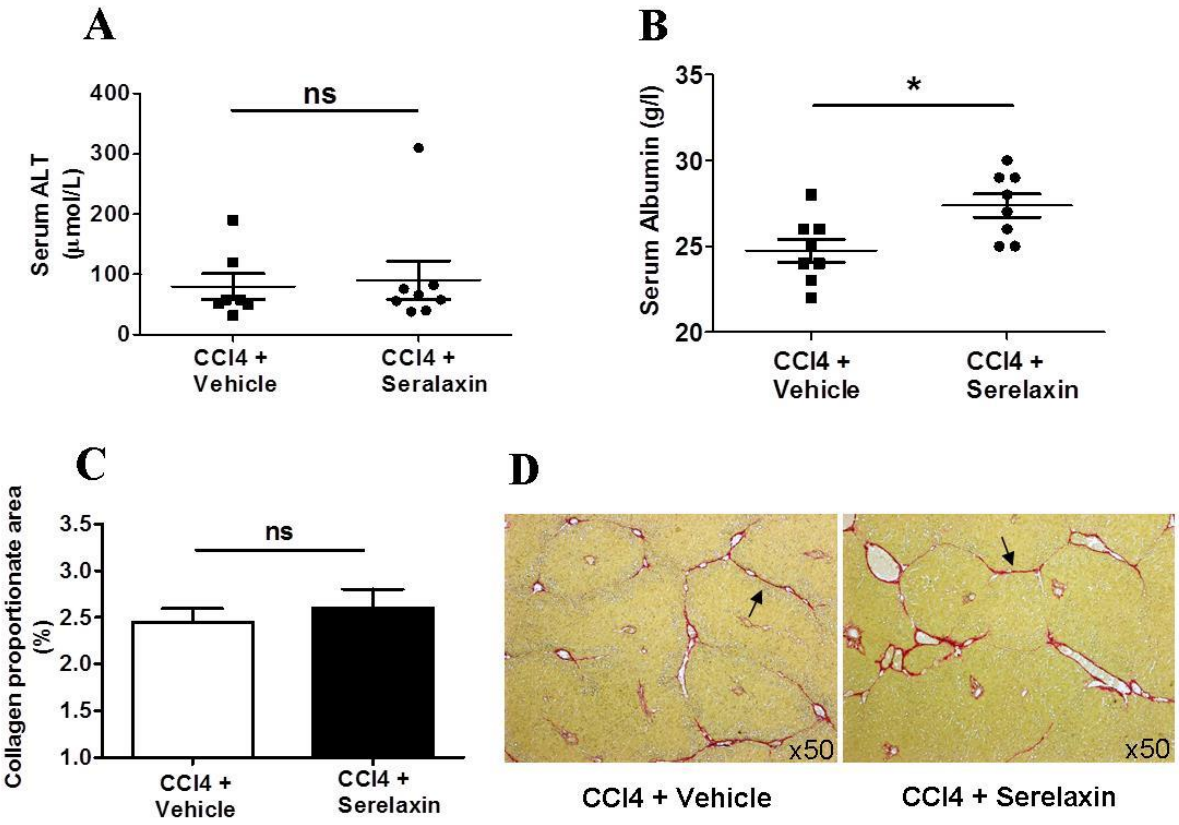


## Figure 5.11 Effect of Sustained 72 Hour Infusion of Relaxin on Hepatic Injury, Function and Fibrosis in CCl4 Cirrhosis

Serum ALT, a marker of liver injury (**A**). Serum albumin, a hepatocyte synthetic marker, **(B**). (**C)**. Morphometric analysis of PSR stained liver sections (n=4/group) from RLN or vehicle treated rats (represented as collagen proportionate area (CPA)**)** (**C).** Representative images shown-arrows indicating fibrosis (**D**). Data expressed as individual data ±SEM and analysed by Students t test. *p<0.05.

### 5.13 Sustained RLN infusion elicits renal vasodilation and improves renal function in bile duct ligated rats

To exclude a model dependent effect of RLN on RBF and GFR and to determine the effect of RLN in a preclinical setting more akin to human HRS, I repeated my analyses from the $CCl_4$ cirrhosis model in decompensated 21 day BDL rats. Sustained treatment with RLN (4µg/hr s.c.) for 72hr in resulted in mean serum RLN levels of 10.6±1.8 ng/mL and elicited a significantly increased RBF compared with vehicle (RLN 2.3±0.2 mL/min vs. vehicle 1.5± 0.2 mL/min, p=0.01; **Fig. 5.12A**). GFR was also increased in RLN treated rats (RLN 2.1±0.5 mL/min vs. vehicle 0.8±0.3 mL/min, p=0.04; **Fig 5.12B**). Importantly this represents an increase in RBF from 22 % to 38% and GFR from 25% to 86% of sham controls after 72 hrs infusion.

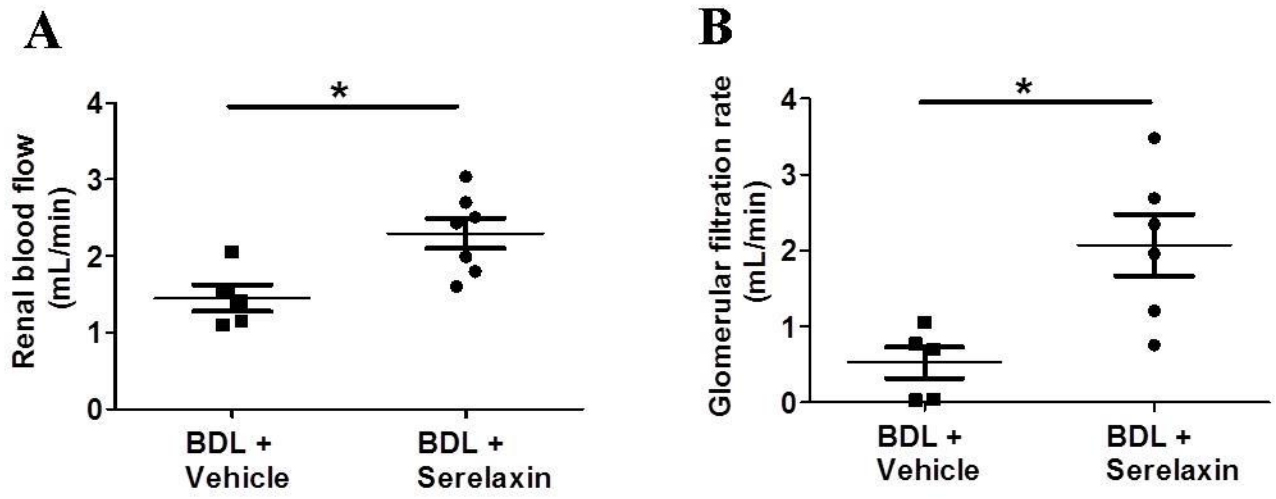


## Figure 5.12 Effect of Sustained 72 Hour Infusion of Relaxin on Renal Blood Flow and Glomerular Filtration Rate in 21 day BDL Rats

Sustained treatment with RLN (4µg/hr s.c.) or vehicle for 72h in 21 day BDL rats. Rats were anaesthetised and RBF, measured by flow probe compared with vehicle **(A)**. GFR by inulin

clearance (**B**). Data expressed as individual data ±SEM and analysed by Students t test. *p<0.05 **p<0.01 ***p<0.001.

### 5.14 Sustained RLN treatment reduces portal pressure but does not affect mean arterial blood pressure or systemic nitric oxide levels in BDL cirrhosis

I invasively measured MAP via a femoral arterial line and found no difference between RLN and vehicle treated 21 day BDL treated rats (RLN 81±8 mmHg after vs. vehicle 73±4 mmHg, p=0.39; **Fig. 5.13A**). In contrast RLN treated rats exhibited a reduction in PP (RLN 8.8±0.7mmHg vs vehicle 14.1±1.3mmHg, p<0.01; **Fig 15.13B**). Again, serum total nitrite levels were unaffected by RLN treatment (RLN 30.7±7.2 µmol/L vs. vehicle 30.8±4.2 µmol/L, p=0.99; **Fig. 5.13C**).

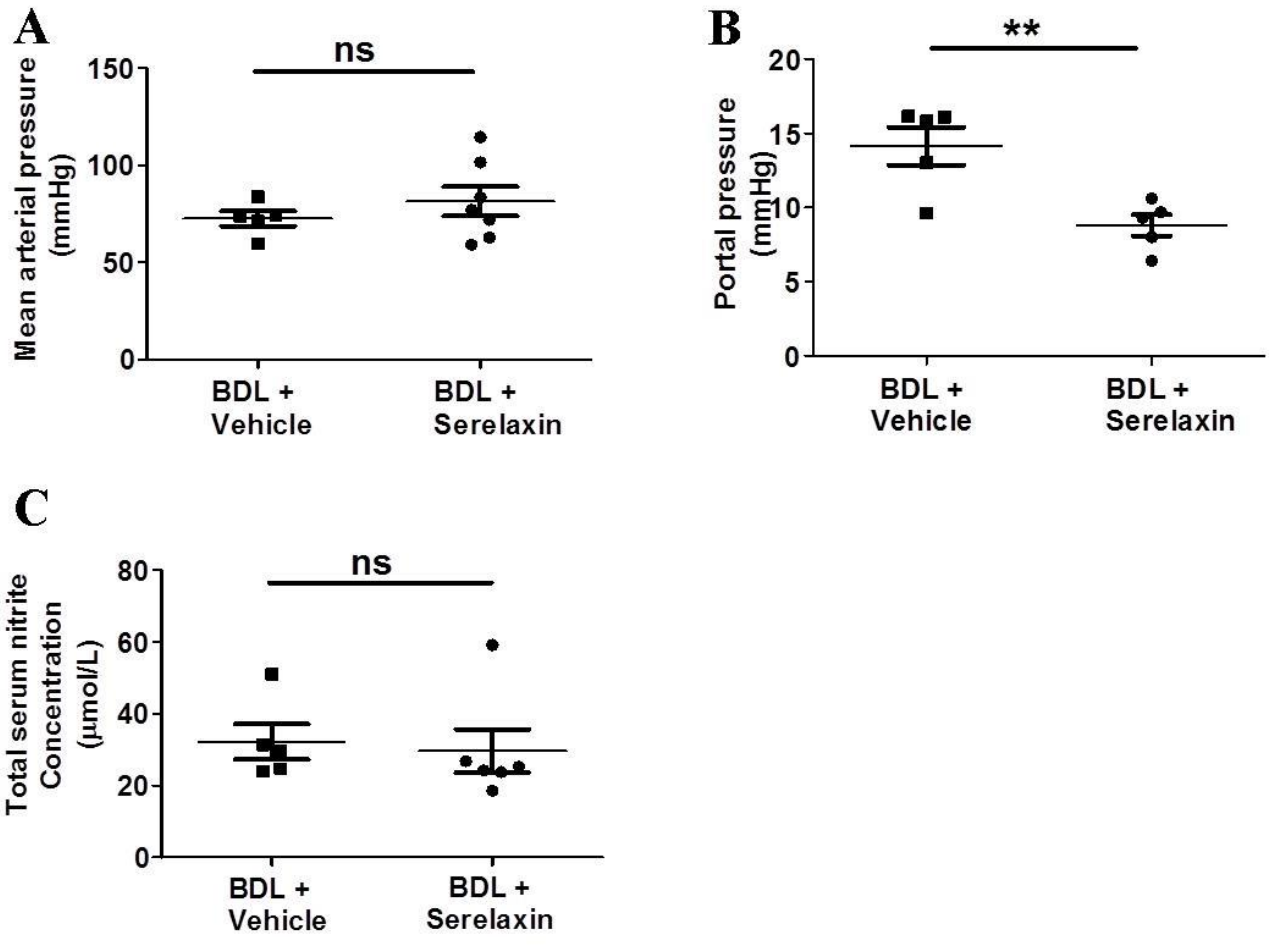

# Figure 5.13 Effect of Sustained 72 Hour Infusion of Serelaxin on Mean Arterial Pressure, Portal Pressure and Serum Nitric Oxide in 21 day BDL Rats

MAP was measured by a femoral arterial line (**A**). PP was measured via portal vein cannulation (**B**). Serum nitrite levels were measured in the blood (**C**) after 72hrs of RLN or vehicle treatment in 21 day BDL cirrhotic rats. Analysed by Students t test. *p<0.05 **p<0.01 ***p<0.001.

### 5.15 72 hours sustained RLN does not affect biliary injury, hepatic fibrosis or function

The haemodynamic effects of RLN appeared to be independent of biliary injury as serum ALP was unaffected (RLN 498±43 µmol/L vs. vehicle 509±69 µmol/L, p=0.8939; **Fig. 5.14A**). Serum albumin was also similar in RLN and vehicle treated rats (RLN 21.5±1.9g/L vs vehicle 26.6±1.3g/L, p=0.062; **Fig 5.14B**). Furthermore there was no difference in liver fibrosis (CPA; RLN 2.3±1.4% vs. vehicle 3.3±1.6%, p=0.65; **Fig. 5.14 C and D**).

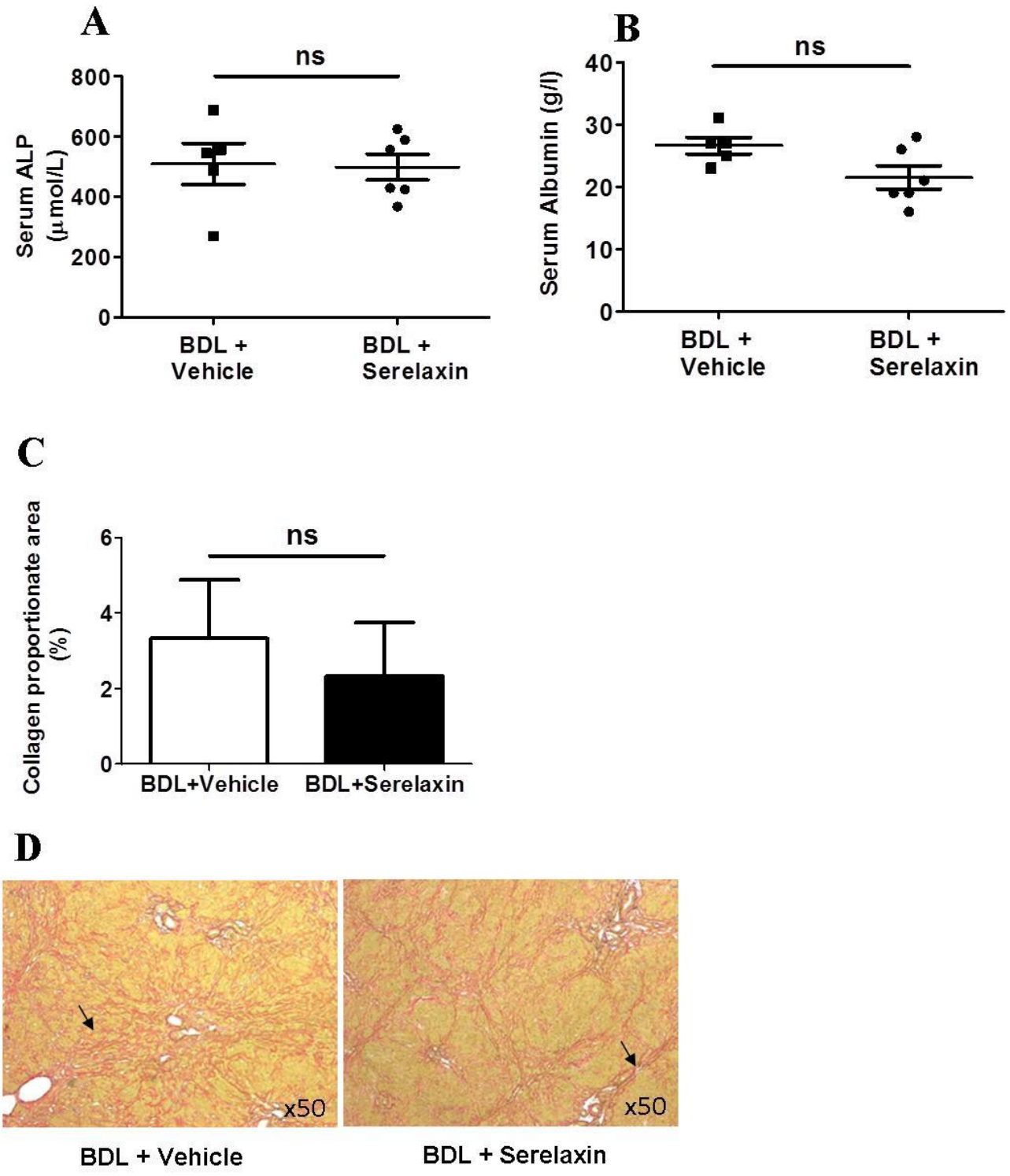


**Figure 5.14 Effect of Sustained 72 Hour Infusion of Relaxin on Hepatic Injury, Function and Fibrosis in BDL Cirrhosis**

Serum ALP, a marker of biliary injury (**A**). Serum albumin, a hepatocyte synthetic marker, **(B**) were measured in blood from BDL rats exposed to 72hrs of either RLN or vehicle. (**C**) Morphometric analysis of PSR stained liver sections (n=4/group) from RLN or vehicle treated rats (represented as collagen proportionate area (CPA)**)**. (**D**) Representative images shown. Analysed by Students t test. *p<0.05 **p<0.01 ***p<0.001.

### 5.16 Cardiac effects of RLN

I measured cardiac output and stroke volume by M-mode Doppler ultrasound at baseline and then at 60 min following either a single i.v. injection of RLN or vehicle but observed no effect on either parameter (**Fig. 5.15A and B**). However, when heart rate was measured invasively through the femoral arterial line in response to RLN, I observed a positive chronotropic effect at 30 and 60 minutes relative to baseline (Baseline 250, 30 mins 333, 60 mins 329;p<0.001; **Fig 5.15C**) which was not seen with vehicle. In contrast, there was no difference in the heart rates of rats exposed to 72 hours of RLN compared to vehicle in either cirrhosis model (**Fig 5.15D and E**). This suggests that this chronotropic effect is acute rather than sustained.

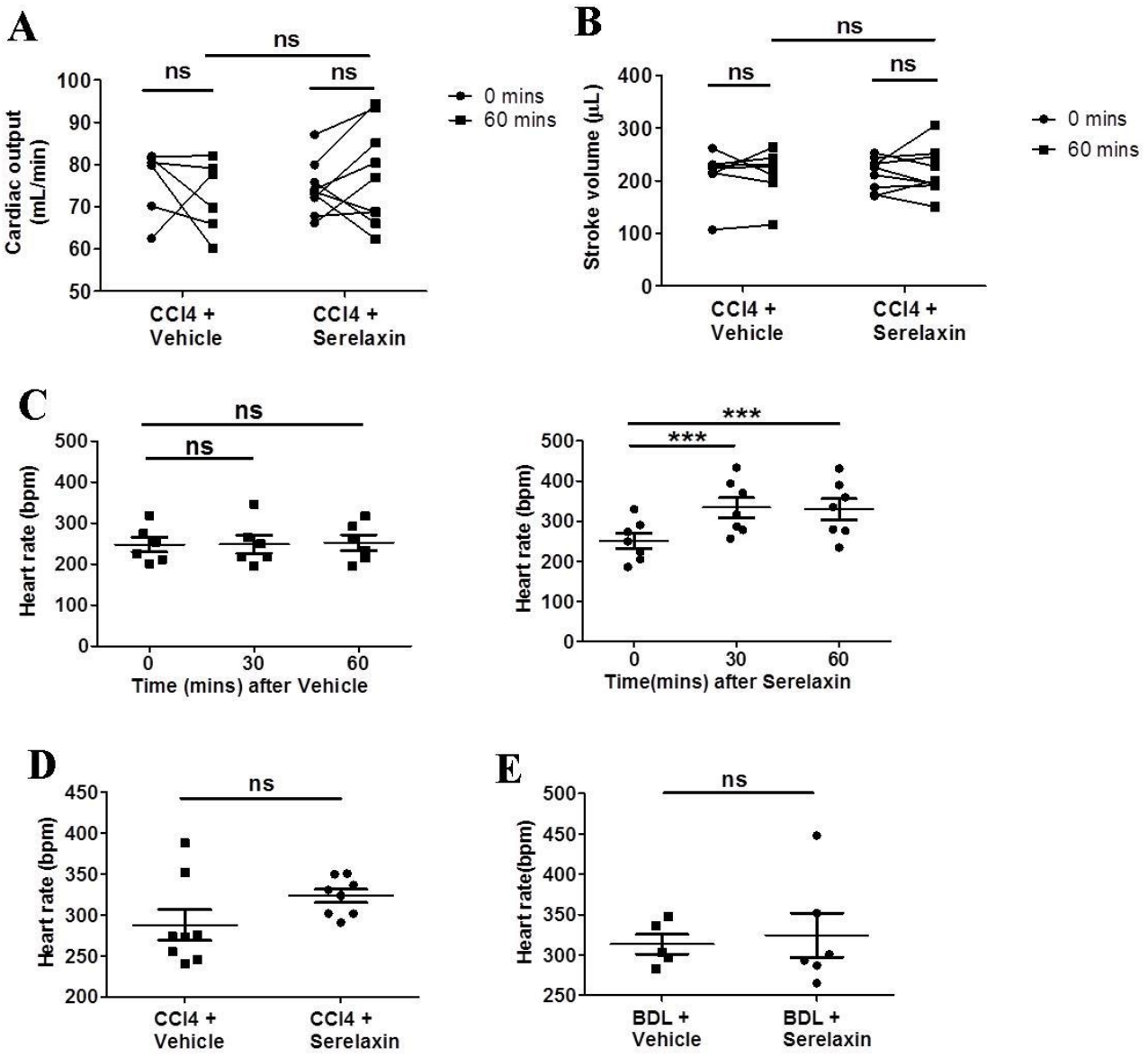


## Figure 5.15 Effect of Relaxin on Cardiac Output, Stroke Volume and Heart Rate

Cardiac output and stroke volume measured by M-mode Doppler ultrasound at baseline and then at 60 min following either a single i.v. injection of RLN or vehicle. (**A and B**). Shown as individual data and analysed by 2 way ANOVA with post hoc Bonferroni test. Heart rate, measured invasively, through the femoral arterial line in response to acute vehicle or RLN **(C**) shown as individual data with mean±SEM and analysed by one way ANOVA with post hoc Bonferroni test. Heart rates of rats measured invasively after 72 hours of RLN or vehicle (**D and E**). Analysed by Students t test. ***p<0.001.

### 5.17 Acute bolus of a non-selective vasodilator does not improve real blood flow

As NO is pivotal to the mechanism of vasodilation proposed for RLN (McGuane, Debrah et al. 2011), I also investigated the acute in vivo haemodynamic response to the NO-releasing drug SNP in the $CCl_4$ rat cirrhosis model (n=6). I used doses of SNP previously shown to increase hind-limb blood flow in rats (Robertson, Gray et al. 2012). In contrast to the selective effects of systemically administered RLN on RBF with preservation of MAP, the vasodilatory agent SNP did not increase renal perfusion (**Fig.5.16A-B**). This experiment adds further evidence that RLN is a selective vasodilator, as the effects seen with a normal vasodilator include hypotension. These results correlate with previous trials of nitrates and vasodilators in HRS showing no success (Salmeron, Ruiz del Arbol et al. 1993).

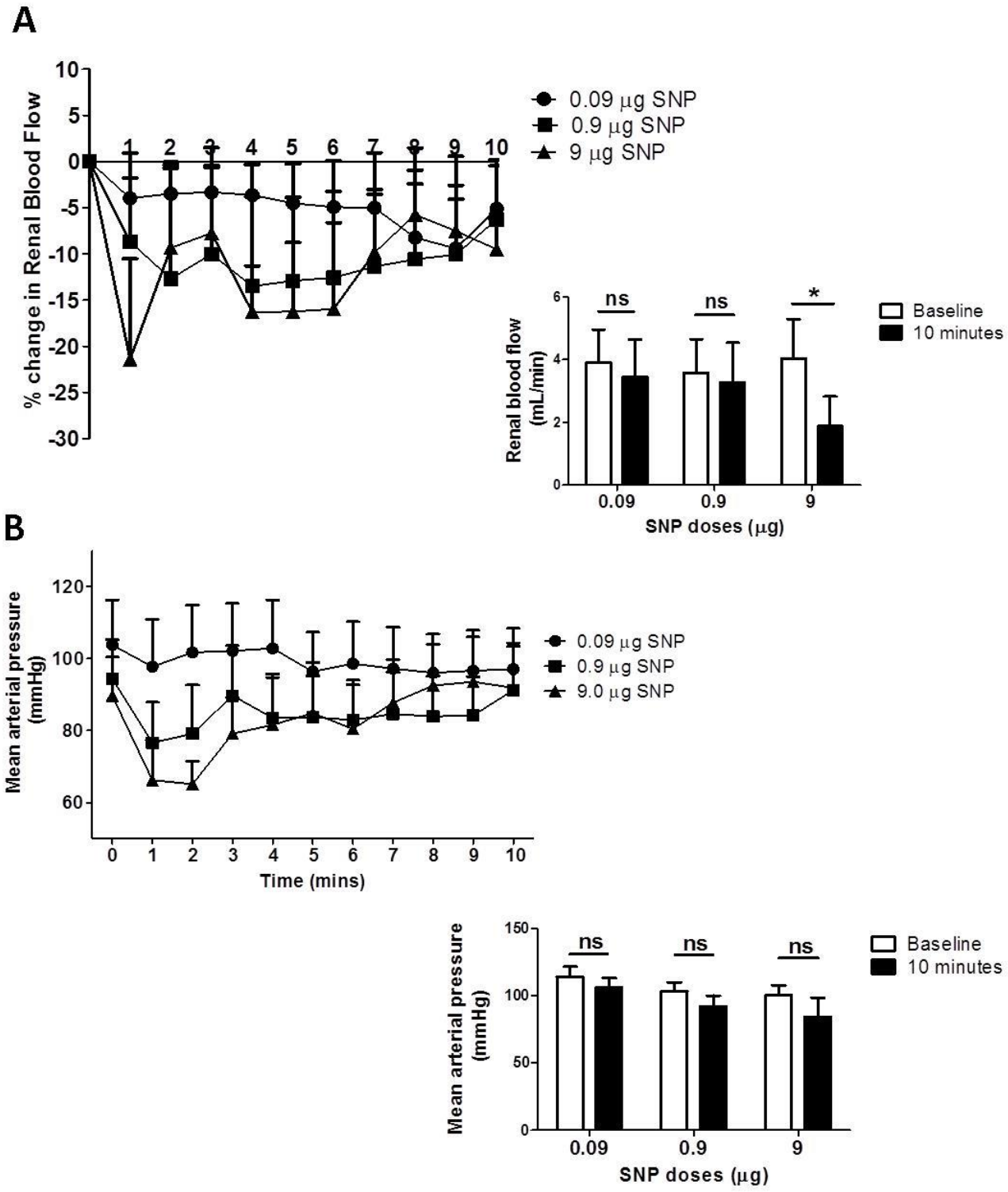


**Figure 5.16 Acute Bolus of the nitrovasodilator SNP on Renal Blood Flow and Mean Arterial Pressure in 16 week $CCl_4$ Cirrhotic Rats**

16 week $CCl_4$ rats were given acute i.v. boluses of SNP and their RBF and MAP measured invasively for 10 minutes. (A) RBF . (B) MAP. Data expressed as mean±SEM and analysed by 2 way ANOVA with post hoc Bonferroni test and Students t test. *$p<0.05$.

## DISCUSSION

In this chapter I have shown for the first time the *in vivo* effects of H2-RLN in two rat models of cirrhosis. To date, work into the effect of exogenous RLN on RBF and GFR has been undertaken in normal and pregnant rats. Acute i.v. bolus RLN rapidly augments RBF in 16 week $CCl_4$ rats without affecting the MAP, suggesting its role as a selective renal vasodilator (**Fig 5.3 and 5.4**). Current pharmacological therapy for HRS in humans consists of an indirect treatment with systemic/splanchnic vasoconstrictors that have been shown to improve renal function in 40-50% of patients but have side effects related to their vasoconstrictor properties. Using a selective vasodilator to target the vasoconstricted renal circulation makes sense therapeutically, but the concern with the use of vasodilators has always been their systemic vasodilatory effects causing deleterious effects on the already labile arterial pressure that is contributing to HRS and to date none have been successful in clinical trials (Salmeron, Ruiz del Arbol et al. 1993). However, here I have also shown that extended RLN treatment in $CCl_4$ cirrhosis increases RBF and GFR without any effect on MAP. Additionally, in the BDL model where the rat is decompensated and hypotensive, no further deleterious effect was observed on the MAP (**Fig 5.13A**). Therefore, the apparently selective renal effects of RLN make it very promising as a novel agent for HRS.

I have shown that acute i.v. bolus RLN augments RBF more in cirrhotic rats than in normal rats (**Fig 5.3C**), with a greater increase seen from baseline in the former. This observation could be explained by my previous data showing a significant increase in RXFP1 expression in the renal vasculature and parenchyma in both cirrhosis models. Alternatively, it could be explained by the observation in hypertensive rats and humans that RLN preferentially dilates pre-constricted vessels (Debrah, Conrad et al. 2005; Teichman, Unemori et al. 2009).

A potential criticism of any invasive *in vivo* animal experiment is that there are confounding factors related to surgery (e.g. insensible fluid loss). To overcome this, I used two non-invasive modalities to monitor changes in RBF indirectly. VTI is an USS measurement of blood flow and confirmed the results seen with invasive flow probes (**Fig 5.5**). Measuring RI was a different way to monitor dynamic vascular modulation by quantifying the resistance to blood flow. This latter parameter is a well-established USS measurement and has been suggested as a potential clinical marker of renal dysfunction/HRS. Currently, although USS is utilised in the diagnosis of HRS by ruling out an obstructive or structural cause, RI is not routinely measured. RI was reduced with RLN by 60 minutes corresponding to the time point when the VTI and RBF were maximally increased (**Fig 5.6).** Furthermore, BOLD MRI measurement of tissue deoxygenated haemoglobin levels also indicated dynamic modulation of RBF with RLN treatment compared to vehicle (**Fig 5.7 and 5.8**). Using these different but complementary techniques allowed me to conclude with confidence that RLN is acting as a renal vasodilator.

I used two distinct models of cirrhosis with reduced RBF and function to ensure that the effects seen with RLN were not model dependent. I have shown that sustained (72 hour) s.c RLN infusion improves RBF and GFR compared to vehicle in both $CCl_4$ and BDL cirrhosis (**Fig 5.9 and 5.12**).

The improvement in GFR is the most clinically relevant finding and probably the most important finding of these experiments. The GFR in $CCl_4$ cirrhosis was restored completely and in BDL was increased to 86% of sham controls. The degree of improvement in GFR compared to that in RBF ($CCl_4$: 59%, BDL 38%) is much greater and suggests, either RLN has increased the RBF enough beyond a threshold to substantially improve renal function, or it suggests that there may be other mechanisms involved in improving renal function, which I will try to address in the next chapter.

This improvement in renal function is a novel finding in cirrhosis models and suggests that RLN could represent a promising therapy for HRS. My experiment only assessed the effect of 72 hours of RLN. In normal rats the effect on RBF and GFR has been shown to be sustained for a further 12 hours post infusion, but was fully normalised by 24 hours (Danielson and Conrad 2003). However, one can only speculate whether this would be the same in cirrhotic rats. With more time it would have been interesting to study the effect of longer and shorter durations of therapy on RBF and GFR and compare pulsed intravenous therapy to a subcutaneous infusion. However, I was trying to test proof of concept with the above experiments in cirrhotic rats to allow translation to cirrhotic humans, where the questions above could be answered more relevantly. It has been shown in vitro that, unlike most G protein coupled receptors RXFP,1 is poorly internalized and lacks the ability to recruit β-arrestins, so less receptor desensitization occurs with prolonged exposure suggesting no tachyphylaxis should occur with chronic treatment with RLN (Callander, Thomas et al. 2009). Additionally, to date, no neutralising antibodies have been detected to RLN in any of the recent clinical trials.

Investigating the mechanism of action of RLN on RBF and GFR, it can be seen from my results that the improvement seen cannot be attributed to an improvement in liver injury as measured by serum

ALT (**Fig 5.11A and 5.14A**) or an improvement in fibrosis measured by CPA (**Fig 5.11C and 5.14C**). The latter seemed unlikely given the duration of infusion was only 72 hours. I did observe an improvement in albumin, which is a synthetic marker of liver function, in the $CCl_4$ model treated with RLN (**Fig 5.11B**) which could suggest some improvement in hepatocyte function. However, it was a marginal change and this was not seen in the BDL model (**Fig 5.14B**). . Furthermore, I witnessed in both models that portal pressure was reduced in the RLN treated rats (Fallowfield, Hayden et al. 2014). Taken together, this raises the possibility that the RLN ligand-receptor axis could represent an integrated treatment target in chronic liver disease and leads to the question: are these effects on RBF and GFR purely via RLN's direct acting renal vasodilatory effects or is the effect on portal pressure contributing to the improvement seen in RBF and GFR? This is a difficult question to answer and in the next Chapter I try to unpick the mechanism in greater detail.

## Summary of important findings:

- Acute i.v. bolus of RLN rapidly increases RBF in cirrhotic rats without affecting the MAP
- USS confirms rapid improvement in renal VTI and RI in response to RLN
- BOLD MRI shows a reduction in deoxygenated haemoglobin in kidney in response to RLN
- Sustained RLN infusion increases RBF and restores renal function in two distinct rat models of cirrhosis without changing the MAP
- Sustained RLN infusion reduces portal pressure, does not affect systemic NO levels, liver injury or fibrosis

## Next steps:

Having established the acute and sustained effects of RLN *in vivo* in models of cirrhosis I wanted to try to unpick its mechanism of action. Before doing this, I wanted to use my models of cirrhosis with renal dysfunction to investigate the pathogenesis of renal vasoconstriction in cirrhosis. My aim was to establish possible targetable pathways for modulation both with RLN and other therapies.

# CHAPTER 6 - RESULTS -

# DEFINING THE PATHOGENESIS OF RENAL ARTERIAL VASOCONSTRICTION IN RAT CIRRHOSIS MODELS

## 6.1 Overview of Chapter

In this chapter I used the $CCl_4$ and BDL rat models of cirrhosis to define the mechanism for renal vasoconstriction and renal dysfunction in experimental HRS. To do this I used myography to measure changes in vascular reactivity and qPCR, Western blot, immunohistochemistry and ELISA to analyse changes to key vasoactive modulators.

## 6.2 Author contributions

I performed all the experiments in this Chapter with significant help initially from Dr Patrick Hadoke (University of Edinburgh/BHF Centre for Cardiovascular Science) to learn the techniques of vessel isolation/preparation and myography.

## 6.3 Background

Functional renal arterial vasoconstriction is hypothesised to be the central mechanism underlying HRS pathophysiology (Epstein, Berk et al. 1970; Platt, Ellis et al. 1994). This vasoconstriction is thought to occur due to the haemodynamic consequences of cirrhosis (splanchnic and peripheral arterial vasodilatation) and the impairment of cardiac function (cirrhotic cardiomyopathy). Eventually, these lead to a reduction in effective circulating volume and subsequent compensatory activation of the renin-angiotensin-aldosterone system, sympathetic nervous system and increased activity of antidiuretic hormone (Schrier, Arroyo et al. 1988; Krag, Bendtsen et al. 2010). Additionally, pooling of blood in the dilated splanchnic circulation (so-called 'splanchnic steal syndrome') may also alter gut permeability and induce bacterial translocation, with the release of

endotoxin and various cytokines which amplify the dysregulated circulation in cirrhosis (Newby and Hayes 2002). Progression of these haemodynamic alterations in cirrhosis and an intra-renal imbalance between vasoconstrictor and vasodilator systems, results in renal blood flow becoming critically dependent on arterial blood pressure, with small changes in perfusion pressure translating into intense renal vasoconstriction and the precipitation of HRS (Stadlbauer, Wright et al. 2008).

At a cellular level in the cirrhotic liver, liver sinusoidal endothelial cells (LSECs) appear to play an important role in contributing to the dynamic component of raised intrahepatic vascular resistance. It has been shown that LSECs in cirrhosis display an abnormal phenotype. Central to this abnormal phenotype is an imbalance in the liver with increased production of vasoconstrictors (e.g. endothelin-1) and reduced release of endogenous vasodilators (mainly NO) (Bhathal and Grossman 1985; de Franchis 2000; Iwakiri and Groszmann 2007). Pivotal to this increase in intrahepatic vascular tone is the endothelial nitric oxide synthase (eNOS)/ NO pathway. Previous work has suggested that either decreased expression of eNOS protein, decreased phosphorylation of eNOS by the serine-threonine kinase AKT, the presence of inhibitory substances (e.g. asymmetric dimethylarginine, ADMA) or hyporesponsiveness to NO may underlie this intrahepatic liver sinusoidal endothelial dysfunction (Rockey and Chung 1998; Laleman, Omasta et al. 2005; Iwakiri 2011). In contrast, extra-hepatic endothelial cells have the opposite phenotype, producing excessive NO which contributes to increased portal blood flow and splanchnic pooling. Further work has explored receptor expression changes in the liver and portal vein in cirrhosis. It has been shown that the relative expression of the Endothelin Type A (ETA) receptor in the portal vein (Ling, Kuc et al. 2012), urotensin 2 receptor (Liu, Chen et al. 2010) and angiotensin 2 receptor (Grace, Herath et al. 2012) in the liver are all upregulated in cirrhosis contributing to the increased vasoconstrictor activity and subsequent worsening of intrahepatic vascular resistance and portal hypertension.

Despite growing evidence about intrahepatic endothelial dysfunction, the key cellular players and receptors involved in HRS development remain to be fully elucidated. The difficulty and limiting step in achieving this is a lack of access to the human 'HRS' kidney vasculature. Therefore, for the following body of work I have used my models of cirrhosis and their clear renal phenotypes to try to help unravel the mechanism of renal vasoconstriction and renal dysfunction development.

### 6.4 Aims:

- To assess renal vascular reactivity in normal and cirrhotic rats
- To delineate in cirrhosis models potential therapeutic targets for inhibition of renal vasoconstriction

## RESULTS:

### 6.5 A failure of endothelium-dependent vasorelaxation underlies the impaired renal blood flow in both rat cirrhosis models

Extra-renal arteries and intra-renal arteries (segmental, interlobar and arcuate) and 3rd order mesenteric arteries were isolated from 16 week $CCl_4$ rats and their olive oil controls and mounted on a wire myograph and their vascular reactivity measured. Owing to how small the arcuate vessels were and subsequent problems with getting them onto the wire, I continued analysis without the latter group. See **Table 6.1** for summary of vessel characteristics. To compare vessel

responsiveness, I compared the concentration response curves (CRC) using 2-way ANOVA to ascertain the effect of cirrhosis and dose on vascular response. Additionally I analysed other parameters of vascular reactivity: sensitivity ($-\log IC_{50}$ or $-\log EC_{50}$: the concentration of vasodilator or vasoconstrictor, respectively, needed to produce a 50% response) and maximal vaso-dilation/constriction (Emax). Renal arteries from 16 week $CCl_4$ cirrhotic rats showed a markedly attenuated response to the endothelium-dependent vasodilator acetylcholine (ACh; $10^{-9}$ to $10^{-5}$M), compared to arteries isolated from control rats (**Fig 6.1A**; $p<0.001$), with a reduced sensitivity and reduced maximal dilatation (Emax). This marked attenuation in response to ACh was also seen in the intra-renal segmental and interlobar arteries (**Fig 6.1B-C**). With the vasoconstrictor phenylephrine (PE; $10^{-9}$ to $10^{-5}$M) the CRCs were not significantly different, however the intra-renal segmental artery from the $CCl_4$ rats had higher $-\log EC_{50}$ suggesting less sensitivity to PE (**Table 6.1**). The Emax was not different. There was no difference in CRC, sensitivity or Emax in response to the endothelium-independent vasodilator sodium nitroprusside (SNP; $10^{-9}$ to $10^{-5}$M) (**Fig. 6.2A-F**). The mesenteric arteries showed no difference in CRCs, sensitivity or Emax to ACh or SNP but did show greater sensitivity to PE, with an enhanced CRC though Emax were the same between cirrhosis and controls (**Fig 6.3A-C**) and **Table 6.1**.

| | | RA | RA | Segmental | Segmental | Interlobar | Interlobar | MA | MA |
|---|---|---|---|---|---|---|---|---|---|
| | | **$CCl_4$** | **OO** | **$CCl_4$** | **OO** | **$CCl_4$** | **OO** | **$CCl_4$** | **OO** |
| | **Number** | **8** | **10** | **11** | **11** | **7** | **5** | **8** | **10** |
| **PE** | **-log$EC_{50}$** | 5.97±0.1 | 6.33±0.08 | **6.15±0.07**** | 6.37±0.03 | 6.29±0.06 | 6.31±0.19 | **6.19±0.04*** | 6.01±0.04 |
| | **Emax (%KPSS)** | 119.4 ± 9.922 | 105.9 ± 6.779 | 111.7 ± 4.185 | 109.7 ± 1.982 | 125.0 ± 4.937 | 119.7 ± 9.404 | 113.5±3.7 | 108.2±4.5 |
| **KPSS** | **Emax (mN.mm-1)** | 5.56 ± 0.71 | 3.77 ± 0.59 | 3.73 ± 0.79 | 3.35 ± 0.79 | 3.05 ± 1.90 | 1.21 ± 0.39 | 4.49±0.98 | 6.79±1.42 |
| **ACH** | **-log Ic50** | **6.42±0.14**** | 6.88±0.11 | **6.31±0.12*** | 7.12±0.17 | **6.56±0.19*** | 7.23±0.21 | 7.37±0.19 | 7.34±0.07 |
| | **Emax (%)** | **47.99±8.57**** | 78.61±5.17 | **43.83±4.98*** | 68.89±7.57 | **42.64±7.07*** | 77.14±13.14 | 69.8±8.0 | 88.2±3.6 |
| **SNP** | **-log Ic50** | 7.31±0.09 | 7.13±0.05 | 7.36±0.06 | 7.314±0.11 | 7.42±0.08 | 7.54±0.18 | 7.99±0.13 | 7.93±0.13 |
| | **Emax (%)** | 85.94 ± 4.78 | 86.60 ± 1.74 | 87.36 ± 3.69 | 88.20 ± 11.80 | 84.76 ± 2.41 | 86.85 ± 5.95 | 96.21±1.69 | 98.4±0.9 |

# Table 6.1 The Effect of $CCl_4$ Cirrhosis on Vascular Reactivity

The extra- renal artery (RA) and intra-renal segmental, interlobar and 3rd order mesenteric arteries were isolated from 16 week CCl4 rats and their olive oil (OO) controls. Viability was measured with response to KPSS and responses to vasoconstrictor (PE), endothelium-dependent vasodilator (ACh) and endothelium-independent vasodilator (SNP) were measured. Parameters included sensitivity ($-\log IC_{50}$ or $-\log EC_{50}$: measured the concentration of vasodilator or vasoconstrictor, respectively, needed to produce a 50% response) and maximal vaso-dilation/constriction (Emax). For PE the Emax was measured relative to % contraction with KPSS and with the vasodilators measured relative to % preconstruction with PE. Data expressed as mean±SEM, analysed by Students t test, *$p<0.05$ **$p<0.01$ ***$p<0.001$. Significant values in bold.

A

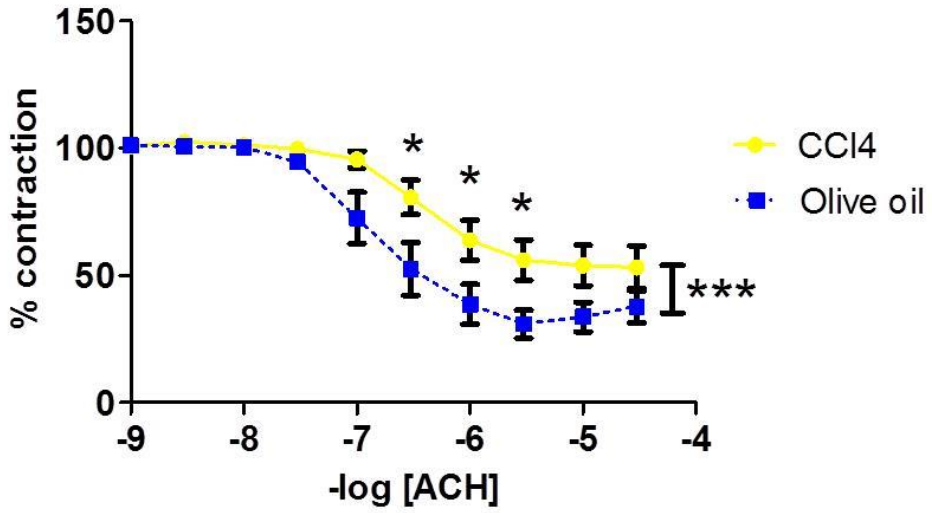
150
100
50
0
% contraction
-9
-8
-7
-6
-5
-4
-log [ACH]
*
*
*
***
CCl4
Olive oil

B

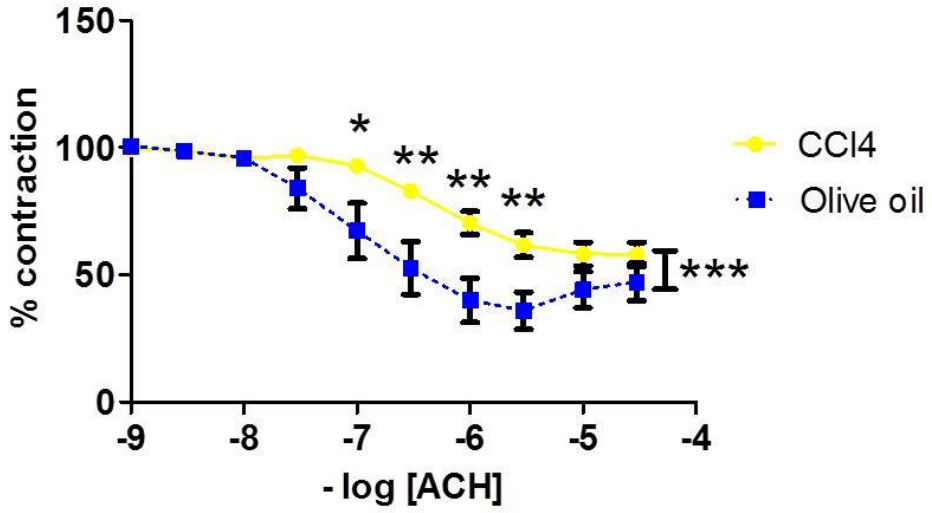
150
100
50
0
% contraction
-9
-8
-7
-6
-5
-4
- log [ACH]
*
**
**
**
***
CCl4
Olive oil

C

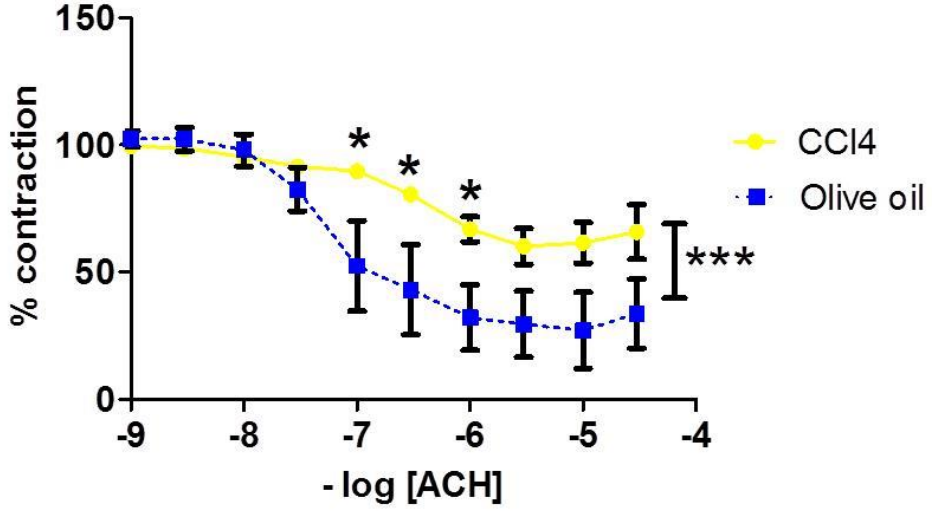
150
100
50
0
% contraction
-9
-8
-7
-6
-5
-4
- log [ACH]
*
*
*
***
CCl4
Olive oil

## Figure 6.1 Concentration Response Curves to ACh in Renal Arteries from 16 week $CCl_4$ rats and Olive Oil Controls

Renal arteries (**A**) extra-renal, (**B**) intra-renal segmental and (**C**) intra-renal interlobar were isolated from 16 week $CCl_4$ cirrhotic rats and olive oil controls, pre-constricted with phenylephedrine and exposed to increasing doses of Acetylcholine (ACH; $10^{-9}$ to $10^{-5}$M). Data expressed as % contraction, relative to pre-constriction with PE, analysed by 2-way ANOVA with post-hoc Bonferroni test comparing individual concentrations. *p<0.05 **p<0.01 ***p<0.001.

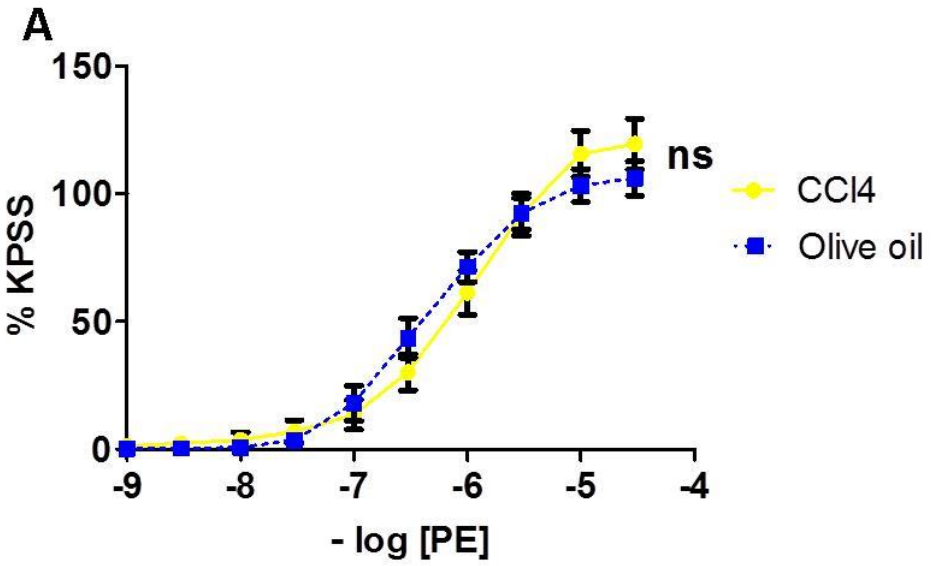
A
150
100
50
0
% KPSS
-9
-8
-7
-6
-5
-4
- log [PE]
ns
CCl4
Olive oil

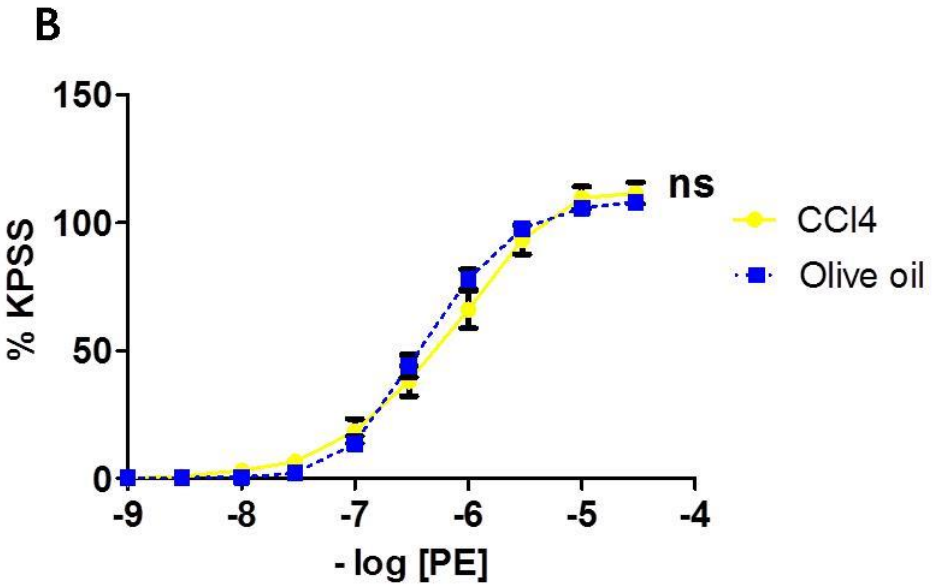
B
150
100
50
0
% KPSS
-9
-8
-7
-6
-5
-4
- log [PE]
ns
CCl4
Olive oil

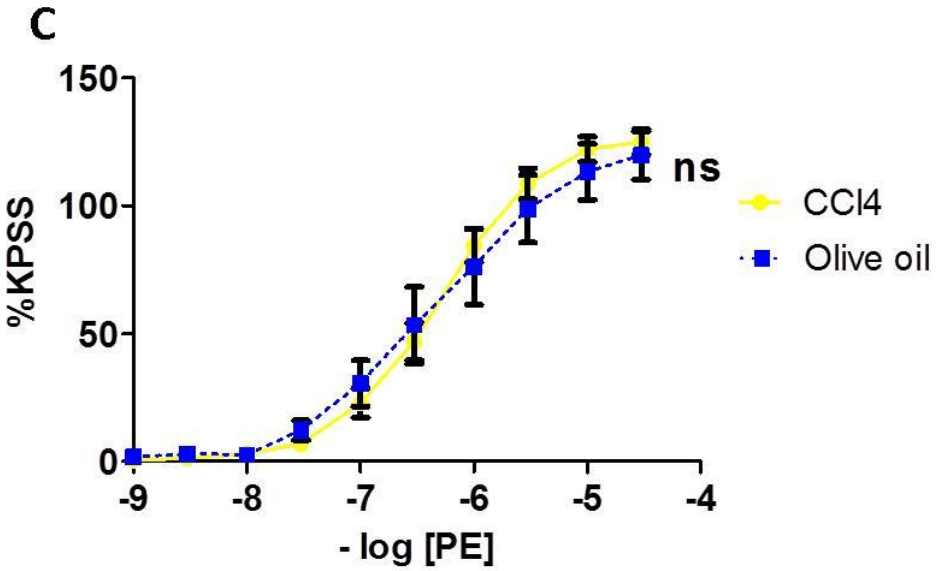
C
150
100
50
0
%KPSS
-9
-8
-7
-6
-5
-4
- log [PE]
ns
CCl4
Olive oil

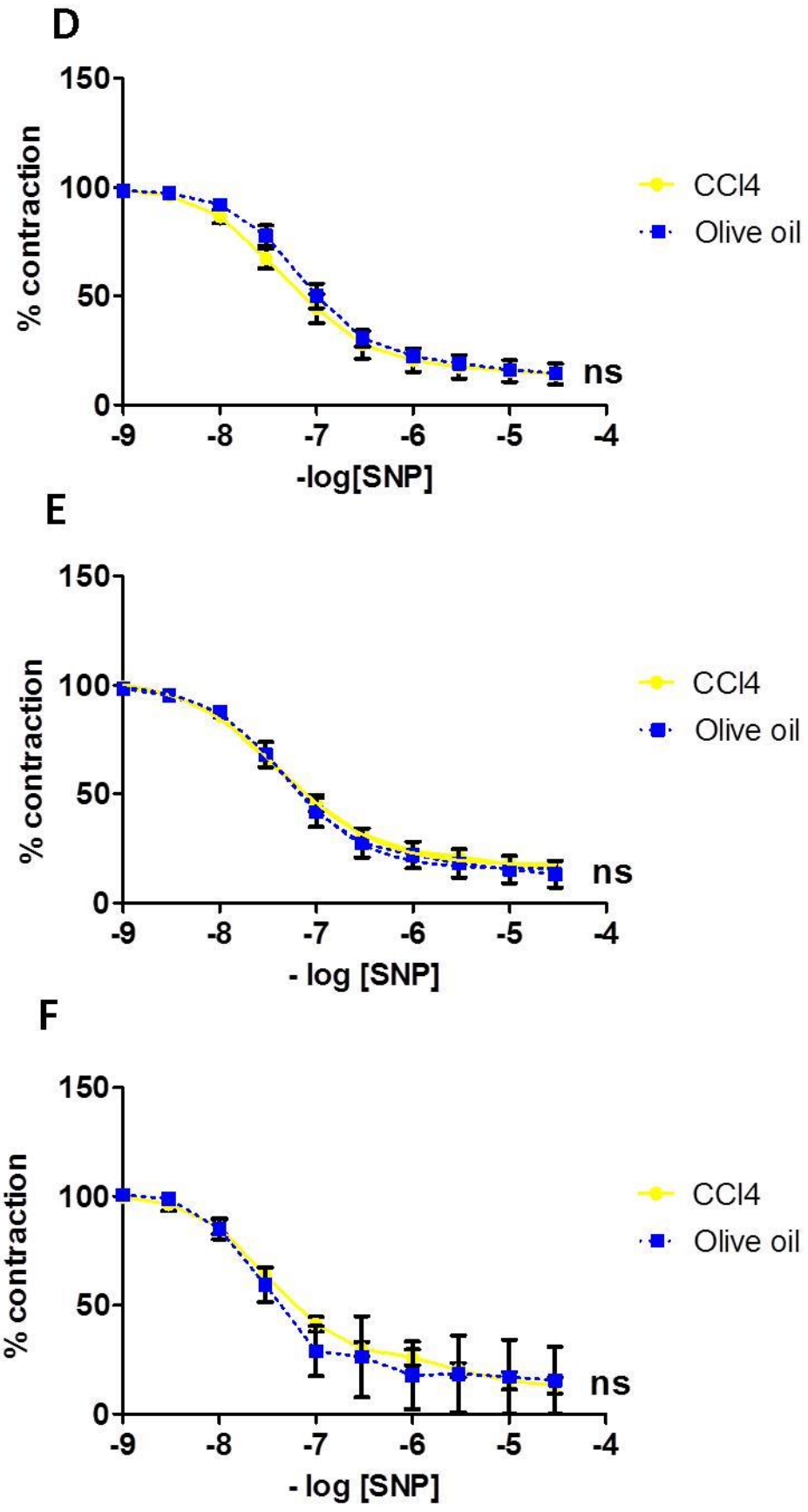
D
150
100
50
0
% contraction
-9
-8
-7
-6
-5
-4
-log[SNP]
CCl4
Olive oil
ns
E
150
100
50
0
% contraction
-9
-8
-7
-6
-5
-4
- log [SNP]
CCl4
Olive oil
ns
F
150
100
50
0
% contraction
-9
-8
-7
-6
-5
-4
- log [SNP]
CCl4
Olive oil
ns

## Figure 6. 2 Concentration Response Curves to PE and SNP in Renal Arteries from 16 week $CCl_4$ rats and Olive Oil Controls

Renal arteries (**A, D**) extra-renal, (**B, E**) intra-renal segmental and (**C, F**) intra-renal interlobar were isolated from 16 week $CCl_4$ cirrhotic rats and olive oil controls, exposed to increasing doses of the vasoconstrictor phenylephedrine (PE; $10^{-9}$ to $10^{-5}$M **A-C**). Data expressed as % contraction relative to KPSS (Potassium rich physiological salt solution). After pre-constriction with PE, arteries were exposed to increasing doses of sodium nitroprusside – an endothelium-independent vasodilator (SNP; $10^{-9}$ to $10^{-5}$M; **D-E**). Data expressed as % contraction, relative to pre-constriction with PE and analysed by 2-way ANOVA with post-hoc Bonferroni test comparing individual concentrations. *p<0.05 **p<0.01 ***p<0.001.

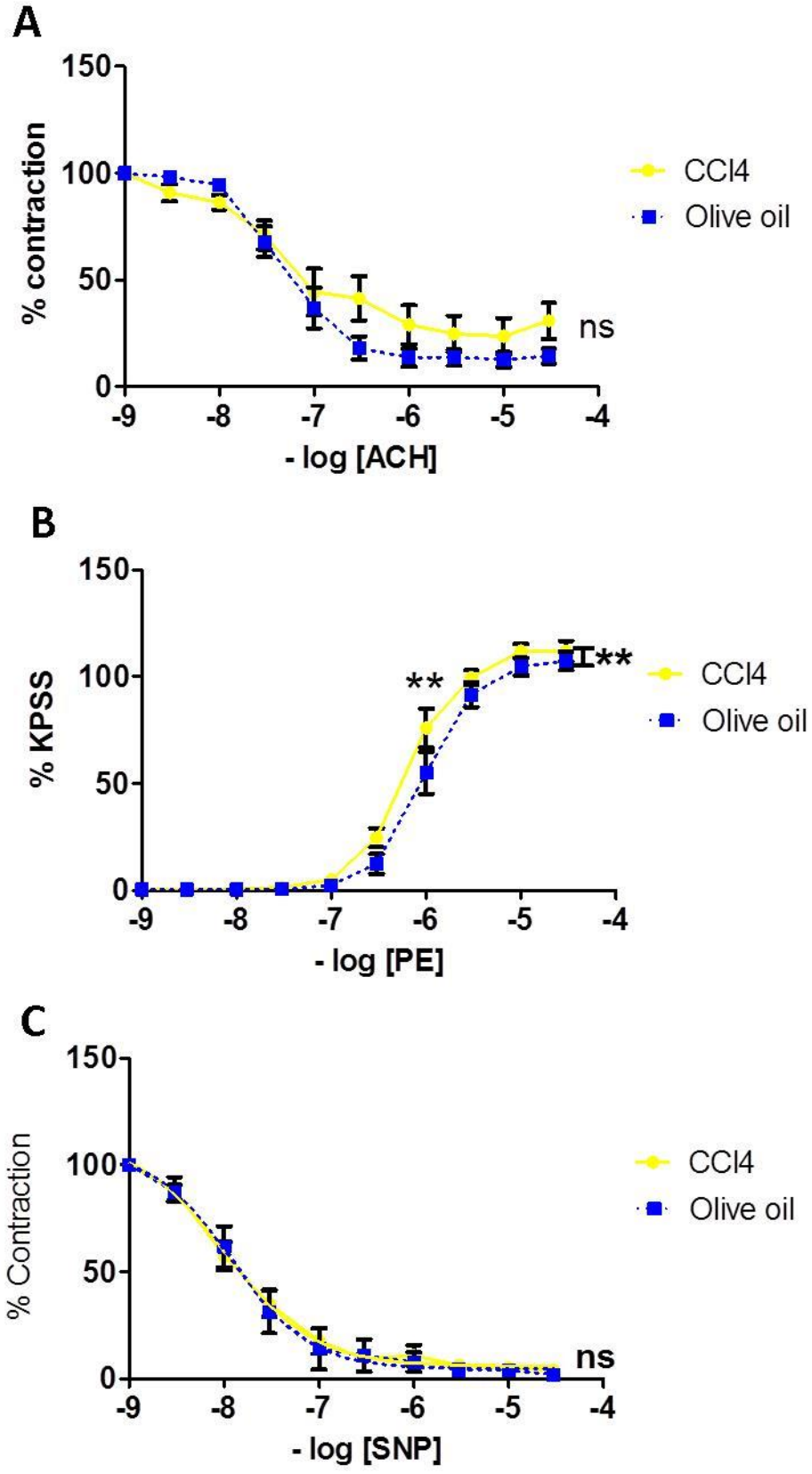
A
150
100
50
0
% contraction
-9
-8
-7
-6
-5
-4
- log [ACH]
ns
CCl4
Olive oil
B
150
100
50
0
% KPSS
**
**
-9
-8
-7
-6
-5
-4
- log [PE]
CCl4
Olive oil
C
150
100
50
0
% Contraction
ns
-9
-8
-7
-6
-5
-4
- log [SNP]
CCl4
Olive oil

## Figure 6.3 Concentration Response Curves in Mesenteric arteries from 16 week $CCl_4$ and Olive Oil Control rats

3rd order mesenteric arteries were isolated from 16 week $CCl_4$ cirrhotic rats and olive oil controls and after pre-constriction with PE, were exposed to increasing doses of the endothelium-dependent vasodilator Acetylcholine (ACH; $10^{-9}$ to $10^{-5}$M; **A**), sodium nitroprusside – an endothelium-independent vasodilator (SNP; $10^{-9}$ to $10^{-5}$M; **C**). Data expressed as % contraction, relative to pre-constriction with PE. (**B**) Mesenteric arteries were also exposed to increasing doses of the vasoconstrictor phenylephedrine (PE; $10^{-9}$ to $10^{-5}$M; **B**). Data expressed as % contraction relative to KPSS and analysed by 2-way ANOVA with post-hoc Bonferroni test comparing individual concentrations. *p<0.05 **p<0.01 ***p<0.001.

To demonstrate that this was not a model dependent observation, I recreated the same experiment in 28 day BDL rats (n=6) and compared them to sham operated controls (n=8). Again, throughout the renal arterial tree there was an attenuated response to the endothelium-dependent vasodilator acetylcholine (ACh; $10^{-9}$ to $10^{-5}$M), with reduced sensitivity throughout (**Table 6.2**) and a reduced Emax in the segmental artery compared to arteries isolated from control rats (**Fig 6.4A-C**). There were no differences in CRC, sensitivity or Emax in response to the vasoconstrictor phenylephrine (PE; $10^{-9}$ to $10^{-5}$M) in the extra-renal artery or interlobar artery. However, the segmental artery from 28 day BDL rats was more responsive to PE, with a higher Emax but no difference in the $-\log EC_{50}$. Finally, there was no difference in CRC, sensitivity or Emax to the endothelium-independent vasodilator sodium nitroprusside (SNP; $10^{-9}$ to $10^{-5}$M) in the extra-renal artery or interlobar, however although the CRC was no different to shams, the segmental artery from 28 day BDL was less sensitive to SNP with a higher $-\log IC_{50}$ (**Fig. 6.5A-E**). The mesenteric arteries showed no difference in the CRC, sensitivity or Emax to Ach (**Fig.6.6A**), PE (**Fig.6.6B**) though mesenteric arteries from BDL rats showed reduced response and a higher $-\log IC_{50}$ to SNP compared to sham controls (**Fig.6.6C**),

| | | RA | RA | Seg | Seg | IL | IL | MA | MA |
|---|---|---|---|---|---|---|---|---|---|
| | | **BDL** | **Sham** | **BDL** | **Sham** | **BDL** | **Sham** | **BDL** | **Sham** |
| | **Number** | 6 | 7 | 6 | 7 | 5 | 7 | 4 | 4 |
| **PE** | **-log$EC_{50}$** | 6.26±0.12 | 6.14±0.09 | 6.30±0.09 | 6.28±0.06 | 6.19±0.23 | 6.43±0.11 | **6.32 ± 0.11** | 6.16 ± 0.07 |
| | **Emax (%KPSS)** | 124.9 ± 4.56 | 124.5 ± 6.52 | **137.6 ± 6.74 **** | 112.7 ± 2.67 | 120.0 ± 22.14 | 124.3 ± 8.96 | 108.2 ± 13.96 | 113.1 ± 6.034 |
| **ACH** | **-log Ic50** | **6.29 ± 0.12***** | 6.52±0.05 | **6.4 ± 0.24*** | 7.28±0.19 | **6.56 ± 0.53*** | 7.09±0.19 | 7.62 ± 1.13 | 7.78 ±0.28 |
| | **Emax (%)** | 51.33 ± 11.76 | 72.84 ± 5.86 | **17.29 ± 3.69***** | 70.81 ± 10.50 | 31.65 ± 10.57 | 59.10 ± 12.20 | 78.08 ± 9.00 | 86.62 ± 8.58 |
| **SNP** | **-log Ic50** | 7.07±0.06 | 7.69±0.71 | **7.17±0.06***** | 7.83±0.21 | 7.59±0.23 | 7.78±0.14 | 7.57 ± 0.15 | 8.7 ± 0.18 |
| | **Emax (%)** | 94.93 ± 2.62 | 88.75 ± 3.57 | 94.38 ± 1.91 | 86.85 ± 5.19 | 96.77 ± 3.23 | 92.75 ± 2.65 | 98.99 ± 1.01 | 99.18 ± 0.710 |

## Table 6.2 The Effect of BDL Cirrhosis on Vascular Reactivity

The extra- renal artery (RA) and intra-renal segmental, interlobar and 3$^{rd}$ order mesenteric arteries were isolated from 28 day rats and their sham controls. Vessels viability was assessed by response to KPSS and then responses to a vasoconstrictor (PE), endothelium-dependent vasodilator (ACh) and endothelium-independent vasodilator (SNP) were measured. Parameters included sensitivity (-log$IC_{50}$ or -log$EC_{50:}$ measured the concentration of vasodilator or vasoconstrictor, respectively, needed to produce a 50% response) and maximal vaso-dilation/constriction (Emax). For PE the Emax was measured relative to % contraction with KPSS and with the vasodilators measured relative to % preconstruction with PE. Data expressed as mean±SEM, analysed by Students t test, *p<0.05 **p<0.01 ***p<0.001. Significant values in bold.

It can be seen from these results that the predominant feature that was observed specifically in the renal arteries, was an impairment in endothelium-dependent vasodilation in response to ACh.

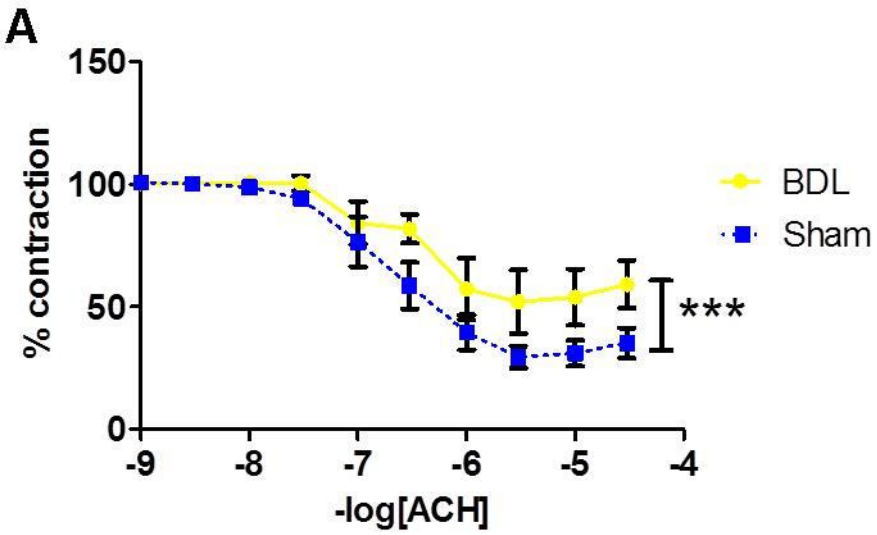
A
150
100
50
0
% contraction
-9
-8
-7
-6
-5
-4
-log[ACH]
BDL
Sham
***

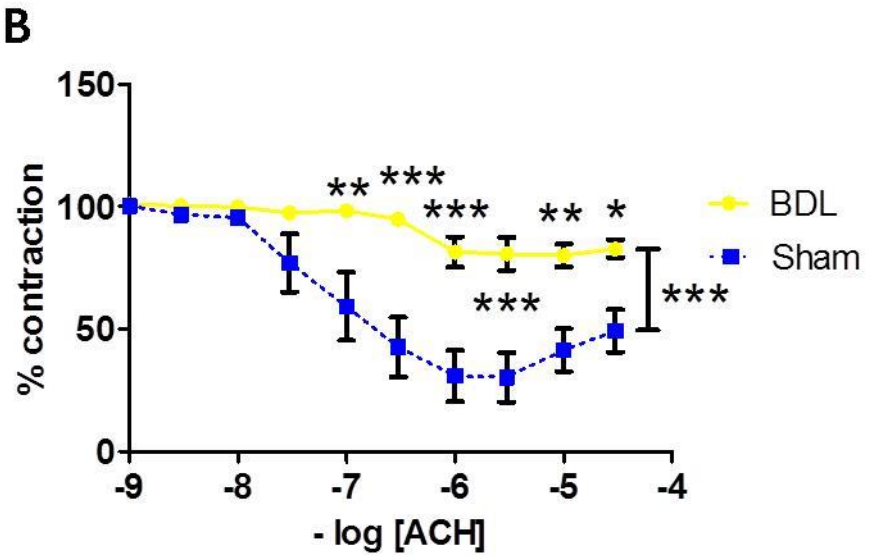
B
150
100
50
0
% contraction
-9
-8
-7
-6
-5
-4
- log [ACH]
** *** *** ** *
***
BDL
Sham
***

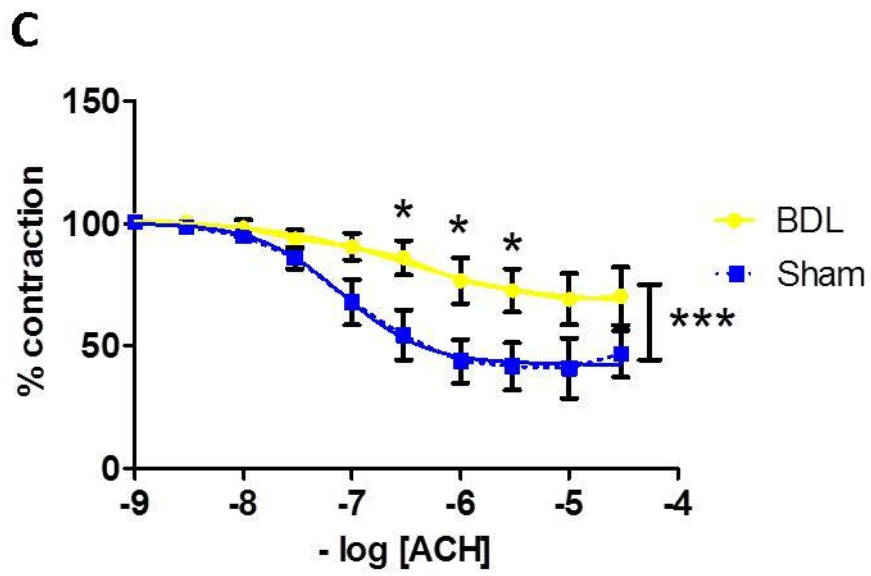
C
150
100
50
0
% contraction
-9
-8
-7
-6
-5
-4
- log [ACH]
* * *
BDL
Sham
***

## Figure 6.4 Concentration Response Curves to ACh in Renal Arteries from 28 day BDL and Sham Controls

Renal arteries (**A**) extra-renal, (**B**) intra-renal segmental and (**C**) intra-renal interlobar were isolated from 28 day BDL rats and sham controls, pre-constricted with phenylephedrine and exposed to increasing doses of Acetylcholine (ACh; $10^{-9}$ to $10^{-5}$M). Data expressed as % contraction, relative to pre-constriction with PE and analysed by 2-way ANOVA with post-hoc Bonferroni test comparing individual concentrations. *p<0.05 **p<0.01 ***p<0.001.

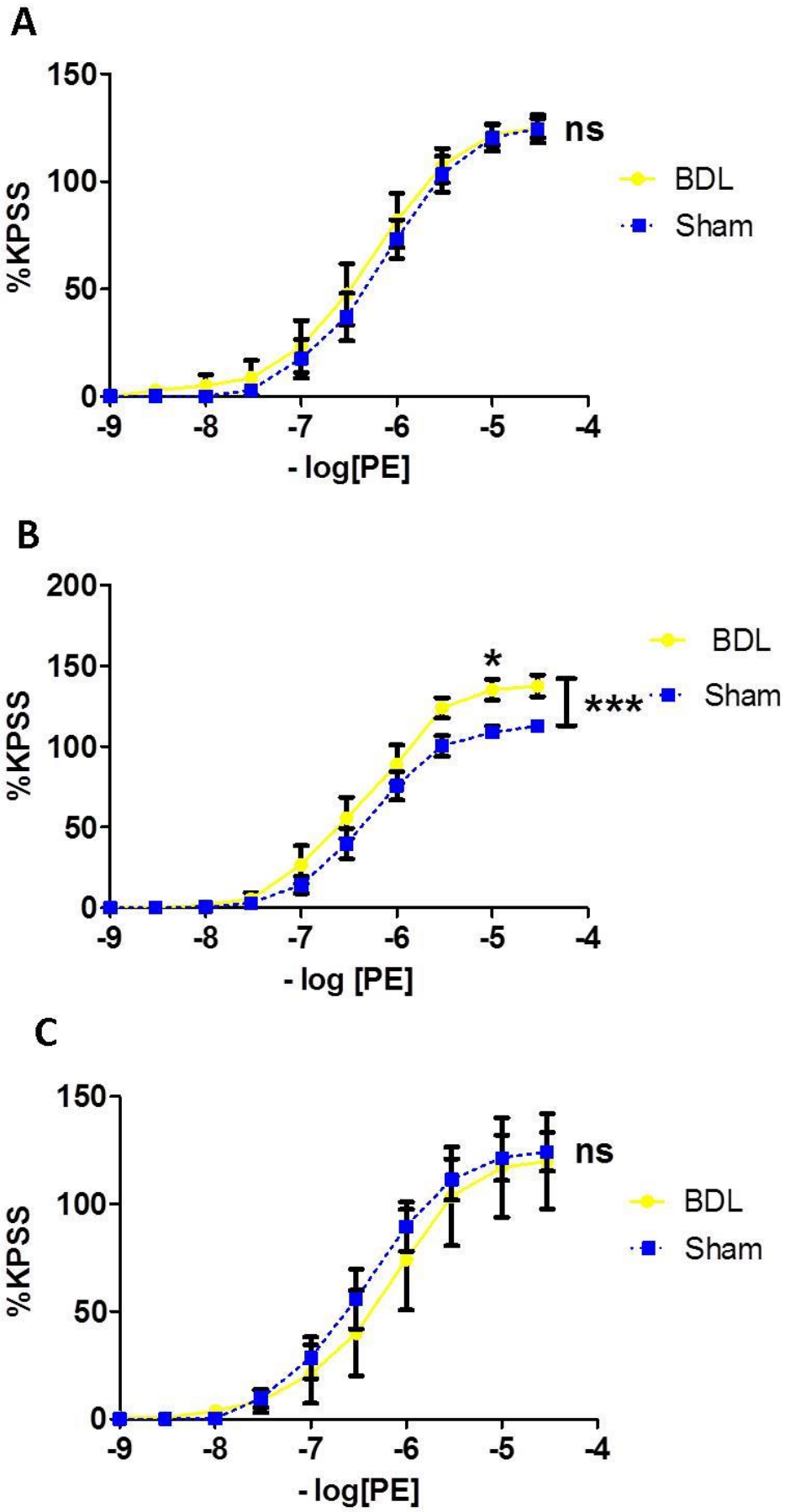
A
150
100
50
0
%KPSS
-9
-8
-7
-6
-5
-4
- log[PE]
ns
BDL
Sham
B
200
150
100
50
0
%KPSS
-9
-8
-7
-6
-5
-4
- log [PE]
*
***
BDL
Sham
C
150
100
50
0
%KPSS
-9
-8
-7
-6
-5
-4
- log[PE]
ns
BDL
Sham

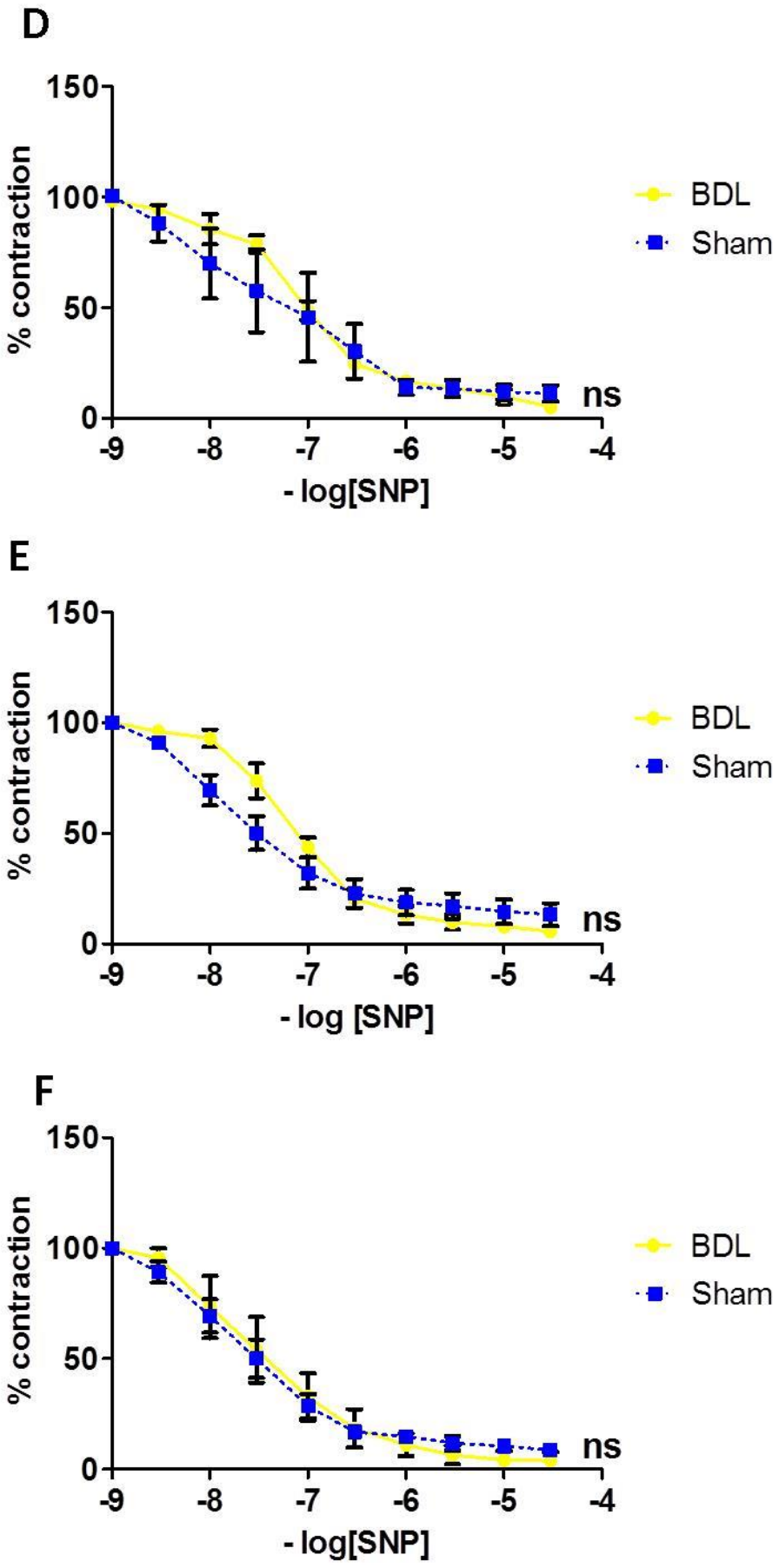
D
150
100
50
0
% contraction
-9
-8
-7
-6
-5
-4
- log[SNP]
ns
BDL
Sham
E
150
100
50
0
% contraction
-9
-8
-7
-6
-5
-4
- log [SNP]
ns
BDL
Sham
F
150
100
50
0
% contraction
-9
-8
-7
-6
-5
-4
- log[SNP]
ns
BDL
Sham

## Figure 6.5 Concentration Response Curves to PE and SNP in Renal Arteries from 28 Day BDL rats and Sham Operated Controls

Renal arteries (**A, D**) extra-renal, (**B, E**) intra-renal segmental and (**C, F**) intra-renal interlobar were isolated from 28 day BDL cirrhotic rats and sham controls, exposed to increasing doses of the vasoconstrictor phenylephedrine (PE; $10^{-9}$ to $10^{-5}$M **A-C**). Data expressed as % contraction relative to KPSS (Potassium rich physiological salt solution). After pre-constriction with PE, arteries were exposed to increasing doses of sodium nitroprusside – an endothelium-independent vasodilator (SNP; $10^{-9}$ to $10^{-5}$M; **D-E**). Data expressed as % contraction, relative to pre-constriction with PE and analysed by 2-way ANOVA with post-hoc Bonferroni test comparing individual concentrations. *p<0.05 **p<0.01 ***p<0.001.

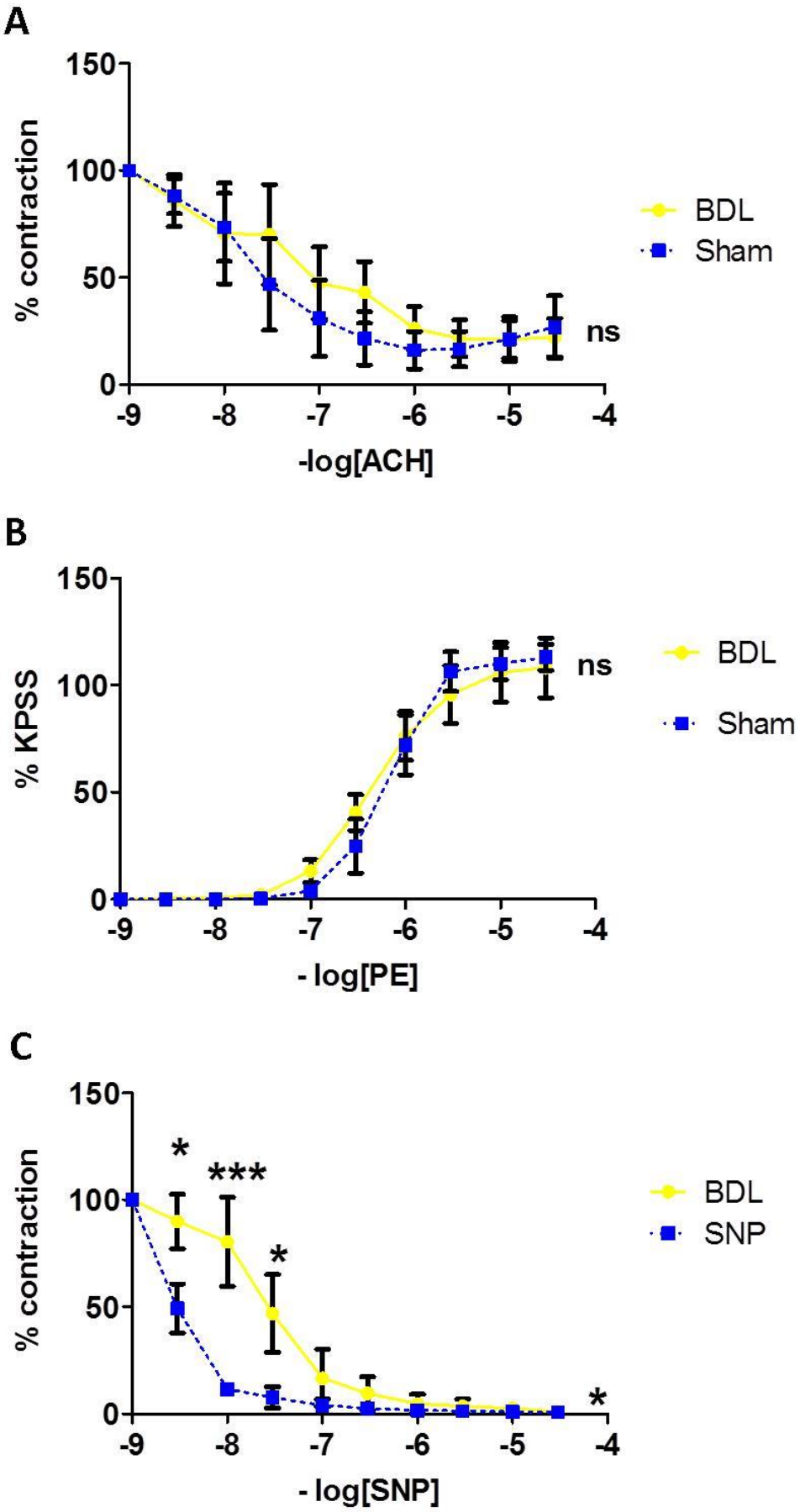
A
150
100
50
0
% contraction
-9
-8
-7
-6
-5
-4
-log[ACH]
ns
BDL
Sham
B
150
100
50
0
% KPSS
-9
-8
-7
-6
-5
-4
- log[PE]
ns
BDL
Sham
C
150
100
50
0
% contraction
-9
-8
-7
-6
-5
-4
- log[SNP]
*
***
*
*
BDL
SNP

## Figure 6.6 Concentration Response Curves in Mesenteric arteries from 28 day BDL Rats and Sham Controls

3rd order mesenteric arteries were isolated from 28 day BDL cirrhotic rats and sham controls and after pre-constriction with PE, were exposed to increasing doses of the endothelium-dependent vasodilator Acetylcholine (ACH; $10^{-9}$ to $10^{-5}$M; **A**), sodium nitroprusside – an endothelium-independent vasodilator (SNP; $10^{-9}$ to $10^{-5}$M; **C**). Data expressed as % contraction, relative to pre-constriction with PE. (**B**) Mesenteric arteries were also exposed to increasing doses of the vasoconstrictor phenylephedrine (PE; $10^{-9}$ to $10^{-5}$M; **B**). Data expressed as % contraction relative to KPSS and analysed by 2-way ANOVA with post-hoc Bonferroni test comparing individual concentrations. *$p<0.05$ **$p<0.01$ ***$p<0.001$.

## 6.6 Nitric oxide synthase is critical to endothelium-dependent renal arterial vasodilation in normal and cirrhotic rats

Having observed that endothelium-dependent vasodilatation is impaired in both models of cirrhosis, I needed to establish the mechanism. In order to do this, I firstly needed to delineate the pathway(s) responsible for normal renal arterial endothelium-dependent function. I used isolated extra-renal renal arteries from normal (uninjured) rats (n=6) and pre-treated them for 45 minutes with inhibitors of the major pathways known to be responsible for endothelium-dependent vasodilatation in different vascular beds. Vessels were exposed to the nitric oxide synthase (NOS) inhibitor L-NAME ($1x10^{-4}$ M), the cyclo-oxygenase (COX) inhibitor indomethacin ($1x10^{-5}$M) and the endothelium-derived hyperpolarisation factor (EDHF) inhibitors apamin ($1x10^{-4}$ M) and charybdotoxin ($1x10^{-5}$M) before stimulation with ACh and SNP. Apamin and charybdoxin have been shown to inhibit calcium-activated potassium channels, selectively inhibiting the smooth muscle response to EDHF (Quinard et al., 2000). From the literature, the relative contribution of different pathways varies between different arteries. In normal uninjured renal arteries endothelium-dependent vasodilation was abrogated by L-NAME pre-treatment and blunted by EDHF inhibitors (**Fig 6.7A**), whereas COX inhibition had no effect.

I repeated this experiment with extra-renal arteries from 16 week $CCl_4$ (n=6) cirrhotic rats. The vasodilatory response to ACh was completely abolished by L-NAME (**Fig 6.7B**). Pre-treatment with EDHF inhibitors alone appeared to have a more modest effect on ACh-mediated vasodilation in 16 week $CCl_4$ rats compared to normal uninjured rats. In contrast, COX inhibition enhanced vasodilation in cirrhotic renal arteries.

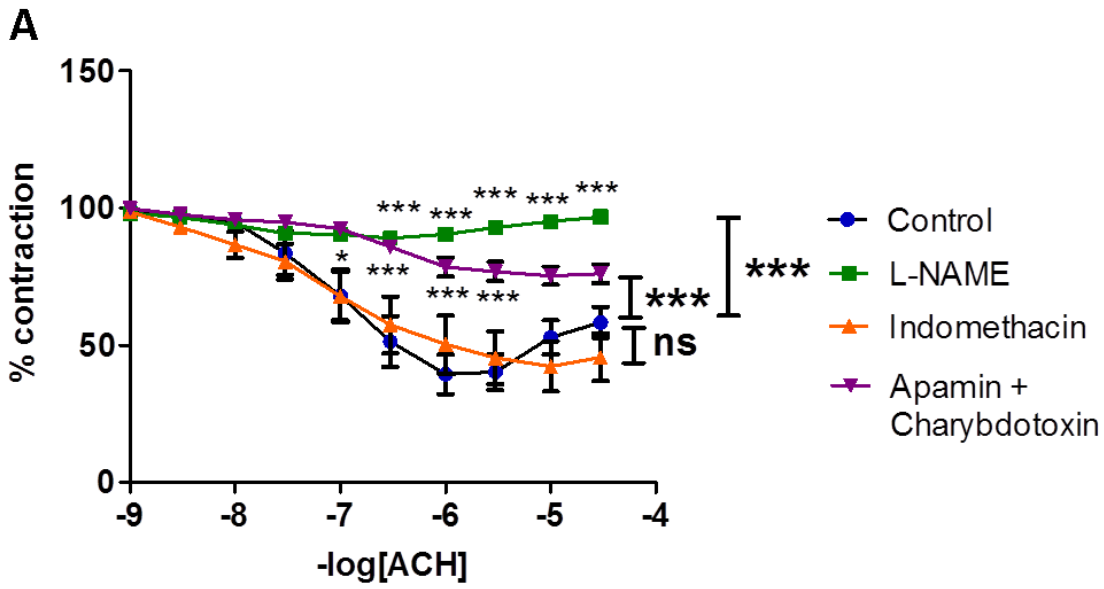
A
150
100
50
0
% contraction
-9
-8
-7
-6
-5
-4
-log[ACH]
***
ns
Control
L-NAME
Indomethacin
Apamin +
Charybdotoxin

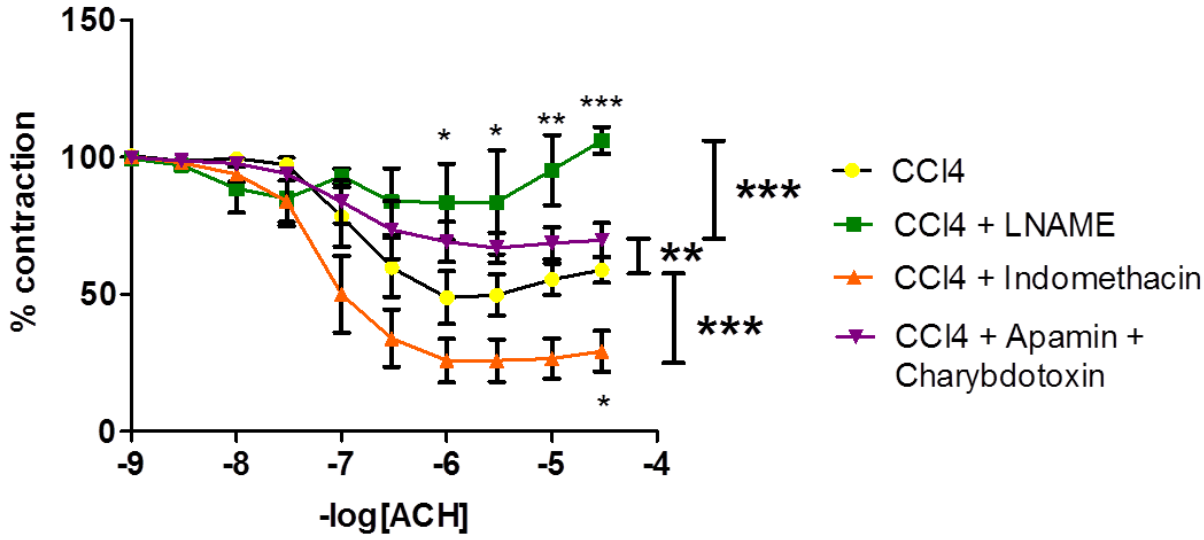
B
150
100
50
0
% contraction
-9
-8
-7
-6
-5
-4
-log[ACH]
***
**
***
CCl4
CCl4 + LNAME
CCl4 + Indomethacin
CCl4 + Apamin +
Charybdotoxin

## Figure 6.7 Ach Concentration Response Curves in Normal Uninjured Controls and 16 week $CCl_4$ cirrhotic rats with inhibitors of NOS, COX and EDHF

Extra-renal renal arteries from control rats (**A**) and 16 week CCl4 rats (**B**) were treated with L-NAME (1x10-4M) to block NOS, indomethacin (1x10-5M) to block COX, and apamin (1x10-4M) and charybdotoxin (1x10-5M) to block EDHF, and then exposed to increasing doses of Ach ($10^{-9}$ to $10^{-5}$M). Data expressed as % contraction, relative to pre-constriction with PE analysed by 2-way ANOVA with post-hoc Bonferroni test comparing individual concentrations. *p<0.05 **p<0.01 ***p<0.001.

To show the selectivity for these inhibitors to the endothelium, in each of the above experiments using the same rings, I created a CRC with SNP in the presence of these inhibitors. In **Fig 6.8A-B** it can be seen that L-NAME and Indomethacin had no effect on endothelium independent vasodilation, suggesting the selectivity of their effects to endothelium dependent function. However Apamin and Charybdotoxin abrogated, more in normal than cirrhotic renal arteries, the smooth muscle response to SNP. As the initial abnormality between control and cirrhotic renal arteries, from both models, appeared to be response to endothelium-dependent vasodilators and the purpose of this experiment was to delineate the mechanism by which renal arteries endothelium dependent vasodilation was mediated I did not look into this abrogation of response to SNP further.

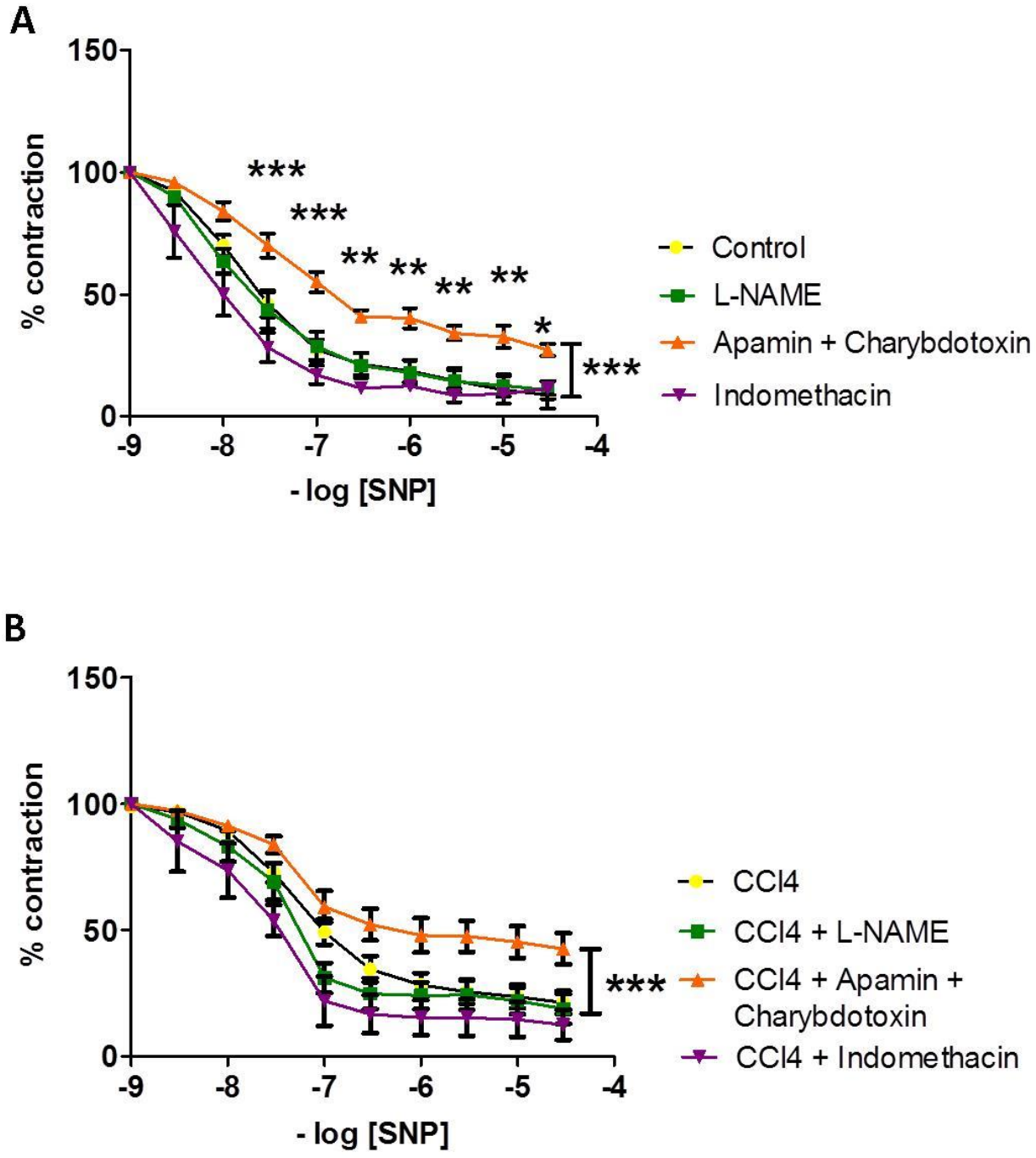
A
150
100
50
0
% contraction
***
***
**
**
**
**
*
***
-9
-8
-7
-6
-5
-4
- log [SNP]
Control
L-NAME
Apamin + Charybdotoxin
Indomethacin
B
150
100
50
0
% contraction
***
-9
-8
-7
-6
-5
-4
- log [SNP]
CCl4
CCl4 + L-NAME
CCl4 + Apamin + Charybdotoxin
CCl4 + Indomethacin

# Figure 6.8 SNP Concentration Response Curves in Normal Uninjured Controls and 16 week $CCl_4$ cirrhotic rats with inhibitors of NOS, COX and EDHF

Extra-renal renal arteries from control rats (**A**) and 16 week $CCl_4$ rats (**B**) were treated with L-NAME ($1x10^{-4}$M) to block NOS, indomethacin ($1x10^{-5}$M) to block COX, and apamin ($1x10^{-4}$M) and charybdotoxin ($1x10^{-5}$M) to block EDHF, and then exposed to increasing doses of SNP ($10^{-9}$ to $10^{-5}$M). Data expressed as % contraction, relative to pre-constriction with PE analysed by 2-way ANOVA with post-hoc Bonferroni test comparing individual concentrations. *p<0.05 **p<0.01 ***p<0.001.

Overall, these findings suggested that renal arteries, from both normal and cirrhotic $CCl_4$ rats, predominantly required NOS to mediate endothelium-dependent relaxation, though there is a definite contribution from EDHF. The relative contributions cannot be delineated from this experiment as I would have needed to repeat this experiment but with multiple inhibitors together.

### 6.7 NOS activity is reduced in the kidneys of cirrhotic rats

As NOS appears critical for renal endothelium-dependent vasodilatation and there is a marked abnormality in endothelium-dependent vasodilatation in renal arteries from the cirrhotic rats, I decided to initially focus my attention on the NOS pathway. Using protein extracted from whole kidney from cirrhotic rats versus their respective controls (n=4/per group) I performed Western blotting and densitometry analysis to quantify the levels of phosphorylated eNOS. In $CCl_4$ kidneys there was a trend to reduction in p-eNOS (**Fig 6.9A-B**), though this did not reach statistical significance, whereas in BDL kidneys there was a definite reduction (**Fig 6.9C-D**). Given Western blotting only determines protein expression levels, I went on to quantify NOS *activity* in whole kidney extracts from control and cirrhotic rats (n=6-8 per group). It should be noted that this assay

measured whole NOS activity. Although the predominant isoform measured will be eNOS there may be some contribution from iNOS. NOS activity was markedly reduced in $CCl_4$ kidneys (**Fig 6.10A**) relative to controls ($p<0.05$) and in BDL kidneys (**Fig 6.10B**) there was a consistent trend to reduction in NOS activity relative to sham controls, although this was not statistically significant ($p=0.0871$).

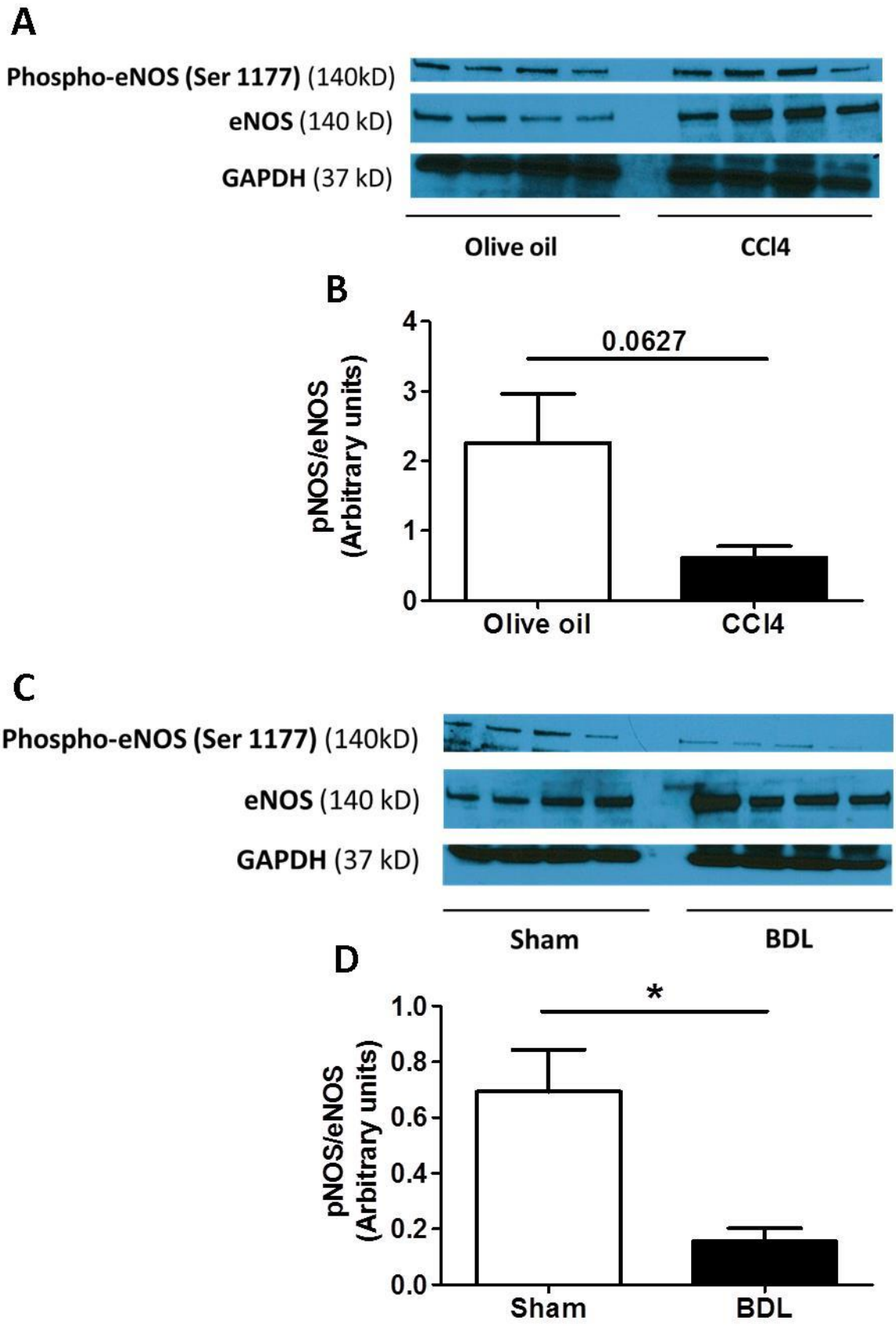
A
Phospho-eNOS (Ser 1177) (140kD)
eNOS (140 kD)
GAPDH (37 kD)
Olive oil
CCl4
B
pNOS/eNOS (Arbitrary units)
0.0627
Olive oil
CCl4
C
Phospho-eNOS (Ser 1177) (140kD)
eNOS (140 kD)
GAPDH (37 kD)
Sham
BDL
D
pNOS/eNOS (Arbitrary units)
*
Sham
BDL

# Figure 6.9 Phosphorylated-endothelial NOS Expression in Rat Models of Cirrhosis

Protein was extracted from whole kidney from both models and their respective controls (n=4/group). Western Blot was performed to assess expression of p-eNOS/eNOS. (**A**) CCl4 model Western Blot with (**B**) densitometry analysis (**C**) BDL model Western Blot with (**D**) densitometry analysis. Data expressed as mean±SEM and analysed by student t test. *$p<0.05$

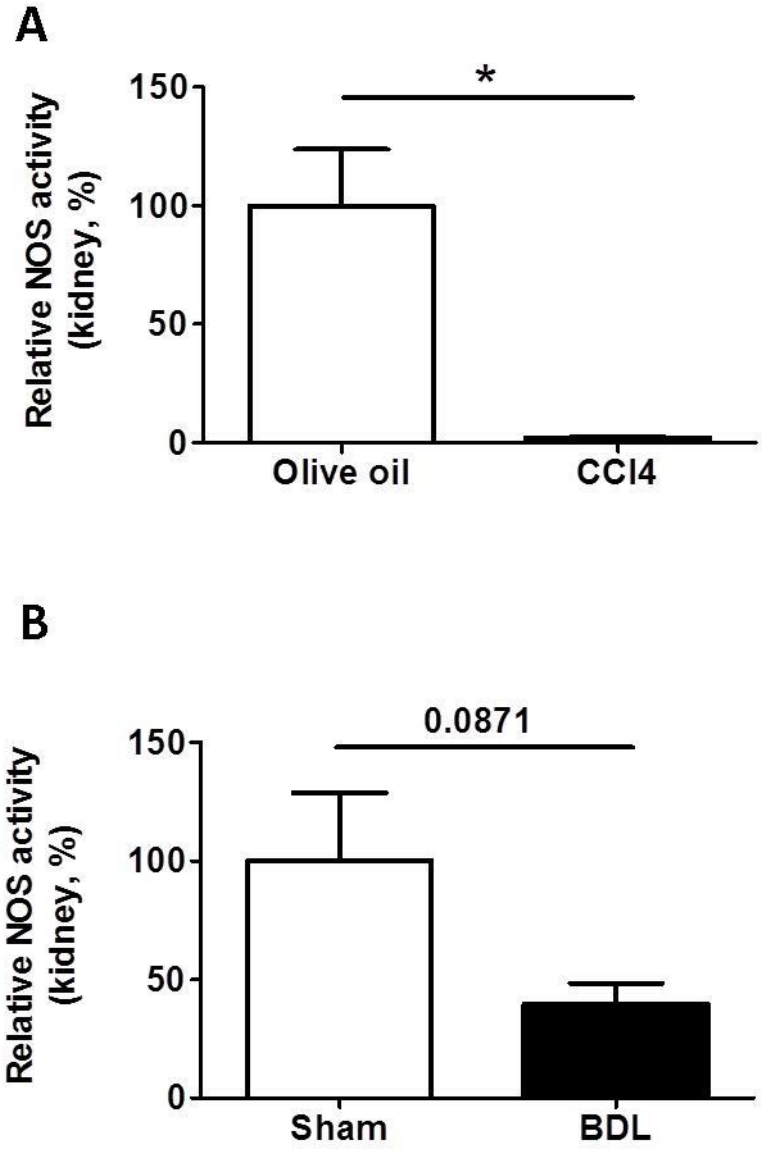


## Figure 6.10 NOS Activity Assay in Rat Models of Cirrhosis

Protein was extracted from whole kidney from 16 week $CCl_4$ and 28 day BDL kidneys and their respective controls (n=6-8/group). NOS activity was measured using the modified Greiss Reaction to measure total Nitrite produced over time in (**A**) $CCl_4$ model and (**B**) BDL model relative to their controls. Data expressed as mean % activity ±SEM relative to mean activity of control and analysed by Students t test. *$p<0.05$.

Taken together, these results showed a reduction in both phosphorylated eNOS protein expression and NOS activity in cirrhotic rat kidneys. This may provide a major explanation for the aberrant vasomotor phenotype observed in cirrhotic renal vessels.

### 6.8 Inhibitors of NOS are upregulated in the kidneys in cirrhosis

To elucidate the mechanism(s) resulting in reduced kidney NOS activity and p-eNOS expression in cirrhosis, I studied transcriptional changes in potentially relevant genes. As an initial unbiased screening tool I used a Hypertension qPCR array (Qiagen) that included 96 different genes involved in vasodilatation and vasoconstriction. I again used whole kidney from 16 week $CCl_4$ cirrhotic rats versus controls (n=3-6/group). All genes that had a fold regulation relative to control of $\geq 2$ with a $p<0.05$ were considered significant. **Fig 6.11A and B** shows genes that were differentially regulated in cirrhosis**.** In cirrhosis, the following key genes were upregulated: endothelin receptors $ET_A$ (Ednra) and $ET_B$ (Ednrb) - both key regulators of vascular tone; the arginine vasopressin receptor 1a (Agtr1a) - responsible for water and sodium retention; and, interestingly, key regulators of NOS (Arg2 (arginase II) and Cav1 (caveolin I). Given the results above, which suggested the importance of functioning NOS in endothelium-dependent vasodilation, I decided to focus on genes that were involved predominantly with its synthesis and receptors already implicated in the altered vascular tone occurring in cirrhosis, $ET_A$ and $ET_B$. To ensure this was not a model dependent result I performed qPCR for genes of interest using kidneys from 4 week BDL versus sham controls (n=4/group) and these showed a similar expression profile, with up-regulation of Arg2 (**Fig 6.12A**), Cav1 (**Fig 6.12B**), Ednra (**Fig 6.12C**), Ednrb (**Fig 6.13D**)

A

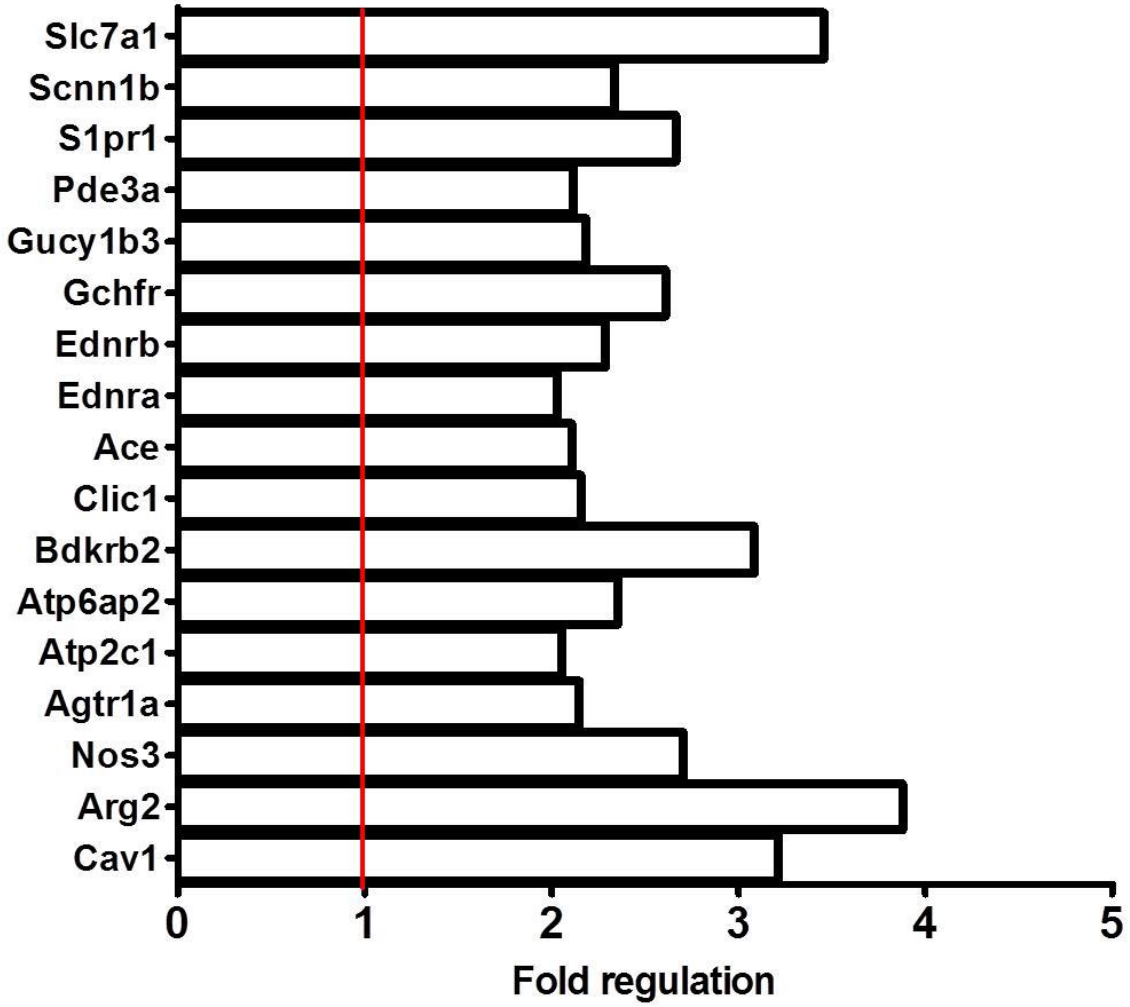
Slc7a1
Scnn1b
S1pr1
Pde3a
Gucy1b3
Gchfr
Ednrb
Ednra
Ace
Clic1
Bdkrb2
Atp6ap2
Atp2c1
Agtr1a
Nos3
Arg2
Cav1
0
1
2
3
4
5
Fold regulation

B

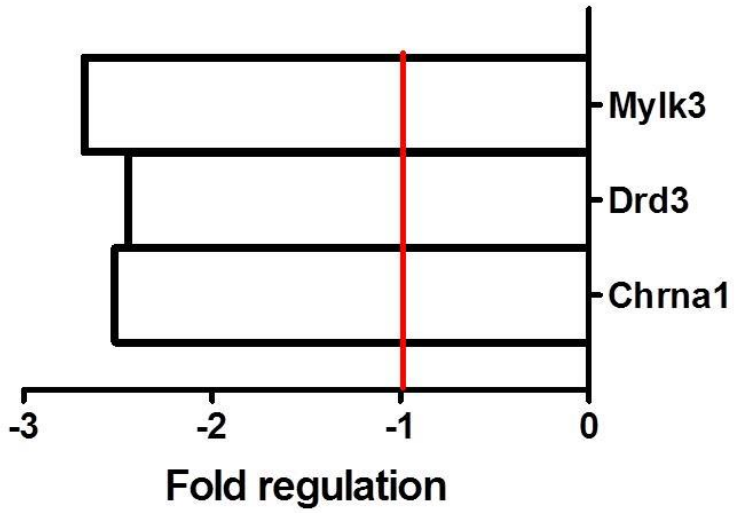
Mylk3
Drd3
Chrna1
-3
-2
-1
0
Fold regulation

## Figure 6.11 Gene Regulation in $CCl_4$ Model of Cirrhosis

RNA was extracted from whole kidney from 16 week $CCl_4$ cirrhotic and Olive oil controls, 2µg RNA was transcribed and the RT2 Hypertension Profile PCR Array (Qiagen) undertaken. All genes that had a fold regulation relative to control of equal to or of $\geq 2$ with a $p<0.05$ were considered significant and shown. (**A**) genes that were upregulated, (**B**) genes that were down regulated in cirrhosis

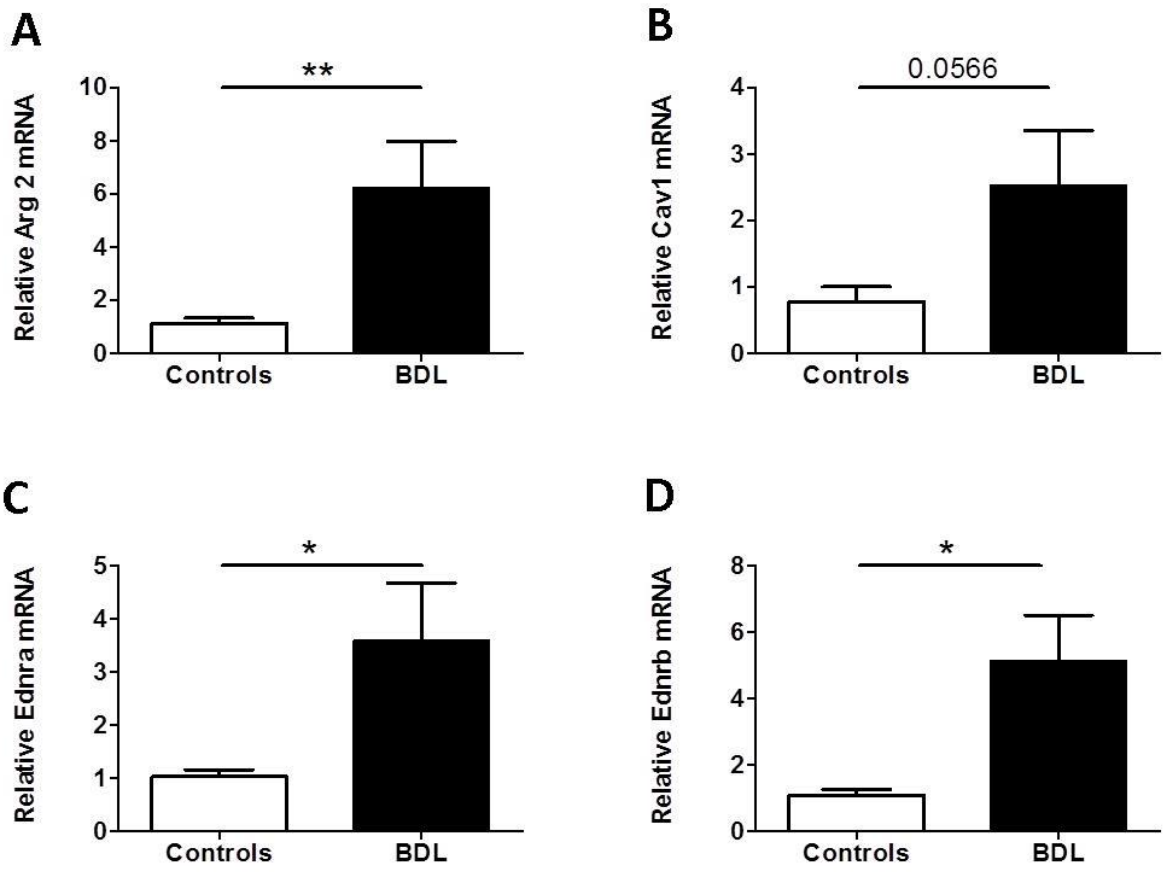


## Figure 6.12 Gene Regulation in BDL Model of Cirrhosis

RNA was extracted from whole kidney from 28 day BDL cirrhotic and sham controls, 2µg RNA was transcribed and qPCR performed for genes of interest (**A**) Arginase 2, (**B**), Caveolin I, (**C**) $ET_A$, (**D**) $ET_B$. Data expressed as mean ± SEM relative to average expression of respective control, and analysed by Students t test. *$p<0.05$, **$p<0.01$.

Arginase II is a mitochondrial enzyme that inhibits NOS metabolism by competing for its predominant substrate arginine. Without arginine, NOS is unable to produce NO. It has increasingly been shown to play a role in the endothelial dysfunction seen in diabetes, obesity and hypertension (Johnson, Peyton et al. 2015) via competition with NOS leading to arterial vasoconstriction. Its role in cirrhosis and particularly HRS has not been defined, but the increase in gene expression made it an interesting factor to study in more detail. Staining of kidney tissue showed its expression was

predominantly in the medulla and in tubular cells (**Fig 6.13A**). Morphometric pixel analysis of kidney sections (n=5/group) stained for arginase II, confirmed increased expression in cirrhosis (**Fig 6.13B**). To confirm this I went on to perform Western blot analysis of arginase II in whole kidney of both cirrhosis models versus their respective controls (n=4/group). The results from Western blot from both models (**Fig 6.13C-D**) indicated increased expression.

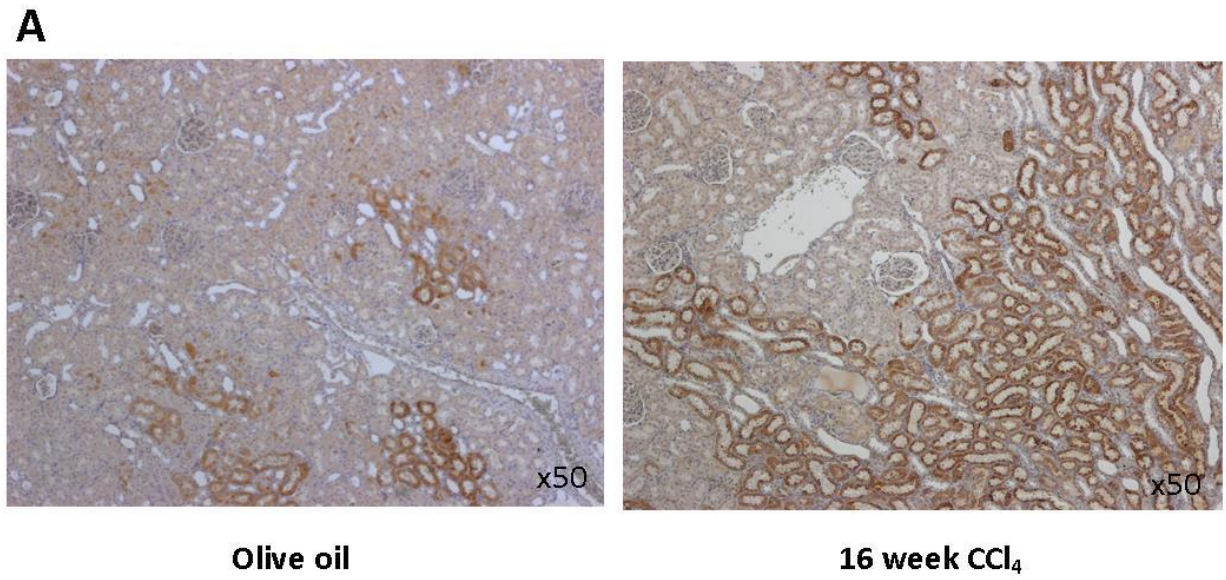
A
x50
x50
Olive oil
16 week CCl4
B
**
% of Arginase staining / kidney section
15
10
5
0
Olive oil
16wk CCl4
C
Arginase 2 (40kD)
GAPDH (37 kD)
Olive oil
CCl4
**
Arginase (Arbitrary units)
1.5
1.0
0.5
0.0
Olive Oil
16 week CCl4
D
Arginase 2 (40kD)
GAPDH (37 kD)
Sham
BDL
**
Arginase (Arbitrary units)
2.5
2.0
1.5
1.0
0.5
0.0
Sham
BDL

## Figure 6.13 Effect of Cirrhosis on Kidney Arginase II Expression

(**A**)Arginase II staining in kidney sections from olive oil and 16 week $CCl_4$ rats (representative images). (**B**) Quantification of Arginase staining (n=5/group) by morphometric pixel analysis. Data expressed as mean % stained per section ±SEM. (**C**)Western Blot and densitometry for Arginase II of protein extracted from whole kidney from olive oil and 16 week CCl4 (n=4/group). (**D**) Western Blot and densitometry for Arginase II of protein extracted from whole kidney from sham and 28 day BDL (n=4/group). Data expressed relative to GAPDH as mean±SEM, and analysed by Students t test. **p<0.01.

Caveolin I is a scaffolding protein that is thought to bind eNOS and in the bound form it is inactive (Minshall, Sessa et al. 2003). Therefore one could hypothesize that increasing amounts of Caveolin I may limit eNOS activity in these models. I stained for Caveolin in kidney tissue and it was predominantly expressed in the endothelium and smooth muscle (**Fig 6.14A**). Quantification of renal Caveolin I protein expression by Western blot and densitometry showed an increase in BDL cirrhosis with a trend in $CCl_4$ cirrhosis (n=4/group) (**Fig 6.14B-C**)

A

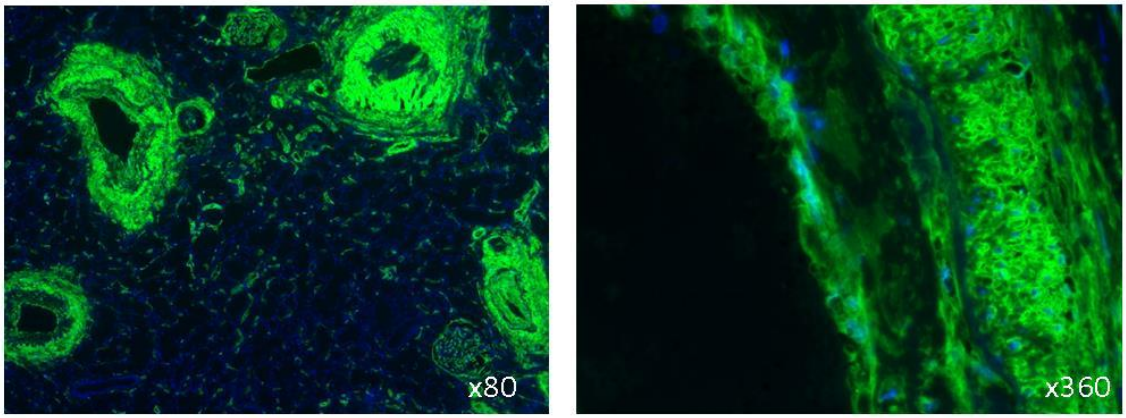


16 week $CCl_4$ Cortex

16 week $CCl_4$ artery wall

B

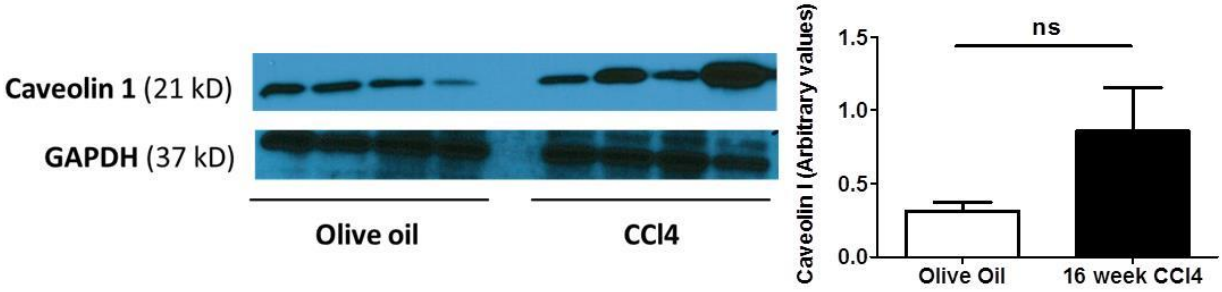


C

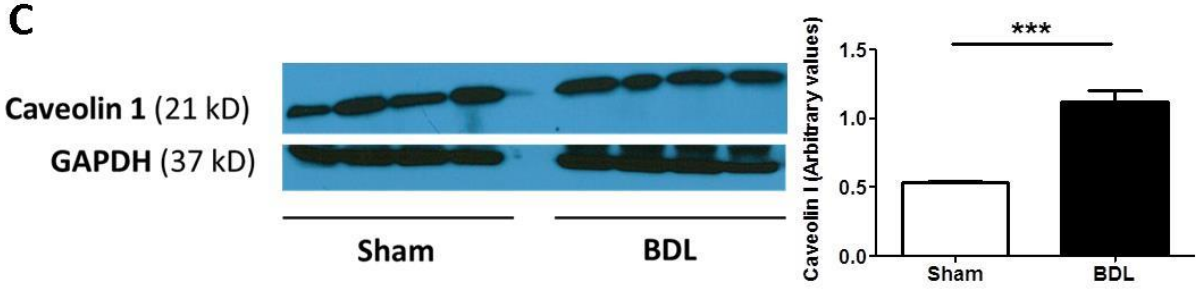

## Figure 6.14 Effect of Cirrhosis on Kidney Caveolin I Expression

(**A**)Caveolin I staining in kidney sections from olive oil and 16 week $CCl_4$ rats (representative images). (**B**)Western Blot and densitometry for Arginase II of protein extracted from whole kidney from olive oil and 16 week $CCl_4$ (n=4/group). (**C**) Western Blot and densitometry for Arginase II of protein extracted from whole kidney from sham and 28 day BDL (n=4/group). Data expressed relative to GAPDH, as mean±SEM, and analysed by Student's t-test. **p<0.01.

In these cirrhosis models there was up-regulation of potential inhibitors of NOS that may account, at least in part, for the endothelial dysfunction observed *ex vivo*. I did not investigate the regulation of these NOS inhibitory proteins or the cellular source, but they represent an interesting focus for future studies.

### 6.9 Serum TNFα is increased in rat cirrhosis models

TNFα is a major pro-inflammatory cytokine that has been shown in numerous studies (Picchi, Gao et al. 2006; Zhang, Xu et al. 2006) to contribute to endothelial dysfunction. I therefore decided to measure circulating TNFα levels in my models. **Fig 6.15A** and **B** show increased levels of serum TNFα in both models, particularly in BDL. The serum was taken from the peripheral circulation so represents 'systemic' TNFα. At present, I have only shown an association between high circulating levels of TNFα and endothelial dysfunction in these models, but future work could focus on a causal relationship by using TNFα inhibitors/anti-inflammatory approaches.

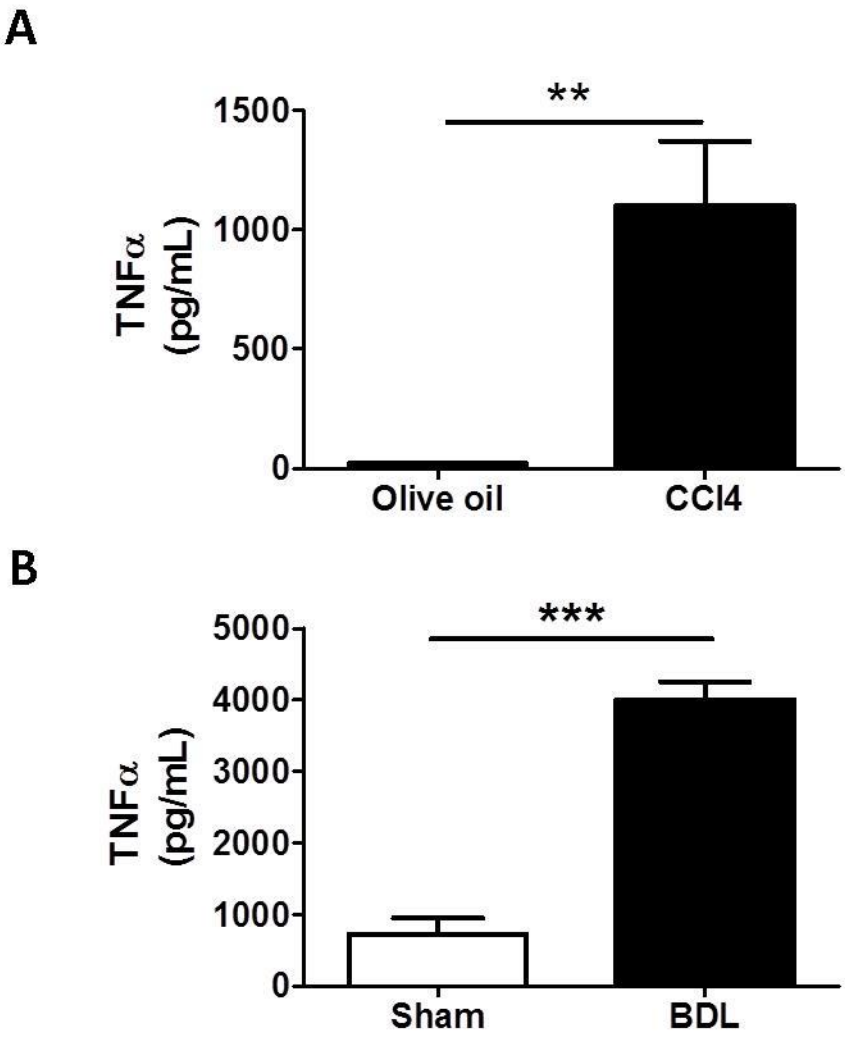


## Figure 6.15 Serum TNFα level in Cirrhosis Models

Circulating serum TNFα levels were measured from blood taken from the femoral artery in (A) olive oil and CCl4 rats (5-6/group). (B) sham and 28 day BDL (4-7/group). Date expressed as mean±SEM, analysed by Students t test. . **p<0.01, ***p<0.001.

## DISCUSSION

In this Chapter I investigated vascular reactivity and gene and protein expression changes in the kidneys of cirrhotic rats to identify potential mechanisms underlying the renal vasoconstriction observed in these models. The first observation, that I will term 'endothelial dysfunction', is that renal arteries from cirrhotic rats showed impairment of endothelium-dependent vasodilatation (**Fig 6.1A-C, Fig 6.4A-C**) and this was seen throughout the renal artery circulation. Importantly, this did not appear to be a systemic phenomenon as the mesenteric arteries did not show the same abnormality (**Fig 6.3 and 6.6**). Previous studies have used myography to assess vascular reactivity in cirrhosis, but this has focussed primarily on other arteries, particularly the portal vein (Hadoke and Hayes 1997). These studies have highlighted that inter-species differences undoubtedly influence individual vascular responses. Ideally, I would have studied vascular responses in human renal arteries from patients with HRS to establish whether this was a species-specific phenomenon. Unfortunately research into this important condition has been limited as kidneys are rarely explanted in patients with HRS and biopsies are not performed as part of routine clinical care. Moreover, biopsy tissue would not permit rings of renal artery to be tested by myography.

From interrogating the pathways important for renal endothelium-dependent vasodilatation, NOS appears critical to vasodilatation in both normal and cirrhotic rats as blocking NOS with L-NAME abrogated normal renal vasodilatation. Interestingly, prostacyclins were previously thought to be integral to renal arterial vasodilatation, but in both normal and cirrhotic renal arteries I observed no impact on endothelium-dependent vasodilatation by inhibition of this pathway. This finding is supported to a certain extent, by clinical data showing that no improvement in renal function was observed in patients treated with prostacyclins (Salo, Gines et al. 1996).

I have shown that p-eNOS expression and NOS activity are reduced in cirrhotic kidney (**Fig. 6.9-10**) which may account for the abnormality in endothelium dependent vasodilation seen in the renal arteries. It is worth noting that these results are from whole kidney and so aren't specific to endothelial cell or renal arterial expression but are inclusive of all kidney cells. The reason I took this approach was that the amount of tissue needed for successful protein extraction, Western blotting and NOS activity assay precluded the use of tiny renal artery segments. Further to this, I have shown that inhibitors of NOS (arginase II, caveolin I) are increased in kidneys from cirrhotic rats and these may account, at least in part, for the abnormal vascular responses observed. The results above are all descriptive and without *in vivo* experiments specifically blocking arginase II, caveolin I or TNFα and determining whether RBF improves and/or there is preservation of endothelial function, I cannot infer the extent to which they contribute. Additionally, as arginase II and caveolin I are abundantly expressed, simply blocking them could cause systemic off-target effects limiting the focus of the experiment.

This renal endothelial dysfunction may account for the reduced RBF and vasoconstricted circulation seen in both the rat models and in human HRS. One could hypothesise that a reduced ability to respond to endothelial vasodilators leads to an increasingly unopposed response to circulating vasoconstrictors, which have been shown to be circulating in abundance in cirrhosis (Ring-Larsen, Hesse et al. 1982; Schrier, Arroyo et al. 1988). Additionally, I have shown increased transcript levels of the $ET_A$ and $ET_B$ receptor in both models. Both receptors are expressed on smooth muscle cells, with the $ET_B$ receptor also being expressed on the endothelium. The former, on activation with endothelin, induces vasoconstriction, whilst the latter also induces vasodilation. It has been shown that in the liver parenchyma in cirrhosis there is a shift to increased $ET_B$ expression, and in the portal

vein a down-regulation of $ET_B$ relative to $ET_A$ in the smooth muscle (Ling, Kuc et al. 2012). One could postulate that the hepatic parenchymal and portal vein receptor expression changes in cirrhosis represent a 'protective mechanism' to try to reduce the raised intravascular resistance by increasing vasodilation in the liver and reducing inflow via the portal vein. Further implicating the $ET_A$ and $ET_B$ receptors in the pathogenesis of endothelial dysfunction is a recent study investigating endothelial function in patients with type 2 diabetes and coronary artery disease, which found that selective $ET_A$ and combined $ET_A/ET_B$ blockade improved endothelium-dependent forearm vasodilation (Rafnsson, Shemyakin et al. 2014).

The abnormalities defined in the results above, in renal endothelial function, are very similar to that which has been proposed in the hepatic sinusoidal endothelial cells (Rockey and Chung 1998). Although I have shown a potential role for NOS in the evolution of this endothelial dysfunction and subsequent renal vasoconstriction, the underlying mechanisms require further study. In addition to NOS dysregulation, the relative balance of vasoconstrictor/vasodilator receptor expression, the sympathetic nervous system, and other circulating cytokines will also play important roles. This needs further delineation. Improved understanding of the major contributors to this endothelial dysfunction would represent an important step towards unravelling the pathogenesis of HRS.

## Summary of important findings:

- Endothelium-dependent vasodilation was blunted in the extra and intra renal arteries from two distinct models of cirrhosis characterized by renal vasoconstriction and renal dysfunction
- *Ex vivo* normal and cirrhotic renal arteries required NOS to respond to endothelium-dependent vasodilators
- In kidneys from both cirrhosis models p-eNOS expression and NOS activity were reduced
- The expression of negative regulators of NOS (Arginase II and Caveolin I) was increased in the kidneys of cirrhotic rats
- Levels of TNFα in the peripheral circulation were increased in both cirrhosis models

## Next steps:

In **Chapter 5** I showed that both acute and sustained RLN treatment improved RBF and GFR. In this Chapter I have shown that renal arteries from cirrhotic rats exhibit abnormal endothelium-dependent vasodilatation and that this 'endothelial dysfunction' may be partially explained by changes in NOS activity due to increased expression of negative regulator proteins. I next wanted to study the effect of RLN on these parameters in order to define the haemodynamic mechanism of action.

# CHAPTER 7 - DEFINING THE MECHANISM OF ACTION OF H2-RELAXIN IN MODULATING RENAL DYSFUNCTION

## 7.1 Overview

In this Chapter I used the $CCl_4$ and BDL models of cirrhosis and used myography to measure changes in vascular reactivity and qPCR, Western blot and ELISA to analyse changes to key vasoactive modulators to establish how RLN mediates the *in vivo* haemodynamic effects reported in **Chapter 5**.

## 7.2 Author contributions

I performed all the experiments in this Chapter.

## 7.3 Background

As covered in detail in the **Introduction**, all mechanistic work with RLN to date has been in undertaken in pregnant or normal rats and in humans with cardiac failure. A consistent feature in these studies was the observation that RLN increases RBF, which I have also shown in cirrhotic rats with renal dysfunction.

The vasoactive effects of RLN are mediated through a number of downstream mechanisms including a reduction in myogenic reactivity of vessels, enhanced nitric oxide (NO) signaling and antagonism of vasoconstrictors such as angiotensin-II (Danielson, Kercher et al. 2000; Novak, Ramirez et al. 2002; McGuane, Debrah et al. 2011). Through inhibitory *in vivo* and *in vitro* experiments, pivotal factors have been identified in mediating the sustained vasodilatory effects of RLN including NOS

(Danielson, Sherwood et al. 1999), endothelial $ET_B$ receptor (Danielson, Kercher et al. 2000), arterial gelatinases (MMP2, MMP9) (Jeyabalan, Novak et al. 2003), and vascular endothelial growth factor (VEGF) (McGuane, Danielson et al. 2011). Rapid vasodilatory effects of RLN have been shown to be mediated through Gαi/o protein coupling to Pi3K, Akt and endothelial NOS, but not via VEGF (Fisher, MacLean et al. 2002).

I wanted to establish in my rat models, in which I had shown robust renal haemodynamic changes in response to RLN, whether the mechanisms mediating its beneficial effects were consistent with previous studies or if other pathways were engaged by RLN in cirrhosis.

### 7.4 Aims

- To assess the effects of H2-RLN on renal vascular reactivity
- To ascertain the potential mechanisms responsible for the *in vivo* effects of H2-RLN

## RESULTS

### 7.4 Isolated renal arteries from cirrhotic rats show no acute vasodilation response to RLN *ex vivo*

In **Chapter 5,** I showed that RLN rapidly increased RBF *in vivo*. To elucidate the underlying mechanism, I took the isolated renal arteries from both control uninjured and 16 week $CCl_4$ cirrhotic rats and after checking viability with KPSS, and endothelial function with ACh I then pre-constricted with PE to achieve an $EC_{50}$ of 80% and exposed them to increasing doses of RLN every 3 minutes (1

$x10^{-13}$ to $1x10^{-7}$M) and observed the degree to which they vasodilated. The dose range was based on previously published work using RLN and wire myography where acute vasodilation was demonstrated in gluteal arteries (Fisher, MacLean et al. 2002). Interestingly, I observed no acute vasodilation response to RLN *ex vivo* in arteries from either control or cirrhotic rats ($CCl_4$ and BDL), even with an extended dose range in the latter (**Fig 7.1A-D**). There are several reasons why this may be the case. Firstly, although the above study showed vasodilation, it was not performed in renal arteries. Furthermore, previous studies showing acute RLN induced vasodilation in small rat renal arteries *ex vivo* used manometry rather than wire myography (McGuane, Debrah et al. 2011) and measured the % change in diameter, which is more sensitive than change in pressure. Finally, isolating the artery *per se* may have destroyed potentially important cell-to-cell interactions.

To establish that this was not just an experimental artefact I needed a positive control. It has been shown previously by wire myography that RLN induced vasodilation *ex vivo* in the uterine artery from pregnant rats (Longo, Jain et al. 2003). I repeated the above experiment with vascular rings obtained from 2 pregnant rats and saw no response (data not shown). Additionally, I modified the degree of vessel pre-constriction (reduced to $EC_{50}$) and still saw no response to RLN. In all of the above experiments the arteries were viable and responded predictably to ACh and SNP, albeit that the response to ACh was blunted in both models of cirrhosis (**Fig 6.1 and 6.4**).

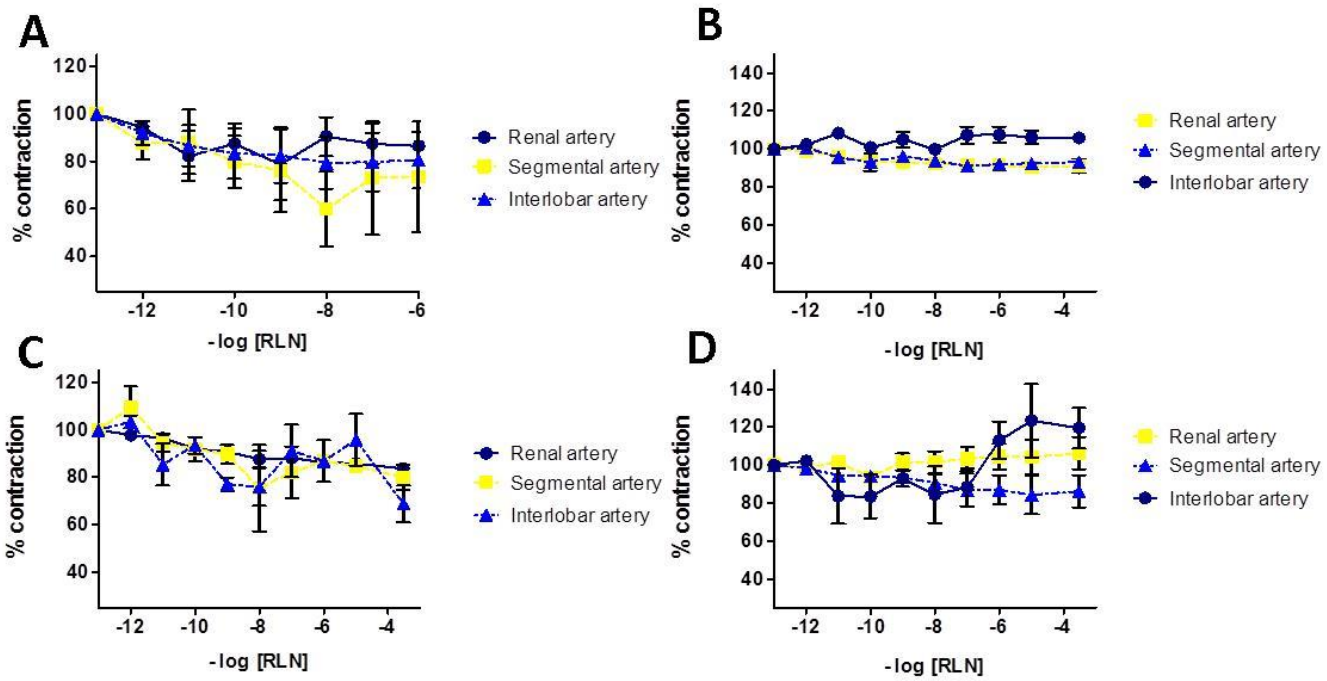


**Figure 7.1 Relaxin Concentration Response Curves in Renal Arteries from Normal, Olive Oil, 28 Day BDL and 16 Week $CCl_4$**

Renal arteries extra-renal, intra-renal segmental and intra-renal interlobar were isolated from Normal (**A**), Olive Oil (**B**), 28 day BDL (**C**) and 16 week $CCl_4$ (**D**) rats. After pre-constriction with PE, arteries were exposed to increasing doses of RLN ( $1 \times 10^{-13}$ to $3 \times 10^{-4}$ M). Data expressed as mean % contraction ± SEM, relative to pre-constriction with PE.

### 7.5 Renal arteries isolated from 72 hour RLN treated cirrhotic rats showed restoration of normal endothelium-dependent vasodilation

Having seen no effects by myography in renal arteries isolated from cirrhotic rats treated *ex vivo* with RLN, I reviewed the literature and decided to change my approach. I had shown *in vivo* that 72 hours of s.c. RLN improved RBF and GFR (**Chapter 5**) and, additionally, that both cirrhosis models exhibited an impairment of endothelium-dependent vasodilatation (**Chapter 6**). In a model of TNFα induced endothelial dysfunction RLN fully restored endothelial function (Dschietzig, Brecht et al. 2012). I hypothesised that the *in vivo* renal haemodynamic effects induced by RLN in rat cirrhosis models could be, at least in part, due to correction of underlying endothelial dysfunction. I harvested extra renal and segmental renal arteries from 16 week $CCl_4$ rats that had been treated for 72 hours with s.c RLN or vehicle (n=6-7/group) and assessed their vascular functional responses by wire myography. Vessels from RLN treated rats showed restoration of the endothelium-dependent response to ACh in the extra-renal renal arteries with increased sensitivity to ACh (**-log $Ec_{50}$ :** RLN 6.86±0.08 vs vehicle 6.51±0.11; p=0.032), restoring the arteries to similar values of olive oil controls (**Table 6.1**). No such response was seen in vessels from vehicle treated rats (**Fig 7.2A**). Interestingly this response to RLN was not seen to the same degree in the segmental arteries (**Fig 7.2B**) and the -log $Ec_{50}$ was also not different. Furthermore, RLN treatment did not alter endothelium-independent vasodilation or vasoconstriction responses in corresponding renal vessels (**Fig 7.3A-D**). This result suggests that RLN specifically augments endothelium-dependent vasodilatation in the extra-renal artery. However, there are clearly subtle differences in the extra- and intra- renal artery responses to RLN.

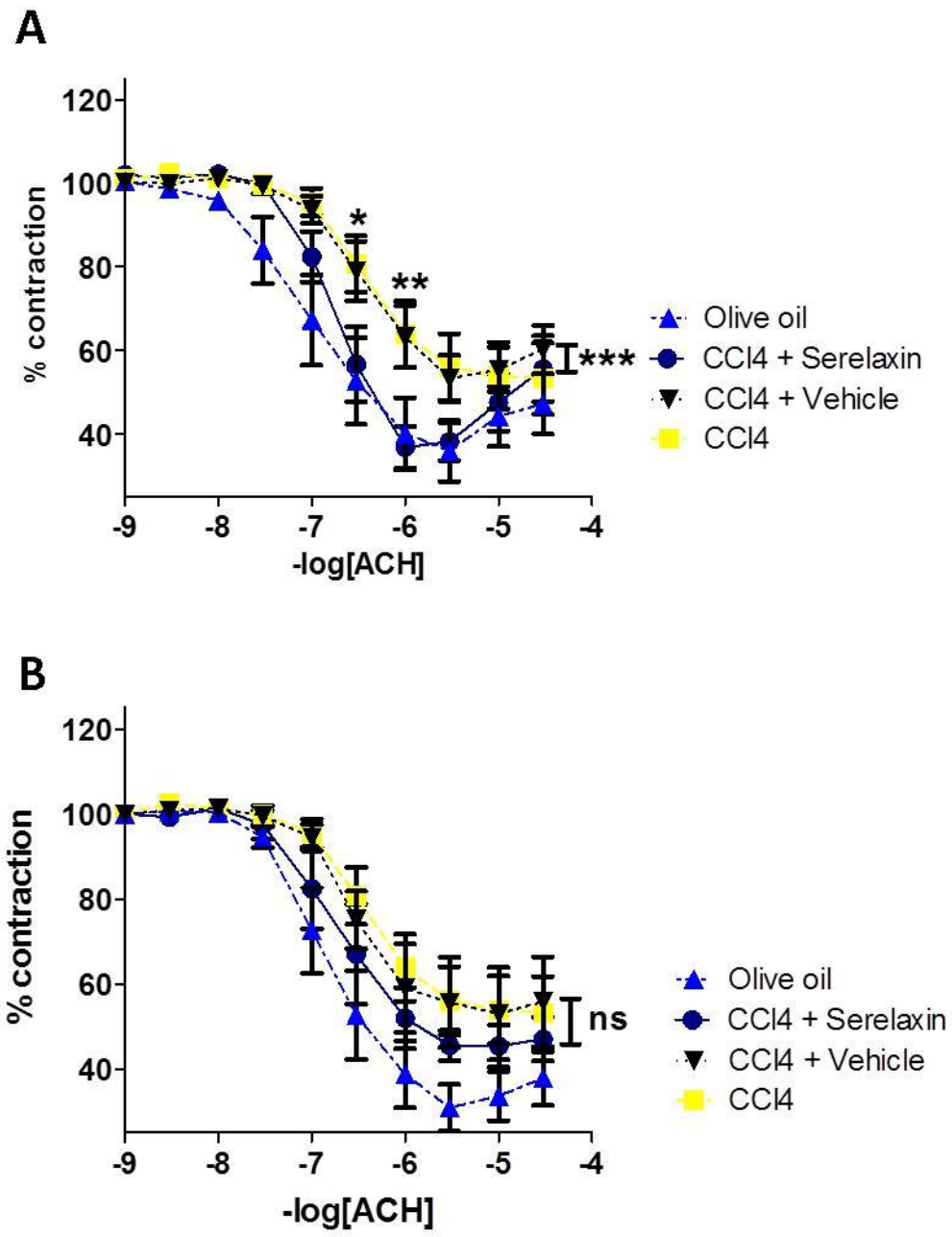
A
120
100
80
60
40
% contraction
*
**
***
-9
-8
-7
-6
-5
-4
-log[ACH]
Olive oil
CCl4 + Serelaxin
CCl4 + Vehicle
CCl4
B
120
100
80
60
40
% contraction
ns
-9
-8
-7
-6
-5
-4
-log[ACH]
Olive oil
CCl4 + Serelaxin
CCl4 + Vehicle
CCl4

# Figure 7.2 ACh Concentration Response Curves after 72 hours of *in vivo* Relaxin

Extra renal (**A**) and intra-renal segmental (**B**) arteries were harvested from 16 week $CCl_4$ rats that had been treated for 72 hours with s.c RLN or vehicle (n=6-7/group). After pre-constriction with PE, arteries were exposed to increasing doses of ACh $10^{-9}$ to $10^{-5}$M . Data expressed as mean % contraction ± SEM, relative to pre-constriction with PE. All analysed by 2-way ANOVA with post-hoc Bonferroni test comparing individual concentrations. *p<0.05 **p<0.01 ***p<0.001.

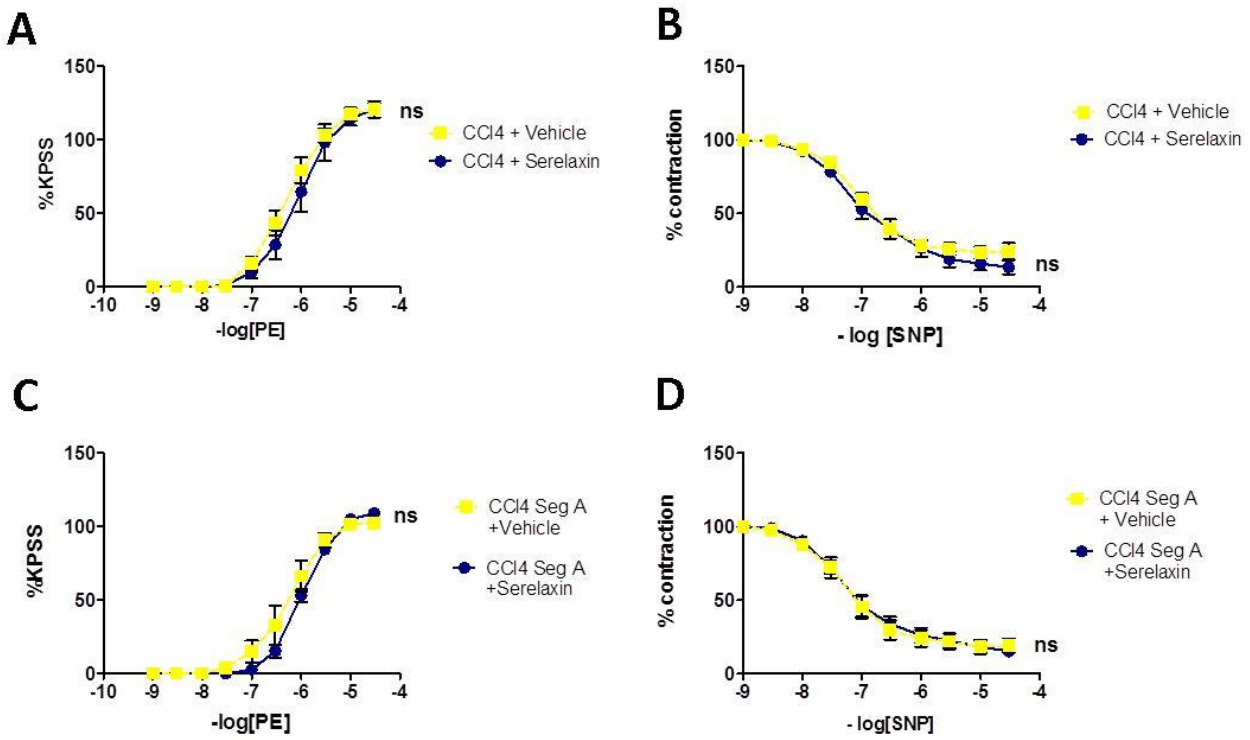


## Figure 7.3 PE and SNP Concentration Response Curves after 72 hours of *in vivo* Relaxin

Extra renal (**A-B**) and intra-renal segmental arteries (**C-D**) were harvested from 16 week $CCl_4$ rats that had been treated for 72 hours with s.c RLN or vehicle (n=6-7/group). (**A,C**) vessels were exposed to increasing doses of the vasoconstrictor phenylephedrine (PE; $10^{-9}$ to $10^{-5}$M; ). Data expressed as % contraction relative to KPSS. (**B, D**) After pre-constriction with PE, arteries were exposed to increasing doses of SNP $10^{-9}$ to $10^{-5}$M . Data expressed as mean % contraction ± SEM, relative to pre-constriction with PE. All analysed by 2-way ANOVA with post-hoc Bonferroni test comparing individual concentrations. *p<0.05 **p<0.01 ***p<0.001.

### 7.6 RLN induces renal arterial vasodilation through activation of the AKT/eNOS/NO signaling pathway

The results from Western blotting and NOS activity assay in cirrhotic rat kidneys indicated that a reduction in activated p-eNOS and NOS activity could account for the endothelial dysfunction seen with myography. Given that RLN appeared to restore a normal endothelial phenotype in the renal artery, I went on to explore this further. I firstly used Western blotting to quantify changes in whole kidney protein expression, focusing on the AKT/eNOS/NO signaling pathway, given my earlier observations on perturbation of this axis in cirrhosis. In both cirrhosis models, I showed increased levels of p-eNOS and p-AKT in kidney after 72hrs RLN treatment compared with vehicle (**Fig. 7.4A-D**). Repeating the NOS assay performed above, in both $CCl_4$ and BDL kidneys treated with 72 hrs of RLN, there was a marked increase in NOS activity compared with vehicle, such that near-normal levels were restored ($CCl_4$: RLN 122±31% vs. vehicle 5±3%, $p<0.01$; BDL: RLN, 86±22% vs. vehicle 26±11%, $p<0.05$; **Fig. 7.5**).

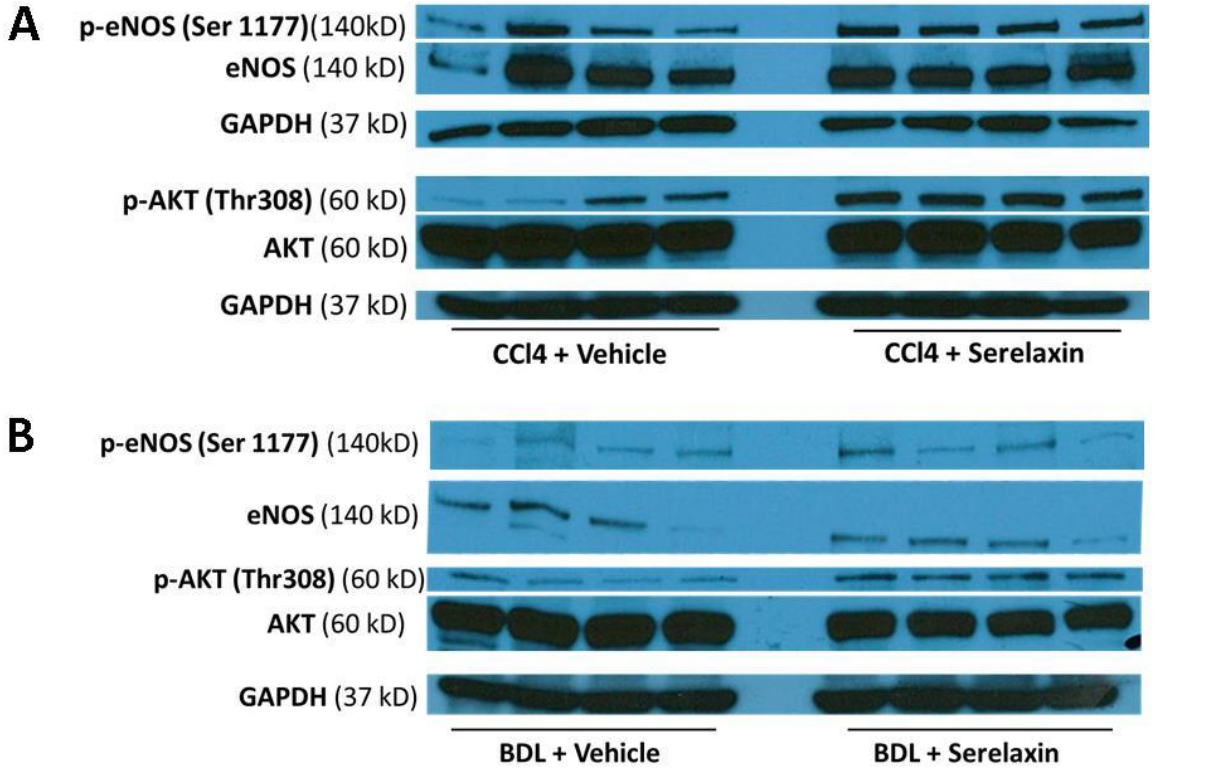
A
p-eNOS (Ser 1177)(140kD)
eNOS (140 kD)
GAPDH (37 kD)
p-AKT (Thr308) (60 kD)
AKT (60 kD)
GAPDH (37 kD)
CCl4 + Vehicle
CCl4 + Serelaxin
B
p-eNOS (Ser 1177) (140kD)
eNOS (140 kD)
p-AKT (Thr308) (60 kD)
AKT (60 kD)
GAPDH (37 kD)
BDL + Vehicle
BDL + Serelaxin

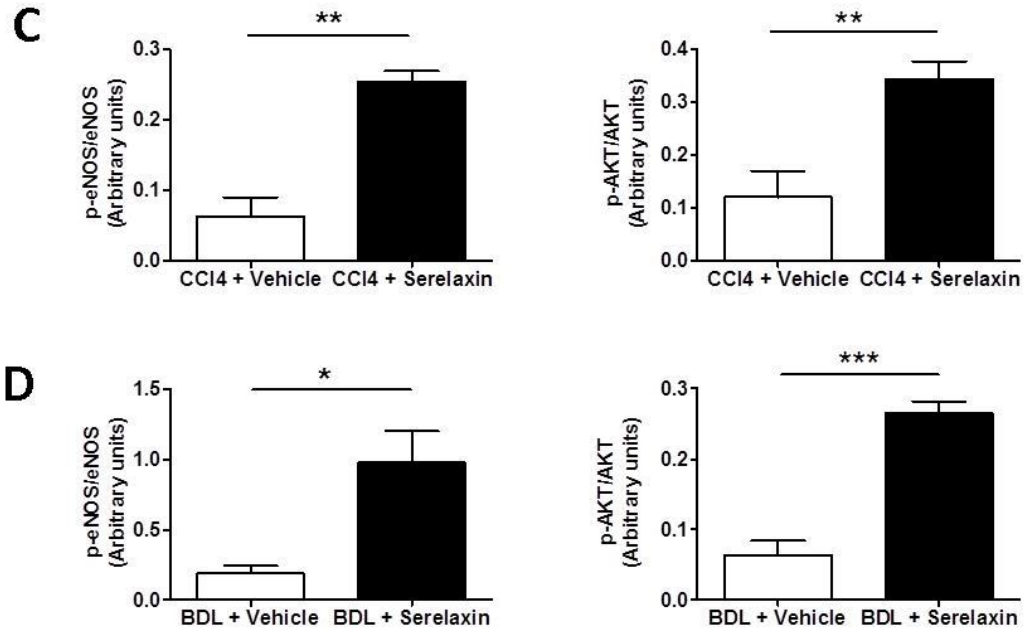
C
**
p-eNOS/eNOS (Arbitrary units)
0.0
0.1
0.2
0.3
CCl4 + Vehicle
CCl4 + Serelaxin
**
p-AKT/AKT (Arbitrary units)
0.0
0.1
0.2
0.3
0.4
CCl4 + Vehicle
CCl4 + Serelaxin
D
*
p-eNOS/eNOS (Arbitrary units)
0.0
0.5
1.0
1.5
BDL + Vehicle
BDL + Serelaxin
***
p-AKT/AKT (Arbitrary units)
0.0
0.1
0.2
0.3
BDL + Vehicle
BDL + Serelaxin

# Figure 7. 4 Effect of 72 Hours of Relaxin *in vivo* on Renal AKT/eNOS/NO Signalling Pathway

Quantification of eNOS, p-eNOS, AKT and p-AKT protein by Western blotting and densitometry in whole kidney extracts from 72hr relaxin or vehicle treated $CCl_4$ (**A, C**) and BDL (**B, D**) rats ($n$=4/group). Data expressed as mean±SEM, analysed by two-tailed unpaired Student's $t$-test; *$p$<0.5 **$p$<0.01 ***$p$<0.001.

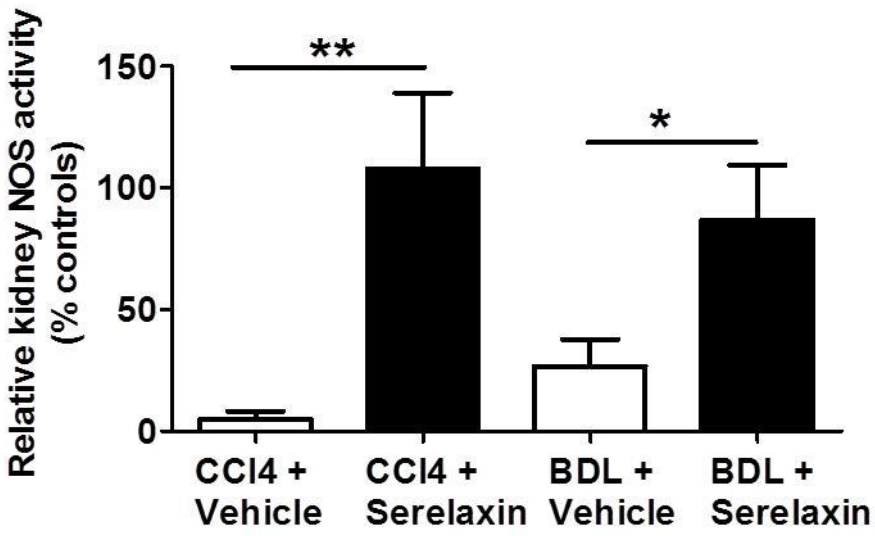


## Figure 7. 5 Effect of 72 Hours of Relaxin *in vivo* on Renal NOS Activity

NOS activity in whole kidney extracts from cirrhotic rats after 72 hrs relaxin or vehicle treatment (*n*=6-8/group). Bars represent mean±SEM relative to respective controls, analysed by two-tailed unpaired Student's *t*-test; *$p$<0.5 **$p$<0.01 ***$p$<0.001.

To confirm NOS dependency in RLN mediated renal vasodilation, I repeated the 72hr RLN *in vivo* analyses in subgroups of $CCl_4$ cirrhotic rats (n=4-8/group) co-treated with L-NAME (250mg/L p.o.). L-NAME abrogated the effects of RLN treatment on RBF (RLN 3.8±0.3 mL/min vs. RLN+L-NAME 2.5±0.3 mL/min, $p$<0.01; **Fig. 7.6A**) and GFR (RLN 2.9±0.3 mL/min vs. RLN+L-NAME 1.8±0.1 mL/min, $p$<0.05; **Fig. 7.6B**). In contrast, L-NAME had no significant effects on RBF or GFR in vehicle treated rats. In all rats treated with L-NAME I observed an increase in MAP (**Fig. 7.6C**). For this experiment I confirmed inhibition of eNOS expression and activity at the level of the kidney by Western blotting and activity assay, respectively (**Fig. 7.7A-C**).

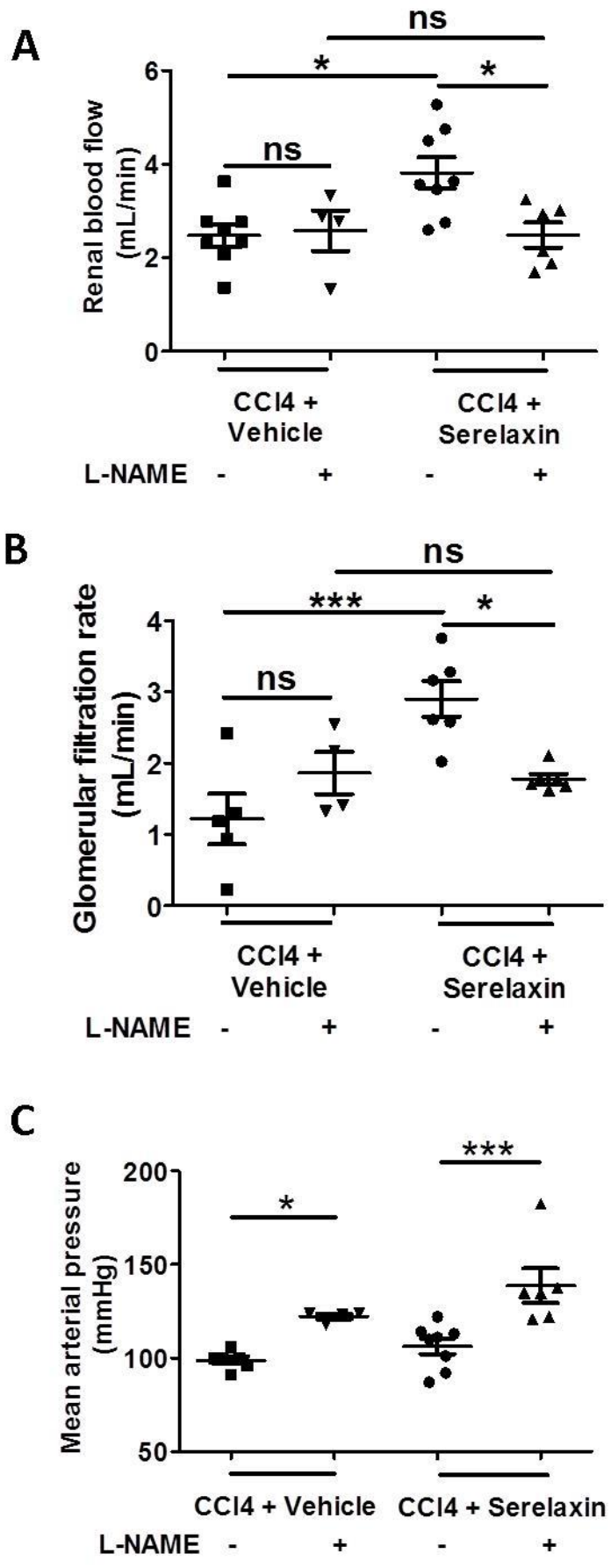
A
ns
*
*
ns
Renal blood flow (mL/min)
6
4
2
0
CCl4 + Vehicle
CCl4 + Serelaxin
L-NAME - + - +
B
ns
***
*
ns
Glomerular filtration rate (mL/min)
4
3
2
1
0
CCl4 + Vehicle
CCl4 + Serelaxin
L-NAME - + - +
C
***
*
Mean arterial pressure (mmHg)
200
150
100
50
CCl4 + Vehicle
CCl4 + Serelaxin
L-NAME - + - +

# Figure 7. 6 Effect of NOS Inhibition on Relaxin *in vivo* Haemodynamic Effects

Subgroups of 16 week $CCl_4$ cirrhotic rats were co-treated with L-NAME with RLN or vehicle for 72 hours and effects on RBF (**A**) and GFR (**B**) measured by perivascular flow probe and inulin clearance, respectively ($n$=4-8/group). MAP was measured via a femoral arterial line (**C**). Data expressed as individual rats with mean±SEM, analysed by one-way ANOVA with post-hoc Bonferroni test; *$P$<0.05, ***$P$<0.001.

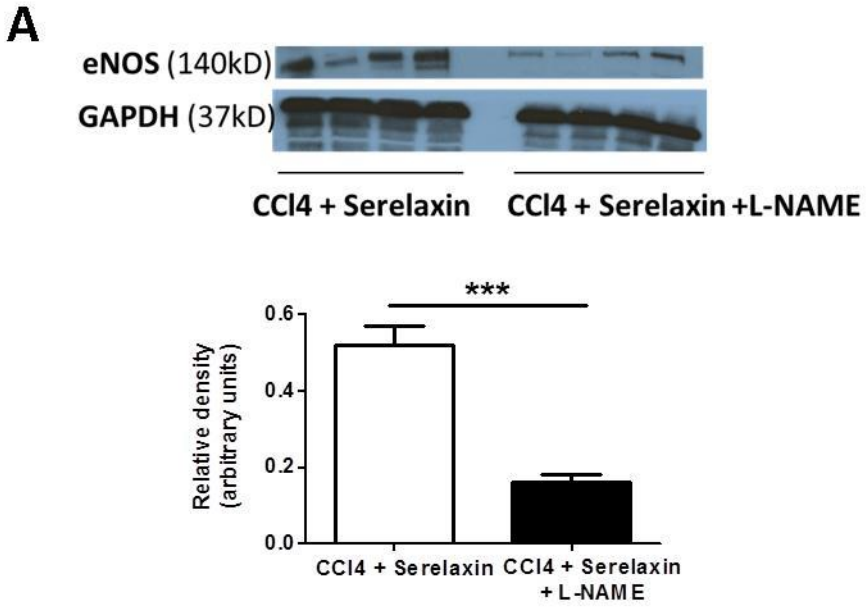
A
eNOS (140kD)
GAPDH (37kD)
CCl4 + Serelaxin
CCl4 + Serelaxin +L-NAME
***
Relative density (arbitrary units)
0.6
0.4
0.2
0.0
CCl4 + Serelaxin
CCl4 + Serelaxin + L-NAME

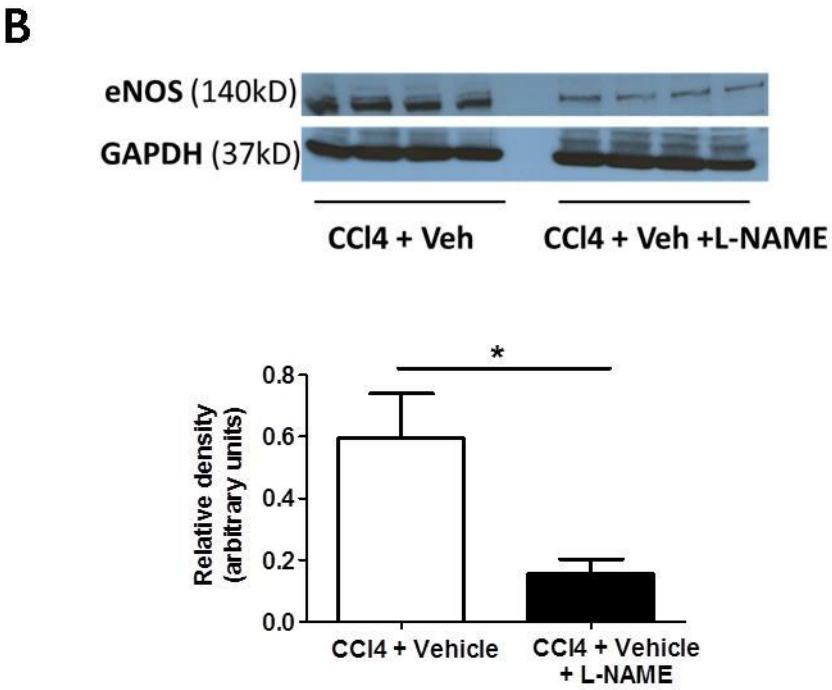
B
eNOS (140kD)
GAPDH (37kD)
CCl4 + Veh
CCl4 + Veh +L-NAME
*
Relative density (arbitrary units)
0.8
0.6
0.4
0.2
0.0
CCl4 + Vehicle
CCl4 + Vehicle + L-NAME

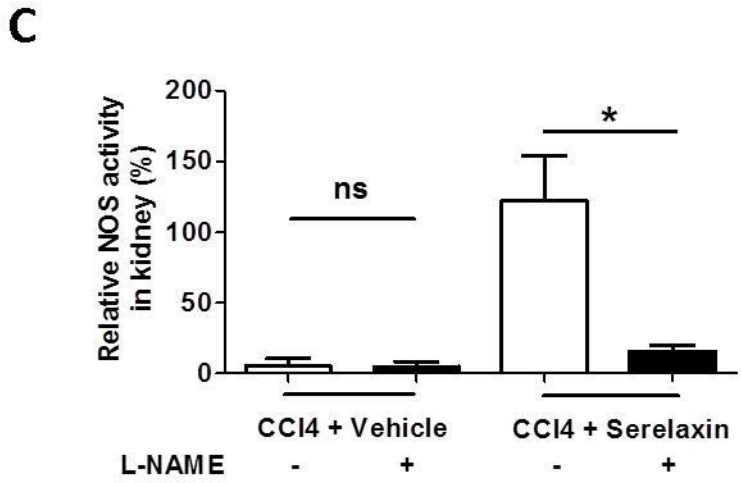
C
Relative NOS activity in kidney (%)
200
150
100
50
0
ns
*
CCl4 + Vehicle
CCl4 + Serelaxin
L-NAME
-
+
-
+

# Figure 7.7 Effect of L-NAME Administration on eNOS Expression and NOS Activity in 16 week $CCl_4$ Rat Kidneys

Subgroups of 16 week $CCl_4$ rats randomized to 72 hr s.c. relaxin or vehicle were co-treated with L-NAME. (**A**) eNOS protein expression (relative to GAPDH loading control) evaluated by Western blotting and quantified by densitometry in whole kidney extracts from 16 week $CCl_4$ rats treated with serelaxin±L-NAME, and (**B**) vehicle±L-NAME (*n*=4/group). Data expressed as mean±SEM, analysed by two-tailed unpaired Student's *t*-test; **p*<0.05, ****p*<0.001. (**C**) Nitric oxide synthase (NOS) activity in corresponding whole kidney extracts (*n*=4-8/group). Data expressed as mean±SEM, analysed by two-tailed unpaired Student's *t*-test; **p*<0.05.

### 7.7 Relaxin downregulates key vasoconstrictor receptors in kidney

Having observed that key inhibitors of eNOS were upregulated at both the gene and protein level in both cirrhosis models (**Chapter 6**), I wanted to establish if RLN was mediating effects on NOS activity by inhibiting these pathways. As an unbiased initial approach I repeated the Hypertension qPCR array (Qiagen). Again I used whole kidney from 16 week $CCl_4$ rats (n=5/group) treated with RLN or vehicle (72hrs), extracted RNA and performed the Hypertension array. Genes that had a fold regulation of over 2 or less than -2 with a significance of <0.5 were included. **Fig 7.8** shows the genes that were differentially regulated by RLN. In the kidney from 16 week $CCl_4$ treated rats, RLN down-regulated expression of the $ET_A$ receptor, which I had previously shown to be increased in both cirrhosis models (**Chapter 6**). Activation of $ET_A$ by endothelin I increases vascular tone (Davenport, Kuc et al. 1995). Additionally, RLN down-regulated expression of the urotensin 2 receptor and urotensin 2 itself. Urotensin is a potent vasoconstrictor of large conductive vessels, but paradoxically it has also been shown to relax mesenteric vessels. In the liver, urotensin and its receptor localize to endothelial cells, bile ducts and Kupffer cells (Leifeld, Clemens et al. 2010). Urotensin levels have been shown to increase in cirrhosis (Pawar, Kemp et al. 2011) and urotensin inhibition appears to reduce fibrosis in rats (Liu, Wang et al. 2009). Furthermore, inhibition of urotensin in rats reduced portal pressure, increased renal blood flow and sodium and water excretion in BDL rats (Trebicka, Leifeld et al. 2008). Finally, RLN also down-regulated expression of the arginine vasopressin receptor 1b (AVR1b). In cirrhosis, due to peripheral vasodilatation and a perceived low volume state, there is increased circulating antidiuretic hormone (ADH) which binds to AVR1b inducing reabsorption of water from the collecting ducts, with associated sodium retention from activation of the RAA and SNS. Inhibition of ADH with Vaptans has been shown to improve ascites in cirrhosis by inhibiting ADH induced reabsorption in the renal collecting ducts, thereby increasing electrolyte free urine excretion (Gines, Wong et al. 2010). RLN had no significant effect

on Arginase II or Caveolin I gene transcription and quantification of IHC staining also showed no difference (data not shown).

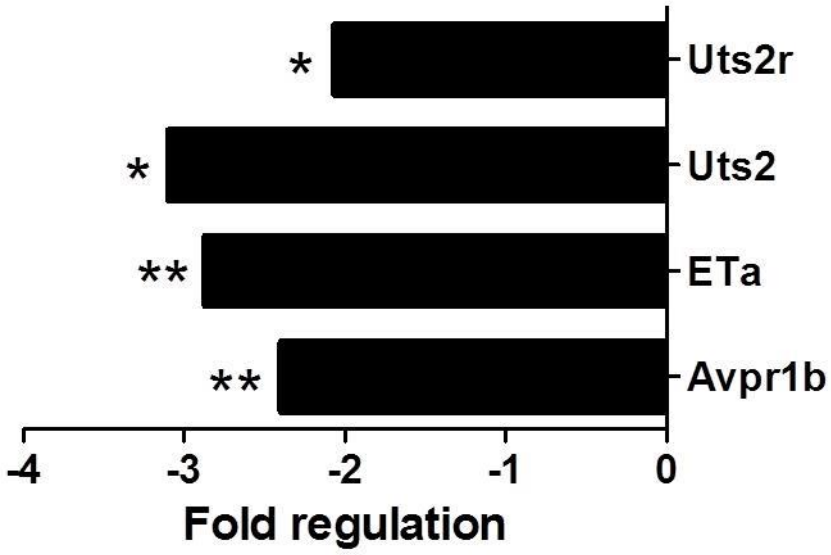


## Figure 7.8 Effect of 72 Hours of Relaxin on Kidney Gene Regulation

RNA was extracted from whole kidney from 16 week $CCl_4$ cirrhotic rats treated with 72hrs of RLN or vehicle. 2µg of RNA was transcribed and the RT2 Hypertension Profile PCR Array (Qiagen) undertaken. All genes that had a fold regulation relative to control of equal to or greater than 2 with a $p<0.05$ were considered significant and shown.

Overall, at the mRNA level at least, RLN regulates some physiologically relevant target genes that represent potential pathways worthy of further investigation.

### 7.8 Relaxin reduces serum TNFα levels

As circulating TNFα levels were increased in both cirrhosis models I investigated the effect of RLN on TNFα levels. Serum analyzed from 16 week $CCl_4$ rats treated with 72 hours of s.c RLN (n= 4-5/group) showed a reduction in TNFα compared to vehicle (**Fig. 7.9A;p<0.01**). I repeated this analysis in serum from BDL rats treated with 72 hours of s.c. RLN (n=6/group) and circulating TNFα levels were also reduced compared to vehicle (**Fig. 6.9B; p<0.01**).

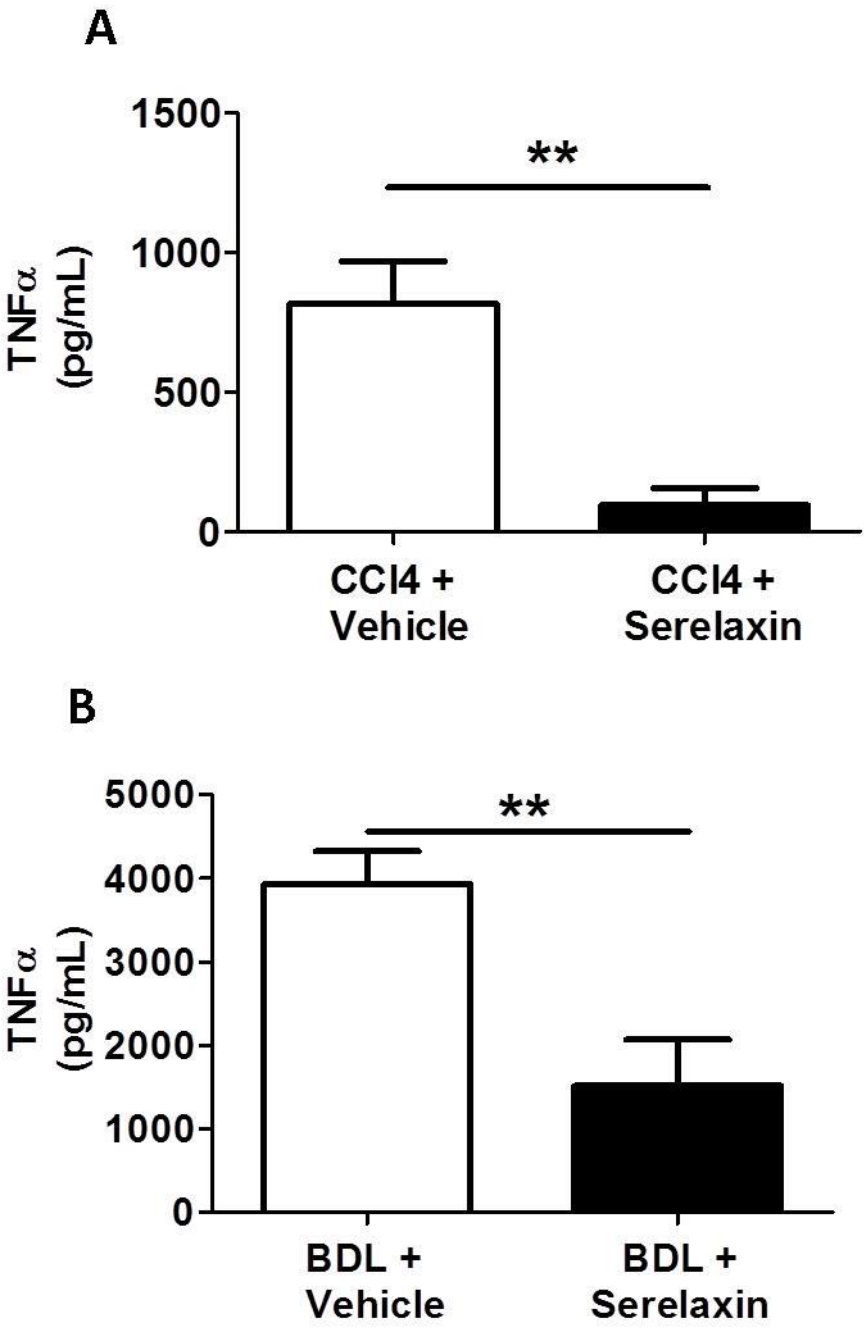


**Figure 7. 9 Effect of 72 Hours of Relaxin Treatment on Serum TNFα levels**

Circulating serum TNFα levels were measured from blood taken from the femoral artery in (**A**) 16 week $CCl_4$ rats (4-5/group), and (**B**) 21 day BDL (6/group) treated with 72 hrs of RLN or vehicle. Date expressed as mean±SEM, analysed by Students t test. . **p<0.01, ***p<0.001.

## DISCUSSION

I have shown that RLN had no vasodilatory effect *ex vivo* in isolated renal arteries from normal and cirrhotic rats (**Fig. 7.1**). The possible reasons for this include, firstly, that the increase in RBF seen by 1 hour *in vivo* is due to arterial changes that take longer than a few minutes to occur. It has been shown previously (Fisher, MacLean et al. 2002) that RLN can rapidly (within minutes) vasodilate small human systemic resistance arteries but this was not the case in pulmonary resistance arteries. It may be a similar situation in renal arteries using this myography technique. Furthermore, it may be that the mechanism of action of RLN on the renal circulation in cirrhosis is related to its vasodilatory effects in the liver (i.e. reducing portal pressure (Fallowfield, Hayden et al. 2014)), antagonism of angiotensin II (Danielson, Sherwood et al. 1999; Sasser, Molnar et al. 2011), or down-regulation of key vasoconstrictor receptors ($ET_A$, Urotensin 2) and that shorter time frame, absence of circulating factors and influence of the liver-renal axis reduces its effects to a level that simply cannot be detected by wire myography. Reviewing the literature, the published DRC's to RLN are relatively modest even with manometry (McGuane, Debrah et al. 2011).

Further to this, having isolated renal arteries from RLN and vehicle treated 16 week $CCl_4$ cirrhotic rats, I have shown that the blunted endothelium-dependent vasodilation seen in renal arteries from both models of cirrhosis was restored to near normal in the extra-renal renal artery, though this was not seen in the segmental renal artery (**Fig 7.2**). My results are supported by recently published data also showing that endothelial dysfunction was improved in mesenteric arteries from rats treated with a single dose of RLN (Leo, Jelinic et al. 2014). The mechanism of this improvement has not been fully delineated though it appeared to be through increased p-eNOS and improved NOS activity, as both were increased in rats treated with RLN compared to vehicle (**Fig 7.4-5**). Additionally, I have shown increased pAKT expression in rats treated with RLN for 72 hrs versus those treated with

vehicle, suggesting a role for the pAKT/eNOS/NO pathway in RLN mediated effects. Indeed, mechanistic studies in normal rat renal arteries have suggested that the PI3K/pAKT/NOS axis is pivotal to the rapid haemodynamic effects of RLN (McGuane, Debrah et al. 2011). I did not perform separate Western blots looking at differential expression of pAKT/p-eNOS after an acute i.v. bolus of RLN. However, a recent study has also shown similar findings with increased p-eNOS in mesenteric arteries exposed to RLN (Leo, Jelinic et al. 2014), suggesting the validity of this result. As a proposed alternative mechanism, there is evidence that RLN reduces levels of the circulating NOS inhibitor asymmetric dimethylarginine (ADMA) in a rat model of angiotensin II induced hypertension (Sasser, Cunningham et al. 2014), which could account for the increased NOS activity observed in my studies. The central importance of NOS activity in mediating the haemodynamic effects of RLN is indicated by the experiments using L-NAME co-treatment. Blocking NOS *in vivo* abrogated the beneficial effects on RBF and GFR observed in RLN treated rats (**Fig 7.6-7.7**), whereas no such effect was seen in vehicle controls.

Finally, serum analysed from both cirrhosis models showed reduced TNFα levels in rats treated for 72 hrs with RLN. The potential importance of TNFα has been discussed in Chapter 5, in particular the role of TNFα in causing endothelial dysfunction (Dschietzig, Brecht et al. 2012). Additionally, it has been shown that reducing gut translocation of microbes with antibiotics reduces kidney TNFα with subsequent protection of rat BDL kidneys from further injury induced by sepsis (Shah, Dhar et al. 2012). Therefore, TNF is strongly implicated in HRS development. It is therefore encouraging that RLN also reduces levels of TNFα and defining the mechanism for this anti-inflammatory effect is an important topic for future study.

## Summary of important findings

- RLN treatment does not induce vasodilatation in the renal arteries of cirrhotic rats *ex vivo*
- Sustained RLN treatment *in vivo* restores endothelium-dependent vasodilatation in harvested renal arteries from cirrhotic rats
- Sustained RLN treatment increases p-eNOS expression and NOS activity, and down-regulates key genes associated with increased vascular tone and water retention in cirrhotic rats
- Sustained RLN treatment reduces serum TNFα levels in cirrhotic rats

# CHAPTER 8 – DISCUSSION AND FUTURE WORK

In this thesis, I have established that by targeting the kidney vasculature with H2-RLN it is possible to improve renal vasoconstriction and impairment of renal function. Both these features characterize HRS, a condition that if untreated or unresponsive to current treatment leads to death in nearly 100% by 3 months (Moreau, Durand et al. 2002). I have provided a proof-of-concept using two distinct rat models of cirrhosis, both with profound renal vasoconstriction and reduction in GFR, that RLN (serelaxin) functions as a potent and selective renal vasodilator. This appears to be through augmentation of intra-renal NOS signaling and restoration of endothelium-dependent vasodilation, both of which I have shown to be abnormal in these models. Critical for potential translation to humans, RLN did not induce systemic hypotension even in the model of decompensated biliary cirrhosis.

As discussed in detail in **Chapter 1**, the prevalence of cirrhosis is increasing and as a result more patients are presenting with complications of cirrhosis and PHT, in particular HRS. Renal dysfunction/AKI occurs in approximately 20% of hospitalized patients with decompensated cirrhosis (Garcia-Tsao, Parikh et al. 2008), conferring a 7 fold increase in death (Fede, D'Amico et al. 2012) and it is often hard to differentiate the cause. HRS occurs in 11 % of patients with cirrhosis and ascites (Planas, Montoliu et al. 2006) and the degree to which other causes of AKI lead to HRS is still relatively unclear (Belcher, Parikh et al. 2013). Current pharmacological therapy is not targeted at the renal circulation but is aimed at increasing MAP and renal perfusion by increasing circulating volume with HAS and by reducing splanchnic vasodilatation with Terlipressin. Although this treatment does reverse HRS in 40-50% of patients (Nazar, Pereira et al. 2010), it does not improve overall survival and is importantly associated with ischaemic complications rendering it unsuitable for some patients. Whereas, RLN has been shown to directly induce renal vasodilatation, increasing the GFR in pregnant rats (Sherwood 2004), importantly this has been recapitulated using exogenous RLN in non-pregnant rats (Conrad 2010), healthy human volunteers (Smith, Danielson et al. 2006)

and more recently in acute (Teerlink, Cotter et al. 2013) and chronic heart failure studies (Dschietzig, Teichman et al. 2009). Hence I sought to establish whether in cirrhosis RLN could be used as a targeted renal vasodilator.

As renal vasoconstriction is central to the pathogenesis of HRS (Epstein, Berk et al. 1970), I needed to establish robust and reproducible models of cirrhosis and portal hypertension with renal vasoconstriction and renal dysfunction. In **Chapter 3** as shown in **Fig 3.1- 3.5** twice weekly i.p. $CCl_4$ injections induced progressive fibrosis with increased portal pressure by 8 weeks and renal vasoconstriction and dysfunction by 16 weeks. These rats all remained pre-ascitic and showed no signs of histological renal damage to account for the profound renal dysfunction observed. As the majority of patients with HRS have ascites, and this is now part of the diagnostic criteria for HRS (Angeli, Gines et al. 2015), I also sought as a means of comparison to $CCl_4$, to evaluate the BDL model of decompensated biliary cirrhosis. As shown in **Fig 3.6 – 3.10** BDL produced a rapidly evolving biliary fibrosis, with jaundice, increased portal pressure, renal vasoconstriction and renal dysfunction developing by 14 days. By 28 days all rats had ascites. As in previous studies (Shah, Dhar et al. 2012) there was evidence of renal ischaemia, demonstrated by histological features of ATN in the kidneys of BDL rats. As renal vasoconstriction in cirrhosis has been shown to be progressive, with reducing RBF seen well before there is a decrease in GFR (Ring-Larsen 1977), these two models serve to represent different stages of this process. In patients with cirrhosis, GFR may be maintained at normal or low/normal levels by a compensatory increase in filtration fraction (likely by angiotensin-II (Ang-II) induced efferent arteriole vasoconstriction) such that the effect of reduced RBF on GFR may be masked (Kew, Brunt et al. 1971). Thus, it is unknown at which stage in the natural history or by which mechanism(s) a reduction in RBF occurs in cirrhosis.

Having established that there was a robust renal phenotype in these models, I next investigated the expression and distribution of RXFP1. Levels of transcripts for the RLN receptor *Rxfp1* in whole liver, kidney and renal artery extracts were increased in rat cirrhosis models (**Fig 4.2**) Moreover, in $CCl_4$ cirrhotic rats RXFP1 localized to renal vascular endothelial cells, smooth muscle cells and pericytes (**Fig 4.8-10**). This is consistent with RXFP1 cellular localization data in normal rat small renal arteries (Jelinic, Leo et al. 2014) and in normal human kidney biopsies in the current study (**Fig 4.11**). All these cells are implicated in the regulation of RBF and GFR. The factors which regulate renal parenchymal and arterial expression of RXFP1 in animal models and human disease are unknown, although a recent *in vitro* study showed that α1- and β1-adrenoceptors regulated cardiac expression of RXFP1 in mice (Moore, Su et al. 2014). I have not delineated the differential expression of RXFP1 in afferent and efferent arterioles, though the *in vivo* results suggest that the former must predominant otherwise such increases in RBF and GFR would not be seen.

A single acute bolus and more prolonged treatment (for 72 hours) with RLN induced a significant increase in RBF *in vivo* (**Fig 5.3**). This increase in RBF occurred without a change in MAP, which is critical to its translational potential as cirrhotic patients normally have low MAP and therefore do not tolerate systemic vasodilatation. Conversely, I have shown in $CCl_4$ cirrhosis that administration of a non-selective nitro-vasodilator (SNP) induced hypotension and a reduction in RBF (**Chapter 5**). Furthermore, studies of vasodilators in cirrhosis also showed hypotension and subsequent worsening of RBF (Salmeron, Ruiz del Arbol et al. 1993). In my models I did not observe an increase in cardiac output in response to RLN (**Fig 5.15**) which in addition to the above adds evidence that RLN acts selectively on the renal vasculature. Interestingly, when isolated renal arteries were exposed to RLN *ex vivo*, there was no acute vasodilatory response detected using wire myography (**Fig 7.1**). This poses the question: how is RLN acting on the renal circulation in my models? It has been shown, measuring myogenic reactivity, that RLN can rapidly dilate small human gluteal arteries

(Fisher, MacLean et al. 2002) and rat and mouse small renal and human subcutaneous arteries (McGuane, Debrah et al. 2011) within minutes, however using wire myography and directly exposing renal arteries from cirrhotic rats to RLN I saw no rapid response (**Fig 7.1**). It may be that this is related to a difference in individual vessel responses *ex vivo* or that myography is less sensitive than myogenic reactivity, or even that direct activation of endothelial/smooth muscle RXFP1 is not the sole mechanism by which RLN induces vasodilatation *in vivo* in these models.

Of central importance is the observation that RLN improved renal function in both models of cirrhosis (**Fig 5.9 and 5.14**), as this is the primary endpoint in clinical trials for AKI/HRS. The GFR in $CCl_4$ cirrhosis was restored completely and in BDL was increased to 86% of sham controls. The degree of improvement in GFR compared to that in RBF (59% for $CCl_4$ rats, 38% for BDL rats) was much greater. This raises the question: why is the improvement in GFR disproportionately greater than that of RBF? It has previously been shown that RBF must reach a critical threshold level after which renal dysfunction and worsening GFR ensues (Ring-Larsen 1977). Therefore, it could be hypothesised that the improvement in RBF is sufficient to restore GFR without a complete restoration of RBF.

In trying to understand the mechanism of RLN's beneficial haemodynamic effects I needed to establish which changes associated with cirrhosis were responsible for the aberrant renal phenotype observed in both models (**Chapter 3**). Given that renal vasoconstriction was common to both models, I decided to evaluate renal vascular reactivity using wire myography. In both rat cirrhosis models extra- and intra-renal arteries exhibited marked impairment in endothelium-dependent vasodilation *ex vivo* (**Figure 6.1 - 6.4**), with normal vasoconstrictor and smooth muscle responses. I also assessed renal arteries to establish the pathways responsible for 'normal' endothelium-dependent vasodilatation and found that blocking NOS with L-NAME completely abrogated

endothelium-dependent vasodilation, indicating its pivotal role in renal vasodilatation. In the kidneys of cirrhotic rats there was a marked reduction in p-eNOS expression and in NOS activity. Alongside this, increased expression of negative regulators of eNOS (arginase II, caveolin 1) and Endothelin receptors $ET_A$ and $ET_B$ was observed. Arginase II has particularly been implicated in endothelial dysfunction from alternative causes such as hypoxia (Krause, Del Rio et al. 2015), hypertension and obesity (Johnson, Peyton et al. 2015). Furthermore serum TNFα was increased in both cirrhosis models. TNFα has been shown to induce endothelial dysfunction (Dschietzig, Brecht et al. 2012) and reducing TNFα has been shown to prevent renal dysfunction in rodent models of cirrhosis (Shah, Dhar et al. 2012). Opposing recent research has suggested that patients with decompensated cirrhosis have increased circulating prostaglandin E2 that drives immunosuppression and therefore reduced TNFα, and that by targeting rodent models with COX inhibitors, or humans with albumin (that binds prostaglandin E2), increased pro-inflammatory cytokines, such as TNFα, are produced and subsequent rodent survival is longer (O'Brien, Fullerton et al. 2014). The haemodynamics in the rodents and, in particular RBF, was not studied in this paper. Although a pro-inflammatory response is clearly needed to 'prevent' infection I would hypothesize, based on my work and work by Shar et al, 2012, that excessive pro-inflammatory cytokines will lead to worsening renal dysfunction.

These results implicate renal endothelial dysfunction in the renal phenotype seen in both models, which is likely secondary to abnormalities in NOS activity (**Fig 8.1**). This renal endothelial dysfunction appears to mimic that of the LSEC's, which contributes to increased intrahepatic intravascular resistance (Iwakiri 2011). A recent study in cirrhotic humans also supports these findings, suggesting an association between endothelial dysfunction and HRS development as with improved renal function concomitant improved endothelial function was observed (Garcia-Martinez, Noiret et al. 2014). Endothelial dysfunction is an aspect of HRS pathogenesis that to date has been

relatively under studied. Further work is needed to fully unravel the dysregulation of eNOS and its inhibitors at a cellular level.

It is known that the molecular mechanisms of RLN induced vasodilation differ according to the duration of exposure to the peptide, but in both rodent and human tissues the final common pathway appears to converge on NO signaling (Conrad 2010). In rats treated with RLN for 72 hours I showed improvement in endothelium-dependent vasodilatation in isolated extra-renal arteries using wire myography (**Chapter 7**). Furthermore, NOS activity and expression of p-eNOS protein was augmented following a 72 hour RLN infusion, though no change in arginase 2 or caveolin 1 expression was observed. The requirement for NOS in mediating the effects of RLN on RBF and GFR in cirrhosis models was demonstrated through co-treatment with L-NAME. Similarly, L-NAME administration has also been shown to abrogate renal vasodilation in pregnant rats (Danielson and Conrad 1995) and in RLN treated non-pregnant rats (Danielson, Sherwood et al. 1999). Furthermore, RLN reduced kidney expression of urotensin 2 receptor, $ET_A$ receptor and the vasopressin V1b receptor - all involved in renal vasoconstriction and sodium conservation. Additionally, I have shown in both models serum TNFα is reduced in rats treated with RLN (**Chapter 7**). Consistent with this, RLN also improved endothelial dysfunction in a rat aortic ring model of LPS-TNFα induced endothelial dysfunction (Dschietzig, Brecht et al. 2012). In summary, my findings suggest that RLN reverses endothelial dysfunction in the renal vasculature, potentially by locally regulating eNOS activity, reducing inflammation, down-regulating expression of vasoconstrictor receptors in the kidney, and in turn restores physiological responses to endothelium-dependent vasodilators (**Fig 8.2**).

I have shown that that RLN decreases PHT in rat cirrhosis (**Fig 5.10 and 13**) and our group has recently shown that RLN also reduces contractility and pro-fibrotic gene expression in human

hepatic myofibroblasts (Fallowfield, Hayden et al. 2014). Given that PHT drives the development of HRS (Jalan, Forrest et al. 1997; Abraldes, Tarantino et al. 2003), it remains possible that the improvements in renal dysfunction detailed above are in part secondary to the portal hypotensive effect of RLN. However, exogenous RLN treatment in *normal* rodents (Danielson and Conrad 2003) and humans (Smith, Danielson et al. 2006) also increased RBF, which suggests that the portal hypotensive effect of RLN cannot be the only mechanism responsible. So far my work has explored the potential role of RLN as a treatment for established HRS, but it is also possible that RLN may be effective in the prophylaxis against HRS in high-risk patients.

All animal studies are subject to the legitimate criticism that they cannot be considered to truly reflect events in the human condition. Nevertheless, my studies have shown a consistent pattern of renal vasoconstriction and renal dysfunction that recapitulate many of the central features of human HRS. There is always concern that preclinical data will not translate to efficacy in human disease. Although it was not possible to confirm RXFP1 expression in human HRS kidney (as biopsies are not routinely performed for clinical diagnosis), RXFP1 was detected in normal human kidney tissue (**Fig 4.11**). Recent clinical data also confer optimism with regard to the use of RLN in human HRS. Firstly, the observation that pharmacokinetic and safety profiles of RLN were not affected in patients with mild, moderate or severe hepatic impairment (Kobalava, Villevalde et al. 2014). Secondly, studies showing beneficial renal haemodynamic effects of RLN (increased RBF and reduced filtration fraction) in patients with chronic heart failure (Voors, Dahlke et al. 2014) and improvement of renal biomarkers (creatinine and cystatin-C) in patients with acute heart failure (Metra, Cotter et al. 2013). To develop RLN as a treatment for human HRS, studies in carefully selected populations will be required. A phase-2 study in patients with cirrhosis and portal hypertension has recently been completed (NCT01640964; www.ClinicalTrials.gov) and will inform about the potential efficacy of RLN as a renal vasodilator, pharmacokinetics, immunogenicity and mechanistic biomarkers.

In conclusion, in this thesis I have shown proof-of-concept in clinically relevant rat models of cirrhosis and renal dysfunction that RLN improves renal function by ameliorating pathological renal vasoconstriction and reversing endothelial dysfunction and is therefore, a promising therapy to take forward in human studies of AKI and HRS.

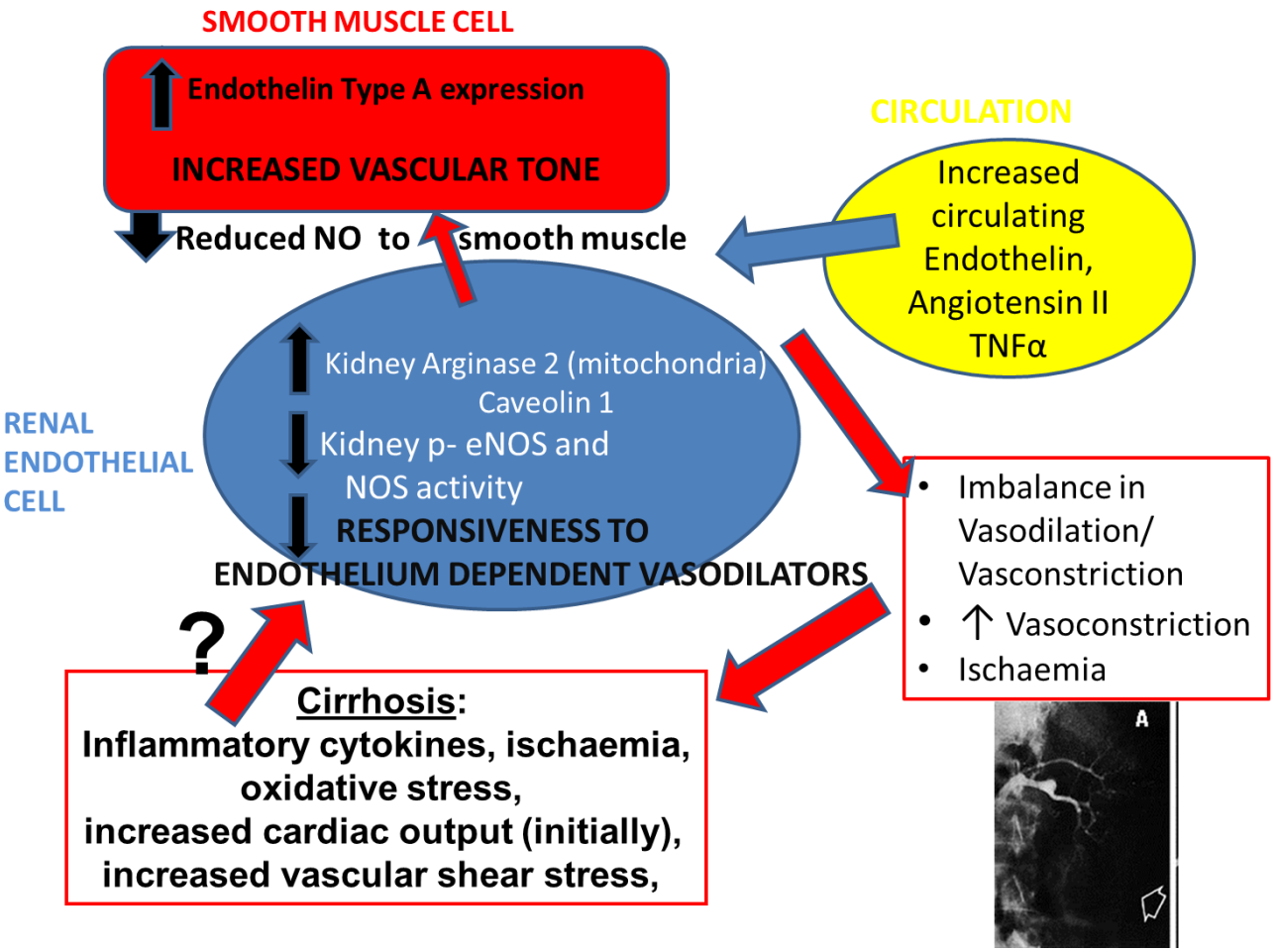


**Figure 8.1 Proposed Mechanism of Pathogenesis of Renal Endothelial Dysfunction in Cirrhosis and HRS Development**

The effect of cirrhosis and PHT on the renal endothelial cell is possibly through increased inflammatory cytokines, oxidative stress, increased cardiac output and shear stress which in turn may lead to increased production of inhibitors of phosphorylated- eNOS, arginase 2 and caveolin 1. As a result of reduced p-eNOS and reduced NOS activity there is less bioavailability of NO in smooth muscle leading to increased vascular tone. Additionally, it is known that there are more circulating vasoconstrictors in cirrhosis and an increase in vasoconstrictor receptor expression, such as the endothelin type A receptor. As a result of this imbalance in dilators/constrictors there is aberrant vasomotor tone which underlies the development of HRS.

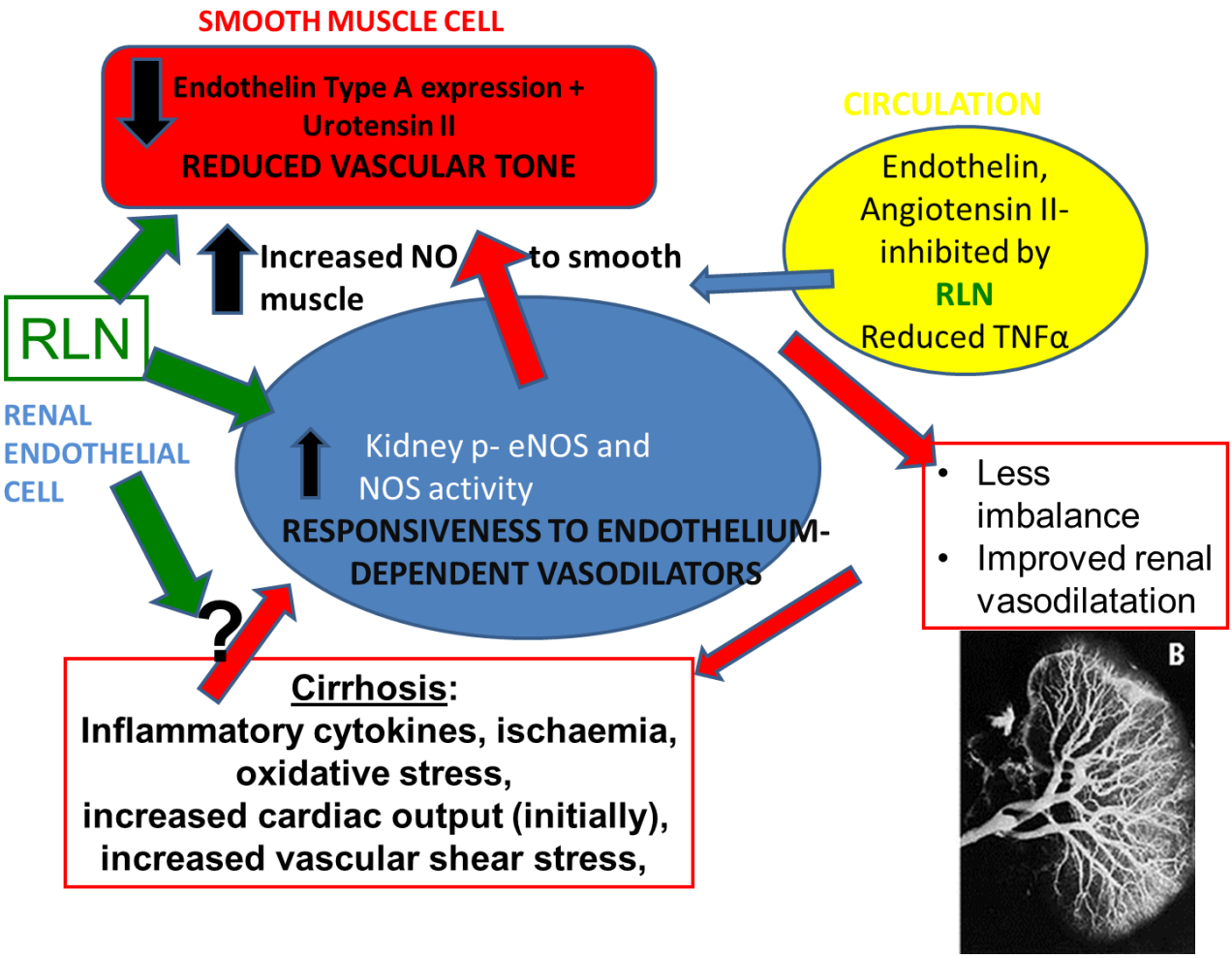


**Figure 8.2 Proposed mechanism of Action of Relaxin on Renal Vascular Endothelial Function and RBF**

RLN has been shown to increase p-eNOS and augment NOS activity in the kidney, reduce $ET_A$ receptor and urotensin II expression, reduce serum TNFα, and inhibit the effect to circulating vasoconstrictors (e.g. Ang II), thereby improving the responsiveness of the kidney vascular endothelial cells to vasodilators, promoting renal vasodilatation and reversing HRS.

# References


Abraldes, J. G., A. Rodriguez-Vilarrupla, et al. (2007). "Simvastatin treatment improves liver sinusoidal endothelial dysfunction in CCl4 cirrhotic rats." Journal of hepatology **46**(6): 1040-1046.

Abraldes, J. G., I. Tarantino, et al. (2003). "Hemodynamic response to pharmacological treatment of portal hypertension and long-term prognosis of cirrhosis." Hepatology **37**(4): 902-908.

Adebayo, D., V. Morabito, et al. (2015). "Renal dysfunction in cirrhosis is not just a vasomotor nephropathy." Kidney international **87**(3): 509-515.

Anand, R., D. Harry, et al. (2002). "Endothelin is an important determinant of renal function in a rat model of acute liver and renal failure." Gut **50**(1): 111-117.

Angeli, P., P. Gines, et al. (2015). "Diagnosis and management of acute kidney injury in patients with cirrhosis: revised consensus recommendations of the International Club of Ascites." Gut.

Angeli, P., P. Gines, et al. (2015). "Diagnosis and management of acute kidney injury in patients with cirrhosis: Revised consensus recommendations of the International Club of Ascites." Journal of hepatology.

Arroyo, V., M. Guevara, et al. (2002). "Hepatorenal syndrome in cirrhosis: pathogenesis and treatment." Gastroenterology **122**(6): 1658-1676.

Arroyo, V., C. Terra, et al. (2007). "Advances in the pathogenesis and treatment of type-1 and type-2 hepatorenal syndrome." Journal of hepatology **46**(5): 935-946.

Assimakopoulos, S. F. and C. E. Vagianos (2009). "Bile duct ligation in rats: a reliable model of hepatorenal syndrome?" World journal of gastroenterology : WJG **15**(1): 121-123.

Bataller, R. and D. A. Brenner (2005). "Liver fibrosis." The Journal of clinical investigation **115**(2): 209-218.

Belcher, J. M., C. R. Parikh, et al. (2013). "Acute kidney injury in patients with cirrhosis: perils and promise." Clinical gastroenterology and hepatology : the official clinical practice journal of the American Gastroenterological Association **11**(12): 1550-1558.

Bhathal, P. S. and H. J. Grossman (1985). "Reduction of the increased portal vascular resistance of the isolated perfused cirrhotic rat liver by vasodilators." Journal of hepatology **1**(4): 325-337.

Bomzon, A., S. Holt, et al. (1997). "Bile acids, oxidative stress, and renal function in biliary obstruction." Seminars in nephrology **17**(6): 549-562.

Bosch, J. and J. C. Garcia-Pagan (2000). "Complications of cirrhosis. I. Portal hypertension." Journal of hepatology **32**(1 Suppl): 141-156.

Boyer, T. D., A. J. Sanyal, et al. (2011). "Impact of liver transplantation on the survival of patients treated for hepatorenal syndrome type 1." Liver transplantation : official publication of the American Association for the Study of Liver Diseases and the International Liver Transplantation Society **17**(11): 1328-1332.

Brensing, K. A., J. Textor, et al. (2000). "Long term outcome after transjugular intrahepatic portosystemic stent-shunt in non-transplant cirrhotics with hepatorenal syndrome: a phase II study." Gut **47**(2): 288-295.

Callander, G. E., W. G. Thomas, et al. (2009). "Prolonged RXFP1 and RXFP2 signaling can be explained by poor internalization and a lack of beta-arrestin recruitment." Am J Physiol Cell Physiol **296**(5): C1058-1066.

Chow, B. S., M. Kocan, et al. (2014). "Relaxin requires the angiotensin II type 2 receptor to abrogate renal interstitial fibrosis." Kidney international **86**(1): 75-85.

Conrad, K. P. (2010). "Unveiling the vasodilatory actions and mechanisms of relaxin." Hypertension **56**(1): 2-9.

Conrad, K. P., D. O. Debrah, et al. (2004). "Relaxin modifies systemic arterial resistance and compliance in conscious, nonpregnant rats." Endocrinology **145**(7): 3289-3296.

Constandinou, C., N. Henderson, et al. (2005). "Modeling liver fibrosis in rodents." Methods in molecular medicine **117**: 237-250.

Culafic, D., M. Stulic, et al. (2014). "Role of cystatin C and renal resistive index in assessment of renal function in patients with liver cirrhosis." World journal of gastroenterology : WJG **20**(21): 6573-6579.

Dagher, L. and K. Moore (2001). "The hepatorenal syndrome." Gut **49**(5): 729-737.
Danielson, L. A. and K. P. Conrad (1995). "Acute blockade of nitric oxide synthase inhibits renal vasodilation and hyperfiltration during pregnancy in chronically instrumented conscious rats." The Journal of clinical investigation **96**(1): 482-490.
Danielson, L. A. and K. P. Conrad (2003). "Time course and dose response of relaxin-mediated renal vasodilation, hyperfiltration, and changes in plasma osmolality in conscious rats." Journal of applied physiology **95**(4): 1509-1514.
Danielson, L. A., L. J. Kercher, et al. (2000). "Impact of gender and endothelin on renal vasodilation and hyperfiltration induced by relaxin in conscious rats." American journal of physiology. Regulatory, integrative and comparative physiology **279**(4): R1298-1304.
Danielson, L. A., O. D. Sherwood, et al. (1999). "Relaxin is a potent renal vasodilator in conscious rats." The Journal of clinical investigation **103**(4): 525-533.
Danielson, L. A., A. Welford, et al. (2006). "Relaxin improves renal function and histology in aging Munich Wistar rats." Journal of the American Society of Nephrology : JASN **17**(5): 1325-1333.
Davenport, A. P., R. E. Kuc, et al. (1995). "ETA receptors predominate in the human vasculature and mediate constriction." J Cardiovasc Pharmacol **26 Suppl 3**: S265-267.
de Franchis, R. (2000). "Stellate cells and the "reversible component" of portal hypertension." Digestive and liver disease : official journal of the Italian Society of Gastroenterology and the Italian Association for the Study of the Liver **32**(2): 104-107.
de Franchis, R. (2010). "Revising consensus in portal hypertension: report of the Baveno V consensus workshop on methodology of diagnosis and therapy in portal hypertension." Journal of hepatology **53**(4): 762-768.
Debrah, D. O., K. P. Conrad, et al. (2005). "Effects of relaxin on systemic arterial hemodynamics and mechanical properties in conscious rats: sex dependency and dose response." J Appl Physiol (1985) **98**(3): 1013-1020.
Debrah, D. O., K. P. Conrad, et al. (2005). "Relaxin increases cardiac output and reduces systemic arterial load in hypertensive rats." Hypertension **46**(4): 745-750.
Debrah, D. O., J. E. Debrah, et al. (2011). "Relaxin regulates vascular wall remodeling and passive mechanical properties in mice." Journal of applied physiology **111**(1): 260-271.
Debrah, D. O., J. Novak, et al. (2006). "Relaxin is essential for systemic vasodilation and increased global arterial compliance during early pregnancy in conscious rats." Endocrinology **147**(11): 5126-5131.
Debrah, J. E. (2008). 5th International Conference on Relaxin and Related Peptides. Maui, Hawaii.
Dschietzig, T., A. Brecht, et al. (2012). "Relaxin improves TNF-alpha-induced endothelial dysfunction: the role of glucocorticoid receptor and phosphatidylinositol 3-kinase signalling." Cardiovasc Res **95**(1): 97-107.
Dschietzig, T., S. Teichman, et al. (2009). "First clinical experience with intravenous recombinant human relaxin in compensated heart failure." Annals of the New York Academy of Sciences **1160**: 387-392.
Dschietzig, T., S. Teichman, et al. (2009). "Intravenous recombinant human relaxin in compensated heart failure: a safety, tolerability, and pharmacodynamic trial." Journal of cardiac failure **15**(3): 182-190.
Du, X. J., R. A. Bathgate, et al. (2010). "Cardiovascular effects of relaxin: from basic science to clinical therapy." Nat Rev Cardiol **7**(1): 48-58.
Epstein, M., D. P. Berk, et al. (1970). "Renal failure in the patient with cirrhosis. The role of active vasoconstriction." The American journal of medicine **49**(2): 175-185.
Fabrizi, F., V. Dixit, et al. (2006). "Meta-analysis: terlipressin therapy for the hepatorenal syndrome." Alimentary pharmacology & therapeutics **24**(6): 935-944.
Fagundes, C., M. N. Pepin, et al. (2012). "Urinary neutrophil gelatinase-associated lipocalin as biomarker in the differential diagnosis of impairment of kidney function in cirrhosis." Journal of hepatology **57**(2): 267-273.
Fallowfield, J. A., A. L. Hayden, et al. (2014). "Relaxin modulates human and rat hepatic myofibroblast function and ameliorates portal hypertension in vivo." Hepatology **59**(4): 1492-1504.

Faul, F., E. Erdfelder, et al. (2007). "G*Power 3: a flexible statistical power analysis program for the social, behavioral, and biomedical sciences." Behav Res Methods **39**(2): 175-191.
Fede, G., G. D'Amico, et al. (2012). "Renal failure and cirrhosis: a systematic review of mortality and prognosis." Journal of hepatology **56**(4): 810-818.
Fernandez, J., M. Navasa, et al. (2007). "Primary prophylaxis of spontaneous bacterial peritonitis delays hepatorenal syndrome and improves survival in cirrhosis." Gastroenterology **133**(3): 818-824.
Fernandez, M., M. Mejias, et al. (2007). "Reversal of portal hypertension and hyperdynamic splanchnic circulation by combined vascular endothelial growth factor and platelet-derived growth factor blockade in rats." Hepatology **46**(4): 1208-1217.
Fisher, C., M. MacLean, et al. (2002). "Is the pregnancy hormone relaxin also a vasodilator peptide secreted by the heart?" Circulation **106**(3): 292-295.
Garcia-Martinez, R., L. Noiret, et al. (2014). "Albumin infusion improves renal blood flow autoregulation in patients with acute decompensation of cirrhosis and acute kidney injury." Liver international : official journal of the International Association for the Study of the Liver.
Garcia-Tsao, G., S. Friedman, et al. (2010). "Now there are many (stages) where before there was one: In search of a pathophysiological classification of cirrhosis." Hepatology **51**(4): 1445-1449.
Garcia-Tsao, G., C. R. Parikh, et al. (2008). "Acute kidney injury in cirrhosis." Hepatology **48**(6): 2064-2077.
Gines, A., A. Escorsell, et al. (1993). "Incidence, predictive factors, and prognosis of the hepatorenal syndrome in cirrhosis with ascites." Gastroenterology **105**(1): 229-236.
Gines, P., M. Guevara, et al. (2003). "Hepatorenal syndrome." Lancet **362**(9398): 1819-1827.
Gines, P., F. Wong, et al. (2010). "Clinical trial: short-term effects of combination of satavaptan, a selective vasopressin V2 receptor antagonist, and diuretics on ascites in patients with cirrhosis without hyponatraemia--a randomized, double-blind, placebo-controlled study." Alimentary pharmacology & therapeutics **31**(8): 834-845.
Gluud, L. L., K. Christensen, et al. (2012). "Terlipressin for hepatorenal syndrome." Cochrane Database Syst Rev **9**: CD005162.
Gonwa, T. A., C. A. Morris, et al. (1991). "Long-term survival and renal function following liver transplantation in patients with and without hepatorenal syndrome--experience in 300 patients." Transplantation **51**(2): 428-430.
Grace, J. A., C. B. Herath, et al. (2012). "Update on new aspects of the renin-angiotensin system in liver disease: clinical implications and new therapeutic options." Clinical science **123**(4): 225-239.
Groszmann, R. J., G. Garcia-Tsao, et al. (2005). "Beta-blockers to prevent gastroesophageal varices in patients with cirrhosis." The New England journal of medicine **353**(21): 2254-2261.
Guevara, M., P. Gines, et al. (1998). "Transjugular intrahepatic portosystemic shunt in hepatorenal syndrome: effects on renal function and vasoactive systems." Hepatology **28**(2): 416-422.
Hadoke, P. W. and P. C. Hayes (1997). "In vitro evidence for vascular hyporesponsiveness in clinical and experimental cirrhosis." Pharmacol Ther **75**(1): 51-68.
Halls, M. L., E. T. van der Westhuizen, et al. (2007). "Relaxin family peptide receptors--former orphans reunite with their parent ligands to activate multiple signalling pathways." Br J Pharmacol **150**(6): 677-691.
Harry, D., R. Anand, et al. (1999). "Increased sensitivity to endotoxemia in the bile duct-ligated cirrhotic Rat." Hepatology **30**(5): 1198-1205.
Hartleb, M. and K. Gutkowski (2012). "Kidneys in chronic liver diseases." World journal of gastroenterology : WJG **18**(24): 3035-3049.
Hsu, S. Y., K. Nakabayashi, et al. (2002). "Activation of orphan receptors by the hormone relaxin." Science **295**(5555): 671-674.
Huang, H. C., O. Haq, et al. (2011). "Intestinal and plasma VEGF levels in cirrhosis: The role of portal pressure." Journal of cellular and molecular medicine.
Huang, X., Y. Gai, et al. (2011). "Relaxin regulates myofibroblast contractility and protects against lung fibrosis." Am J Pathol **179**(6): 2751-2765.

Issa, R., X. Zhou, et al. (2004). "Spontaneous recovery from micronodular cirrhosis: evidence for incomplete resolution associated with matrix cross-linking." Gastroenterology **126**(7): 1795-1808.
Iwakiri, Y. (2011). "Endothelial dysfunction in the regulation of cirrhosis and portal hypertension." Liver international : official journal of the International Association for the Study of the Liver.
Iwakiri, Y. and R. J. Groszmann (2007). "Vascular endothelial dysfunction in cirrhosis." Journal of hepatology **46**(5): 927-934.
Iwatsuki, S., M. M. Popovtzer, et al. (1973). "Recovery from "hepatorenal syndrome" after orthotopic liver transplantation." The New England journal of medicine **289**(22): 1155-1159.
Jalan, R., E. H. Forrest, et al. (1997). "Reduction in renal blood flow following acute increase in the portal pressure: evidence for the existence of a hepatorenal reflex in man?" Gut **40**(5): 664-670.
Jaramillo-Juarez, F., M. L. Rodriguez-Vazquez, et al. (2008). "Acute renal failure induced by carbon tetrachloride in rats with hepatic cirrhosis." Annals of hepatology : official journal of the Mexican Association of Hepatology **7**(4): 331-338.
Jelinic, M., C. H. Leo, et al. (2014). "Localization of relaxin receptors in arteries and veins, and region-specific increases in compliance and bradykinin-mediated relaxation after in vivo serelaxin treatment." FASEB journal : official publication of the Federation of American Societies for Experimental Biology **28**(1): 275-287.
Jeyabalan, A., J. Novak, et al. (2003). "Essential role for vascular gelatinase activity in relaxin-induced renal vasodilation, hyperfiltration, and reduced myogenic reactivity of small arteries." Circulation research **93**(12): 1249-1257.
Jeyabalan, A., J. Novak, et al. (2007). "Vascular matrix metalloproteinase-9 mediates the inhibition of myogenic reactivity in small arteries isolated from rats after short-term administration of relaxin." Endocrinology **148**(1): 189-197.
Johnson, F. K., K. J. Peyton, et al. (2015). "Arginase promotes endothelial dysfunction and hypertension in obese rats." Obesity (Silver Spring) **23**(2): 383-390.
Kew, M. C., P. W. Brunt, et al. (1971). "Renal and intrarenal blood-flow in cirrhosis of the liver." Lancet **2**(7723): 504-510.
Kobalava, Z., S. Villevalde, et al. (2014). "Pharmacokinetics of serelaxin in patients with hepatic impairment: A single-dose, open-label, parallel-group study." Br J Clin Pharmacol.
Kong, H. Y., F. Chen, et al. (2013). "Intrarenal resistance index for the assessment of acute renal injury in a rat liver transplantation model." BMC Nephrol **14**: 55.
Koppel, M. H., J. W. Coburn, et al. (1969). "Transplantation of cadaveric kidneys from patients with hepatorenal syndrome. Evidence for the functionalnature of renal failure in advanced liver disease." The New England journal of medicine **280**(25): 1367-1371.
Krag, A., F. Bendtsen, et al. (2010). "Low cardiac output predicts development of hepatorenal syndrome and survival in patients with cirrhosis and ascites." Gut **59**(1): 105-110.
Krag, A., S. Moller, et al. (2011). "Hyponatremia in patients treated with terlipressin: mechanisms and implications for clinical practice." Hepatology **53**(1): 368-369; author reply 369-370.
Krag, A., S. Moller, et al. (2007). "Terlipressin improves renal function in patients with cirrhosis and ascites without hepatorenal syndrome." Hepatology **46**(6): 1863-1871.
Krause, B. J., R. Del Rio, et al. (2015). "Arginase-endothelial nitric oxide synthase imbalance contributes to endothelial dysfunction during chronic intermittent hypoxia." J Hypertens **33**(3): 515-524; discussion 524.
Laleman, W., A. Omasta, et al. (2005). "A role for asymmetric dimethylarginine in the pathophysiology of portal hypertension in rats with biliary cirrhosis." Hepatology **42**(6): 1382-1390.
Leifeld, L., C. Clemens, et al. (2010). "Expression of urotensin II and its receptor in human liver cirrhosis and fulminant hepatic failure." Digestive diseases and sciences **55**(5): 1458-1464.
Leo, C. H., M. Jelinic, et al. (2014). "Acute intravenous injection of serelaxin (recombinant human relaxin-2) causes rapid and sustained bradykinin-mediated vasorelaxation." J Am Heart Assoc **3**(1): e000493.
Li, L. P., S. Halter, et al. (2008). "Blood oxygen level-dependent MR imaging of the kidneys." Magnetic resonance imaging clinics of North America **16**(4): 613-625, viii.

Lieber, C. S. (2004). "CYP2E1: from ASH to NASH." Hepatol Res **28**(1): 1-11.
Ling, L., R. E. Kuc, et al. (2012). "Comparison of endothelin receptors in normal versus cirrhotic human liver and in the liver from endothelial cell-specific ETB knockout mice." Life Sci **91**(13-14): 716-722.
Liu, D., J. Chen, et al. (2010). "Increased expression of urotensin II and GPR14 in patients with cirrhosis and portal hypertension." Int J Mol Med **25**(6): 845-851.
Liu, D. G., J. Wang, et al. (2009). "The urotension II antagonist SB-710411 arrests fibrosis in CCL4 cirrhotic rats." Mol Med Rep **2**(6): 953-961.
Longo, M., V. Jain, et al. (2003). "Effects of recombinant human relaxin on pregnant rat uterine artery and myometrium in vitro." Am J Obstet Gynecol **188**(6): 1468-1474; discussion 1474-1466.
Manibusan, M. K., M. Odin, et al. (2007). "Postulated carbon tetrachloride mode of action: a review." J Environ Sci Health C Environ Carcinog Ecotoxicol Rev **25**(3): 185-209.
Marik, P. E., K. Wood, et al. (2006). "The course of type 1 hepato-renal syndrome post liver transplantation." Nephrology, dialysis, transplantation : official publication of the European Dialysis and Transplant Association - European Renal Association **21**(2): 478-482.
Martin-Llahi, M., M. N. Pepin, et al. (2008). "Terlipressin and albumin vs albumin in patients with cirrhosis and hepatorenal syndrome: a randomized study." Gastroenterology **134**(5): 1352-1359.
McGuane, J. T., L. A. Danielson, et al. (2011). "Angiogenic growth factors are new and essential players in the sustained relaxin vasodilatory pathway in rodents and humans." Hypertension **57**(6): 1151-1160.
McGuane, J. T., J. E. Debrah, et al. (2011). "Relaxin induces rapid dilation of rodent small renal and human subcutaneous arteries via PI3 kinase and nitric oxide." Endocrinology **152**(7): 2786-2796.
Mehta, R. L., J. A. Kellum, et al. (2007). "Acute Kidney Injury Network: report of an initiative to improve outcomes in acute kidney injury." Crit Care **11**(2): R31.
Melnikov, V. Y., S. Faubel, et al. (2002). "Neutrophil-independent mechanisms of caspase-1- and IL-18-mediated ischemic acute tubular necrosis in mice." The Journal of clinical investigation **110**(8): 1083-1091.
Menzies, R. I., R. J. Unwin, et al. (2013). "Effect of P2X4 and P2X7 receptor antagonism on the pressure diuresis relationship in rats." Front Physiol **4**: 305.
Metra, M., G. Cotter, et al. (2013). "Effect of serelaxin on cardiac, renal, and hepatic biomarkers in the Relaxin in Acute Heart Failure (RELAX-AHF) development program: correlation with outcomes." J Am Coll Cardiol **61**(2): 196-206.
Mindikoglu, A. L., T. C. Dowling, et al. (2014). "A pilot study to evaluate renal hemodynamics in cirrhosis by simultaneous glomerular filtration rate, renal plasma flow, renal resistive indices and biomarkers measurements." Am J Nephrol **39**(6): 543-552.
Minshall, R. D., W. C. Sessa, et al. (2003). "Caveolin regulation of endothelial function." Am J Physiol Lung Cell Mol Physiol **285**(6): L1179-1183.
Moore, K. (1999). "Renal failure in acute liver failure." European journal of gastroenterology & hepatology **11**(9): 967-975.
Moore, X. L., Y. Su, et al. (2014). "Diverse regulation of cardiac expression of relaxin receptor by alpha1- and beta1-adrenoceptors." Cardiovasc Drugs Ther **28**(3): 221-228.
Moreau, R., F. Durand, et al. (2002). "Terlipressin in patients with cirrhosis and type 1 hepatorenal syndrome: a retrospective multicenter study." Gastroenterology **122**(4): 923-930.
Nazar, A., G. H. Pereira, et al. (2010). "Predictors of response to therapy with terlipressin and albumin in patients with cirrhosis and type 1 hepatorenal syndrome." Hepatology **51**(1): 219-226.
Newby, D. E. and P. C. Hayes (2002). "Hyperdynamic circulation in liver cirrhosis: not peripheral vasodilatation but 'splanchnic steal'." QJM : monthly journal of the Association of Physicians **95**(12): 827-830.
Novak, J., L. A. Danielson, et al. (2001). "Relaxin is essential for renal vasodilation during pregnancy in conscious rats." The Journal of clinical investigation **107**(11): 1469-1475.
Novak, J., L. J. Parry, et al. (2006). "Evidence for local relaxin ligand-receptor expression and function in arteries." FASEB journal : official publication of the Federation of American Societies for Experimental Biology **20**(13): 2352-2362.

Novak, J., R. J. Ramirez, et al. (2002). "Myogenic reactivity is reduced in small renal arteries isolated from relaxin-treated rats." American journal of physiology. Regulatory, integrative and comparative physiology **283**(2): R349-355.
O'Brien, A. J., J. N. Fullerton, et al. (2014). "Immunosuppression in acutely decompensated cirrhosis is mediated by prostaglandin E2." Nat Med **20**(5): 518-523.
Pawar, R., W. Kemp, et al. (2011). "Urotensin II levels are an important marker for the severity of portal hypertension in children." Journal of pediatric gastroenterology and nutrition **53**(1): 88-92.
Pereira, R. M., R. A. dos Santos, et al. (2008). "Development of hepatorenal syndrome in bile duct ligated rats." World journal of gastroenterology : WJG **14**(28): 4505-4511.
Perez Tamayo, R. (1983). "Is cirrhosis of the liver experimentally produced by CCl4 and adequate model of human cirrhosis?" Hepatology **3**(1): 112-120.
Picchi, A., X. Gao, et al. (2006). "Tumor necrosis factor-alpha induces endothelial dysfunction in the prediabetic metabolic syndrome." Circulation research **99**(1): 69-77.
Pinzani, M., K. Rombouts, et al. (2005). "Fibrosis in chronic liver diseases: diagnosis and management." Journal of hepatology **42 Suppl**(1): S22-36.
Planas, R., S. Montoliu, et al. (2006). "Natural history of patients hospitalized for management of cirrhotic ascites." Clinical gastroenterology and hepatology : the official clinical practice journal of the American Gastroenterological Association **4**(11): 1385-1394.
Platt, J. F., J. H. Ellis, et al. (1994). "Renal duplex Doppler ultrasonography: a noninvasive predictor of kidney dysfunction and hepatorenal failure in liver disease." Hepatology **20**(2): 362-369.
Rafnsson, A., A. Shemyakin, et al. (2014). "Selective endothelin ETA and dual ET(A)/ET(B) receptor blockade improve endothelium-dependent vasodilatation in patients with type 2 diabetes and coronary artery disease." Life Sci **118**(2): 435-439.
Ramachandran, P. and J. P. Iredale (2009). "Reversibility of liver fibrosis." Annals of hepatology : official journal of the Mexican Association of Hepatology **8**(4): 283-291.
Ring-Larsen, H. (1977). "Renal blood flow in cirrhosis: relation to systemic and portal haemodynamics and liver function." Scand J Clin Lab Invest **37**(7): 635-642.
Ring-Larsen, H., B. Hesse, et al. (1982). "Sympathetic nervous activity and renal and systemic hemodynamics in cirrhosis: plasma norepinephrine concentration, hepatic extraction, and renal release." Hepatology **2**(3): 304-310.
Ripoll, C., R. Groszmann, et al. (2007). "Hepatic venous pressure gradient predicts clinical decompensation in patients with compensated cirrhosis." Gastroenterology **133**(2): 481-488.
Rivera-Huizar, S., A. R. Rincon-Sanchez, et al. (2006). "Renal dysfunction as a consequence of acute liver damage by bile duct ligation in cirrhotic rats." Exp Toxicol Pathol **58**(2-3): 185-195.
Robertson, S., G. A. Gray, et al. (2012). "Diesel exhaust particulate induces pulmonary and systemic inflammation in rats without impairing endothelial function ex vivo or in vivo." Part Fibre Toxicol **9**: 9.
Rockey, D. C. (2001). "Hepatic blood flow regulation by stellate cells in normal and injured liver." Seminars in liver disease **21**(3): 337-349.
Rockey, D. C. and J. J. Chung (1998). "Reduced nitric oxide production by endothelial cells in cirrhotic rat liver: endothelial dysfunction in portal hypertension." Gastroenterology **114**(2): 344-351.
Salerno, F., A. Gerbes, et al. (2007). "Diagnosis, prevention and treatment of hepatorenal syndrome in cirrhosis." Gut **56**(9): 1310-1318.
Salmeron, J. M., L. Ruiz del Arbol, et al. (1993). "Renal effects of acute isosorbide-5-mononitrate administration in cirrhosis." Hepatology **17**(5): 800-806.
Salo, J., A. Gines, et al. (1996). "Renal and neurohormonal changes following simultaneous administration of systemic vasoconstrictors and dopamine or prostacyclin in cirrhotic patients with hepatorenal syndrome." Journal of hepatology **25**(6): 916-923.
Samuel, C. S. (2005). "Relaxin: antifibrotic properties and effects in models of disease." Clin Med Res **3**(4): 241-249.

Samuel, C. S., T. D. Hewitson, et al. (2007). "Drugs of the future: the hormone relaxin." Cellular and molecular life sciences : CMLS **64**(12): 1539-1557.
Sanyal, A. J., T. Boyer, et al. (2008). "A randomized, prospective, double-blind, placebo-controlled trial of terlipressin for type 1 hepatorenal syndrome." Gastroenterology **134**(5): 1360-1368.
Sasser, J. M., M. W. Cunningham, Jr., et al. (2014). "Serelaxin reduces oxidative stress and asymmetric dimethylarginine in angiotensin II-induced hypertension." Am J Physiol Renal Physiol **307**(12): F1355-1362.
Sasser, J. M., M. Molnar, et al. (2011). "Relaxin ameliorates hypertension and increases nitric oxide metabolite excretion in angiotensin II but not N(omega)-nitro-L-arginine methyl ester hypertensive rats." Hypertension **58**(2): 197-204.
Schrier, R. W., V. Arroyo, et al. (1988). "Peripheral arterial vasodilation hypothesis: a proposal for the initiation of renal sodium and water retention in cirrhosis." Hepatology **8**(5): 1151-1157.
Seibold, J. R., J. H. Korn, et al. (2000). "Recombinant human relaxin in the treatment of scleroderma. A randomized, double-blind, placebo-controlled trial." Annals of internal medicine **132**(11): 871-879.
Shah, N., D. Dhar, et al. (2012). "Prevention of acute kidney injury in a rodent model of cirrhosis following selective gut decontamination is associated with reduced renal TLR4 expression." Journal of hepatology **56**(5): 1047-1053.
Sherwood, O. D. (2004). "Relaxin's physiological roles and other diverse actions." Endocr Rev **25**(2): 205-234.
Shi, J., K. Aisaki, et al. (1998). "Evidence of hepatocyte apoptosis in rat liver after the administration of carbon tetrachloride." Am J Pathol **153**(2): 515-525.
Smith, M. C., L. A. Danielson, et al. (2006). "Influence of recombinant human relaxin on renal hemodynamics in healthy volunteers." Journal of the American Society of Nephrology : JASN **17**(11): 3192-3197.
Smith, M. C., A. P. Murdoch, et al. (2006). "Relaxin has a role in establishing a renal response in pregnancy." Fertility and sterility **86**(1): 253-255.
Snowdon, V. K. and J. A. Fallowfield (2011). "Models and mechanisms of fibrosis resolution." Alcoholism, clinical and experimental research **35**(5): 794-799.
Snowdon, V. K., N. Guha, et al. (2012). "Noninvasive evaluation of portal hypertension: emerging tools and techniques." Int J Hepatol **2012**: 691089.
Sort, P., M. Navasa, et al. (1999). "Effect of intravenous albumin on renal impairment and mortality in patients with cirrhosis and spontaneous bacterial peritonitis." The New England journal of medicine **341**(6): 403-409.
Stadlbauer, V., G. A. Wright, et al. (2008). "Relationship between activation of the sympathetic nervous system and renal blood flow autoregulation in cirrhosis." Gastroenterology **134**(1): 111-119.
Teerlink, J. R., G. Cotter, et al. (2013). "Serelaxin, recombinant human relaxin-2, for treatment of acute heart failure (RELAX-AHF): a randomised, placebo-controlled trial." Lancet **381**(9860): 29-39.
Teichman, S. L., E. Unemori, et al. (2009). "Relaxin, a pleiotropic vasodilator for the treatment of heart failure." Heart failure reviews **14**(4): 321-329.
Testino, G., C. Ferro, et al. (2003). "Type-2 hepatorenal syndrome and refractory ascites: role of transjugular intrahepatic portosystemic stent-shunt in eighteen patients with advanced cirrhosis awaiting orthotopic liver transplantation." Hepato-gastroenterology **50**(54): 1753-1755.
Thabut, D., J. Massard, et al. (2007). "Model for end-stage liver disease score and systemic inflammatory response are major prognostic factors in patients with cirrhosis and acute functional renal failure." Hepatology **46**(6): 1872-1882.
Trawale, J. M., V. Paradis, et al. (2010). "The spectrum of renal lesions in patients with cirrhosis: a clinicopathological study." Liver international : official journal of the International Association for the Study of the Liver **30**(5): 725-732.
Trebicka, J., L. Leifeld, et al. (2008). "Hemodynamic effects of urotensin II and its specific receptor antagonist palosuran in cirrhotic rats." Hepatology **47**(4): 1264-1276.
Velez, J. C. and P. J. Nietert (2011). "Therapeutic response to vasoconstrictors in hepatorenal syndrome parallels increase in mean arterial pressure: a pooled analysis of clinical trials." Am J Kidney Dis **58**(6): 928-938.

Verma, S., K. Ajudia, et al. (2006). "Prevalence of septic events, type 1 hepatorenal syndrome, and mortality in severe alcoholic hepatitis and utility of discriminant function and MELD score in predicting these adverse events." Digestive diseases and sciences **51**(9): 1637-1643.

Vodstrcil, L. A., M. Tare, et al. (2012). "Relaxin mediates uterine artery compliance during pregnancy and increases uterine blood flow." FASEB journal : official publication of the Federation of American Societies for Experimental Biology **26**(10): 4035-4044.

Voors, A. A., M. Dahlke, et al. (2014). "Renal hemodynamic effects of serelaxin in patients with chronic heart failure: a randomized, placebo-controlled study." Circ Heart Fail **7**(6): 994-1002.

Williams, E. J., R. C. Benyon, et al. (2001). "Relaxin inhibits effective collagen deposition by cultured hepatic stellate cells and decreases rat liver fibrosis in vivo." Gut **49**(4): 577-583.

Williams, R., R. Aspinall, et al. (2014). "Addressing liver disease in the UK: a blueprint for attaining excellence in health care and reducing premature mortality from lifestyle issues of excess consumption of alcohol, obesity, and viral hepatitis." Lancet **384**(9958): 1953-1997.

Woodward W, Rusnak M, et al. (2014). "Vascular reactivity is altered in mice with a conditional knockout of relaxin receptor in endothelial cells " FASEB journal : official publication of the Federation of American Societies for Experimental Biology **28 no.1 supplement 681.11**.

Zhang, C., X. Xu, et al. (2006). "TNF-alpha contributes to endothelial dysfunction in ischemia/reperfusion injury." Arteriosclerosis, thrombosis, and vascular biology **26**(3): 475-480.

# Appendix 1 – PCR array gene names

| Abbreviation | Gene name |
|---|---|
| **Ace** | Angiotensin I converting enzyme (peptidyl-dipeptidase A) 1 |
| **Ace2** | Angiotensin I converting enzyme (peptidyl-dipeptidase A) 2 |
| **Acta2** | Smooth muscle alpha-actin |
| **Adm** | Adrenomedullin |
| **Adra1b** | Adrenergic, alpha-1B-, receptor |
| **Adra1d** | Adrenergic, alpha-1D-, receptor |
| **Adrb1** | Adrenergic, beta-1-, receptor |
| **Agt** | Angiotensinogen (serpin peptidase inhibitor, clade A, member 8) |
| **Agtr1a** | Angiotensin II receptor, type 1a |
| **Agtr1b** | Angiotensin II receptor, type 1b |
| **Agtr2** | Angiotensin II receptor, type 2 |
| **Alox5** | Arachidonate 5-lipoxygenase |
| **Arg2** | Arginase type II |
| **Atp2c1** | ATPase, Ca++ transporting, type 2C, member 1 |
| **Atp6ap2** | ATPase, H+ transporting, lysosomal accessory protein 2 |
| **Avp** | Arginine vasopressin |
| **Avpr1a** | Arginine vasopressin receptor 1A |
| **Avpr1b** | Arginine vasopressin receptor 1B |
| **Bdkrb1** | Bradykinin receptor B1 |
| **Bdkrb2** | Bradykinin receptor B2 |
| **Bmpr2** | Bone morphogenetic protein receptor, type II (serine/threonine kinase) |
| **Cacna1c** | Calcium channel, voltage-dependent, L type, alpha 1C subunit |
| **Calca** | Calcitonin-related polypeptide alpha |
| **Cav1** | Caveolin 1, caveolae protein |
| **Chrna1** | Cholinergic receptor, nicotinic, alpha 1 (muscle) |
| **Chrnb1** | Cholinergic receptor, nicotinic, beta 1 (muscle) |
| **Clic1** | Chloride intracellular channel 1 |
| **Clic4** | Chloride intracellular channel 4 |
| **Clic5** | Chloride intracellular channel 5 |
| **Cnga1** | Cyclic nucleotide gated channel alpha 1 |
| **Cnga2** | Cyclic nucleotide gated channel alpha 2 |
| **Cnga3** | Cyclic nucleotide gated channel alpha 3 |
| **Cnga4** | Cyclic nucleotide gated channel alpha 4 |
| **Cngb1** | Cyclic nucleotide gated channel beta 1 |
| **Cps1** | Carbamoyl-phosphate synthetase 1 |
| **Drd3** | Dopamine receptor D3 |
| **Drd5** | Dopamine receptor D5 |
| **Ece1** | Endothelin converting enzyme 1 |
| **Edn1** | Endothelin 1 |
| **Edn2** | Endothelin 2 |
| **Ednra** | Endothelin receptor type A |
| **Ednrb** | Endothelin receptor type B |
| **Ephx2** | Epoxide hydrolase 2, cytoplasmic |
| **Gch1** | GTP cyclohydrolase 1 |
| **Gchfr** | GTP cyclohydrolase I feedback regulator |
| **Gucy1a3** | Guanylate cyclase 1, soluble, alpha 3 |
| **Gucy1b3** | Guanylate cyclase 1, soluble, beta 3 |
| **Hif1a** | Hypoxia-inducible factor 1, alpha subunit (basic helix-loop-helix transcription factor) |

| | |
|---|---|
| **Itpr1** | Inositol 1,4,5-triphosphate receptor, type 1 |
| **Itpr2** | Inositol 1,4,5-triphosphate receptor, type 2 |
| **Itpr3** | Inositol 1,4,5-triphosphate receptor, type 3 |
| **Kcnj8** | Potassium inwardly-rectifying channel, subfamily J, member 8 |
| **Kcnma1** | Potassium large conductance calcium-activated channel, subfamily M, alpha member 1 |
| **Mylk** | Myosin light chain kinase |
| **Mylk2** | Myosin light chain kinase 2 |
| **Mylk3** | Myosin light chain kinase 3 |
| **Nos3** | Nitric oxide synthase 3, endothelial cell |
| **Nosip** | Nitric oxide synthase interacting protein |
| **Nostrin** | Nitric oxide synthase trafficker |
| **Nppb** | Natriuretic peptide precursor B |
| **Nppc** | Natriuretic peptide precursor C |
| **Npr1** | Natriuretic peptide receptor A/guanylate cyclase A (atrionatriuretic peptide receptor A) |
| **Npy1r** | Neuropeptide Y receptor Y1 |
| **P2rx4** | Purinergic receptor P2X, ligand-gated ion channel 4 |
| **Pde3a** | Phosphodiesterase 3A, cGMP inhibited |
| **Pde3b** | Phosphodiesterase 3B, cGMP-inhibited |
| **Pde5a** | Phosphodiesterase 5A, cGMP-specific |
| **Plcg1** | Phospholipase C, gamma 1 |
| **Plcg2** | Phospholipase C, gamma 2 |
| **Prkg1** | Protein kinase, cGMP-dependent, type 1 |
| **Prkg2** | Protein kinase, cGMP-dependent, type II |
| **Ptgir** | Prostaglandin I2 (prostacyclin) receptor (IP) |
| **Ptgs1** | Prostaglandin-endoperoxide synthase 1 |
| **Ptgs2** | Prostaglandin-endoperoxide synthase 2 |
| **Ren** | Renin |
| **S1pr1** | Sphingosine-1-phosphate receptor 1 |
| **Scnn1a** | Sodium channel, nonvoltage-gated 1 alpha |
| **Scnn1b** | Sodium channel, nonvoltage-gated 1, beta |
| **Scnn1g** | Sodium channel, nonvoltage-gated 1, gamma |
| **Slc7a1** | Solute carrier family 7 (cationic amino acid transporter, y+ system), member 1 |
| **Sphk1** | Sphingosine kinase 1 |
| **Sphk2** | Sphingosine kinase 2 |
| **Uts2** | Urotensin 2 |
| **Uts2r** | Urotensin 2 receptor |

# Appendix 2 - Published paper

HEPATOLOGY
Official Journal of the American Association for the Study of Liver Diseases



# Relaxin Modulates Human and Rat Hepatic Myofibroblast Function and Ameliorates Portal Hypertension *In Vivo*

Jonathan A. Fallowfield,[1] Annette L. Hayden,[2] Victoria K. Snowdon,[1] Rebecca L. Aucott,[1] Ben M. Stutchfield,[3] Damian J. Mole,[1] Antonella Pellicoro,[1] Timothy T. Gordon-Walker,[1] Alexander Henke,[4] Joerg Schrader,[1] Palak J. Trivedi,[5] Marc Princivalle,[6] Stuart J. Forbes,[3] Jane E. Collins,[2] and John P. Iredale[1]

**Active myofibroblast (MF) contraction contributes significantly to the increased intrahepatic vascular resistance that is the primary cause of portal hypertension (PHT) in cirrhosis. We sought proof of concept for direct therapeutic targeting of the dynamic component of PHT and markers of MF activation using short-term administration of the peptide hormone relaxin (RLN). We defined the portal hypotensive effect in rat models of sinusoidal PHT and the expression, activity, and function of the RLN-receptor signaling axis in human liver MFs. The effects of RLN were studied after 8 and 16 weeks carbon tetrachloride intoxication, following bile duct ligation, and in tissue culture models. Hemodynamic changes were analyzed by direct cannulation, perivascular flowprobe, indocyanine green imaging, and functional magnetic resonance imaging. Serum and hepatic nitric oxide (NO) levels were determined by immunoassay. Hepatic inflammation was assessed by histology and serum markers and fibrosis by collagen proportionate area. Gene expression was analyzed by quantitative reverse-transcription polymerase chain reaction (qRT-PCR) and western blotting and hepatic stellate cell (HSC)-MF contractility by gel contraction assay. Increased expression of RLN receptor (RXFP1) was shown in HSC-MFs and fibrotic liver diseases in both rats and humans. RLN induced a selective and significant reduction in portal pressure in pathologically distinct PHT models, through augmentation of intrahepatic NO signaling and a dramatic reduction in contractile filament expression in HSC-MFs. Critical for translation, RLN did not induce systemic hypotension even in advanced cirrhosis models. Portal blood flow and hepatic oxygenation were increased by RLN in early cirrhosis. Treatment of human HSC-MFs with RLN inhibited contractility and induced an antifibrogenic phenotype in an RXFP1-dependent manner. *Conclusion*: We identified RXFP1 as a potential new therapeutic target for PHT and MF activation status. (HEPATOLOGY 2014;59:1492-1504)**

See Editorial on Page 1223

The dynamic component of portal hypertension (PHT), mediated by active contraction of myofibroblasts (MFs) predominantly derived from activated hepatic stellate cells (HSCs),[1,2] accounts for about 30% of the increased intrahepatic vascular resistance (IHVR) in cirrhosis and is potentially reversible.[3,4] The increase in sinusoidal tone reflects a functional disturbance of the liver circulation in response to excessive production of contractile agonists (e.g., endothelin-1 [ET-1]), reduced

*Abbreviations:* α*-SMA, alpha-smooth muscle actin; ALT, alanine aminotransferase; BDL, bile duct ligation; BOLD-MRI, blood oxygen dependent-magnetic resonance imaging; CCl4, carbon tetrachloride; CPA, collagen proportionate area; (e)NOS, (endothelial) nitric oxide synthase; ET-1, endothelin-1; (H2)-RLN, (human2)-relaxin; (h)HSC, (human) hepatic stellate cell; ICG, indocyanine green; IHVR, intrahepatic vascular resistance; L-NAME, L-N$^G$-Nitroarginine methyl ester; MAP, mean arterial pressure; MF, myofibroblast; NO, nitric oxide; PHT, portal hypertension; RXFP, relaxin receptor family peptide.*

*From the [1]Medical Research Council/University of Edinburgh Centre for Inflammation Research, Queen's Medical Research Institute, Edinburgh, UK; [2]Clinical and Experimental Sciences, Sir Henry Wellcome Laboratories, School of Medicine, University of Southampton, UK; [3]Scottish Centre for Regenerative Medicine, University of Edinburgh, UK; [4]Medical Research Council/University of Edinburgh Centre for Reproductive Health, Queen's Medical Research Institute, Edinburgh, UK; [5]Centre for Liver Research/NIHR Biomedical Research Unit, 5th floor IBR Building, University of Birmingham, UK; [6]Ferring Research Ltd., Southampton, UK.*

*Received May 9, 2013; accepted July 3, 2013.*

bioavailability of relaxant factors (mainly nitric oxide [NO]), and impaired responses to NO.[5,6] The structural component of IHVR may be decreased by effective etiological treatment,[7] but this is not achievable in the majority of patients with PHT. Current treatments for PHT (vasopressin and somatostatin analogs, nonselective beta-blockers) decrease portal pressure by splanchnic vasoconstriction, but this may further compromise hepatic perfusion in cirrhosis and impair organ function.[8]

Relaxin (RLN) is a naturally occurring peptide hormone with a two-chain structure similar to insulin.[9] Although initially identified as a hormone of pregnancy, gene knockout studies and observations in rodents and humans treated with exogenous RLN have revealed diverse effects in nonreproductive tissues in both males and females.[9] The product of the human *RLN2* gene, human gene 2-relaxin (H2-RLN), is the major stored and circulating form. H2-RLN circulates in women at low concentrations during the luteal phase of the menstrual cycle (~50 pg/mL) and at increased levels (~1 ng/mL) throughout pregnancy. In men, H2-RLN is expressed locally in the prostate and may also be present at very low levels (1-5 pg/mL) in the circulation. The primary receptor for H2-RLN, relaxin receptor family peptide-1 (RXFP1), is a member of the leucine-rich repeat family of G-protein coupled receptors[10] and is widely distributed in many tissues in both sexes. RLN is thought to mediate its physiological actions in an autocrine or paracrine manner, whereby activation of RXFP1 results in the stimulation of multiple signal transduction pathways including 3′-5′-cyclic adenosine monophosphate (cAMP) (influenced by a variety of Gα isoforms), extracellular signal-regulated kinases, tyrosine kinases, and NO signaling.[10,11] The effects of RLN on connective tissue remodeling in reproductive and nonreproductive tissues are well documented.[9,12] Although circulating RLN has been detected in patients with chronic liver disease, serum concentrations were either stable or rose very slowly over 15 years of follow-up and did not correlate with the histological stage of fibrosis (M. Mayo, pers. commun.).

A number of humoral agents that elicit either HSC contraction or relaxation have been identified.[1] In human cirrhosis, circulating and tissue levels of the HSC contractile agonist ET-1 are elevated[13] and HSC sensitivity to ET-1 is also enhanced. Exogenous NO has been shown to abolish the contractile effects of ET-1 in isolated perfused liver and in cultured HSCs.[14] Through binding to RXFP1, RLN may induce activation of the NO pathway in target cells. Furthermore, RLN has also been shown to inhibit the vasoconstrictive properties of ET-1 and angiotensin-II in rodent models.[15,16]

Here we show that RLN can modulate the dynamic component of PHT, through effects on intrahepatic NO and MF contractility; thereby identifying the RLN-RXFP1 axis as a novel vasoactive target in cirrhosis.

## Materials and Methods

Tissue was used in accordance with the local ethical review committees and the Human Tissue Act 2004. Procedures involving animals were conducted with ethical approval and in accordance with the Use of Animals in Scientific Procedures Act 1986.

***Isolation and Culture of Cells.*** Primary HSCs and hepatic sinusoidal endothelial cells (HSECs) were isolated and cultured as described in the online Supporting Information.

***Quantitation of HSC Apoptosis.*** Apoptosis of human HSCs was assessed using acridine orange as described in the online Supporting Information.

***Quantitative Polymerase Chain Reaction (qPCR).*** Total RNA was extracted using the RNeasy kit (Qiagen, Manchester, UK) and qPCR performed. Full details are provided in the online Supporting Information and primer sequences listed in Supporting Table 1.

*Jonathan Fallowfield and Damian Mole are supported by Academy of Medical Sciences / The Health Foundation Clinician Scientist Fellowships. Annette Hayden was funded jointly by Ferring Research Ltd as part of an industrial collaborative studentship with the Medical Research Council (MRC) UK and the University of Southampton. Victoria Snowdon and Ben Stutchfield are funded by Scottish Translational Medicine and Therapeutics / Wellcome Trust Clinical Research Fellowships. John Iredale gratefully acknowledges the support of the Medical Research Council and the Wellcome Trust.*

*Address reprint requests to: Professor John P. Iredale, BM (Hons), FMedSci, FRCP, FRSE, Medical Research Council/University of Edinburgh Centre for Inflammation Research, Queen's Medical Research Institute, 47 Little France Crescent, Edinburgh, EH16 4TJ, UK. E-mail: john.iredale@ed.ac.uk; fax: +44-(0)131-242-6682.*



*View this article online at wileyonlinelibrary.com.*

*DOI 10.1002/hep.26627*

*Potential conflict of interest: Nothing to report.*

*Additional Supporting Information may be found in the online version of this article.*

***cAMP Assay.*** Intracellular cAMP measurement in HSCs was performed using the HitHunter cAMP II kit (DiscoveRx, Birmingham, UK) following the manufacturer's instructions. Cells were resuspended in antibody solution at 10,000 cells/well with 0.5 mM isobutylmethylxanthine (IBMX).

***Cyclic Guanosine Monophosphate (cGMP) Immunoassay.*** cGMP in whole liver homogenates and HSC lysates was measured by enzyme immunoassay (Cayman Chemical, Cambridge, UK). Full details are provided in the online Supporting Information.

***Gel Contraction Assay.*** Activated passage-1 human HSCs (hHSCs) suspended in Dulbecco's Modified Eagle Medium (DMEM; Gibco, Paisley, UK) / 10% fetal bovine serum (FBS; Gibco) were layered on top of type-1 collagen lattices at a density of 100,000 cells/well in 24-well flat-bottom tissue culture plates and contractility assessed in response to 1 $\mu$M H2-RLN ± *RXFP1* small interfering RNA (siRNA). Full details are provided in the online Supporting Information.

***NO Measurement.*** Rat serum was centrifuged at 13,000*g* for 2 minutes before filtration using a 10,000 Da molecular weight cutoff filter (Millipore, Watford, UK). $NO/NO_3^-/NO_2^-$ determination was performed using a Parameter Kit (R&D Systems, Abingdon, UK).

***Histology, Immunohistochemistry, and Confocal Microscopy.*** Full details are provided in the online Supporting Information.

***Western Blotting.*** Full details are provided in the online Supporting Information and antibody dilutions listed in Supporting Table 3.

***Rat Carbon Tetrachloride Models.*** Cirrhosis and PHT was induced in age-matched male Sprague-Dawley rats by 8 or 16 weeks administration of carbon tetrachloride ($CCl_4$; Sigma). Littermates (~250-300 g body weight) were randomly allocated to treatment with either twice-weekly injections of intraperitoneal $CCl_4$ (0.1 mL/100g $CCl_4$ for 2 weeks then 0.05 mL $CCl_4$/100g for 6-14 weeks) or sterile vehicle (olive oil; Sigma). 72h RLN Model: Twenty-four hours after the final injection of $CCl_4$ or olive oil ("peak fibrosis"), rats either underwent portal pressure measurement (n = 4-6/group) or insertion of subcutaneous osmotic minipumps (2ML2 Alzet; Durect, Cupertino, CA) under isoflurane anesthesia. Minipumps were preloaded with recombinant human H2-RLN (0.5 mg/kg/day; Corthera, San Carlos, CA) or vehicle (sodium acetate pH 5) for 72h continuous infusion (n = 10). Subgroups of rats (n = 5) were also coadministered L-$N^G$-Nitroarginine methyl ester (L-NAME; Sigma) 250 mg/mL in drinking water starting 24h before minipump insertion and continuing for the 72h infusion period. Serum RLN levels were measured using the Quantikine Human Relaxin-2 Immunoassay (R&D Systems). Blood was collected from the inferior vena cava (systemic blood) or portal vein (splanchnic blood), tissues were fixed in 10% buffered formalin or snap-frozen in liquid nitrogen. Acute RLN Model: Groups of $CCl_4$ or olive oil treated anesthetized rats were randomly allocated to treatment with intravenous RLN (4 $\mu$g/mL over 2 minutes) or equivalent volume of vehicle by way of an internal jugular vein catheter (PE-50; Durect), with continuous hemodynamic monitoring for 180 minutes. Animals were warmed using a heat pad and received intraoperative 0.9% NaCl 10 mL/kg/h.

***Rat Bile Duct Ligation Model.*** Liver fibrosis and PHT was induced in age-matched male Sprague-Dawley rats (~250-300 g) by bile duct ligation (BDL) under isoflurane anesthesia. Briefly, the common bile duct was exposed after laparotomy, ligated with 7-0 silk and cut. Intraoperatively, animals were warmed and received 0.9% NaCl 10 mL/kg/h. Eighteen days post-BDL, animals were randomly allocated to 72h subcutaneous treatment with RLN (0.5 mg/kg/day) or vehicle by minipump (n = 5).

***Hemodynamic Measurements.*** Hemodynamic data were recorded from the femoral artery by way of a PE-50 catheter and portal vein by way of a 24G cannula or indwelling PE-50 catheter using Powerlab 4/35 with LabChart 7 Pro software (ADInstruments, Oxford, UK). Portal blood flow was measured using a perivascular flowprobe (Transonic MA1.5PRB; ADInstruments).

***Dynamic Indocyanine Green (ICG) Imaging.*** Noninvasive *in vivo* imaging was performed using the IVIS Spectrum Imaging System and Living Image v. 3.2 software (PerkinElmer, Waltham, MA). Hepatic uptake and peripheral disappearance rate of 2.5 mg/kg ICG (Cardiogreen; Sigma) was assessed by dynamic fluorescence imaging in anesthetized 8-week $CCl_4$ rats after pretreatment with 4 $\mu$g/mL intravenous H2-RLN or vehicle. Full details are provided in the online Supporting Information.

***Blood Oxygen Level-Dependent Magnetic Resonance Imaging (BOLD-MRI).*** BOLD-MRI uses the paramagnetic properties of deoxyhemoglobin to acquire images sensitive to local tissue oxygen concentration.[17] MRI data were acquired using a 7-Tesla preclinical MRI scanner (Agilent Technologies, Edinburgh, UK) in anesthetized 8-week $CCl_4$ rats, 30 and 60 minutes after administration of 4 $\mu$g/mL intravenous H2-RLN or vehicle. Full details are provided in the online Supporting Information.

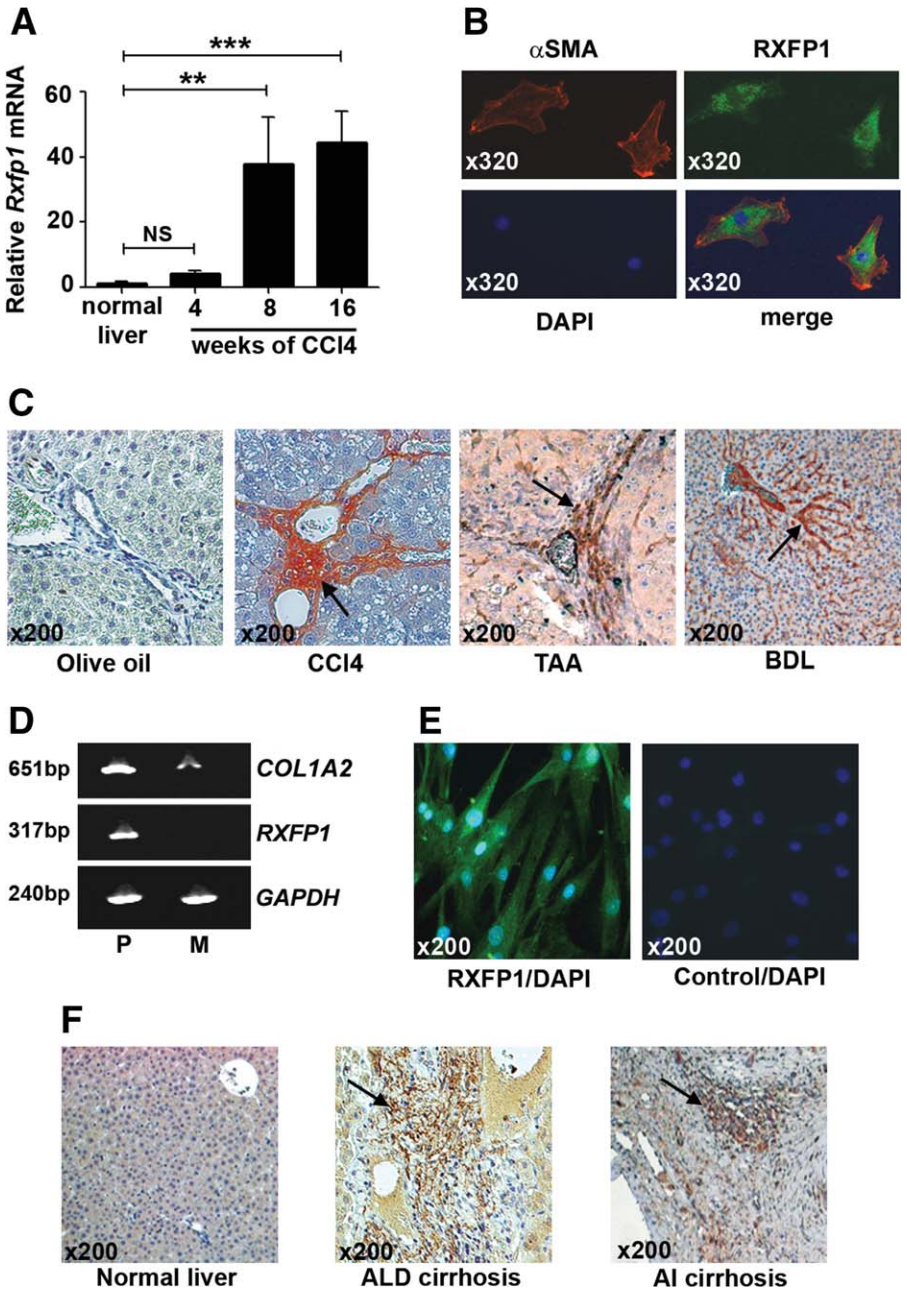


Fig. 1. (A) Hepatic expression of *Rxfp1* mRNA in progressive rat $CCl_4$ injury (**$P < 0.01$, ***$P < 0.001$; NS, not significant; n = 4). (B) Dual immunofluorescence in activated rat HSCs (α-SMA, red; RXFP1, green; DAPI (diamidino-2-phenylindole) nuclear stain, blue). (C) Hepatic RXFP1 immunostaining in rat fibrosis models (TAA, thioacetamide). Positive staining indicated in fibrotic scars and sinusoids (arrows). (D) Representative gels showing gene expression by RT-PCR in hHSCs activated on plastic (P) and deactivated on Matrigel (M) (*COL1A2*, procollagen-1; *GAPDH*, glyceraldehyde 3-phosphate dehydrogenase). (E) RXFP1 immunofluorescence in activated hHSCs. (F) Immunostaining for RXFP1 in normal and cirrhotic (explanted) human liver, with localization to areas of fibrotic scarring (arrows). ALD, alcohol-related liver disease; AI, autoimmune.

***Statistics.*** GraphPad Prism 5 was used for statistical analysis. Data are presented as mean ± standard error of the mean or 95% confidence intervals. Parametric data were compared by unpaired *t* test or one-way analysis of variance (ANOVA) with post-hoc Tukey test for multiple groups, and nonparametric data by equivalent methods.

## Results

***RXFP1 Is Expressed in Rat and Human Cirrhotic Liver and MFs Are the Major Cellular Source.*** We studied hepatic expression of the primary receptor for RLN, RXFP1, in progressive rat $CCl_4$ fibrosis. *Rxfp1* messenger RNA (mRNA) was barely detectable in

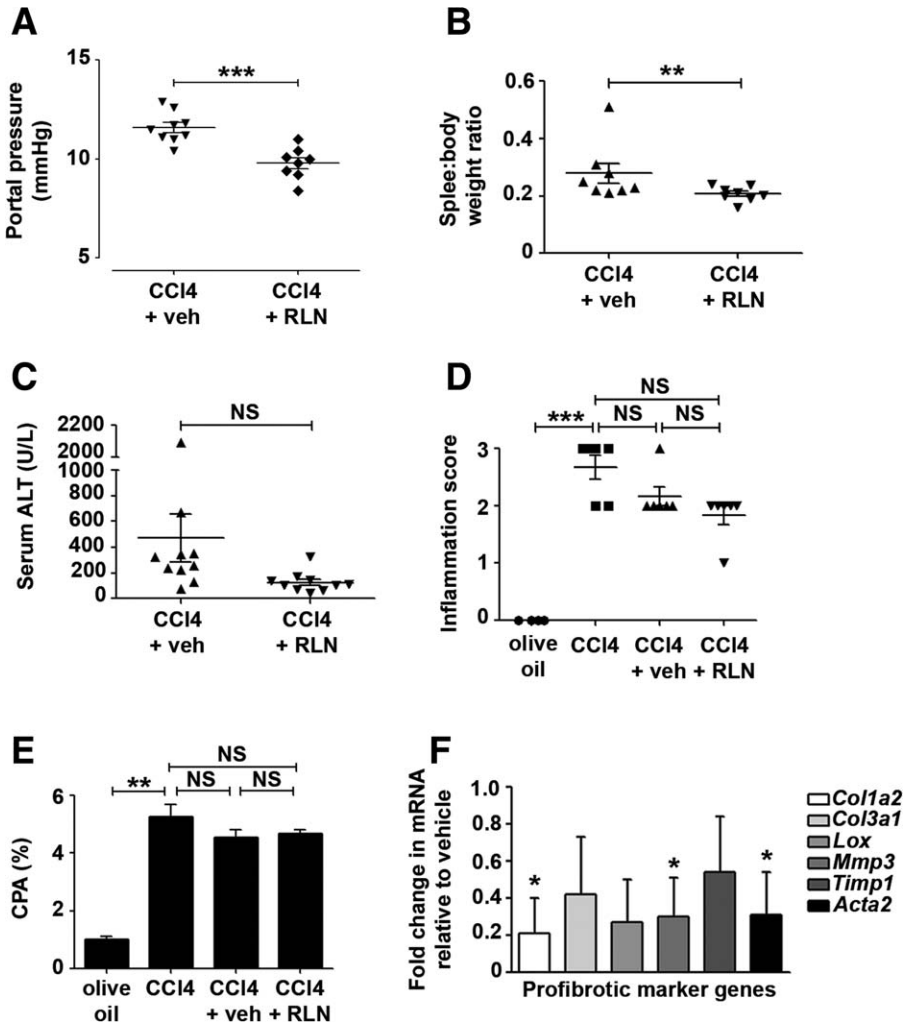


Fig. 2. Effect of 72h RLN treatment on portal pressure, hepatic inflammation, and fibrosis in 8-week $CCl_4$ rats. (A) Portal pressure (***$P = 0.0003$) and (B) spleen size (**$P = 0.01$) were compared after 72h subcutaneous RLN (0.5 mg/kg/day) or vehicle (veh; sodium acetate pH 5) (n = 8-9). (C) Serum ALT, (D) hepatic histological inflammation score (0 (absent), 1 (<2 foci), 2 (2-4 foci), 3 (>4 foci), and (E) collagen proportionate area (CPA) (n = 5-10). (F) Relative hepatic expression of profibrotic genes by qRT-PCR (mean ± 95% confidence intervals; *$P < 0.05$ for *Col1a2* (procollagen-1), *Mmp3* (matrix metalloproteinase-3) and *Acta2* (α-smooth muscle actin). *Col3a1*, procollagen-3; *Lox*, lysyl oxidase; *Timp1*, tissue inhibitor of metalloproteinases-1; n = 6.

normal rat liver but transcripts were increased 38-fold and 44-fold, respectively, after 8 weeks and 16 weeks of $CCl_4$ (Fig. 1A). Quiescent primary rat HSCs did not express *Rxfp1* mRNA (data not shown) but RXFP1 and alpha-smooth muscle actin (α-SMA) colocalized in culture-activated rat HSCs (Fig. 1B). Neither hepatocytes nor hepatic macrophages expressed RXFP1 (data not shown). Expression of RXFP1 protein was shown in a range of mechanistically distinct rat liver fibrosis models (Fig. 1C) in areas of fibrosis and within the sinusoids. No RXFP1 protein was detected in olive oil-treated (Fig. 1C) or normal rat liver (data not shown). Quiescent human HSCs (hHSCs) did not express *RXFP1* or other HSC activation markers, but culture-activated hHSCs expressed RXFP1 mRNA (Fig. 1D) and protein (Fig. 1E). We have previously demonstrated that the activated HSC is not a committed phenotype and HSCs can effectively become "deactivated" *in vitro* after replating onto a synthetic basement membrane-type matrix.[18] Culture of activated hHSCs on Matrigel abrogated expression of *RXFP1* and *COL1A2* mRNA. (Fig. 1D). In addition, human sinusoidal endothelial cells (HSECs) isolated from fibrotic liver also expressed RXFP1 (Supporting Fig. 2D). Finally, we showed that RXFP1 was undetectable in normal human liver but abundant in areas of fibrous scarring within explanted cirrhotic livers (Fig. 1F). Taken together, these data indicate that expression of RXFP1 is restricted to activated HSC-MFs and HSECs in fibrotic liver.

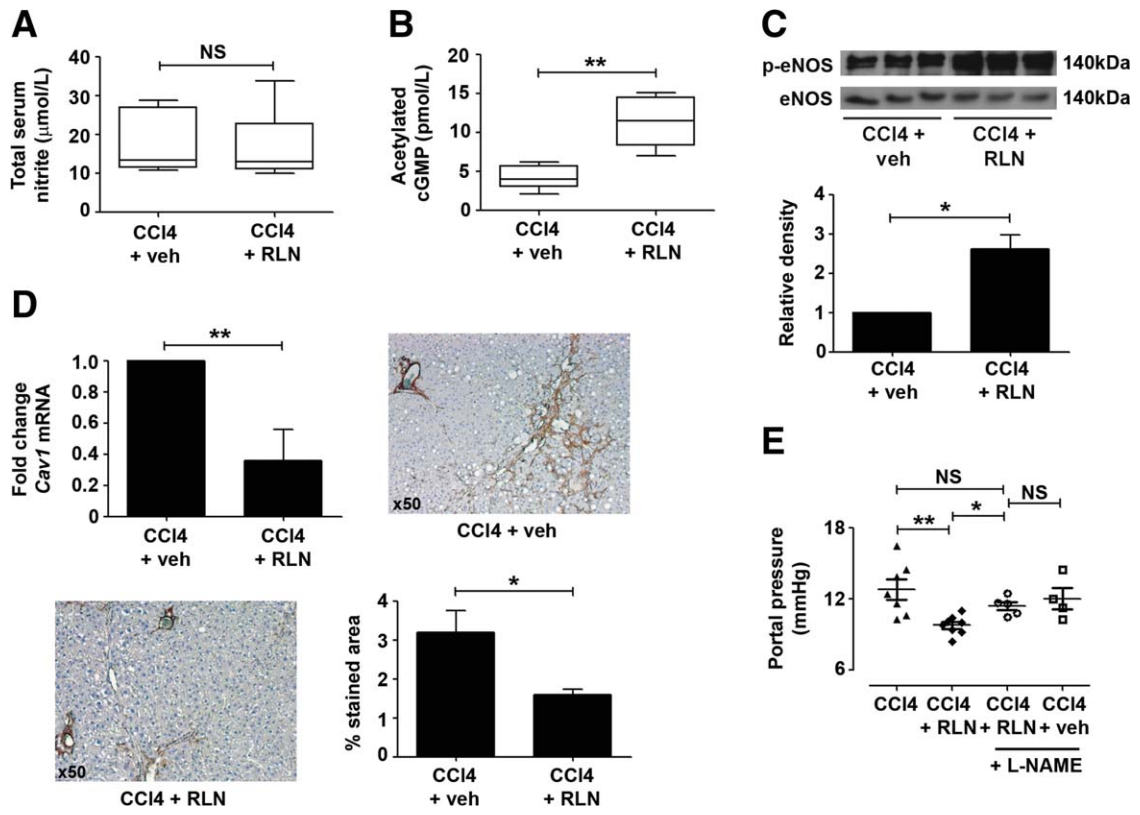


Fig. 3. Effect of 72h RLN treatment on NO bioavailability and signaling in 8-week $CCl_4$ rats. (A) Serum total nitrite ($P = 0.9372$) and (B) intrahepatic acetylated cGMP (**$P = 0.0018$) levels were compared after 72h subcutaneous RLN (0.5 mg/kg/day) or vehicle (veh; sodium acetate pH 5) (n = 6). (C) Relative p-eNOS protein by western blotting and densitometry (*$P = 0.0125$; n = 6). (D) Hepatic caveolin-1 (*Cav1*) mRNA by qRT-PCR (**$P = 0.0059$) and representative photomicrographs showing protein by immunohistochemistry with quantitation by morphometry (*$P = 0.0253$) (n = 6). (E) Effect of cotreatment with the NOS inhibitor L-NAME on portal pressure (*$P < 0.05$; n = 5-8).

***RLN Treatment Reduces Portal Pressure in 8-Week $CCl_4$ Rats.*** Cirrhosis and preascitic PHT was induced by 8 weeks $CCl_4$ (Supporting Fig. 1A-D). After 72h subcutaneous RLN the mean serum concentration was $62 \pm 10$ ng/mL, whereas in controls it was undetectable. Rats receiving RLN had lower portal pressures (Fig. 2A; $9.7 \pm 0.28$ mmHg versus $11.7 \pm 0.29$ mmHg) and a reduction in splenomegaly (Fig. 2B; spleen:body weight ratio $0.20 \pm 0.01$ versus $0.27 \pm 0.03$). Livers were assessed for hepatocellular injury and fibrosis (Supporting Fig. 1E,F). There was no difference in serum alanine aminotransferase (ALT) level (Fig. 2C), hepatic necro-inflammatory score (Fig. 2D), or collagen proportionate area (CPA; Fig. 2E) between RLN-treated rats and controls. Acknowledging that matrix remodeling was unlikely within the short time-frame chosen for our hemodynamic study, we quantified hepatic expression of profibrogenic marker genes (Fig. 2F). Relative to control, transcripts for all profibrotic genes were reduced by RLN.

***RLN Increases Intrahepatic But Not Systemic NO Levels in 8-Week $CCl_4$ Rats.*** To define the role of NO in mediating the portal hypotensive effect of RLN, we measured serum NO metabolites and intrahepatic cGMP as a surrogate index of NO bioavailability. We found no difference in total nitrite levels in systemic venous (Fig. 3A) and portal venous blood (data not shown), but RLN-treated rats had increased intrahepatic cGMP levels compared to controls (Fig. 3B). Hepatic expression of phosphorylated Akt $^{(Ser473)}$ (Supporting Fig. 2A) and phosphorylated eNOS$^{(Ser1179)}$ protein (Fig. 3C) were also increased. The eNOS regulatory protein caveolin-1 is abundant in cirrhotic liver but, relative to control, RLN reduced caveolin-1 mRNA and protein (Fig. 3D). These data indicate that RLN can stimulate intrinsic NO generation in fibrotic liver by activating the Akt/eNOS/cGMP pathway. The pivotal role of NO was confirmed by showing that NOS inhibition with L-NAME inhibited hepatic eNOS expression (Supporting Fig. 2B) and abrogated the effect of RLN on portal pressure (Fig. 3E) and splenomegaly (Supporting Fig. 2C). We went on to demonstrate that primary HSECs cultured from fibrotic human liver expressed RXFP1 (Supporting Fig. 2D) and increased NO production when treated with RLN (Supporting Fig. 2E).

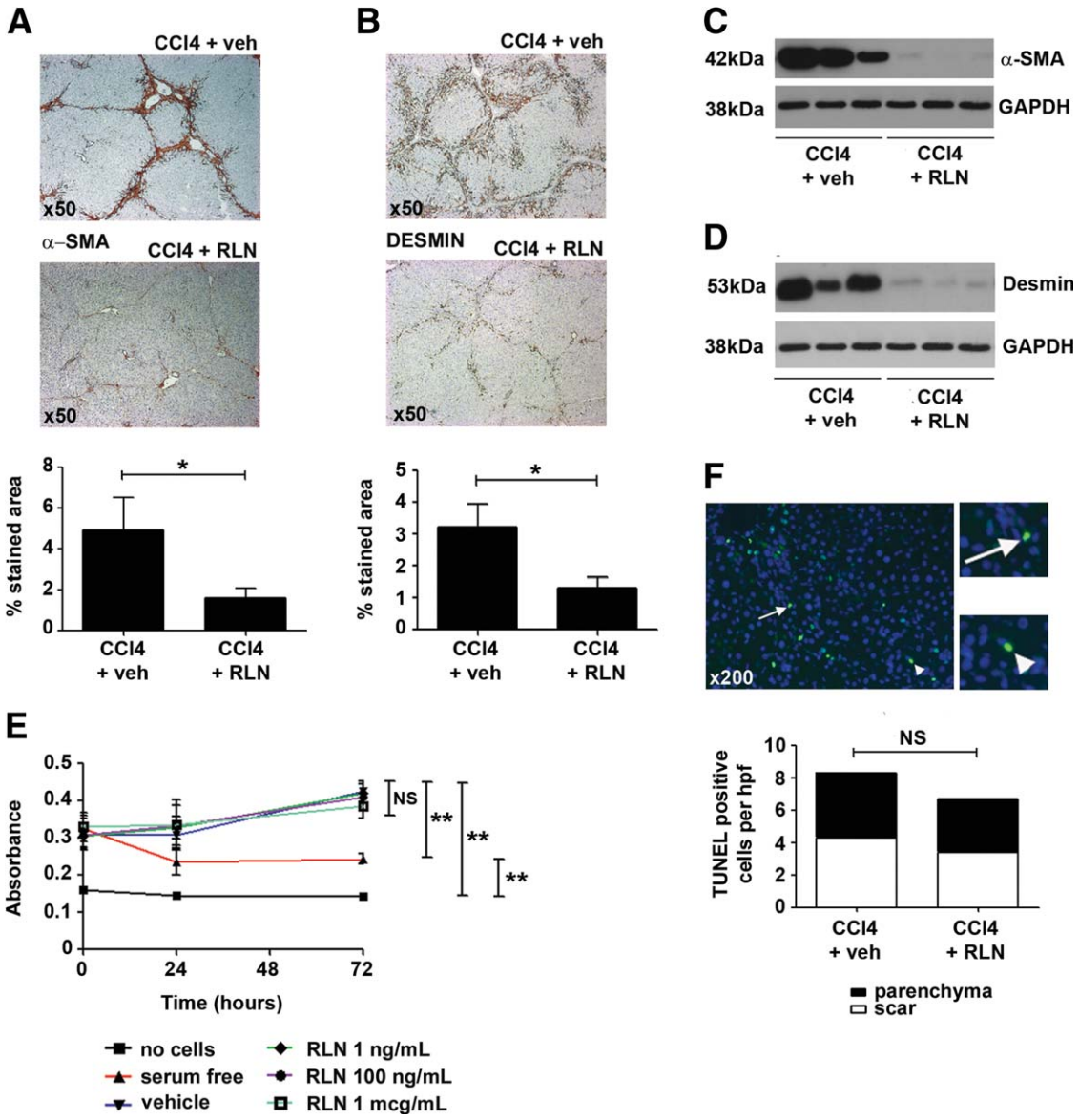


Fig. 4. Effect of 72h RLN treatment on hepatic expression of cytoskeletal proteins in 8-week $CCl_4$ rats. Representative photomicrographs of (A) α-SMA (*$P = 0.026$) and (B) desmin ($P = 0.0422$) immunostaining in liver after 72h subcutaneous RLN (0.5 mg/kg/day) or vehicle (veh; sodium acetate pH 5) with quantitation by morphometry (n = 6). Representative western blots showing (C) α-SMA and (D) desmin protein expression in whole liver extracts. (E) Effect of RLN on numbers of activated rat HSCs by MTS assay ($P < 0.001$; n = 4). (F) Representative image showing TUNEL (green) immunofluorescence from a vehicle-treated $CCl_4$ rat liver with DAPI (blue) nuclear counterstain. Enlarged panels show TUNEL-positive cells within a fibrotic band (arrow) and in liver parenchyma (arrowhead) (n = 6).

***RLN Treatment Down-Regulates Expression of Cytoskeletal Filament Proteins in 8-Week $CCl_4$ Rats.*** Liver fibrosis is characterized by increased contractile filament expression and increased cytoskeletal tension. After 72h RLN, we observed a profound reduction in hepatic α-SMA protein by immunostaining (Fig. 4A) and western blotting (Fig. 4C). Desmin filaments run between anchorage points of the contractile apparatus in cells (the foci of mechanical stress) and are also a marker of the activated HSC-MF phenotype.[19] We also observed a marked reduction in desmin protein by immunostaining (Fig. 4B) and western blotting (Fig. 4D) following RLN. In contrast, glial fibrillary acidic protein (GFAP), predominantly a marker of quiescent HSCs, did not decrease significantly (Supporting Fig. 3A). Additionally, treatment of activated rat HSCs with a range of RLN doses *in vitro* had no effect on cell numbers (Fig. 4E). Indeed, we observed no difference in apoptotic markers in liver (TUNEL staining [Fig. 4F] and cleaved caspase-3 levels [Supporting Fig. 3B]), indicating that the observed decrease in hepatic α-SMA and desmin by RLN

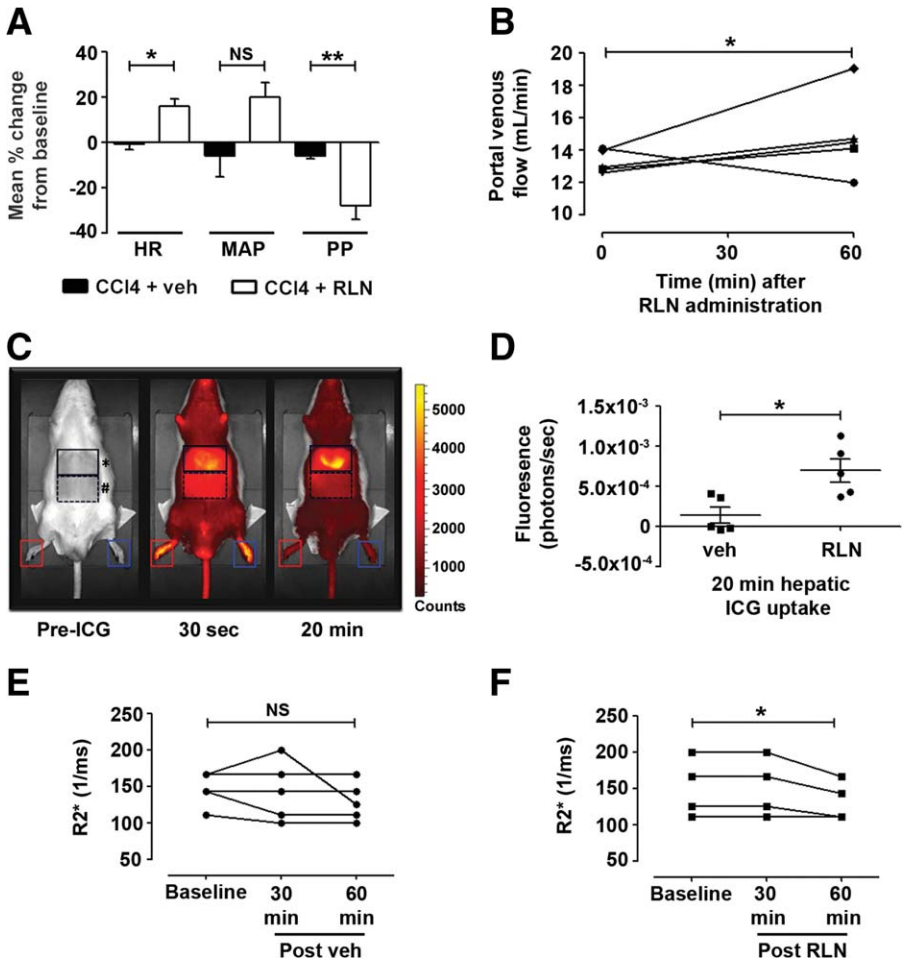


Fig. 5. Acute hemodynamic effects of RLN treatment in 8-week $CCl_4$ rats. (A) Mean change in portal pressure (PP; $^{**}P = 0.0035$), heart rate (HR; $^{*}P = 0.0324$), and mean arterial pressure (MAP; $P = 0.0869$) from baseline after intravenous RLN (4 $\mu$g/mL) or vehicle (veh; sodium acetate pH 5) (n = 4). (B) Effect of RLN on portal venous blood flow by perivascular flowprobe ($^{*}P = 0.0352$ baseline versus 60 minutes; n = 5). (C) Representative whole-animal fluorescence images in an RLN-treated $CCl_4$ rat pre-ICG, 30 seconds and 20 minutes after tail vein ICG injection (2.5 mg/kg) with regions of interest indicated over liver (*), abdominal wall (background; #), right paw (red box). (D) Hepatic ICG uptake rate after pretreatment with 100 $\mu$L intravenous RLN (4 $\mu$g) or equivalent volume of vehicle ($^{*}P = 0.0303$; n = 5). (E) BOLD-MRI showing change in R2* (1/T2*) after 1 mL intravenous vehicle ($P = 0.3343$ baseline versus 60 minutes; n = 5) and (F) after intravenous RLN (4 $\mu$g/mL) ($^{*}P = 0.0346$ baseline versus 60 minutes; n = 4).

involved a specific reduction of fibrotic markers in these cells. We found no evidence for inhibition of hepatic Rho/Rho-kinase by RLN in our study (Supporting Fig. 4A,B).

The major profibrogenic cytokine responsible for initiation and perpetuation of HSC activation is transforming growth factor beta-1 (TGF$\beta$1). After 72h subcutaneous RLN we showed reduced hepatic expression of TGF$\beta$1 mRNA and protein and reduced transcription of other genes associated with TGF$\beta$ activity and signaling (Supporting Fig. 3C-E).

***Acute Intravenous RLN Treatment Decreases Portal But Not Systemic Pressure in 8-Week $CCl_4$ Rats.*** To exclude the impact of systemic hypotension on the apparent portal hypotensive effect of RLN, we measured the hemodynamic effects of intravenous RLN in 8 week $CCl_4$ rats (Fig. 5A). Dose-response studies had previously been undertaken by our group (data not shown) and others.[15,20] Rats were monitored for 180 minutes after injection of RLN (4 $\mu$g/mL over 2 minutes) or vehicle. RLN induced a rapid (<60 minutes) and robust reduction in portal pressure (mean change from baseline $28 \pm 6\%$ versus $-6.2 \pm 1.5\%$), an increase in heart rate (mean change from baseline $16 \pm 3\%$ versus $-1 \pm 2.5\%$), and modest increase in mean arterial pressure (MAP; mean change from baseline $20 \pm 6.4$ versus $-6 \pm 9.5\%$). Vehicle had no significant hemodynamic effects (Fig. 5A). There was no difference is spleen size between RLN and vehicle-treated rats in this acute model.

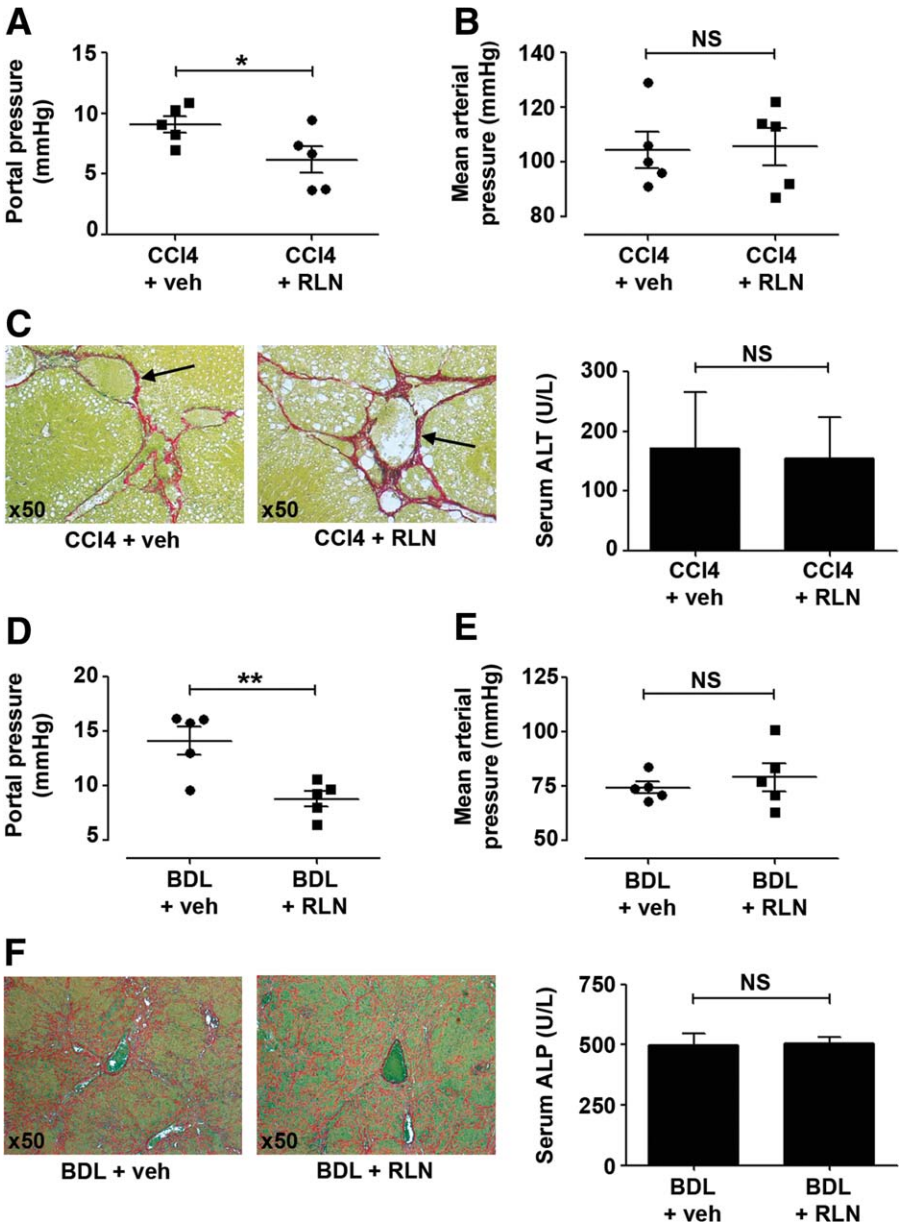


Fig. 6. Effect of 72h RLN treatment in 16-week $CCl_4$-treated and bile duct ligated rats. (A) Portal pressure (*$P = 0.0414$), (B) MAP ($P = 0.8574$), (C) Sirius red staining and serum ALT levels ($P = 0.8808$) were compared in 16-week $CCl_4$ rats after 72h subcutaneous RLN (0.5 mg/kg/day) or vehicle (veh; sodium acetate pH 5) (n = 5). (D) Portal pressure (**$P = 0.0067$), (E) MAP ($P = 0.3072$), (F) Sirius red staining and serum alkaline phosphatase (ALP) levels ($P = 0.8713$) were compared in 3-week BDL rats after 72h subcutaneous RLN (0.5 mg/kg/day) or vehicle (veh; sodium acetate pH 5) (n = 5).

***Acute Intravenous RLN Treatment Increases Portal Venous Blood Flow and Hepatic Oxygenation in 8-Week $CCl_4$ Rats.*** Given its effects on intrahepatic NO, we went on to study portal blood flow and hepatic oxygenation in response to RLN. By perivascular flowprobe we demonstrated an increase in portal venous flow in response to RLN in 4 of 5 rats studied (Fig. 5B; baseline $12.8 \pm 0.42$ mL/min versus 60 minutes $15.0 \pm 1.1$ mL/min), but no significant change was observed in controls (data not shown). Injection of ICG with dynamic fluorescence imaging[21] was used to measure blood flow noninvasively (Fig. 5C,D; Supporting Fig. 5A). Hepatic uptake of ICG at 20 minutes was increased in rats pretreated with RLN compared to vehicle (Fig. 5D), as was peripheral disappearance rate, although the difference was not statistically significant (Supporting Fig. 5B). Assessment of tissue oxygenation by BOLD-MRI (Fig. 5E,F) showed that RLN decreased R2* (1/T2* = deoxyhemoglobin) after 60 minutes, whereas vehicle had no effect.

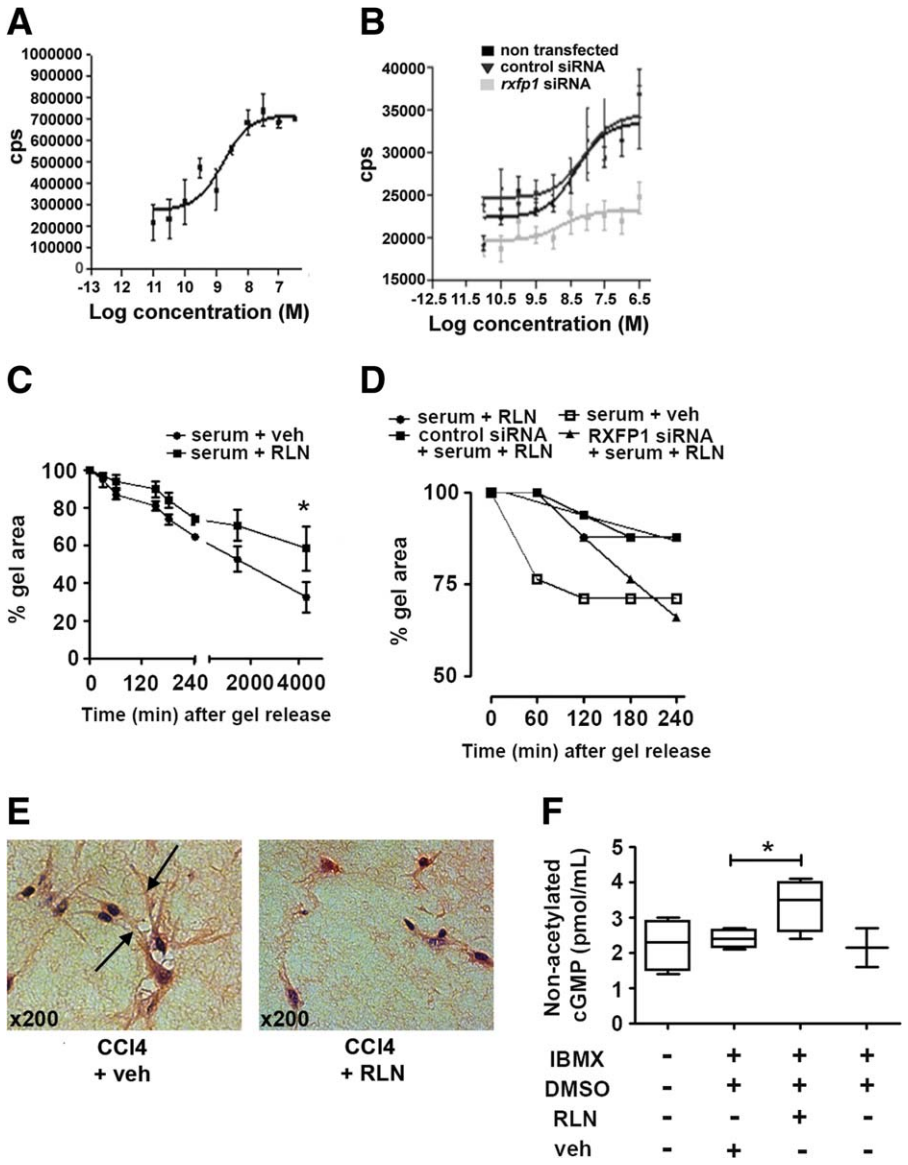


Fig. 7. Effects of RLN on human HSCs *in vitro*. (A) cAMP accumulation in hHSCs after stimulation with RLN for 90 minutes (cps = counts per second; n = 6). (B) Effect of RXFP1 siRNA pretreatment on RLN-induced cAMP accumulation (n = 3). (C) Effect of RLN (1 $\mu$M) on 10% serum-induced hHSC contraction by collagen gel contraction assay (*$P < 0.05$; n = 4) and (D) after pretreatment with *RXFP1* siRNA (n = 2). (E) Representative photomicrographs showing hematoxylin and eosin (H&E)-stained hHSCs in collagen gel lattices after RLN and vehicle treatment. Arrows indicate long cellular processes. (F) Intracellular cGMP levels after 30 minutes treatment with 100 ng/mL RLN or vehicle (*$P < 0.05$ versus hHSCs incubated with vehicle/untreated hHSCs/DMSO control; n = 3).

***RLN Reduces Portal But Not Systemic Pressure and Improves Liver Function in Advanced Cirrhosis.*** We then confirmed that RLN mediated a portal hypotensive effect in advanced $CCl_4$ cirrhosis and also in a mechanistically distinct model of fibrosis (BDL). Rats injured for 16 weeks with $CCl_4$ had PHT but no significant ascites. Treatment with subcutaneous RLN for 72h reduced portal pressure (Fig. 6A; $6.1 \pm 1.1$ mmHg versus $9.12 \pm 0.9$ mmHg), but not spleen size (Supporting Fig. 6A), heart rate (Supporting Fig. 6B), or MAP (Fig. 6B). Serum albumin levels were increased following RLN (Supporting Fig. 6C; $27.4 \pm 0.54$ g/L versus $24.7 \pm 0.67$ g/L), but there was no difference in liver fibrosis (Fig. 6C) by CPA (Supporting Fig. 6D), or hepatocellular injury by serum ALT (Fig. 6A) and histology (data not shown).

The livers of BDL rats were intensely scarred and inflamed and PHT was marked with most rats developing ascites. Treatment with 72h subcutaneous RLN reduced portal pressure (Fig. 6D; $8.8 \pm 0.73$ mmHg versus $14.13 \pm 1.28$ mmHg), although there was no significant difference in spleen:liver weight ratio

(Supporting Fig. 7A), heart rate (Supporting Fig. 7B), or MAP (Fig. 6E). There were no significant differences in fibrosis (Fig. 6F; Supporting Fig. 7C), hepatocellular injury (Supporting Fig. 7D,E), serum alkaline phosphatase (ALP; Fig. 6F), or albumin (Supporting Fig. 7F).

***RXFP1 Activation and Signaling in Human HSCs* In Vitro.** Functional activity of RXFP1 was investigated by cAMP accumulation assay following treatment with exogenous RLN. hHSCs exhibited a full cAMP dose-response curve with the preferential RXFP1 ligand H2-RLN (Fig. 7A). Transfection of hHSCs (and LX-2 cells, not shown) with *RXFP1* siRNA inhibited the cAMP response to RLN (Fig. 7B). No significant effects were observed following treatment with RXFP1 siRNA in H2-RLN unstimulated forskolin-spiked assays (data not shown).

***Modulation of hHSC Contraction by RLN* In Vitro *Supports a Role for a Portal Hypotensive Effect in Humans.*** In collagen gel contraction assays, RLN reduced basal (10% serum-induced) hHSC contractility by ~40% after 72h measured by final gel area (Fig. 7C). Visualization of hHSCs seeded into collagen lattices revealed morphological differences associated with RLN treatment, including a reduction in the number of cytoplasmic protrusions (Fig. 7E). Knockdown of *RXFP1* with siRNA completely inhibited the cell relaxation effect of RLN, indicating that this was mediated by way of RXFP1 (Fig. 7D). Treatment with RLN also increased intracellular cGMP in hHSCs (Fig. 7F).

***Exogenous RLN Induces an Antifibrotic Phenotype in Activated Human HSCs.*** Treatment of activated hHSCs with RLN for 72h decreased expression of profibrotic genes and increased expression of MMPs in an RXFP1-dependent manner (Supporting Fig. 8A,B). Additionally, RLN reduced TGF$\beta$1 mRNA and protein expression (Supporting Fig. 8C), and inhibited basal and TGF$\beta$-stimulated $\alpha$-SMA protein expression in hHSCs (Supporting Fig. 8D), but had no effect on hHSC apoptosis (Supporting Fig. 8E).

## Discussion

In this study we show comprehensively that RLN induced a selective and significant portal hypotensive effect in the most relevant rodent model of sinusoidal PHT ($CCl_4$),[22] through augmentation of intrahepatic NO signaling and down-regulation of contractile filament expression. Critically, reduction in portal pressure was also reproduced in advanced cirrhosis and a second mechanistically distinct model of fibrosis (BDL). Finally, we showed that activated hHSCs expressed functional RLN receptors *in vitro* and that stimulation with exogenous RLN decreased cellular contractility and induced an antifibrogenic phenotype. Therapeutic deployment of RLN in diseases such as cirrhosis that are characterized by fibrosis and pathological vasoconstriction is therefore an appealing approach. Increased IHVR, resulting from structural changes related to scarring and increased vascular tone mediated by dynamic contraction of hepatic MFs, is the primary cause of PHT in cirrhosis. As such, it is the ideal target for treatment.

The primary (H2-)RLN receptor, RXFP1, was undetectable in normal rat liver and quiescent HSCs but highly expressed in fibrotic liver and HSC-MFs. By subcutaneous infusion in cirrhotic rats we generated steady-state serum RLN concentrations comparable to midterm pregnancy levels, when gestational renal vasodilation is maximal,[23] and induced a portal hypotensive effect that would be clinically meaningful if translated in humans. Reduction in portal pressure was not due to regression of fibrosis or inflammation (both of which contribute to the mechanical component of PHT) or loss of HSC-MFs by apoptosis. Recent studies have demonstrated hepatic MF plasticity even in an advanced activated phenotype.[24] We conclude that RLN altered the fibrogenic state of MFs rather than influencing cell numbers, consistent with studies in renal and cardiac models.[25]

In experimental cirrhosis and human disease, impaired NO production by eNOS contributes to increased IHVR. Decreased expression of eNOS protein, decreased phosphorylation of eNOS by the serine-threonine kinase Akt, and inhibition of eNOS by enhanced expression of caveolin-1[26] underlies this endothelial dysfunction. Replenishing NO in cirrhotic liver by NOS gene transfer or drug therapy in rats and humans[27] has been shown to ameliorate PHT. In treating cirrhotic rats with RLN, we increased hepatic eNOS, Akt-dependent eNOS phosphorylation, and cGMP levels, and down-regulated caveolin-1 expression. Inhibition by L-NAME demonstrated the importance of this axis in mediating the portal hypotensive effect of RLN *in vivo*. Clinical application of nonselective NO donors such as nitrates in cirrhosis is complicated by impairment of systemic hemodynamics and subsequent risk of kidney dysfunction.[28] However, we showed that 72h subcutaneous RLN did not significantly increase systemic or portal venous nitrite levels and did not reduce MAP, even in advanced cirrhosis, indicating that RLN may represent a new liver-selective NO donor. Interestingly, RLN has been

shown to preferentially dilate preconstricted vessels and vasodilatory effects were observed in small renal arteries of rats and mice but not in mesenteric or coronary septal arteries.[29]

We demonstrated a rapid and robust reduction in portal pressure following acute intravenous RLN with no effect on MAP. This is in agreement with rodent[30] and human[31] studies, where RLN elicited hemodynamic effects consistent with vasodilatation without inducing hypotension. The goal of therapy in PHT is to reduce portal pressure below critical thresholds without further deteriorating liver function. We showed that RLN infusion in early cirrhosis increased portal venous flow and tissue oxygenation while decreasing portal pressure, indicating a reduction in IHVR. Furthermore, in advanced $CCl_4$ cirrhosis serum albumin levels were significantly increased.

We went on to underscore the potential for RLN in human disease by showing RXFP1 expression in explanted human cirrhosis specimens and activated hHSC-MFs, and confirmed H2-RLN as the cognate ligand for RXFP1 in these cells. Treatment with exogenous RLN *in vitro* inhibited HSC contractility and induced an antifibrogenic gene expression profile in an RXFP1-dependent manner. Compared to contraction, relatively little is known about the signaling pathways which regulate HSC or MF relaxation.[1] Both an increase in intracellular cAMP[32] and cGMP[6] have been shown to reduce HSC contraction. We showed that RLN increased intracellular cAMP and cGMP in hHSC-MFs. Interestingly, the observation that α-SMA expression in rat HSCs is regulated by NO and cGMP production[33] may provide a link between RLN induced intrahepatic NO generation and down-regulation of α-SMA protein in HSC-MFs *in vivo*. Indeed, we also showed that human HSECs isolated from fibrotic liver expressed RXFP1 *in vitro* and increased NO production in response to RLN treatment. Further work will define the HSEC response to RLN and crosstalk between HSECs and HSCs.

Our data demonstrate that short-term RLN treatment effectively down-regulates HSC-MF contractile filament expression and contractile function and exerts a significant portal hypotensive effect *in vivo* even in advanced cirrhosis models (Supporting Fig. 9). Although initial application in humans would likely involve short-term hemodynamic modulation (e.g., for variceal bleeding), it is tempting to speculate that longer-term targeting of RXFP1 might have dual effects on PHT through relaxation and deactivation of HSC-MFs, particularly as RXFP1 desensitization has not been reported to occur.[11] We have provided proof of concept for the use of RLN in cirrhotic PHT and other conditions associated with MF activation and pathological vasoconstriction and, given its excellent safety profile in clinical trials, support its evaluation in selected patients in early-phase studies.

*Acknowledgment:* We thank Will Mungall, Ross Lennen, Maurits Jansen, Cathy Payne and Deborah Mauchline (all University of Edinburgh) and Shishir Shetty (University of Birmingham, UK) for assistance; Hector Garcia (Hepatic Vascular Biology Lab, University of Barcelona, Spain), and Don Rockey (University of Texas Southwestern, USA) for technical advice; and Professor David Adams (University of Birmingham, UK) for access to human liver material. We thank Dr. Dennis Stewart (Corthera, USA) for supply of clinical grade recombinant human H2-RLN and placebo (vehicle).

## References

1. Reynaert H, Thompson MG, Thomas T, Geerts A. Hepatic stellate cells: role in microcirculation and pathophysiology of portal hypertension. Gut 2000;50:571-581.
2. Thimgan MS, Yee HF Jr. Quantitation of rat hepatic stellate cell contraction: stellate cells' contribution to sinusoidal resistance. Am J Physiol 1999;277:137-143.
3. De Franchis R. Stellate cells and the "reversible component" of portal hypertension. Dig Liv Dis 2000;32:104-107.
4. Bhathal PS, Grossman HJ. Reduction of the increased portal vascular resistance of the isolated perfused cirrhotic rat liver by vasodilators. J Hepatol 1985;1:325-337.
5. Rockey DC, Chung JJ. Reduced nitric oxide production by endothelial cells in cirrhotic rat liver: endothelial dysfunction in portal hypertension. Gastroenterology 1998;114:344-351.
6. Perri RE, Langer DA, Chatterjee S, Gibbons SJ, Gadgil J, Cao S, et al. Defects in cGMP-PKG pathway contribute to impaired NO-dependent responses in hepatic stellate cells upon activation. Am J Physiol Gastrointest Liver Physiol 2006;290:G535-G542.
7. Carrión JA, Navasa M, García-Retortillo M, García-Pagan JC, Crespo G, Bruguera M, et al. Efficacy of antiviral therapy on hepatitis C recurrence after liver transplantation: a randomized controlled study. Gastroenterology 2007;132:1746-1756.
8. Cardoso JE, Giroux L, Kassissia I, Houssin D, Habib N, Huet PM, et al. Liver function improvement following increased portal blood flow in cirrhotic rats. Gastroenterology 1994;107:460-467.
9. Sherwood OD. Relaxin's physiological roles and other diverse actions. Endocrine Rev 2004;25:205-234.
10. Hsu SY. New insights into the evolution of the relaxin-LGR signaling system. Trends Endocrinol Metab 2003;14:303-309.
11. Halls ML. Constitutive formation of an RXFP1-signalosome: a novel paradigm in GPCR function and regulation. Br J Pharmacol 2012;165:1644-1658.
12. Williams EJ, Benyon RC, Trim N, Hadwin R, Grove BH, Arthur MJ, et al. Relaxin inhibits effective collagen deposition by cultured hepatic stellate cells and decreases rat liver fibrosis in vivo. Gut 2001;49:577-583.
13. Moller S, Emmeluth C, Henriksen JH. Elevated circulating plasma endothelin-1 concentrations in cirrhosis. J Hepatol 1993;19:285-290.
14. Kawada N, Tran-Thi TA, Klein H, Decker K. The contraction of hepatic stellate (Ito) cells stimulated with vasoactive substances. Possible involvement of endothelin 1 and nitric oxide in the regulation of the sinusoidal tonus. Eur J Biochem 1993;213:815-823.

15. Danielson LA, Sherwood OD, Conrad KP. Relaxin is a potent vasodilator in conscious rats. J Clin Invest 1999;103:525-533.
16. Danielson LA, Kercher LJ, Conrad KP. Impact of gender and endothelin on renal vasodilation and hyperfiltration induced by relaxin in conscious rats. Am J Physiol Regul Integr Comp Physiol 2000;279:1298-1304.
17. Ramachandran P, Pellicoro A, Vernon M, Boulter L, Aucott RL, Ali A, et al. Differential Ly-6C expression identifies the recruited macrophage phenotype which orchestrates the regression of murine liver fibrosis. Proc Natl Acad Sci U S A 2012;109:E3186-E195.
18. Foley LM, Picot P, Thompson RT, Yau MJ, Brauer M. In vivo monitoring of hepatic oxygenation changes in chronically ethanol-treated rats by functional magnetic resonance imaging. Magn Reson Med 2003;50:976-983.
19. Gaca MD, Zhou X, Issa R, Kiriella K, Iredale JP, Benyon RC. Basement membrane-like matrix inhibits proliferation and collagen synthesis by activated rat hepatic stellate cells: evidence for matrix-dependent deactivation of stellate cells. Matrix Biol 2003;22:229-239.
20. Cassiman D, Libbrecht L, Desmet V, Denef C, Roskams T. Hepatic stellate cell/myofibroblast subpopulations in fibrotic human and rat livers. J Hepatol 2002;36:200-209.
21. Debra DO, Conrad KP, Danielson LA, Shroff SG. Effects of relaxin on systemic arterial hemodynamics and mechanical properties in conscious rats: sex dependency and dose response. J Appl Physiol 2005;98:1013-1020.
22. Kawaguchi Y, Ishizawa T, Miyata Y, Yamashita S, Masuda K, Satou S, et al. Portal uptake function in veno-occlusive regions evaluated by real-time fluorescent imaging using indocyanine green. J Hepatol 2013;58:247-253.
23. Abraldes JG, Pasarín M, García-Pagán JC. Animal models of portal hypertension. World J Gastroenterol 2006;12:6577-6584.
24. Conrad KP. Renal hemodynamics during pregnancy in chronically catheterized, conscious rats. Kidney Int 1984;26:24-29.
25. Kisseleva T, Cong M, Paik Y, Scholten D, Jiang C, Benner C, et al. Myofibroblasts revert to an inactive phenotype during regression of liver fibrosis. Proc Natl Acad Sci U S A 2012;109:9448-9453.
26. Heeg MHJ, Koziolek MJ, Vasko R, Schaefer L, Sharma K, Muller GA, et al. The antifibrotic effects of relaxin in human renal myofibroblasts are mediated in part by inhibition of the Smad2 pathway. Kidney Int 2005;68:96-109.
27. Shah V, Toruner M, Haddad F, Cadelina G, Papapetropoulos A, Choo K, et al. Impaired endothelial nitric oxide synthase activity associated with enhanced caveolin binding in experimental cirrhosis in the rat. Gastroenterology 1999;117:1222-1228.
28. Zafra C, Abraldes JG, Turnes J, Berzigotti A, Fernandez M, Garcia-Pagan JC, et al. Simvastatin enhances hepatic nitric oxide production and decreases the hepatic vascular tone in patients with cirrhosis. Gastroenterology 2004;126:749-755.
29. Salmerón JM, Ruiz del Arbol L, Ginès A, García-Pagán JC, Ginès P, Feu F, et al. Renal effects of acute isosorbide-5-mononitrate administration in cirrhosis. HEPATOLOGY 1993;17:800-806.
30. McGuane JT, Debrah JE, Sautina L. Relaxin induces rapid dilation of rodent small renal and human subcutaneous arteries via PI3 kinase and nitric oxide. Endocrinology 2011;52:2786-2796.
31. Debrah DO, Conrad KP, Jeyabalan A, Danielson LA, Shroff SG. Relaxin increases cardiac output and reduces systemic arterial load in hypertensive rats. Hypertension 2005;46:745-750.
32. Dschietzig T, Teichman S, Unemori E, Wood S, Boehmer J, Richter C, et al. Intravenous recombinant hunman relaxin in compensated heart failure: a safety, tolerability, and pharmacodynamic trial. J Cardiac Fail 2009;15:182-190.
33. Kawada N, Kuroki T, Kobayashi K, Inoue M, Kaneda K. Inhibition of myofibroblastic transformation of cultured rat hepatic stellate cells by methylxanthines and dibutyryl cAMP. Dig Dis Sci 1996;41:1022-1029.
34. Kawada N, Kuroki T, Uoya M, Inoue M, Kobayashi K. Smooth muscle alpha-actin expression in rat hepatic stellate cell is regulated by nitric oxide and cGMP production. Biochem Biophys Res Commun 1996;4;229:238-242.